ICOMAT PRAGUE 2025

INTERNATIONAL CONFERENCE ON MARTENSITIC TRANSFORMATIONS

September 7-12, 2025

OREA Hotel Pyramida, Prague, Czech Republic

PROGRAM and ABSTRACTS

www.icomat2025.org

Welcome

Dear Friends and Colleagues,

Welcome to the International Conference on Martensitic Transformations 2025 (ICOMAT2025) held in Prague, Czech Republic. The conference is the 17th ICOMAT conference since the 1st conference held in Kobe, Japan, on May 10-12, 1976. As is the tradition of ICOMAT meetings, the conference will offer participants an interesting program and will stipulate many discussions that will move the field of martensitic transformations forward.

The research to be presented at ICOMAT2025 covers latest developments in a wide range of topics related to martensitic transformations. You will hear lectures from leading as well as young scientists active in the field, including six plenary speakers and 32 invited speakers selected by members of the International Advisory Committee and Local Advisory Committee. The conference will provide many opportunities to discuss research details during poster presentations, lunches and coffee breaks. Although we tried to prepare the program with the utmost care and effort, glitches may appear for which we apologize beforehand.

In addition to the scientific content, we will have a memorial section reminding the participants on the work and legacy of excellent scientists from the martensite community who passed away recently. We will also have a section dedicated to public outreach of martensite research focusing on issues concerned with attracting a new generation to the field, or science in general.

The conference offers a social program that includes a welcome drink in the conference hall of the Hotel Pyramida on Sunday. On Wednesday, we will have a conference dinner in the beautiful Renaissance Martinický Palace, located next to the Prague Castle just a short distance walk from the conference venue.

We hope that ICOMAT2025 will be remembered as a meeting where you can reconnect with old friends, make new ones, and exchange new ideas with colleagues in the pleasant setting of Hradčany in Prague. We appreciate your kind participation and look forward to well-prepared contributions, which will help to further strengthen the long tradition of ICOMAT conferences.

We wish you all a pleasant stay at the 17th ICOMAT conference in Prague.

Oleg Heczko, Hanuš Seiner and Petr Šittner

Organised by:

FZU Institute of Physics of the Czech Academy of Sciences

INSTITUTE OF THERMOMECHANICS Czech Academy of Sciences

General information ICOMAT 2025

Conference venue: OREA Hotel Pyramida, Bělohorská 24, 169 01 Praha 6
https://www.orea.cz/en/hotel-pyramida

Conference date: September 7 - 12, 2025

Conference website: https://www.icomat2025.org/

Registration Desk: Located in the ground floor, close to the main entrance of the OREA Hotel Pyramida

Sunday (September 7)	16:00 - 20:00
Monday – Thursday (September 8-11)	08:30 - 17:00
Friday (September 12)	08:30 - 12:00

Welcome party: Sunday, September 7, 18:00 – 20:00, Conference venue

Internet: SSID: „Pyramida“ without password

Conference Dinner: Wednesday, September 10, 19:00 – 22:00, Martinický palác
https://www.martinickypalac.cz/en/

Walking tour: Tuesday, September 9, 9:00 – 13:00, start at Conference venue **(for registered accompanying persons)**

How to get to conference venue:

You can scan qr code to map and select your travel to hotel:

From Vaclav Havel Airport:

- Bus 59 → „Nádraží Veleslavín“ → Metro A to „Hradčanská“ → Tram 25 or 8 to „Malovanka“ → 3-min walk to Orea Hotel Pyramida.
- Bus 191 → „Vypich“ → Tram 22 or 25 to „Malovanka“ → 3-min walk to Orea Hotel Pyramida.
  Bus stops are right outside the Terminal 1 or Terminal 2 https://www.dpp.cz/en/travelling/transport-to-airport
- Time of travel: approx. 35-40 minutes.
  Ticket: one 90-minute ticket (40 CZK) is valid for the whole journey. Ticket must be validated when boarding the firts bus.
  Public transport tickets can be purchased at counters/stands in Arrivals Halls of Terminals 1 & 2 (from 7:00 am to 9:00 pm) or at self-service vending machines placed directly at bus stops (cash required).

From Prague Main Railway Station (Praha Hlavní nádraží):

- Tram 15 → „Malostranská“ → Tram 22 to „Malovanka“ → 3-min walk to Orea Hotel Pyramida.
- Tram 9 → „Národní třída“ → Tram 22 to „Malovanka“ → 3-min walk to Orea Hotel Pyramida.
- Time of travel: approx. 23-27 minutes.
  Ticket: one 30-minute ticket (30 CZK) is valid for the whole journey. Ticket must be validated when boarding the first tram. Public transport tickets can be purchased in the hall of the Main Railway Station at self-serving vending machines placed near the entrance to the metro.

By own car:

- GPS position data : 50,085750 14,380292
- https://www.orea.cz/en/hotel-pyramida/contacts

By taxi:

- We recommend you NOT catch taxi at the street. Always order your taxi in advance by phone or internet order – only time-proven taxi companies can guarantee fair price and are usually at your service anywhere in Prague in about 10-15 minutes.
- Recommended English speaking taxi services:
  http://www.aaataxi.cz/en/
  http://www.modryandel.cz/en
  http://taxi14007.cz/en/

How to get to conference dinner venue – Martinický palác:

- Address: Hradčanské náměstí 67/8, Praha 1
- No transfer provided.
- ***There will be organized guided walk from the conference venue to Martinický palác at 18:45.***
- Individual transport by public transportation:
  Tram 22 to „Brusnice“ → 6-min walk to Martinický palác.
  Time of travel: approx. 17 minutes.
  Ticket: one 30-minute ticket (30 CZK) is valid for the whole journey. Ticket must be validated when boarding the first tram.

Public Transportation:

- The most recent information on Prague's transportation system can be found on the official website: www.dpp.cz

Important numbers:

- 112 - general emergency number (Emergency telephone numbers can be dialled from mobile telephones and phone boxes free of charge)
- +420 734 204 334 - Conference secretariat: Mrs. Anděla Barotová

Currency:

- The official currency of the Czech Republic is the Czech Crown (CZK = Kč)
- The majority of hotels, shops, restaurants and other establishments' accept a credit card. Money can be withdrawn from Automatic Teller machines ATM´s or banks, which can be found in various locations around the city.

Copyright:

ICOMAT2025 - PROGRAM

Sunday-September 7

16:00-20:00		**Registration**	
18:00-20:00		**Welcome Party**	

Monday-September 8

			room: SUN I+II	
9:00			Opening Ceremony	
9:40	**P1**	**001_404**	**Towards Autonomous Discovery and Development of Alloys and their Manufacturing**	**Aaron Stebner (GATECH, US)**
10:20	**P2**	**002_402**	**What distinguishes and resembles bainite and martensite?.**	**Francisca Caballero (CENIM-CSIC, ES)**
11:00			***Coffee***	
			room: SUN II	Chair: Mohammad Elahinia
11:30	*Additive manufacturing*	**003_203**	**Voxel-Level Design of Functionally Graded NiTi and NiTiHf Shape Memory Alloys via Laser Powder Bed Fusion for Multi-Stage Actuation**	**Ibrahim Karaman (TAMU, US)**
12:00		004_201	Effect of Powder Characteristics on the Printability of NiTi Alloys in Laser Powder Bed Fusion	Kadri C. Atli (TAMU, US)
12:20		005_205	Additive Manufacturing of SMA Ni-Ti using Sinter-Based Methods	Eilon Faran (Technion, Haifa, IL)
12:40		006_299	Laser powder bed fusion vs. single track laser remelting of α'' Ti-Nb	Matthias Bönisch (KU Leuven, BE)
			room: SUN I	Chair: Robert Chulist
11:30	*Fundamental characterization*	**007_267**	Crystallographic analysis of stress-induced martensite in β titanium alloy by combined in-situ measurements	**Masaki Tahara (TITECH, JP)**
12:00		008_349	A Synchrotron Diffraction Study of the Total Stress Approach to Martensitic Transformations in Metastable β-Ti alloys	Nicole Church (Cambridge Uni, UK)
12:20		009_350	The formation, evolution and deformation of stress induced martensite in Ti-Nb based alloys	Nick Jones (Cambridge Uni, UK)
12:40		010_232	Mechanism of Hysteresis Widening in NiTi-Nb: Beyond the β-Nb Phase	Oliver Reed (Cambridge Uni, UK)
			room: JUPITER	Chair: Franziska Scheibel
11:30	*Elastocaloric and multicaloric*	**011_249**	**Flexocaloric effect in shape-memory alloys**	**Antoni Planes (FMC, UB, ES)**
12:00		012_283	Elastocaloric effect of NiTi alloy under multiaxial stress states	Andrej Žerovnik (Uni Ljubljana, SI)
12:20		013_285	Analysis of the elastocaloric effect in CuAlNi shape memory alloys through nano-compression experiments	Jose F. Gómez-Cortés (UPV/EHU, ES)
12:40		014_194	Elastocaloric investigation of NiTi 3D lattice structures fabricated via laser powder bed fusion under coupled mechanical deformation	Emanuele Bestetti (CNR-ICMATE, IT)
13:00			***Lunch***	
			room: SUN II	Chair: Eilon Faran
14:00	*Additive manufacturing*	015_368	Advances in Powder Sintering-Based Binder Jet Additive Manufacturing of NiTi-Cu Shape Memory Alloys: Opportunities and Challenges	Mohammad Elahinia (Utoledo, US)
14:20		016_279	Additive Manufacturing processing of Superelastic Cu–Al–Ni Shape Memory Alloys	Pérez Cerrato (UPV/EHU, ES)
14:40		017_166	Revealing the Friction and Wear Behavior of Additively Manufactured NiTi Alloy Under Different Operating Temperature Levels	Sougata Roy (Iowa State Uni, US)
15:00		018_346	Resonant Ultrasound Spectroscopy: An efficient tool for high throughput characterization of additively manufactured biomedical Ti-Nb-Zr-O alloys	Michaela Janovská (IT, CAS, Cz)

			room: SUN I	Chair: Dominique Schryvers
14:00	*Fundamental characterization*	019_165	The Martensitic Transformation in In-Tl Alloys Revisited	Trevor Finlayson (UNIMELB, AU)
14:20		020_200	Composition dependence of the distribution and hysteresis width of Martensite phases in the Au50-xCu25+xAl25 pseudobinary system	Yuki Matsuoka (Nara WU, JP)
14:40		021_300	The change of the martensitic transformation temperature on each composition by aging treatment in Cu-Al-Mn alloys	Kotaro Tomioka (TUS, JP)
15:00		022_352	Isothermal behavior of reverse ε → γ martensitic transformation in Fe-Mn-Si functional alloys with shape memory effect	Boris Kustov (UIB, ES)
15:20		023_358	Shear and shuffle-based mechanisms in modulated NiMnGa alloys	Robert Chulist (AGH/Krakow, PL)
			room: JUPITER	Chair: Antoni Planes
14:00	*Elastocaloric and multicaloric*	024_193	NiMnGa-based multicaloric alloys: functional thermo-mechanical investigation under magnetic field	Elena Villa (CNR ICMATE, IT)
14:20		025_230	Specific heat and entropy change during martensitic transformation in Ni50Mn50-xTix alloys	Tomoya Miyakawa (Tohoku Uni., JP)
14:40		026_234	Exploration of CuZnAl for elasto-caloric applications	Oneil Goisot (INP Grenoble, FR)
15:00		027_219	Development of elastocaloric device	Jaka Tusek (Uni Ljubljana, SI)
15:20		028_363	New generation of Shape Memory Alloys (SMAs) for elastocaloric solid-state heat pumps	Jan Pilch (Exergyn Ltd., IR/CZ)
15:40			***Coffee***	
			room: SUN II	Chair: Ibrahim Karaman
16:20	*Additive manufacturing*	**029_364**	**Additive Manufacturing Meets Multicalorics: Microstructure Design of Heusler Alloys for Multi-Stimuli Cycling**	**Franziska Scheibel (TU Darmstadt, DE)**
16:50		030_378	Additive manufacturing of metamagnetic shape memory alloys: heat exchangers for magnetic refrigeration	Daniel Salazar (BCMat, ES)
17:10		031_160	Mechanical properties of heterogeneous-structured 18Ni300 maraging steel manufactured by directed energy deposition	Jung Gi Kim (Gyeongsang NU, KR)
17:30		032_164	Superelastic Ti-Nb-Sn porous alloys prepared by material extrusion additive manufacturing	Tae-hyun Nam (Gyeongsang NU, KR)
			room: SUN I	Chair: Tomonari Inamura
16:20	*Fundamental characterization*	**033_161**	**The weak twins in martensite**	**Cyril Cayron (EPFL, CH)**
16:50		034_162	Beyond Martensitic Transformations: Intrinsic Orientation Relationships via Generalized Lattice Correspondences	Wenzheng Zhang (Tsinghua Uni, CN)
17:10		035_206	Disclination-mediated twin-twin reactions in martensitic transformation of titanium	Yipeng Gao (Jilin Uni, CN)
17:30		036_301	Texture Evolution in Transforming and Twinning Materials: A Comparison of Neutron Diffraction and MTEX-Based Simulations	Jan Čapek (CUNI, CZ)
			room: JUPITER	Chair: Elena Villa
16:20	*Elastocaloric and multicaloric*	**037_217**	**Latent thermal energy storage driven by martensitic transformation in shape memory materials**	**Žiga Ahčin (Uni Ljubljana, SI)**
16:50		038_235	Development of Film-Based Elastocaloric Cooling Using Shape Memory Alloy Actuators	Yi-Ting Hsiau (KIT, Karlsruhe, DE)
17:10		039_244	Elastocaloric effect covering wide temperature range in a Ti-Al-Cr shape memory alloy	Yuxin Song (Tohoku Uni., JP)

Tuesday-September 9

			room: SUN I+II	
9:00	**P3**	**040_297**	**Development and challenges of Ni-free Ti-based biomedical superelastic alloys**	**Hideki Hosoda (TITECH, JP)**
9:40	**P4**	**041_407**	**A Multiscale Approach to the Structure and Migration of α/β Interfaces and Screw Dislocations in Titanium**	**David Srolovitz (HK Uni, HK)**
10:20			***Coffee***	
			room: SUN II	Chair: Francisca Caballero
11:00	*Steels-part I*	**042_179**	**Strain accommodation in microstructure development of lath-shaped martensite and bainite**	**Tadashi Furuhara (Tohoku Uni., JP)**
11:30		043_157	The Role of Plastic Deformation in Martensitic Transformation of Low Carbon Steel	Hesham Salama (Ruhr Uni. Bochum, DE)
11:50		044_275	In situ neutron diffraction study on the development of martensitic transformation in hydrogen-charged Type 316L steel at low temperature	Tatsuya Ito (JAEA, JP)
12:10		045_247	Sustaining the TRIP Effect in High-Strength Steels for Enhanced Mechanical Performance	Xuejun Jin (SJTU, CN)
12:30		046_274	Improving the ductility of ultrahigh-strength high-carbon martensite by prior bainitic transformation	Sien Liu (U-Tokyo, JP)
			room: SUN I	Chair: Sebastian Fähler
11:00	*NiTi-part I*	**047_171**	**Detwinning Elasticity of NiTi**	**Yinong Liu (UWA, AU)**
11:30		048_370	Elastic instabilities in NiTi shape memory alloy	Petr Sedlák (IT, CAS, CZ)
11:50		049_373	Martensite Textures and Recoverable Strain Limits of NiTi: Taylor Model vs. Experiment	Luděk Heller (FZU-IoP, CAS, CZ)
12:10		050_192	Energies of type II twin boundaries and martensite plates in NiTi	Meron Doar (Technion, Haifa, IL)
12:30		051_367	A numerical tool to predict the dynamical behavior and the damping effect of Shape Memory Alloys: Application for design of NiTi based passive dampers.	Frédéric Thiebaud (Uni. Lorraine, FR)
12:50			***Lunch***	
			room: SUN II	Chair: Yuri Shinohara
14:00	*Steels-part I*	**052_238**	**Substructures and crystallographic features of as-quenched lath martensite in medium-carbon steel**	**Akinobu Shibata (NIMS, JP)**
14:30		053_211	Phase-field simulation of internal stress distribution during martensitic transformation in low-carbon steel	Yuhki Tsukada (Nagoya Uni, JP)
14:50		054_175	A novel observation of hcp martensite layer formed at bcc martensite lath boundaries in medium-Mn steel during quenching	Haiwen Luo (USTB, CN)
15:10		055_189	Deformation microstructure developed via anisotropic slip behaviour in lath martensite blocks of ultra-low carbon steel	Shohei Ueki (Kyushu Uni, JP)
			room: SUN I	Chair: Yinong Liu
14:00	*NiTi-part I*	**056_215**	**High-Rate Actuation of Shape Memory Alloys**	**Doron Shilo (Technion, Haifa, IL)**
14:30		057_343	How to transform martensite in NiTi within picoseconds	Klara Lünser (Uni-DuE, DE)
14:50		058_395	Elastic and Thermal Properties of NiTi investigated by Transient Grating Spectroscopy	Jakub Kušnír (IT, CAS, CZ)
15:10		059_289	Dynamic characterisation of NiTi during martensite–austenite transformation	Carolina Guerra (Nottingham Uni, UK)
			room: JUPITER	Chair: Toshihiro Omori
14:00	*Novel characterization and processing*	**060_305**	**Variant Selection in Polycrystalline CuAlNi and NiTi Shape Memory Alloys Investigated with In-Situ X-ray Topotomography**	**Janice Moya (UMICH, US)**
14:30		061_386	3D Characterization of Austenite-Martensite Microstructures During Mechanical Loading Using In Situ Dark-Field X-Ray Microscopy and X-Ray Topotomography	Celeste Perez (UMICH, US)
14:50		062_260	Application of full-field measurement techniques for the thermomechanical analysis of Ti-26Nb, Ti-25Nb-0.3O and Ti-25Nb-0.3N shape memory alloys under ten-	Karol Marek Golasiński (UKSW, PL)
15:10		063_281	Mechanical splicing of superelastic Cu-Al-Mn alloy bars with rolled threads	Sumio Kise (Furukawa Techno Material Co, JP)

15:30			**Coffee + Posters**	
			room: SUN II	Chair: Andersan S. Paula
16:20	*Steels-part I*	064_195	Enhancement of Shear-Band Formation During Bending through Tempering and Its Influence on Crack Suppression in Low-Carbon Martensitic Steel	Naoki Maruyama (Osaka Uni, JP)
16:40		065_381	Competing effects of grain refinement and Cr23C6 carbide precipitation on martensitic transformation behavior in low-Ni austenitic stainless steel	Yeonggeun Cho (POSTECH, KR)
17:00		066_256	Plastic Deformation Mechanism of Low-Carbon Steel Lath Martensite by Multi-scale Deformation Analysis	Shuang Gong (U-Tokyo, JP)
17:20		067_268	Variant selection in deformation-induced martensitic transformation during tensile deformation of ultrafine grained metastable austenitic steel	Yuanhong Liu (Kyoto Uni, JP)
17:40		068_263	Fatigue crack growth in metastable austenitic stainless steels related to martensitic transformation-induced hydrogen embrittlement	Yuhei Ogawa (NIMS, JP)
			room: SUN I	Chair: Nick Jones
16:20	*High-temperature*	069_317	Complex Thermomechanical Loading Paths for High Temperature Shape Memory Alloys	Dimitris C. Lagoudas (TAMU, US)
16:40		070_323	Shape memory behavior of additively manufactured Ti-Ta high-temperature shape memory alloy lattice structures	Christian Lauhoff (Uni Kassel, DE)
17:00		071_357	Effects of Chemistry and Annealing Treatments on HTSMA Ni-Ti-Hf-Nb Alloys	Alberto Coda (CNR-ICMATE, IT)
17:20		072_212	On designing Aging of Stress-Induced Martensite in Order to Produce High Temperature Shape Memory Alloys	Asmaa Hassan (Uni Debrecen, HU)
17:40		073_369	Effect of Fast Laser Shape Setting on Functional Performances of Thin NiTiHf based Shape Memory Alloy for High Temperature Applications	Carlo Alberto Biffi (CNR, Lecco, IT)
			room: JUPITER	Chair: Klara Lünser
16:20	*Novel characterization and processing*	074_314	Acoustic emission-a promising tool to study the functional stability of superelasticity of shape memory alloys	Anja Weidner (TU Freiberg, DE)
16:40		075_158	Investigation of TiNi Shape Memory Alloy, Polymer and TiNb Ni -free High Elastic Alloys by using Digital Image Correlation, Infrared and Acoustic Emission Tech-	Elżbieta Pieczyska (IPPT PAS, PL)
17:00		076_408	Acoustic Emission Characteristics of Martensitic Transformation in Superelastic NiTinol	Lukáš Kadeřávek (FZU-IoP, CAS, CZ)
17:20		077_330	Growth kinetics and property tuning in magnetic shape memory alloys prepared by optical floating zone growth	Denys Musiienko (FZU-IoP, CAS, CZ)
17:40		078_398	Microstructural features of NiMnGa polycrystalline alloys manufactured by rapid solidification methods	Anna Wojcik (AGH/Krakow, PL)
19:00-21:00			**International Advisory Committee Meeting**	

Wednesday-September 10

			room: SUN II	Chair: Cyril Cayron
9:00	*Microstructures in shape memory alloys & ceramics*	**079_204**	**Suppression of transformation-induced dislocations in supercompatible martensite microstructure satisfying the triplet condition in Ti-Ni based all-**	**Tomonari Inamura (TITECH, JP)**
9:30		080_307	Analysis of complex microstructures in Ti76Nb22Al2	John M. Ball (Heriot-Watt Uni, UK)
9:50		081_169	Crystallographic and morphological changes during successive stress-induced martensitic transformations in single crystal Cu-Al-Mn shape memory alloys	Hiroshi Akamine (Kyushu Uni, JP)
10:10		082_173	Reorientation Behavior of Martensitic Variants and Mechanical Response in Aged Ti–Mo–Al Shape Memory Alloys	Naoki Nohira (TITECH, JP)
10:30		083_366	Supercompatibility and nucleation in martensite	Mohd Tahseen (IISC, IN)
			room: SUN I	Chair: Masaki Tahara
9:00	*High-temperature*	**084_371**	**NiTi-Hf Shape Memory Alloys via Binder Jet Printing: Materials Insights and Process Strategies**	**Mohammad Elahinia (Utoledo, US)**
9:30		085_329	Microstructure Evolution of Ni-Ti-Hf Shape Memory Alloys Manufactured via Additive Manufacturing Processes	Philipp Krooß (Uni Kassel, DE)
9:50		086_181	Effect of Hf on the martensitic transformation behavior and self-accommodation in Ti-Ni-Hf and Ti-Pd-Hf alloys	Mitsuhiro Matsuda (Kumamoto Uni, JP)
10:10		087_391	Exploring Crack Dynamics and Actuation Fatigue in NiTiHf High-Temperature Shape Memory Alloys with High Hf Content	Benat Kockar (Hacettepe Uni, TR)
10:30		088_412	Tensile actuation using NiTiHf HTSMA fabricated via LPBF additive manufacturing	Petr Šittner (FZU-IoP, CAS, CZ)
			room: JUPITER	Chair: Oleg Heczko
9:00	*Modelling*	**089_354**	**Nanotwinning and magnetoelastic coupling in Ni-Mn-based Heusler compounds from first principles**	**Markus Gruner (Uni-DuE, DE)**
9:30		090_190	Investigation on the electronic structure of modulated martensite phase of magnetic shape memory alloy Ni2MnGa via quasi-particle self-consistent GW approach	Masao Obata (Kanazawa Uni., JP)
9:50		091_345	Predictions of modulation and structural stability of Ni-Mn-X (X = Al, Ga, In) from first-principles	Jakub Luštinec (FZU-IoP, CAS, CZ)
10:10		092_227	Ab initio study of long-period commensurate structures of Ni2MnGa modulated martensite	Martin Zelený (FME, TU Brno, CZ)
10:30		093_397	Antiphase boundaries in Ni2MnGa: an atomistic perspective	Jan Zemen (FZU-IoP, CAS, CZ)
10:50			***Coffee***	
			room: SUN II	Chair: Avadh Saxena
11:30	*Microstructures in shape memory alloys & ceram.*	**094_380**	**Crystallographically compatible ceramic shape memory materials**	**Eckhard Quandt (Uni Kiel, DE)**
12:00		095_262	An EBSD Study of Crystallographic Correspondences and Variant Selection in Zirconia-Based Shape Memory Ceramics	Alejandra Slagter (Northwestern Uni, US)
12:20		096_372	Martensitic phase transformations in a compositionally graded thin film	Ole Martin Løvvik (SINTEF, NO)
12:40		097_401	Supercritical martensitic phase transformations in NiFeGaCo ferromagnetic shape memory alloys	Timothy Thompson (UMICH, US)
			room: SUN I	Chair: Denys Musiienko
11:30	*Small scales in SMAs*		**Functional behaviour of shape memory alloys at the nanoscale: An overview.**	**Jose M. San Juan (UPV/EHU, ES)**
12:00		099_322	Magnetic Manipulation of Spatially Confined Multiferroic Heuslers by Martensitic Microstructure Engineering	Milad Takhsha (IMEM-CNR, IT)
12:20		100_242	Martensitic transformation in Ni2FeGa Glass-Coated Microwires	Ondrej Milkovič (Rvmagnetics, SK)
12:40		101_411	Coherent electron imaging of magnetic nanoparticles	Marco Beleggia (UNIMORE, IT)

			room: JUPITER	Chair: Martin Zelený
11:30	*Modelling*	**102_375**	**Simulating the early stages of martensite band formation in pseudoelastic wires**	**Maximilian Hinze (TU Chemnitz, DE)**
12:00		103_396	Constitutive modeling of martensite plasticity and TRIP in polycrystalline shape memory alloys	Miroslav Frost (IT, CAS, CZ)
12:20		104_389	High-resolution strain-field mapping during nucleation and propagation of martensite bands in pseudoelastic NiTi	Martin Wagner (TU Chemnitz, DE)
12:40		105_298	Shell-based finite element modelling for predicting buckling stability of superelastic SMA tubes	Adam Plantarič (Uni Ljubljana, SI)
13:00			***Lunch***	
			room: SUN I+II	
14:00			**Memorial Session** (chaired by Petr Šittner)	
14:40	**P5**	**106_224**	**Probing theory of martensite by epitaxial films**	**Sebastian Fähler (HZDR, DE)**
			Coffee	
15:50	**P6**	**107_406**	**Development of high-performance shape memory alloys for elastocaloric refrigeration technology**	**Qingpin Sun (UST HK, HK)**
16:30-17:20			**Popularization & Outreach Roundtable** (Julie Nováková, Hanuš Seiner, Dominique Schryvers, Aaron Stebner, Yinong Liu)	
19:00-22:00			**Conference Dinner**	

Thursday-September 11

			room: SUN II	Chair: Manabu Takahashi
9:00	*Steels-part II*	108_187	Microstructure refinement of 0.1C-4Mn martensitic steel utilizing heterogeneous Mn distribution	Ji Hoon Kim (Pusan NU, KR)
9:20		109_177	Effect of microstructure on hole expansion ratio of advanced high strength steel	Jin Sung Hong (Hyundai Steel R&D Center, KR)
9:40		110_248	Effect of microstructure on mechanical properties of 1.0G TRIP steels produced by quenching and partitioning process	Wontae Cho (POSCO, Kwang., KR)
10:00		111_311	Effect of the manufacturing method and heat treatment on martensite formation in maraging 250 steel	Andersan dos Santos Paula (IME-EB, BR)
			room: SUN I	Chair: Qingping Sun
9:00	*NiTi-part II*	112_258	Fatigue performance of low-temperature aged NiTi filaments	Ondřej Tyc (FZU-IoP, CAS, CZ)
9:20		113_252	Third element diffusion induced amorphization of NiTi	Hong Yang (UWA, AU)
9:40		114_400	Aging effect on orientation dependent superelastic behavior of NiTi Shape Memory Alloy by multicycle nanoindentation	Akhil Bhardwaj (FZU-IoP, CAS, CZ)
10:00		115_213	Standard and repetitive load-unload nanoindentation studies on superelastic and shape memory NiTi	Sneha Samal (FZU-IoP, CAS, CZ)
			room: JUPITER	Chair: Markus Gruner
9:00	*Modelling*	116_319	Hydrogen Outgassing from FCC Metal Surfaces under Thermal Treatment	Avadh Saxena (LANL, US)
9:20		117_347	Development of neural network interatomic potentials for molecular dynamics: Application for martensitic nickel titanium	Petr Jaroš (IT, CAS, CZ)
9:40		118_270	Reversible domain switching induced by gradient precipitation with high dissipative superelasticity at low temperature	Dong Wang (XJTU, CN)
10:00		119_231	Grain boundary network-induced martensitic transformations in polycrystals at finite strains: Multiphase-field approach and scale-effect	Newton (IITTP, IN)
10:20			***Coffee***	
			room: SUN II	Chair: Tadashi Furuhara
11:00	*Steels-part II*	**120_312**	**Analysis of Variant Pair Formation on Σ3 Boundaries in Lenticular Martensite Microstructures**	**Yuri Shinohara (UEC, JP)**
11:30		**121_198**	**Martensitic Transformation-Dominated Lüders Deformation in Ultrafine-Grained 304 Steel at 77K**	**Stefanus Harjo (JAEA, JP)**
12:00		122_324	Revisiting γ-ε martensitic transformation: sluggish plate growth and significant TRIP effect.	Kaneaki Tsuzaki (Kyushu Uni, JP)
12:20		123_333	Effects of Cryogenic Rolling and Metallographic Preparation on Martensitic Transformation and Residual Stress in 304L TRIP Steel	Andersan dos Santos Paula (IME-EB, BR)
12:40		124_280	Cyclic Transformation Strengthening in Fine-Grained Fe-24Ni-0.3C Metastable Austenitic Steel Studied by In-Situ Synchrotron XRD	Mayu Dono (Kyoto Uni, JP)
			room: SUN I	Chair: Rubén Santamarta
11:00	*New alloys*	**125_293**	**Prospects and challenges in Fe-based shape memory alloys**	**Thomas Niendorf (Uni Kassel, DE)**
11:30		**126_228**	**Crystal structure and superelasticity in novel Fe-Mn-Al-Si alloy**	**Toshihiro Omori (Tohoku Uni., JP)**
12:00		127_254	Ordering and Martensitic Transformation in Fe-Mn-Al-Ga Alloys	Ji Xia (Tohoku Uni., JP)
12:20		128_315	In situ studies on the functional stability of a polycrystalline highly textured Fe-Ni-Co-Al-Ti-B shape memory alloy using synchrotron X-ray diffraction and acoustic emission measurements	Anja Weidner (TU Freiberg, DE)
12:40		129_272	Change in Reverse Transformation Start Temperatures of Fe-33%Ni and Fe-28%Ni-20%Co Alloys by Shot-Peening	Hisashi Sato (NITECH, JP)

			room: JUPITER	Chair: Doron Shilo
11:00	*Magnetic shape memory*	**130_342**	**Bridging Fundamental Crystallography and Magnetic Shape Memory: Minor Diffraction Features Reveal Anharmonic Incommensurate Modulation in Ni-Mn-Ga Single Crystals**	**Petr Veřtát (FZU-IoP, CAS, CZ)**
11:30		**131_382**	**Modulated structures & Elasticity: On the road towards understanding the supermobility in Ni-Mn-Ga**	**Tomáš Grabec (IT, CAS, CZ)**
12:00		132_339	Long-period Commensurate States in Ni-Mn-Ga Modulated Martensite	Ladislav Straka (FZU-IoP, CAS, CZ)
12:20		133_310	Temperature and stress induced structural transformations in Ni50Mn27Ga22Fe1 alloy	Mariia Vinogradova (LUT Uni., FI)
12:40		134_207	Austenite-Martensite interface propagation in Ni-Mn-Ga single crystal	Xingke Gao (Uni. Paris-Saclay, FR)
13:00			***Lunch***	
			room: SUN II	Chair: Akinobu Shibata
14:00	*Steels-part II*	**135_176**	**Variant selection in deformation-induced martensite transformation**	**Manabu Takahashi (Kyushu Uni, JP)**
14:30		136_210	Microstructure and bending fatigue behavior of martensite steel with 0.4%C subjected to different heat treatments	Jiaqiang Dang (U-Tokyo, JP)
14:50		137_208	In-situ 3D characterization of deformation-induced martensitic transformation in metastable austenitic alloy by synchrotron X-ray micro-and nano-tomography	Tatsuya Iwano (Kyushu Uni, JP)
15:10		138_174	Hydrogen Cation-Induced Martensitic Transformation During Electrochemical Hydrogen Charging in Metastable Austenitic Stainless Steel	Heung Nam Han (Seoul NU, KR)
			room: SUN I	Chair: Hiroshi Akamine
14:00	*New alloys*	**139_296**	**Enhanced Mechanical Properties by FCC-HCP Martensitic Transformation in Co-Cr-Mo-Ni Medium Entropy Alloys**	**Koichi Tsuchiya (NIMS, JP)**
14:30		140_257	Structure formation in high entropy shape memory alloys	Georgiy Firstov (IMP Kyev, NASU, UA)
14:50		141_291	Fe-based near HEA with shape memory effect: microstructure and quantitative characterization of the martensitic transformation	Lucia del Río (UPV/EHU, ES)
15:10		142_184	A polymer-like ultrahigh-strength metal alloy	Yuanchao Ji (XJTU, CN)
			room: JUPITER	Chair: Anja Weidner
14:00	*Magnetic shape memory*	**143_229**	**Sharp Atomic Structure of Highly Mobile Type I and Type II Twin Boundaries in Ni-Mn-Ga Magnetic Shape Memory Single Crystal**	**Marek Vronka (FZU-IoP, CAS, CZ)**
14:30		144_374	Demagnetization tensor for a parallelepiped with a mirror symmetry in the xy plane and its use for magnetically induced reorientation in Ni-Mn-Ga crystal	David Vokoun (FZU-IoP, CAS, CZ)
14:50		145_390	Elastic moduli measurements in 10M martensite of Ni-Mn-Ga-based alloys with commensurate and incommensurate lattice modulation	Andrey Saren (LUT Uni., FI)
15:10		146_348	Magnetic anomalies in Ni-Mn-Ga-x austenite and premartensite	Alexej Perevertov (FZU-IoP, CAS, CZ)
15:30			**Coffee + Posters**	
			room: SUN II	Chair: Luděk Heller
16:20	*NiTi-part III*	147_196	Transformation behaviors and microstructur aspects in hydrogen-charged Ti-Ni alloys	Minoru Nishida (Kyushu Uni, JP)
16:40		148_159	EBSD and TKD Study of Microstructure Evolution in NiTi Alloys	Junfeng Xiao (EPFL, CH)
17:00		149_359	In-situ DMA studies during thermomechanical loading of NiTi wires	Elizaveta Iaparova (FZU-IoP, CAS, CZ)
17:20		150_331	Unraveling the precipitation-controlled martensite self-accommodation and shape memory effect in NiTi alloy across atomic scale and microscale	Shanshan Cao (SCUT, CN)

			room: SUN I	Chair: Dimitris C. Lagoudas
16:20	*New alloys*	151_222	In situ neutron diffraction examination of anomalous hysteresis behavior in Co-Cr-Al-Si superelastic alloys	Xiao Xu (Tohoku Uni., JP)
16:40		152_379	Elastic behavior of Co-Cr-Ga-Si: Resonant ultrasound spectroscopy at Weyl's asymptote and giant negative magnetoelastic coupling	Hanuš Seiner (IT, CAS, CZ)
17:00		153_220	Realization of tensile plasticity and shape memory effect in NiMnGa shape memory alloys by constructing a unique dual-phase configuration	Jiaxi Meng (Beihang Uni, CN)
17:20		154_214	The origin of the β-relaxation phenomenon in strain glass: a phase field modeling	Chuanxin Liang (XJTU, CN)
			room: JUPITER	Chair: Jan Frenzel
16:20	*Magnetic shape memory*	155_328	Effect of solidification rate on martensitic transformation behavior of Cu-doped Ni-Mn-Ga metamagnetic shape memory ribbons	Natalia A. Río-López (UPV/EHU, ES)
16:40		156_250	Magnetic-field-induced martensitic transformation with small hysteresis in Mn3Ga alloys	Daisuke Imatomi (Tohoku Uni., JP)
17:00		157_265	Correlation of Crystallographic and Magnetic Domain Structures in Fe-61.8at%Pd Alloy	Yuto Tomita (Kyushu Uni, JP)
17:20		158_303	Magnetostructural behaviour of Ni35Co13Mn35-xFexTi17 melt spun-ribbons	Mariana Ríos Naranjo (BCMat, ES)

Friday-September 12

			room: SUN II	Chair: Minoru Nishida
9:00	*Fatigue & fracture*	**159_393**	**Influence of Ni-content and Precipitates on the Mechanical and Actuation Fatigue Crack Growth of NiTiHf High-Temperature Shape Memory Alloys**	**Dimitris C. Lagoudas (TAMU, US)**
9:30		160_362	Micro crack growth in NiTi based shape memory alloys	Jan Frenzel (Ruhr Uni. Bochum, DE)
9:50		161_182	On the origin of functional fatigue of nanocrystalline NiTi wires	Petr Šittner (FZU-IoP, CAS, CZ)
			room: SUN I	Chair: Georgiy Firstov
9:00	*New alloys*	**162_325**	**Characterization and influence of Ni3Ti precipitates on functional properties of All-d-Metal Ni-Mn-Ti Magnetic Shape Memory Alloys**	**Rubén Santamarta (UIB, ES)**
9:30		163_277	Observation of strain-spin dual-glass state in all-d-metal Heusler alloy Ni2MnTi	Qiusa Ren (IoP CAS, CN)
9:50		164_341	Development of Cu-doped Ni-Mn-Ga metamagnetic shape memory alloy powders	Daniel Salas (UIB, ES)
			room: JUPITER	Chair: Ladislav Straka
9:00	*Smart applications and processing*	**165_304**	**Origami-Inspired Reprogrammable Shape Memory Alloy Microactuator System**	**Vincent Gottwald (KIT, Karlsruhe, DE)**
9:30		166_202	Interlocking Metasurfaces: A New Paradigm for Adaptive and Reconfigurable Joining	Abdelrahman Elsayed (TAMU, US)
9:50		167_226	Proof-of-concept of superelastic active mechanical metamaterials using Cu-Al-Ni shape memory alloys.	Ander Abadín (UPV/EHU, ES)
10:10			***Coffee***	
			room: SUN II	Chair: Kaneaki Tsuzaki
11:50	*Steels-part III*	**168_241**	**Introduction to 3D in-situ characterization technique for deformation-induced martensitic transformation using synchrotron X-ray**	**Osamu Takakuwa (Kyushu Uni, JP)**
11:20		169_261	A novel quench cracking characterisation method for induction-hardened steels with different thermal histories	Aysu Catal Isık (UCL, London, UK)
11:40		170_170	Anisotropic cleavage fracture caused by transformation-induced internalstress in an as-quenched martensite	Nobuo Nakada (TITECH, JP)
12:00		171_178	Development of Cold-rolled Martensitic Steels with excellent flatness and resistance to hydrogen delayed fracture	Min-Ho Jang (Hyundai Steel R&D Center, KR)
			room: SUN I	Chair: Petr Sedlák
11:50	*New alloys*	**172_191**	**A lightweight yet strong Ti-Al-based superelastic alloy operating across a wide temperature range**	**Sheng Xu (Tohoku Uni., JP)**
11:20		173_269	Tunable High Contrast Changes in Transport Properties of Metamagnetic Phase Change Materials	Serdar Torun (TAMU, US)
11:40		174_245	Effect of Composition on the Degree of B2 Ordering in Ti-Al-Cu Shape Memory Alloys	Hirobumi Tobe (Iwate Uni, JP)
12:00		175_290	Design and characterization of a new quaternary Cu-Al-Ni-Ga shape memory alloy	Maria L. Nó (UPV/EHU, ES)
			room: JUPITER	*Chair: Petr Veřtát*
11:50	*Smart applications and processing*	**176_225**	**An Implantable Device Based on Shape Memory Alloys**	**Israel Alexandron (BGU, IL)**
11:20		177_163	Recovery stress and tensile behavior under recovery stress of cold-drawn superelastic SMA wires	Eunsoo Choi (Hongik Uni., KR)
11:40		178_318	Recycling of NiTi shape memory alloys-effects of melting methods and processing conditions	Sakia Noorzayee (Ruhr Uni. Bochum, DE)
12:20			**Short break**	
			room: SUN I	
12:30-12:50			**Closing Ceremony**	

LIST OF POSTERS

Code	Abstract title	Presenting
P01_282	Changes of martensitic transformation temperature by adding Mn into 68Cu-16Al-16Zn alloys	Ayaka Ibato
P02_266	The relationship between degree of order and martensitic transformation behavior in 68Cu–16Al–16Zn	Megumi Takayama
P03_199	In-situ crystallographic analysis of habit plane in stress-induced martensitic transformation of Ti-Ni alloy single crystals	Kosei Ono
P04_321	On interaction between deformation twins and LPSO phases in Mg alloys	Andrej Ostapovec
P05_167	Lattice Distortion - Atomic Shuffle Coupling of the R phase in NiTi	Yuxuan Chen
P06_188	R-Phase transformation in Ti-Ni-Co alloys	Jaeil Kim
P07_286	Electrical Resistivity Changes during Successive Transformations in Ti-Ni Alloy under Stress Loading	Yohei Soejima
P08_403	Effect of molten zone geometry on compositional homogeneity in NiMnGa crystals obtained by optical floating zone method	Valentina Moskvina
P09_185	Characterization of Ti50Ni50-XMoX (X=2; 6) alloy produced by high-energy ball milling	Tomasz Goryczka
P10_264	Laser focal length influence in H13 Tool Steel Deposition Through L-DED	Andersan Paula
P11_183	Influence of two-step aging treatment on precipitation behavior of as-built 18Ni-maraging steel fabricated by laser powder bed fusion	Sung Hwan Hong
P12_394	A Fast-Track Approach to Ti–20Nb–6Ta Alloy via PBF-LB for Biomedical Applications	João Felipe Queiroz Rodrigues
P13_399	Digital Image Correlation-Based Local Strain Evaluation in EBM-Additive Manufactured NiTi Part	SAVAS DILIBAL
P14_327	Microstructural Aspects Ti6Al4V Alloy Processed by LBPF Investigated by EBSD Technique	Fábio Oliveira
P15_338	Acoustic emission from displacive phase transitions: comparison of martensitic and ferroelectric model materials	Uwe Klemradt
P16_276	Characterization of permanent lattice defects and strain generated by forward or reverse martensitic transformation in NiTi wire	Orsolya Molnárová
P17_351	In-situ Measurement of Elasticity During Thermally Induced Phase Changes Using Dove Prism-Enhanced Transient Grating Spectroscopy	Pavla Stoklasová
P18_334	Actuation characteristics of spring-biased NiTi shape memory alloy wires under pulsed current stimulation	Xiao Ma
P19_313	Thermomechanical Characterization of very thin Ni50Fe27Ga23 Shape Memory Microwire	Limpat Nulandaya
P20_365	Influence of Sputtering Parameters on Functional and Mechanical Behavior of Ni-Rich NiTi Films	Andersan dos Santos Paula
P21_377	Martensitic transformation in Heusler alloy nanostructures	Michal Varga
P22_353	Angular dependence in magnetically induced reorientation	David Hruška
P23_246	Elastic properties of Ni-Mn-Ga-1%Fe 10M martensite with incommensurate lattice modulation	Alexei Sozinov
P24_410	Tuning magneto-structural transitions in Ni-Mn-Ga melt-spun ribbons through Co and Cu doping	Milena Kowalska
P25_388	Substrate-induced martensitic transformation in thin epitaxial Ni-Mn-Ga films	Matěj Makeš
P26_361	Search for criterion for martensitic transformation in ferromagnetic Heusler alloys	Michal Rameš
P27_385	Scanning twin boundary mobility in 10M martensite of Ni-Mn-Ga alloy from subatomic to macroscopic scale	Andrey Saren
P28_344	Probing martensitic transformation in Ni-Mn-Ga via high-frequency ferromagnetic resonance	Sviatoslav Vovk
P29_259	Elastocaloric effect in polycrystalline NiMnGa produced through hot-rolling powder consolidation	Francesca Villa
P30_384	Microstructure and Elastocaloric Effect of a Ti-Ni-Zr-Sn Shape Memory Alloy	Zhiyong Gao
P31_392	Modulation of NI2MnGa described by generalized susceptibility based on Wannier functions.	Dominik Váňa
P32_209	Tensile deformation of cold rolled Fe-Ni-C metastable austenitic steel investigated by in-situ synchrotron XRD	Naoki HARADA
P33_302	Mechanical Testing at Elevated and Cryogenic Temperatures with Concurrent Acoustic Emission and Electrical Resistivity Monitoring	Jan Čapek
P34_271	Surface Microstructures Formed by Shot-Peening of Fe-33mass%Ni Alloy	Marie Kondo
P35_292	Acoustic emission measurements during plastic deformation of FeMn(Cr) TWIP steel.	Lajos Daróczi
P36_186	Novel sub-grain structures in B2 of a cold-rolled TiNi shape memory alloy with unique property	Qianglong Liang
P37_218	Effect of excess Ti solutes on the martensitic transformation behavior and microstructure of Ti-rich Ti50+xNi (x = 0, 0.5, 1, 1.5, 2) shape memory alloys via rapid solidification	Nian-Hu Lu

Code	Abstract title	Presenting
P38_335	Superelasticity over a wide temperature range in a NiTiCu shape memory alloy via laser powder bed fusion	Haizhou Lu
P39_172	Antwerp outreach activity for children	Dominique Schryvers
P40_308	Strain glass boundary in TiNiCu alloys showing enhancement of superelasticity over a wide temperature range	Yang Yang
P41_309	Martensitic transformation behaviors and damping properties of Cu-Al-Fe-Co high-temperature shape memory alloys	Wei Ting Guo
P42_295	Damping characteristics of Cu-13.5Al-4Ni-xTi shape memory alloys	KAI-MIN HUANG
P43_284	Effects of Au addition on the internal friction of Cu-Al-Mn shape memory alloys	Wei-Jhen Hsu
P44_360	Influence of Particle Size and Microstructure on the First-Order Magnetostructural Phase Transition in Ni-Mn-Sn Heusler Alloy	Johannes Puy
P45_337	Low melting point composites based on metamagnetic Ni-Co-Mn-In-Cu alloy for magnetic refrigeration	Vicente Sánchez-Alarcos
P46_356	Optimizing NiTi Interatomic Potentials Through Atomic Cluster Expansion	Petr Šesták
P47_243	Phase-field study on austenite-martensite interface formation in Shape Memory Alloys	Bingqian WANG
P48_326	Automated Classification of Martensitic Microstructures in Ti6Al4V via Transfer Learning: A Metallographic and Literature-Based Approach	Edilvando Eufrazio
P49_216	Phase-field simulation of martensitic transformation during continuous cooling in polycrystalline low-carbon steel	Takumi Okamoto
P50_340	Regular Twinning in Epitaxial Rh2MnSb Thin Films	Artem Shamardin
P51_223	Effect of Carbon Content on Microstructures of Low-Carbon Lath Martensite	Shigekazu Morito
P52_180	Phase-field modeling of martensitic transformation in ferrous shape memory alloy exhibiting superelasticity	Miyu Takagi
P53_405	In-situ characterization of supercritical martensitic phase transformations in NiFeGaCo single crystals using high-energy diffraction microscopy	Timothy Thompson
P54_251	Hydrogen-Induced Modifications in Nickel-Titanium Alloys: Correlating Electronic Transport and Phase Transformations	Torben Tappe
P55_240	Microstructural Studies of Fe-Pd Martensitic Crystals using Elastic and Inelastic Neutron Scattering	Trevor Finlayson
P56_278	Analysis of Fatigue Behavior of Martensitic Steel Using Digital Holographic Microscope	Yusuke Matsui
P57_316	Hybrid Modeling Framework for Shape Memory Alloys	Dimitris C Lagoudas
P58_409	A Multiphase-Field Model for Grain Boundary-Induced Martensitic Transformations in Polycrystals at Finite Strains with Scale Dependence.	Newton .
P59_332	Structure and Microstructure-based Elastic Property study on a Co41Ni32Al27 Ferromagnetic Shape Memory Alloy Melt-spun ribbon	RAJINI KANTH BHOGOJU
P60_383	Structural-functional integrated TiBw/Ti–V–Al lightweight shape memoryalloy composites	Xianglong Meng
P61_336	High tensile stress actuation with NiTiHf high-temperature shape memory alloys additively manufactured via laser powder bed fusion	Hongwei Ma
P62_237	Phase transformation and texture evolution in a metastable medium entropy alloy	Ibrahim Ondicho
P63_253	Functional properties comparison for high entropy and conventional shape memory alloys: few application perspectives	Vira Filatova
P64_355	Microstructural aspects of bcc-hcp-fcc displacive transformations in annealed HEA melt spun ribbons	Wojciech Maziarz
P65_273	In-situ Observation of the Formation of Lath Martensite Microstructurein Fe-Ni-Cr-C Alloy	Wataru Aoki
P66_236	Tensile properties and deformation-induced martensitic transformation in Fe-Ni-C steel	Ryoya OISHI

ABSTRACTS

001_404

PLENARY: Towards Autonomous Discovery and Development of Alloys and their Manufacturing

Aaron Paul Stebner
Georgia Institute of Technology, Atlanta, Ga, USA

We have created an Artificial Intelligence Manufacturing Pilot Facility (AIMPF) that extends the concepts of “self-driving labs” and “mobile robotic scientists” to create a semi-autonomous user facility toward enabling AI to assist people with materials and manufacturing science and engineering. AIMPF provides a world-leading environment for cooperative industry-academia-government pilot trials, innovation of new technologies, and workforce training. Foundational efforts are establishing automated research and development workflows for discovering new alloys and developing their manufacturing by learning and optimizing process-structure-property relationships. This presentation will highlight recent advancements in automating research and development of shape memory alloys and steels.

002_402

PLENARY: What distinguishes and resembles bainite and martensite?

Francisca G Caballero
National Centre for Metallurgical Research (CENIM-CSIC), Avda. Gregorio del Amo 8, 28040, Madrid, Spain

Both bainite and martensite reactions involve a sudden, ordered movement of iron atoms, which is accompanied by a given crystal correspondence, and a macroscopic shape strain of the transformed structure. Carbon supersaturation and tetragonality are not exclusive of martensite. A high level of carbon supersaturation in bainitic ferrite accompanied by a change in symmetry of the unit cell from cubic to tetragonal have been observed at low transformation temperatures confirming that, as martensite, bainitic ferrite grows without diffusion of carbon. It is therefore difficult to identify the morphological differences to discriminate metastable ferritic structures. This study investigates the differences and similarities between bainitic and martensitic structures obtained by isothermal heat treatments such as austempering, quench and partitioning (Q&P), and quench and tempering (Q&T) using a variety of techniques such as X-ray diffraction, electron backscatter diffraction, scanning and transmission electron microscopy, and atom probe tomography. The results show that by varying the isothermal holding temperature, identical austenite concentration may be obtained in ferritic structures that resemble laths. Nonetheless, some diversity in hardness is noted, which is compatible with variations in the crystallographic size distribution of ferritic grains and variations in the precipitation state as shown by the structure's nanoscale analysis.

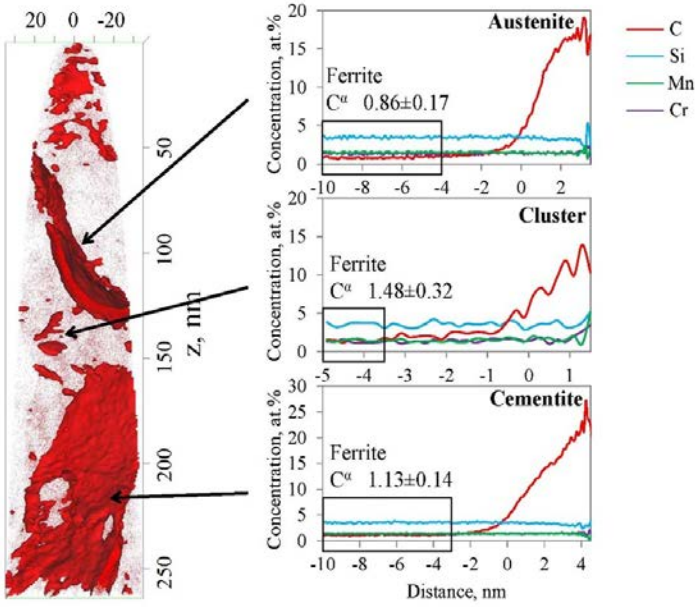

Complex Carbon Distribution in Bainitic Ferrite by Atom Probe Tomography.

003_203

Voxel-Level Design of Functionally Graded NiTi and NiTiHf Shape Memory Alloys via Laser Powder Bed Fusion for Multi-Stage Actuation

Ibrahim Karaman[1], Abdelrahman Elsayed[1], Taresh Guleria[2], Haoyi Tian[3], Bibhu P. Sahu[1], Kadri C. Atli[1], Alaa Olleak[4], Alaa Elwany[2], Raymundo Arroyave[1], Dimitris Lagoudas[3]
[1]Department of Materials Science and Engineering, Texas A&M University, College Station, TX, USA. [2]Department of Industrial and Systems Engineering, Texas A&M University, College Station, TX, USA. [3]Department of Aerospace Engineering, Texas A&M University, College Station, TX, USA. [4]Ansys Inc., Canonsburg, PA, USA

This study presents a comprehensive framework for the successful additive manufacturing of functionally graded shape memory alloys (FG-SMAs) via Laser Powder Bed Fusion (LPBF), encompassing both NiTi and high-temperature NiTiHf systems. A novel approach was implemented to achieve precise voxel-level control of local chemistry and microstructure starting from a single feedstock composition, enabling location-specific phase transformation characteristics. By systematically analyzing the relationships between volumetric energy density, Ni evaporation, and transformation temperatures, the study achieved accurate control of Ni content across different segments of the functionally graded materials (FGMs). Thermal modeling further elucidated the influence of thermal history change, due to changes in the process parameters and sample size, on Ni evaporation and oxide formation, findings that were experimentally validated by local transmission electron microscopy analyses. Wavelength dispersive spectroscopy confirmed the localized control of Ni content, while differential scanning calorimetry identified multiple transformation peaks, indicating multi-stage transformation behavior throughout the FG segments. The transformation range spanned over 150°C in the FG NiTiHf SMAs, demonstrating the capability to engineer tailored thermomechanical responses across different regions within the printed components. Simultaneously, the FG NiTi parts exhibit combined superelastic and shape memory responses under variable loading, with transformation strains up to 6% in both tension and compression. A novel thermomechanical modeling approach effectively predicted the global actuation response of the FG parts, and mechanical testing demonstrated broader transformation ranges and high strain recovery in the samples. These results highlight the potential of FG SMAs for applications requiring tailored actuation and reliable performance across varying temperature ranges, offering a viable path forward for enhancing their functionality.

004_201

Effect of Powder Characteristics on the Printability of NiTi Alloys in Laser Powder Bed Fusion

Kadri C. Atli[1], Abdelrahman Elsayed[1], Taresh Guleria[2], Alaa Elwany[2], Raymundo Arroyave[1], Ibrahim Karaman[1]
[1]Department of Materials Science and Engineering, Texas A&M University, College Station, TX, USA. [2]Department of Industrial and Systems Engineering, Texas A&M University, College Station, TX, USA

The printability of NiTi shape memory alloys (SMAs) in Laser Powder Bed Fusion (LPBF) is highly sensitive to powder characteristics, including particle size distribution (PSD), morphology, chemistry, and impurity content. This study systematically investigates six NiTi powders with varying Ni contents (50.0–51.2 at.%) and powder characteristics to understand how these factors influence melt pool behavior, defect formation, print quality, shape memory and superelastic responses during and after LPBF. Using a combination of numerical melt pool modeling and experimental single-track tests, printability maps were developed for Ni-50.1, Ni-50.8, and Ni-51.2. These maps identified optimum processing windows to print defect free parts and highlighted regions susceptible to lack of fusion, keyholing, and balling. Ni-50.1 exhibited broad optimum printable regions, while Ni-50.8 and Ni-51.2 showed smaller regions and higher defect susceptibility due to lower packing density and thermal conductivity associated with their powder characteristics.

To streamline parameter development, a universal printability map was developed by overlaying defect-free processing windows of multiple NiTi compositions, establishing optimal process parameters for any given NiTi SMA powder to fabricate defect-free parts using LPBF, independent of initial composition or powder characteristics, without extensive process parameter optimization experiments. This map successfully predicted processing parameters for Ni-50.0, Ni-50.9, and Ni-51.1, all of which achieved high-density, crack-free builds without additional single-track validation. Powder characterization revealed that optimal flowability and minimal porosity were achieved with PSDs having a D50 of 30–35 µm and a D10–D90 range of 13–20 µm. Ni-rich powders, while essential for superelastic behavior, exhibited inferior printability due to their lower thermal conductivity and higher susceptibility to processing defects. The findings offer key insights for screening and tailoring powder characteristics and process parameters, demonstrating the effectiveness and generalizability of the proposed framework, which enables reliable, high-quality fabrication of NiTi parts and accelerates the development of new printable alloy compositions in LPBF.

005_205

Additive Manufacturing of SMA Ni-Ti using Sinter-Based Methods

Alon Addess[1], Yeshurun Cohen[1], Eugen Rabkin[1], Doron Shilo[1], Eilon Faran[1], Carlo Burkhardt[2], Lucas Vogel[2], Yael Paskovitch[3], Boaz Glass[3]
[1]Technion, Haifa, Israel. [2]Pforzheim university, Pforzheim, Germany. [3]Tritone, Rosh Hayain, Israel

Additive Manufacturing (AM) of Shape Memory Alloys (SMA), and specifically Ni–Ti, is a rapidly evolving field with significant potential to applications in actuation, energy harvesting, and refrigeration. Currently, most AM processes rely on melting-based methods that locally melt the metallic feedstock of Ni-Ti. However, the repeated melting impairs the resulting microstructure, thus limiting the ability of the printed material to undergo a reversible thermo-elastic martensitic transformation. Recent advances in sinter-based AM offer new possibilities for tailoring the microstructure and properties of the printed SMA. Here, we present the first production and characterization of Ni-Ti SMA using two sinter-based AM methods: Lithography-based Metal Manufacturing (LMM) [1], and Moldjet, a novel adaptation of metal injection molding [2]. Our findings show that microstructure and properties are highly sensitive to oxide and carbide content introduced primarily during the sintering stage. Notably, Ni–Ti produced via MoldJet, which employs a metallic paste with minimal organic binder, exhibits lower carbon and oxygen contamination than other sinter-based methods. As a result, it demonstrates a superelastic response with a substantial recoverable strain of 5.6% in tension and 4.5% in compression, and irrecoverable plastic strain below 0.2%. Additionally, we propose a new approach for improving process parameters and microstructure in sinter-based AM by pretreating the metallic powder with high-energy ball milling [3]. The effects of the milling pretreatment on the printing process and the final properties of Ni-Ti are evaluated and discussed. Specifically, our results indicate that the ball milling facilitates sintering at lower temperatures, without impairing the thermo-mechanical response. This is particularly advantageous for SMA containing highly reactive elements like Ni and Ti.

[1] Cohen et al, Sinter-Based Additive Manufacturing of Ni–Ti Shape Memory Alloy, Shap. Mem. Superelasticity 9 (2023) 492–503. https://doi.org/10.1007/s40830-023-00436-y.

[2] Addess et. al, Additive Manufacturing of Ni–Ti SMA by the Sinter-Based MoldJet Method, Shap. Mem. Superelasticity 11 (2025) 89–99. https://doi.org/10.1007/s40830-025-00522-3.

[3] Mechanical ball-milling as a powder pretreatment for additive manufacturing of shape memory alloys, In preparation.

006_299

Laser powder bed fusion vs. single track laser remelting of α'' Ti-Nb

Florian Senftleben[1], Mariana Calin[1], Jürgen Eckert[2,3], Matthias Bönisch[4]
[1]IFW Dresden, Institute for Materials Chemistry, Dresden, Germany. [2]Austrian Academy of Sciences (ÖAW), Erich Schmid Institute of Materials Science, Leoben, Austria. [3]Montanuniversität Leoben, Department of Materials Science, Leoben, Austria. [4]KU Leuven, Department of Materials Engineering, Leuven, Belgium

Titanium alloyed with moderate amounts of β stabilizers (e.g. Nb, Ta) exhibits shape memory and tailorable thermal expansion, rooted on orthorhombic martensite α''. Conventional fabrication of those alloys involves classical ingot metallurgy, thermomechanical processing, and shaping by forming and subtractive methods, limiting geometric freedom and restricting application specific design. In contrast, additive manufacturing techniques like laser powder bed fusion (LPBF) combine the benefits of (near-) net-shape production of complex parts from Ti alloys with the intrinsic potential to locally tailor microstructures to the requirements dictated by the end application. In addition, due to its characteristic rapid cooling rates, LPBF favours the formation of metastable phases as-built, such as hexagonal martensite α' in β stabilizer-lean parts, and metastable β phase in β stabilizer-rich parts. LPBF may also allow controlled formation of orthorhombic martensite α''-which is an open question that needs systematic validation and exploration.

However, the limited availability and relatively high cost of commercially pre-alloyed, atomized powders is a significant challenge for the widespread production of LPBF α'' parts. Taking Ti-Nb as example, this work thus explores the fabrication of α'' Ti-Nb via LPBF from pre-alloyed Ti-29Nb powders, prepared by mechanical alloying of elemental Ti and Nb powders. The powders were characterized for homogeneity, particle size, and phase constitution, and subsequently consolidated into cuboids via LPBF. Various combinations of laser power and scan speed were tested to study their effects on as-built microstructures and porosity. To isolate the influence of the layerwise build process on the resulting phases and microstructures, experiments will be discussed, for which α'' martensitic substrates were remelted along single laser tracks. Single track remelting revealed different microstructures depending on the melt pool location, including planar growth at the roots and cellular-dendritic growth near the surface.

The results of this study suggest that proper selection of alloy content and LPBF parameters can lead to α'' martensitic Ti-Nb parts for functional 3D-printed components.
This work benefitted from financial support by KU Leuven Internal Funds (grant no. STG/23/008) and by the European Commission (grant agreement no. 264635, BioTiNet-ITN).

007_267

Crystallographic analysis of stress-induced martensite in β titanium alloy by combined in-situ measurements

Masaki Tahara, Naoki Nohira, Hideki Hosoda
Institute of Science Tokyo (Formerly: Tokyo Institute of Technology), Yokohama, Kanagawa, Japan

It is a common understanding that the crystallographic characteristics of thermally induced martensite are consistent with the phenomenological theory of martensitic crystallography (PTMC). On the other hand, there are only a limited number of reports on the crystallographic characteristics of stress-induced martensite. In previous studies on some alloys (Cu-Al-Ni, Au-Cd, Ni-Al), the crystallographic features were reported to be consistent with PTMC. However, in Ti-Ni and β-Ti, the observed crystallographic features were reported to be inconsistent with PTMC. The reason for this is unclear, and we are attempting to clarify this reason. In this study, we used β-Ti alloy single crystals to investigate the crystallographic characteristics (habit plane, lattice-invariant deformation, and crystal orientation relationship) and lattice constants of the parent phase and martensitic phase under stress using in-situ measurements. This study aims to deepen our understanding of stress-induced martensitic transformation.

In this study, Ti-6Mo-10Al (mol%) was used as a β-Ti alloy that exhibits stress-induced martensitic transformation at room temperature. The alloy ingot was prepared using the arc melting method, and the single crystal was obtained using the optical levitation zone melting method. The single crystal was homogenized at 1273 K for 172.8 ks, and the back-reflection Laue method identified the crystal orientation. Using a diamond cutter and an electrical discharge machine, the test specimen was cut out with the [277] direction of the parent phase as the tensile direction. This test specimen was subjected to a solution treatment at 1273 K for 3.6 ks. The tensile test specimen was mounted on a small tensile device, and the following in-situ measurements were performed under tensile stress using the same sample: optical microscopy, scanning electron microscopy, electron backscatter diffraction, and X-ray diffraction.

The lattice parameters and crystallographic characteristics of martensitic transformation under tensile stress were experimentally determined. The lattice parameters of stress-induced martensite significantly differed from those of thermally induced martensite used in the PTMC. The lattice parameters during stress-induced transformation were used to re-calculate the PTMC, and the results were compared with the experimentally measured crystallographic features. The two were found to be in good agreement.

008_349

A Synchrotron Diffraction Study of the Total Stress Approach to Martensitic Transformations in Metastable β-Ti alloys

Nicole Church, Nicholas Jones
University of Cambridge, Cambridge, United Kingdom

Metastable β titanium alloys can undergo a reversible martensitic transformation from a disordered bcc phase to an orthorhombic martensite in response to a change in temperature or load. However, variations in the critical transformation parameters significantly limits their industrial acceptance. For example, in the commercial alloy Ti2448 (Ti-24Nb-4Zr-8Sn wt%), the critical stress for martensite formation has been shown to vary by over 250 MPa between studies, whilst the reported martensite start temperature can differ by ~200°C. These discrepancies are not unique to this alloy and can be seen in a range of binary and higher order systems.

Historically, discrepancies in the initial transformation behaviour have been attributed to differences in the formation of the hexagonal ω phase, which forms rapidly in some alloy compositions within the 200-400°C temperature range, and is known to suppress the martensitic transformation. However, in other compositions, such as Ti2448, the incorporation of Sn dramatically suppresses ω phase formation, and as such this explanation has been called into question. Furthermore, both thermal and mechanical transformation parameters are known to change on cycling through the martensitic transformation. A mechanism based on ω phase formation is therefore insufficient to address these observations.

Through a combination of *in situ* synchrotron X-ray diffraction and *ex situ* mechanical testing and microscopy experiments, we will demonstrate how these observations are underpinned by differences in residual stresses and defect structures. However, we will show how initial differences in residual stress levels only have a transient effect on mechanical response, as dislocations are formed to accommodate the bcc/martensite interface. We will present a detailed characterisation of martensite evolution during a range of thermomechanical tests and provide unique insight into the heterogenous nature of martensite nucleation. Finally, we will also demonstrate how this understanding can be utilised to achieve more consistent transformation behaviour, with important consequences for both alloy and component design.

009_350

The formation, evolution and deformation of stress induced martensite in Ti-Nb based alloys

Nick Jones, Nicole Church, Jai Sai Nichenametla, Oliver Reed
University of Cambridge, Cambridge, United Kingdom

Many metastable β titanium alloys undergo a transformation from the parent bcc β phase to an orthorhombic α" martensite, which can be driven by temperature, stress or a combination of the two. This transformation can be reversible, giving rise to superelastic and shape memory behaviours, or irreversible leading to transformation induced plasticity (TRIP). Such behaviours make these alloys highly attractive for a wide range of industrial applications including those in the aerospace, defence, biomedical and energy sectors. Yet, industrial uptake of these materials has been limited, as engineering their transformation properties to specific application requirements and achieving stable cyclic performance has proven challenging.

The persistence of these issues is rooted in an incomplete understanding of the factors that influence the formation, evolution and deformation of the martensite. For example, within the extensive literature relating to Ti-Nb based alloys, significant variations exist in the reported martensite start temperatures, even when considering alloys with nominally identical compositions. Given the dynamic nature of these transformations, an enhanced understanding, capable of rationalising the variations in the literature, can only be achieved via *in situ* through-transformation experiments using modern advanced characterisation techniques.

In this talk, a substantial body of high energy synchrotron diffraction data will be used to discuss the micromechanics of the β to α″ transformation in Ti-Nb based alloys when subjected to tensile deformation. These data enable a detailed characterisation of martensite formation, variant evolution, and interphase strain partitioning during mechanical loading. Such unique observations give rise to new insights into the nature of the transformation in these materials, including the role of type II and III strains on the ease of martensite formation, dynamic strain relaxation during loading and how the active deformation mechanism can transition from superelasticity to TRIP.

010_232

Mechanism of Hysteresis Widening in NiTi-Nb: Beyond the β-Nb Phase

Oliver Reed, Nicole Church, Nicholas Jones
University of Cambridge, Cambridge, United Kingdom

NiTi-based alloys typically undergo a reversible martensitic transformation between a high temperature B2 austenitic phase and a low temperature B19′ martensitic phase. The transformation occurs at different temperatures on heating or cooling, leading to a thermal hysteresis. This transformation allows for the shape memory effect, where deformations of the martensitic phase can be recovered by heating to the austenitic phase. Such behaviour enables NiTi-based alloys to be used in a range of applications, such as pipe couplings, actuators, valves and sensors. However, each application requires different transformation temperatures and thermal hysteresis. For example, a pipe coupling application requires a large thermal hysteresis, in order to ensure the alloy is stable during storage and application.

The addition of Nb has been shown to increase the thermal hysteresis of NiTi-based alloys, from around 10 K, to over 50 K. However, the reasons for the increase in hysteresis remain under debate. Early literature attributed this effect to the presence of a β-Nb phase, which hinders the transformation from martensite to austenite. However, more recent studies have shown that large thermal hysteresis can be achieved in alloys containing Nb, but without any β-Nb. The mechanism for the increase in hysteresis in these alloys is unknown, and this understanding is crucial to developing improved wide hysteresis shape memory alloys.

To address this issue, a range of NiTi-Nb alloys with differing Nb concentrations have been produced and the effect of these additions on the transformation behaviour and alloy microstructure assessed. Here we will present data obtained from electron microscopy, differential scanning calorimetry and *in situ* synchrotron X-ray diffraction experiments. These data indicate that the wide hysteresis in NiTi-Nb alloys is due to the combined effect of Nb on the microstructure, the crystallographic compatibility of the martensite and austenite phases, and the thermodynamics of the transformation. The talk will conclude by showing how this new understanding of the effects of Nb may aid in finding other alloying additions which can further increase the hysteresis width of these alloys, and tailor the transformation temperatures to a specific application.

011_249

Flexocaloric effect in shape-memory alloys

Antoni Planes[1], Marcel Porta[1], Emma Valdés[1], Lluís Mañosa[1], Eduard Vives[1], Avadh Saxena[2]
[1]Universitat de Barcelona, Barcelona, Catalonia, Spain. [2]Los Alamos National Laboratory, Los Alamos, New Mexico, USA

We will present experiments on flexocaloric effect carried out in a single crystalline Cu-Al-Ni shape memory alloy and will discuss the obtained results within the framework of a Ginzburg-Landau model adequate to study the martensitic transition induced by bending. Then, we will show that a reliable comparison of elastocaloric and flexocaloric performances requires that the mechanical work exchanged in both cases is the same. Comparison of both modes confirms that the flexocaloric effect is more efficient at low work since less driving force is required to nucleate the martensitic phase by bending.

012_283

Elastocaloric effect of NiTi alloy under multiaxial stress states

Andrej Žerovnik, Jaka Tušek
University of Ljubljana, Faculty of Mechanical Engineering, Ljubljana, Slovenia

Elastocaloric cooling is a promising solid-state refrigeration technology offering an efficient and environmentally friendly alternative to conventional systems. It relies on reversible temperature changes during stress-induced martensitic transformations in shape memory alloys. Early research focused on tensile loading, showing high temperature change but suffering from material fatigue and limited lifetime. This led to increased interest in compressive loading, where mechanical stability improves, yet significantly higher transformation stresses are required.

While tensile and compressive regimes have been extensively studied, the elastocaloric response under shear (particularly in torsional loading) remains poorly understood. Even more unexplored is the elastocaloric effect under multiaxial stress states, where combinations of torsion with tension or compression could provide beneficial transformation paths. This is especially relevant due to the asymmetric nature of the transformation surface in stress space, which suggests that different stress components can activate phase transitions more effectively.

This contribution presents a comparative analysis of the elastocaloric effect under tension, compression, torsion, and combined multiaxial loading conditions. The study highlights differences in stress-strain behaviour, transformation efficiency, and the potential of combined loading strategies to enhance system performance and durability.

013_285

Analysis of the elastocaloric effect in CuAlNi shape memory alloys through nano-compression experiments

Jose F. Gómez-Cortés[1], Emilio Ruiz Reina[2], Eduardo Gonzáles[3], Maria L. Nó[1], Jose M. San Juan[1]
[1]Dept. of Physics, Fac. of Science and Technology, University of the Basque Country UPV/EHU, Bilbao, Basque Country, Spain. [2]Dept. of Physics II, University of Málaga, Málaga, Andalucía, Spain. [3]COMSOL AB, Stockholm, Sweden

The elastocaloric effect (eCe) in shape memory alloys (SMA), such as Cu–Al–Ni, has garnered significant interest due to its potential for compact, efficient, and environmentally friendly cooling technologies. Unlike conventional refrigeration methods, elastocaloric cooling relies on solid-state phase transformations, offering a promising alternative with high energy efficiency. This study investigates the eCe at the nanoscale in Cu–Al–Ni SMA using finite element analysis with COMSOL Multiphysics software to analyze adiabatic temperature changes (ΔT) during nanocompression experiments on Cu–Al–Ni pillars.

We use the Souza-Auricchio shape memory model to capture the superelastic response of the SMA. The analysis combines non-linear structural mechanics and heat transfer modules to simulate the relationship between mechanical loading-unloading and temperature changes. Our simulations effectively reproduce the elastocaloric cycle across different strain rates and loading conditions, showing significant temperature variations that align with the experimental data. The methodology could be applied to any SMA to model the elastocaloric effect during nano-compression tests.

The results demonstrate an enhanced elastocaloric response at the nanoscale, indicating that miniaturization can improve performance metrics for cooling applications. These findings deepen our understanding of nanoscale elastocaloric behavior and lay the groundwork for the design of advanced micro-and nanoscale cooling devices. By optimizing material properties and device architectures, this research contributes to the development of next-generation shape memory alloy-based elastocaloric refrigeration systems, which have the potential to revolutionize thermal management technologies across various industries.

014_194

Elastocaloric investigation of NiTi 3D lattice structures fabricated via laser powder bed fusion under coupled mechanical deformation

Emanuele Bestetti[1], Francesca Villa[1], Elena Villa[1], Francesca Passaretti[1], Nicola Bennato[1], Enrico Bassani[1], Ehsan Marzban Shirkharkolaei[2], Shirin Dehgahi[2], Davoud Jafari[2]
[1]CNR-ICMATE, Lecco, Italy. [2]University of Twente, Enschede, Netherlands

Future cooling technologies based on solid-state phase-changing materials attract increasing interest as efficient and compact alternatives to traditional gas-based systems, which can satisfy sustainability requirements on energy/power consumption and pollution emissions. Mechanocaloric Shape Memory Alloys (SMAs) are materials that undergo a first-order phase transformation upon mechanical stress/deformation. The variation of latent heat associated with the Thermoelastic Martensitic Transformation (TMT) enables caloric effects exploited in cooling applications. In application, prospective, compact materials with large heat exchange surface area offer superior cooling efficiency/capability. Metalworking of bulk SMAs prepared with conventional methods, such as induction melting, arc remelting, and sintering, to obtain large surface areas is often hindered by the mechanical properties of the alloy. Conversely, bed powder fusion or direct energy deposition, techniques of additive manufacturing, enable the manufacturing of materials with high surface area and they are mostly exploited for NiTi. In particular, lattice structures composed by the repetition in the space of a unit cell, not only enhance the heat exchange upon phase transformation but also decrease the required stress to induce TMT while maintaining their structural integrity. Moreover, it is also possible to introduce the lattice compositional or microstructural gradients which can further enhance the mechanocaloric efficiency of the material. In our work, we prepared 3D printed almost equiatomic NiTi samples with different kinds of lattices and we performed mechanocaloric investigation by unidirectional compression and torsional deformation. The functional caloric parameters such as DT_{ad} are measured by thermocouples with high-frequency sampling devices and by thermo-camera records. Moreover, the mechanical properties at different temperatures, cycling fatigue, and structural degradation were assessed. Based on these results, we adopted this approach also for NiMnTi systems and we present the first results on superelastic NiMnTi processed with the Laser Bed Powder Fusion (LPBF) technique. This work put together the promising performances of NiMnTi with the enhanced functionality of architected lattice structures in order to achieve superior cooling capacity.

015_368

Advances in Powder Sintering-Based Binder Jet Additive Manufacturing of NiTi-Cu Shape Memory Alloys: Opportunities and Challenges

Mohammad Elahinia[1], Alireza Behvar[1], Mahyar Sojoodi[1], Harsh Bajaj[1], Shiva Mohajerani[1], Saeedeh Vanaei[1], Nasrin Taheri[1], Ahu Celebi[1], Ausonio Tuissi[2], Carlo Biffi[2]
[1]UToledo, Toledo, OH, USA. [2]CNR ICMATE Lecco, Lecco, Italy

NiTi-Cu shape memory alloys (SMAs) offer tunable thermomechanical behavior, superior fatigue resistance, and minimized transformation hysteresis, positioning them as next-generation functional materials for biomedical, aerospace, and solid-state cooling systems. The strategic addition of Cu to NiTi alloys enables control over phase transformation sequences and thermal stability, but conventional and fusion-based additive manufacturing (AM) methods often introduce thermal gradients, residual stresses, and undesirable phase segregation. Binder Jet Additive Manufacturing (BJAM), a powder sintering-based AM technique, emerges as a promising non-fusion alternative capable of producing complex geometries while mitigating melt-induced defects. This study provides the first in-depth, critical analysis of the feasibility and roadmap for fabricating NiTi-Cu SMAs via BJAM. Emphasis is placed on the influence of Cu content on microstructural evolution, transformation pathways (B2 → B19/B19′), and elastocaloric efficiency. Key parameters such as powder morphology, binder saturation, sintering dynamics, and contamination control are analyzed for their roles in shaping phase uniformity, densification, and functional properties. Computational alloy design strategies, particularly CALPHAD and machine learning integration, are highlighted for their predictive power in optimizing composition, thermal behavior, and printability. Current knowledge gaps, especially the absence of experimental BJAM studies on NiTi-Cu, are addressed with a proposed research roadmap that outlines alloy design, sintering optimization, and post-processing approaches for achieving high-performance, low-hysteresis, and defect-free components. This study sets a foundation for scalable production of NiTi-Cu SMAs via BJAM and offers a forward-looking framework for expanding their deployment in smart actuators, biomedical devices, and thermal management systems.

Keywords: NiTi-Cu alloys, Binder Jet Additive Manufacturing, Shape Memory Alloys, Powder Sintering, Thermal Hysteresis, Alloy Design, Additive Manufacturing

016_279

Additive Manufacturing processing of Superelastic Cu–Al–Ni Shape Memory Alloys

Mikel Pérez-Cerrato[1], José F. Gómez-Cortés[1], Lucia Del-Río[1,2], Josu Leunda[3], Ernesto Urionabarrenetxea[4,5], Isabel Ruiz-Larrea[1], Ízaro Ayesta[6], Iban Quintana[3], Maria L. Nó[1], Nerea Burgos[4,5], José M. San Juan[1]
[1]Department of Physics, University of the Basque Country (UPV/EHU), Bilbao, Bizkaia, Spain. [2]National Institute for Materials Science (NIMS), Tsukuba, Ibaraki, Japan. [3]TEKNIKER, Eibar, Gipuzkoa, Spain. [4]CEIT, Donostia, Gipuzkoa, Spain. [5]Universidad de Navarra, Tecnum, Donostia, Gipuzkoa, Spain. [6]Aeronautics Advanced Manufacturing Centre (CFAA), Zamudio, Bizkaia, Spain

Shape Memory Alloys (SMA) have an increasingly widespread interest due to their ability to work as actuators in a huge variety of sectors such as in medical, automotive or aerospace applications. Moreover, the rapid growth of the Additive Manufacturing (AM) technologies can greatly benefit the field of SMA as it allows for the fabrication of near-net-shape actuators tailored for each individual application. Cu-Al-Ni based SMA present a wide range of transformation temperatures and, in particular, can be used as high temperature SMA. However, one of the challenging aspects of AM is that the final samples will be polycrystalline. For this reason, the focus of the present work is not only the optimization of the building parameters, but of the thermo-mechanical performance of AM produced samples through various techniques, such as Laser Powder Bed Fusion (LPBF) [1].

In this work, the design and characterization of a Cu-Al-Ni SMA produced through AM is presented. After the design and atomization of the alloy, the powders are characterized. Then, the powders are sieved into different size ranges, and each of them is used for different processing techniques: LPBF, Laser Melting Deposition (LMD) and Powder Metallurgy (PM). With this kind of approach the losses of material can be greatly reduced. Moreover, the PM produced samples can be used as a reference material for the AM produced samples [2]. Once the samples are built, they are extensively characterized through differential scanning calorimetry (DSC), scanning electron microscopy (SEM) and X-ray tomography. This information is then used for the optimization of the building parameters that improve the overall performance of the samples. Later, the mechanical properties are studied on both tension and compression. In addition, the effect of the different textures can be observed in the results of the superelastic effect curves. Finally, some conclusions are drawn in order to highlight the strengths of each technique and pave the road for further works and improvements.

[1] M. Pérez-Cerrato et al., *Optimising the laser powder bed fusion processing parameters of Cu-Al-Ni shape memory alloys: microstructure and functional properties relationship*. Virtual & Physical Prototyping 20 (2025) e2458679.

[2] M. Pérez-Cerrato et al., *Powder Metallurgy Processing to Enhance Superelasticity and Shape Memory in Polycrystalline Cu–Al–Ni Alloys: Reference Material for Additive Manufacturing*. Materials 17 (2024) 6165.

017_166

Revealing the Friction and Wear Behavior of Additively Manufactured NiTi Alloy Under Different Operating Temperature Levels

Sougata Roy[1], Hyunsuk Choi[2]
[1]Iowa State University, Ames, IA, USA. [2]University of Toronto, Toronto, ON, Canada

Nitinol, an alloy made of Ni and Ti, has two special characteristics: shape memory and superelasticity. Due to its capacity to withstand significant elastic strains and superior mechanical properties compared to martensitic NiTi, austenitic NiTi alloy was studied for load-bearing applications. In this study, dry sliding wear tests at room temperature, 50°C, 100°C, and 200°C were carried out on samples of NiTi alloy samples fabricated using Laser-Powder and Laser Wire Directed Energy Deposition (LP-DED and LW-DED) processes. A set of systematic experiments including microstructure, hardness, porosity measurement, and thermal analysis via DSC were conducted. This investigation marks the first demonstration of a comparison between the tribological behavior of LP-DED and LW-DED fabricated NiTi alloys to the best of the author's knowledge.

Nitinol 55 wires, Nitinol 55 powders, and Nitinol 55 substrate plates were used for deposition. The phase composition of the as-printed LW-DED and LP-DED NiTi samples was studied to understand the major constituting phases of the printed samples at room temperature. Secondary phases which are widely reported in additively manufactured NiTi alloys were not detected in the XRD analysis for both as printed samples. The as-printed LP-DED sample was primarily composed of the B2 austenite phase with a measured phase fraction of 97 wt% and only minimal amounts of the B19' martensite phase at room temperature. The presence of the major constituting phase, austenite, in the LP-DED sample agrees with the phase transformation temperature observed through DSC analysis since room temperature is significantly higher than the austenite finish temperature for that particular sample. The LP-DED printed samples exhibited 47.2% higher hardness than the LW-DED printed samples. The LW-DED and LP-DED printed samples exhibited different characteristics in their frictional behavior against the steel balls. The coefficient of friction for the LW-DED samples exhibited a decreasing trend from room temperature to 200°C. A similar trend in the frictional response of the cold-rolled NiTi alloy between operating temperature at room temperature to 200°C. Decrease in friction coefficient with increasing operating temperature was observed in both additively manufactured and cold rolled Nitinol. These findings from this study will reveal the benefits and challenges of fabricating NiTi alloy AM technique as compared to conventional routes.

018_346

Resonant Ultrasound Spectroscopy: An efficient tool for high throughput characterization of additively manufactured biomedical Ti-Nb-Zr-O alloys

Michaela Janovska[1], Dalibor Preisler[2], Martin Koller[1], Petr Sedlak[1], Hanuš Seiner[1]
[1]Institute of Thermomechanics of the Czech Academy of Sciences, Prague, Czech Republic. [2]Faculty of Mathematics and Physics of Charles University, Prague, Czech Republic

Additive manufacturing is now a popular method for preparing new types of alloys, as it allows the production of small amounts of material with promising material properties. Since some newly developed alloys contain a higher number of elements, high-throughput characterization methods can effectively map the properties of a large number of alloys with different phase compositions. We present a combination of this method and ultrasonic methods for the characterization of a relatively wide range of compositionally graded biomedical alloys (Ti-Nb-Zr-O) produced by the field-assisted sintering technique. We show that the alloys prepared by this technique are suitable for reliable determination of the elastic constants of each of the prepared alloys.

Resonant ultrasonic spectroscopy (RUS) is a suitable method for determining the elastic constants of various types of materials. This technique allows to determine elasticity of the measured sample, using only a small amount of material to obtain reliable results. Typical dimensions of the investigated samples are about a few millimeters. In addition, fully contactless laser-based RUS device allows in-situ measurements of resonant spectra during temperature cycles. In the case of metastable titanium alloys, the elastic response for individual phases differs significantly, especially for the β and ω phases. In-situ observation of the temperature dependences of shear moduli and internal friction provides information about the individual phases and about the processes that occur in the alloy with a given composition. By mapping the elasticity of alloys with gradually changing niobium and oxygen compositions, it can be shown that the influence of niobium and oxygen is similar and both have a β-stabilizing effect.

References:
P. Sedlák, et. al., Experimental Mechanics, 54 (6) (2014), pp. 1073-1085.
D. Preisler, et. al., Journal of Alloys and Compounds, 932(2023), 16765

This work was financially supported by the Ministry of Education, Youth and Sports of the Czech Republic in the frame of the project 'Ferroic multifunctionalities' (project No.CZ.02.01.01/00/22_008/0004591), co-funded by the European Union.

019_165

The Martensitic Transformation in In-Tl Alloys Revisited

Trevor Finlayson[1], Garry McIntyre[2], Kirrily Rule[2], Lucie Bodnarova[3], Hanus Seiner[3]
[1]University of Melbourne, Parkville, Victoria, Australia. [2]Australian Centre for Neutron Scattering, Lucas Heights, New South Wales, Australia. [3]Czech Academy of Sciences, Prague, Czech Republic

The traditional view for the martensitic transformation in In-x at%Tl alloys, for $15.5 \leq x \leq 30.5$, was via a double shear such as, (101)[-101]; (011)[0-11], on the basis of optical microscopy, x-ray diffraction observations and measurements[1] of the c' (i.e., $(c_{11}-c_{12})/2$) elastic constant which was reported to approach zero at the transformation temperature[2]. Some of these reports for c' had been based on separate measurements of c_{11} and c_{12} and subtraction, on account of the high damping for the appropriate ultrasonic pulse. Nevertheless, a theoretical calculation of the phonon dispersion relations for In-Tl predicted phonon softening along the T_1 branch at low q[3]. Phonon dispersion measurements failed to detect this phonon softening and indeed, quite the reverse, i.e., an increase of low-q phonon frequencies with decreasing temperature, along the T_1 branch, was found[4]. The initial measurements were performed using a crystal of only moderate quality. But subsequent measurements done on a crystal which had been grown directly from an oriented crystal seed using a specially designed furnace to produce an oriented flat-plate crystal of excellent quality, confirmed this result. These most recent measurements were performed on the modern cold triple axis spectrometer, Sika, at the Australian Research Reactor, OPAL.

The presentation of these data at the 2017 International Conference on Martensitic Transformations in Chicago, prompted a question from the audience as to whether or not Resonant Ultrasonic Spectroscopy (RUS) had ever been applied to measure c' in In-Tl alloys? This question has given rise to the results to be reported in this presentation. RUS has been carried out on small crystals which have been shown to exhibit the martensitic transformation at a particular temperature using neutron Laue diffraction measured on Koala at the OPAL Reactor. While an anomaly in c' versus temperature has been observed near the transformation temperature, c' certainly does not go to zero.

These new results will be discussed in relation to the traditional view for the transformation in In-Tl alloys.

1. J.S. Bowles, *et al. Trans. Metall. Soc. A.I.M.E.* **188**, 1478 (1960).
2. D.J. Gunton and G.A. Saunders, *Solid State Commun.* **14**, 865 (1974).
3. D.J. Gunton and G.A. Saunders, *Solid State Commun.* **12**, 569 (1973).
4. T.R. Finlayson, *et al. Proc. ICOMAT2017* eds. A.P. Stebner and G.B. Olsen (The Minerals, Metals & Materials Soc., 2018) p 291.

020-200

Composition dependence of the distribution and hysteresis width of Martensite phases in the $Au_{50-x}Cu_{25+x}Al_{25}$ pseudobinary system

Yuki Matsuoka[1], Kyoko Kubo[2], Ayane Saeki[2], Hideki Hosoda[3,4]
[1]Faculty of Science, Department of Physics and Mathematics, Nara Women's University, Nara, Japan. [2]Graduate school of Humanities and Sciences, Nara Women's University, Nara, Japan. [3]Institute of Integrated Research, Materials and Structures Laboratory, Institute of Science Tokyo, Yokohama, Japan. [4]Laboratory for Future Interdisciplinary Research of Science and Technology, Institute of Science Tokyo, Yokohama, Japan

In the previous ICOMAT, we reported a detailed structural analysis of Au_2CuAl, showing that the alloy transforms from beta phase of ideal $L2_1$ atomic order to an orthorhombic martensite phase regardless of the sample alloy synthesize method.

In this time, we report the composition dependence of the distribution and abundance of the martensite phase in the $Au_{50-x}Cu_{25+x}Al_{25}$pseudobinary system.

The crystal system of the martensite phase changes from the single orthorhombic phase to a single monoclinic martensite phase when Au is substituted for Cu to be the composition ratio of $Au_{45}Cu_{30}Al_{25}$. Further substitution of Au with Cu results in the coexistence of both orthorhombic and monoclinic phases, with the monoclinic phase tending to increase as the substitution ratio increases.

The two martensite phases are observed together just below the M_s, but analysis of the reverse transformation process shows that the ratio of monoclinic phase decreases first, followed by a rapid decrease in orthorhombic phase. This suggests that A_s of the two martensite phases is clearly different.

Although the hysteresis width is wider in the single monoclinic martensite region ($Au_{45}Cu_{30}Al_{25}$) than in single orthorhombic phase (Au_2CuAl), it is about 10 K to 30 K in both cases, but it sharply widens to about 80 K in the composition region where the two martensite phases coexist. As the substitution proceeds, both M_s and A_s increase, but the rate of change of A_s is particularly large. Therefore, the reverse transformation process is considered to become less likely to proceed than the transformation process by the substitution of Au with Cu in the $Au_{50-x}Cu_{25+x}Al_{25}$.

021_300

The change of the martensitic transformation temperature on each composition by aging treatment in Cu-Al-Mn alloys

Kotaro Tomioka[1], Takuro Dazai[1], Akihisa Aimi[2], Ichiro Takeuchi[3], Kenjiro Fujimoto[1]
[1]Tokyo University of Science, Noda, Chiba, Japan. [2]National Defense Academy of Japan, Hashirimizu, Yokosuka, Japan. [3]University of Maryland, College Park, Maryland, USA

Cu-based shape memory alloys with an elastocaloric effect are attracting attention as the next-generation refrigerants that are free of fluorocarbons. To be commercially available as solid state refrigerants, the martensitic transformation temperature of the alloys must remain constant over the long-term. However, in the alloys, it is recognized that the temperature change due to stabilization of the martensite or austenite, which is known as aging[1)]. And this phenomenon results in degradation of elastocaloric effect and fatigue properties[2)]. In this study, we focused on Cu-Al-Mn alloys, which have a wider range of composition in the β-phase than other Cu-based, and investigated the composition dependence of the change of the martensitic transformation temperature and the crystalline phase by aging treatment. Approximately 200 alloys were prepared using arc melting method in the composition range of 64.8-78.23 at% Cu, 12.2-31.6 at% Al, and 0-17.87 at% Mn. The alloys were quenched in iced water after homogenized at 1173 K for 1 hour, and then cooled down to room temperature after aged treatment at 323 K for 0.25 hours. ICP-AES, XRD and DSC were used for compositional analysis of the alloys, identification of crystalline phases and martensitic transformation temperatures, respectively. Figure 1 shows the correlation between the average number of valence electrons per atom ratio (e/a) and temperature difference of the martensitic reverse transformation finish temperature before and after aging (ΔA_f). From this figure, it was clear that a structure of the austenitic phase changed on the border in e/a = 1.34. Alloys with e/a ≤ 1.34 had the A2 structure. In them, ΔA_f increased with an increase in e/a. This is thought that the degree of order in the A2 structure increased[3)]. On the other hand, alloys with e/a > 1.34 had the $L2_1$ structure. Especially for alloys with e/a between 1.34 and 1.4, ΔA_f decreased with an increase in e/a. This is known to be due to the increasing degree of order in the $L2_1$ structure[3)]. Therefore, it is assumed the $L2_1$ structure with e/a > 1.4 is almost perfect ordered, because ΔA_f of the alloys is smaller than the others. Therefore, alloys in this system must satisfy e/a > 1.4, which is less affected by ageing when applied to solid state refrigerants.

1) R. Kainuma *et al*., Metall. Mater. Trans. A, **23** (1996) 2187-2195.
2) R. Kainuma *et al*., Shape Mem. Superelasticity, **4** (2018) 428–434.
3) Y. Sutou, Ph.D. Thesis, Tohoku University (2001).

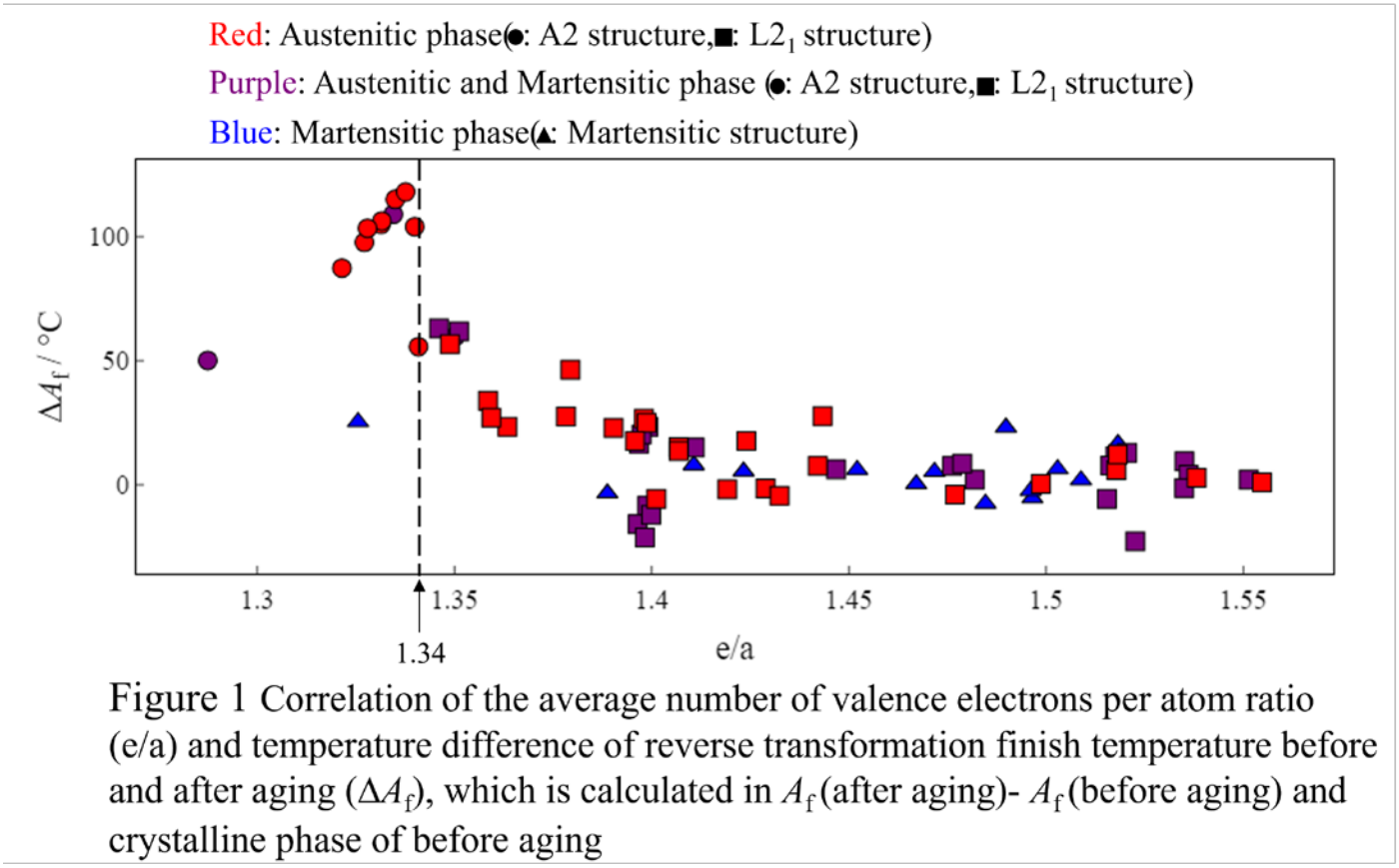

Figure 1 Correlation of the average number of valence electrons per atom ratio (e/a) and temperature difference of reverse transformation finish temperature before and after aging (ΔA_f), which is calculated in A_f(after aging)- A_f(before aging) and crystalline phase of before aging

022_352

Isothermal behavior of reverse ε → γ martensitic transformation in Fe-Mn-Si functional alloys with shape memory effect

Boris Kustov[1], Erkki Lähderanta[2], Jan Van Humbeeck[3], Joan Torrens-Serra[1]
[1]University of the Balearic Islands, Palma de Mallorca, Spain. [2]Lappeenranta-Lahti University of Technology, Lappeenranta, Finland.
[3]University of Leuven, Leuven, Belgium

We report thermally activated isothermal phenomena in functional Fe-Mn-Si-based alloys during the reverse martensitic transformation (MT). Two commercial alloys: Fe-17Mn-5Si-10Cr-4Ni-1VC (wt%) and Fe-28Mn-6Si-5Cr (wt%) are studied using dilatometry and electric resistivity measurements. Experiments point to simultaneous occurrence of two isothermal effects during interruptions of heating between the start As and finish Af temperatures of the reverse MT of temperature-and stress-induced HCP ε-martensite: stabilization of martensite and accumulation of austenite. We report thus the first observation of the isothermal reverse MT in functional Fe-Mn-Si alloys.

The temperature-induced martensite (TIM) and stress-induced martensite (SIM) in Fe-Mn-Si alloys are very different in terms of their reverse MTs: firstly, Af-As ~100K for the SIM and Af-As~ 20K for the TIM and, secondly, the As of the reverse MT of the SIM is lower than that of TIM by ca. 70K [1]. Despite substantial difference in the width and temperatures of the reverse MT in TIM and SIM, two isothermal phenomena persist in martensites of both origins. The most important experimental observations are as follows:

-stabilization of martensite. The stabilization effect does not notably increase the transformation range, keeping essentially Af temperature unchanged. This behavior points to the relaxation of internal stresses as a major contributor to the stabilization.

-isothermal reverse MT. The isothermal accumulation of austenite during reverse MT of stress-and temperature-induced martensites follows the logarithmic kinetics, where is the variation of the austenite fraction. We found that the parameter *Z* correlates with the temperature rate of uninterrupted reverse MT, which is the typical feature of the isothermal direct MTs [2]. Thus, similar to the isothermal direct transformations, we interpret the isothermal reverse MT in Fe-Mn-Si alloys as a relaxation of the system of independent bistable units with a broad distribution of activation energies.

[1]. B. Kustov, E. Lähderanta, J. Van Humbeeck, J. Torrens-Serra, “Reverse ε→γ transformations of temperature-induced and stress-induced martensites in Fe-Mn-Si alloys with shape memory effect”, *J. of Mat. Res. and Technology*, 30 (2024) 6641-6652

[2]. S. Kustov, I. Golovin, M. L. Corró, E. Cesari; Isothermal martensitic transformation in metamagnetic shape memory alloys. *J. Appl. Phys.* 1 March 2010; 107 (5): 053525

023_358

Shear and shuffle-based mechanisms in modulated NiMnGa alloys

Robert Chulist[1], Anna Wojcik[1], Arkadiusz Szewczyk[1], Norbert Schell[2], Alexei Sozinov[3], Wojciech Maziarz[4]
[1]AGH University of Krakow, Krakow, Poland. [2]Helmholtz-Zentrum Hereon, Geesthacht, Germany. [3]LUT University, Lappeenranta, Finland. [4]Institute of Metallurgy and Materials Science, Krakow, Poland

The origin of structural modulation, the extraordinarily low twinning stresses, and the mechanism of intermartensitic transformation in NiMnGa alloys have been subjects of discussion for at least three decades. In this context, the nature of the modulation and the atomic structure of type I and type II twin boundaries have attracted significant interest, as they may provide definitive answers to these long-standing questions.

In this work, we demonstrate that the macroscopic irrational character of the type II twin boundary is represented at the atomic scale by two faceted rational components. Additionally, we propose a dislocation-free mechanism for the facile motion of twin boundaries, which involves the shuffling of atomic layers and an extremely soft elastic response.

Furthermore, by applying a temperature gradient, we stabilized an austenite/twinned martensite interface, revealing both the crystal structure and microstructure, as well as the transformation sequence across the interface. Based on crystallographic analyses, both shear and shuffle mechanisms were identified.

Overall, distinguishing between these two mechanisms enables us to explain the exceptionally low twinning stress of type II twin boundaries, their practical temperature independence, the mechanism of intermartensitic transformation, and the crystallographic nature of modulated phases.

Acknowledgement:
The work was carried out within the project 2021/42/E/ST5/00367 of the National Science Centre of Poland.

024_193

NiMnGa-based multicaloric alloys: functional thermo-mechanical investigation under magnetic field

Elena Villa, Francesca Villa, Emanuele Bestetti, Francesca Passaretti, Enrico Bassani, Nicola Bennato
CNR ICMATE, Lecco, Italy

The Ferromagnetic Shape Memory Alloys (FeSMA) attracted increasing interest as multicaloric materials for solid state cooling. The most important field coupling corresponds to the magnetic and mechanical co-induction of thermoelastic martensitic transformation (TMT) to develop an elasto and magneto-caloric effect in the material. In our work we present an experimental investigation on NiMnGa-based polycrystalline alloys, using an experimental setup ad hoc developed for measuring stress-strain curves in isothermal conditions under a magnetic field. We carried out experimental measurements at different temperature above Af and under 4 values of magnetic field: 0.1, 0.26, 0.46 and 0.56 T. In this way we measured the elastocaloric and magnetocaloric effects at the same time. With Maxwell equations, the entropy changes DS are evaluated, and the influence of magnetic field is discussed. The functional caloric parameters as DT_{ad} vs. magnetic field until 0.56 T are measured by thermocouples system with high frequency sampling device. The application of a magnetic field seems to act like an additional mechanical axial stress. The precise contribution of the magnetic field is considered and discussed starting from a magnetostrictive approach.

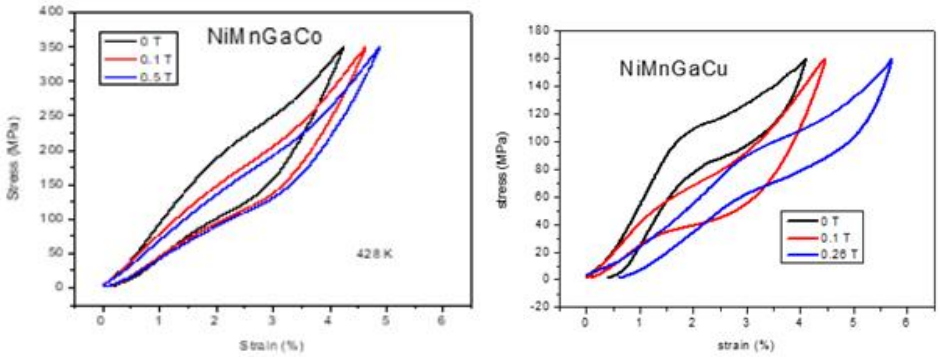

These preliminary results confirm the synergy between mechanical and magnetic forces to improve the overall caloric effect in these systems. Our measurements are important to complete the understanding and modeling of coupled multicaloric phenomenon.

025_230

Specific heat and entropy change during martensitic transformation in $Ni_{50}Mn_{50-x}Ti_x$ alloys

Tomoya Miyakawa[1], Sheng Xu[2], Xiao Xu[1], Toshihiro Omori[1], Ryosuke Kainuma[1]
[1]Department of Material Science, Graduate School of Engineering, Tohoku University, Sendai, Japan. [2]Frontier Research Institute for Interdisciplinary Sciences, Tohoku University, Sendai, Japan

The elastocaloric effect (eCE) in shape memory alloys (SMAs), which exhibits a remarkable stress-induced adiabatic temperature change (ΔT_{ad}), has been considered a key technology for alternative refrigeration systems. Recently, Ni-Mn-Ti SMAs have attracted attention as promising candidate materials for realizing elastocaloric cooling systems, owing to their large eCEs, with ΔT_{ad} exceeding -30 K [1-3]. However, the entropy change (ΔS) associated with the martensitic transformation, which is considered the origin of the large ΔT_{ad}, in Ni-Mn-Ti alloys has not been thoroughly investigated. In this work, we investigated the temperature and composition dependence of the ΔS to clarify why Ni-Mn-Ti alloys show the giant eCE compared to other alloys.

From the specific heat measurements by the heat flow method, the ΔS of $Ni_{50}Mn_{50-x}Ti_x$ alloys from 997 K to 133 K were determined. It was found that the ΔS above 200 K showed relatively large values, with ΔS >3 J/(mol・K). From the specific heat measurements using the relaxation method, magnetic transition-like behaviors were observed in the martensite phase, which may influence the magnitude of ΔS. A comprehensive analysis of the temperature and composition dependence of ΔS, along with the results of magnetization measurements and crystal structure determinations, will be explained further in the presentation.

REFERENCES

[1] D.Cong *et al.*, *Phys. Rev. Lett.*, **122** (2019) 255703.
[2] G. Zhang *et al.*, *Scr. Mater.*, **234** (2023) 115584.
[3] G. Zhang *et al.*, *Scr. Mater.*, **237** (2023) 115725.

026_234

Exploration of CuZnAl for elasto-caloric applications

Oneil Goisot[1,2], Odile Robach[3], Richard Haettel[2], Laureline Porcar[2], Marc Verdier[1]
[1]Univ Grenoble Alpes, CNRS UMR 5266 Grenoble INP, SIMaP, Grenoble, France. [2]CNRS UPR 2940 Institut Néel, Grenoble, France.
[3]CEA Grenoble/IRIG/MEM, Grenoble, France

The need for efficient and environmentally friendly heating/cooling systems is increasing worldwide. The use of heat-pumps based on reversible solid-state phase transformation is promising and can achieve higher COP than conventional heat-pumps [US14]. They also avoid the use of high global warming power (GWP) or flammable fluids.

For realistic heat pump, a sustained number of cycling must be above ten million, the bottleneck is to find a material that can withstand such a large cycling number at total strain greater than few % without loss of latent heat ($\Delta T_{adiabatic}$). The primary cause of irreversible mechanisms comes from the lattice mismatch between austenite and martensite [Karami24].

Fatigue life can be greatly improved by phase, microstructure engineering and size [Gu18]. By investigating composition effect, a strategy has been explored to ensure the best reversibility, namely supercompatibility [Gu18]. Exceptional fatigue up to 10^7 cycles is obtained, but only for costly alloys in NiTiCu and ZnAuCu systems and in micron size samples. Super compatible alloys show very low thermal hysteresis and can exhibit a very specific flexible microstructure.

Our strategy is to explore β-brass domain to find minima in thermal hysteresis (fig.2) and to carry out microstructural observations and crystallographic data collection. Calorimetry measurements (DSC), resistivity, microstructural investigations optic and µLaue (BM32 @ESRF) (fig.3), are conducted on both bulk and composition gradient samples (fig.1).

The methodology will be presented and results from our measurements on the transition characteristics will be discussed as a function of composition and lattice parameters.

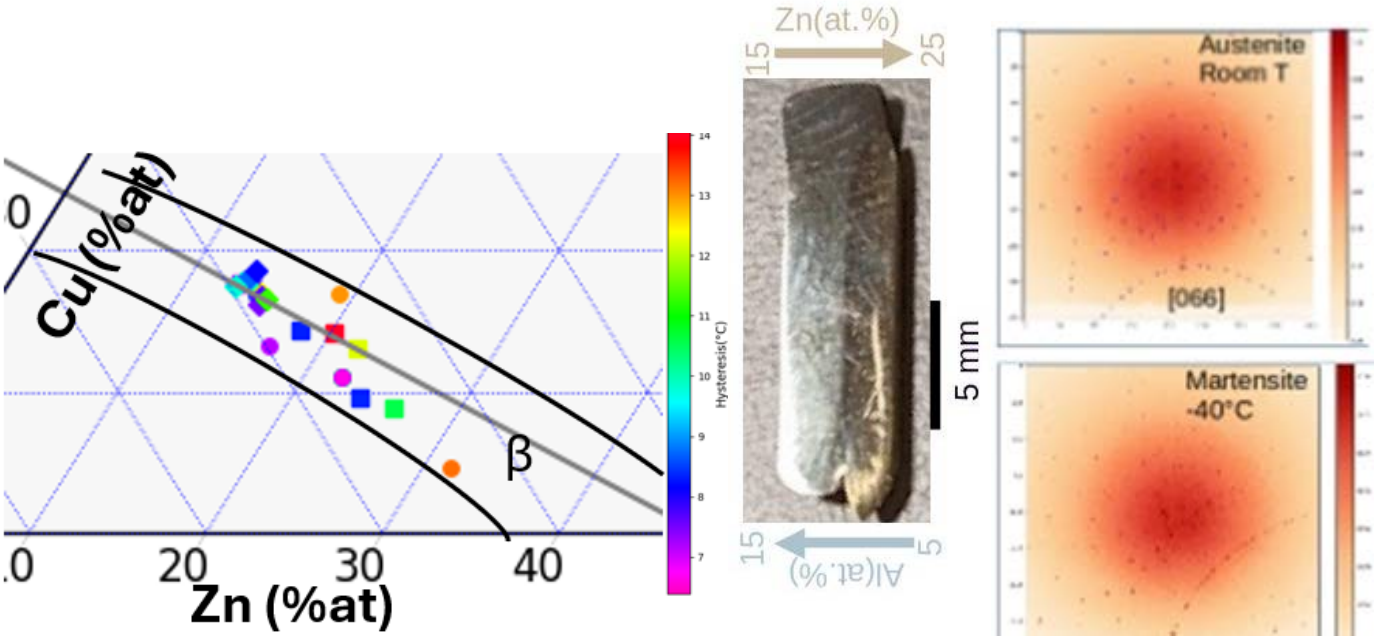

027_219

Development of elastocaloric device

Andrej Žerovnik, Žiga Ahčin, Stefano Dall'Olio, Miha Brojan, Jaka Tusek
Faculty of Mechanical Engineering, University of Ljubljana, Ljubljana, Slovenia

Elastocaloric cooling/heating is emerging as a promising alternative to nowadays widely used, but environmentally harmful vapor compression technology. It is based on the elastocaloric effect that occurs during a stress-induced martensitic transformation in superelastic shape memory materials. Here, we will discuss the concept of active elastocaloric regeneration [1], which has been recently shown to be the most effective method for utilization of the elastocaloric effect in practical applications [2-4]. We will then focus on the development of two crucial components of an elastocaloric device, namely the fatigue resistant elastocaloric regenerator and efficient loading system. We have developed a durable tube-based elastocaloric regenerator loaded in compression, which worked both in a cooling and heating mode and demonstrated a temperature span of above 30 K (see Fig. 1) [2]. We have further designed and tested a cam-disc-based loading system that enables simultaneous loading of multiple elastocaloric regenerators and recovery of the work released upon unlading. At the end we will discuss future improvements, such as more efficient elastocaloric materials, required for further boosting the efficiency of elastocaloric devices.

[1] J. Tušek et al., Nature Energy 1 (2016)

[2] Ž. Ahčin et al., Joule 6 (2022)

[3] S. Qian et al., Science 380 (2023)

[4] G. Zhou et al., Nature 639 (2025)

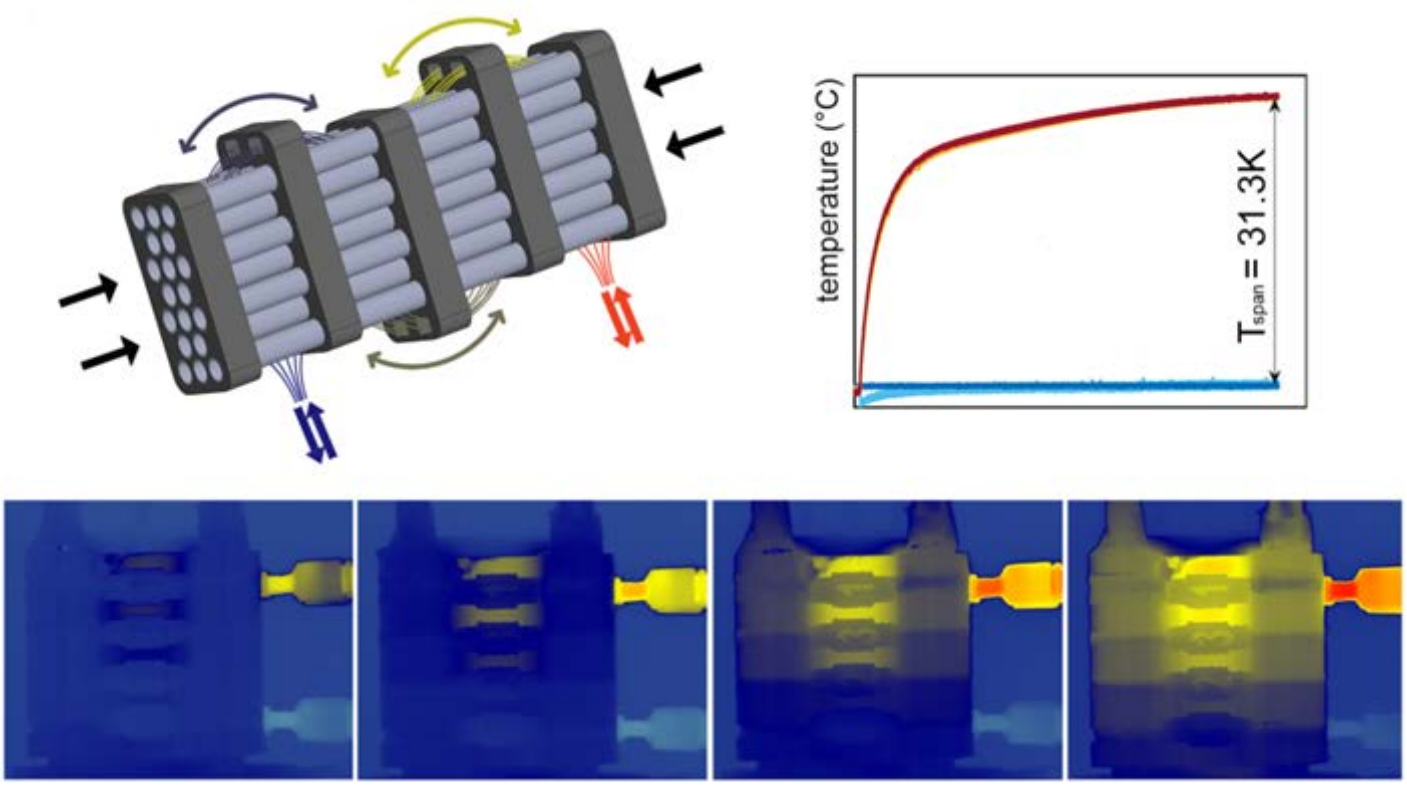

Figure 1: Schematic representation of tube-based elastocaloric regenerator (left), time evolution of the temperature span between the hot and cold side (right), IR images of the elastocaloric regenerator in the heat-pumping mode from the initial state until the steady-state is reached [2].

028_363

New generation of Shape Memory Alloys (SMAs) for elastocaloric solid-state heat pumps

Jan Pilch[1,2], David Vokoun[2], Kristyna Stepanovska[2], Ivo Marek[2], Lucie Petrusova[2], Erik Skobrtal[2], Jan Mikeska[2], Petr Vondrous[2], Kevin O'Toole[1]
[1]Exergyn Limited, Dublin, Ireland. [2]Exergyn CR s.r.o., Zdiby, Czech Republic

Heat pumps (HP) are an integral part of modern society. With over a century of history, vapor compression technology is used, including various types of refrigerants, which are currently regulated to meet stringent environmental criteria. Regulations lead to the selection of refrigerants that reduce the efficiency of HP and that are, for example, flammable. Alternative technology using SMAs as Elastocaloric Materials (EMs) instead of refrigerants has recently attracted considerable attention. EMs undergo a first order reversible phase transformation under the influence of an external force and have the following key advantages. There is no risk of the medium leaking into the atmosphere, which allows easy recyclability, and it can compete with or even outperform established vapour compression systems in terms of efficiency. On the other hand, these EMs face multiple challenges.

The key selection criteria are fatigue resistance-structural stability and efficiency degradation resistance-functional stability. State-of-the-art commercial EMs, mostly based on nanocrystalline structures, offer sufficient stability and good fatigue properties under compressive loading, however, are generally limited to expensive thin structures such as filaments, thin wires and tubes. In the case of cheaper commercial bulk SMAs, e.g. thick plates, rods, etc., we face massive instability and degradation of properties within several dozens of load cycles.

This work presents a new generation of SMAs produced in large-format volumes, exhibiting excellent structural and functional stability in compression, giant superelastic window greater than 80°C, temperature operational scalability in the range from -50°C to 140°C, high latent heat greater than 15 J/g available for energy transfer in each loading cycle within the whole superelastic window, extraordinal cyclic overload capacity above 2GPa and a small hysteresis response (~100 MPa, Fig. 1). A major advantage of these new generation SMAs is the elimination of the need to ”train” them to achieve a stabilized latent heat output under superelastic cycling. In this work, the thermomechanical response of this new generation SMAs after 1 million full superelastic fatigue cycles is presented for various operational conditions.

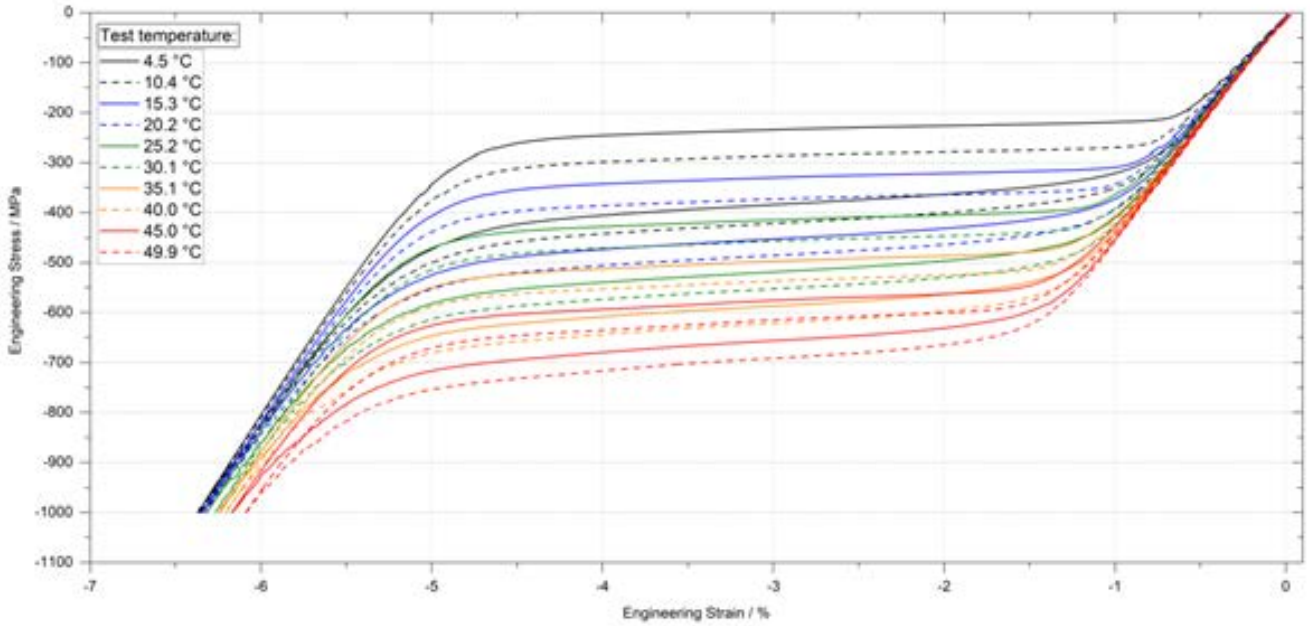

Fig. 1 The stress-strain isothermal behavior under compression loading of the new generation SMA purposely developed for efficient elastocaloric solid-state heat pumps.

029_364

Additive Manufacturing Meets Multicalorics: Microstructure Design of Heusler Alloys for Multi-Stimuli Cycling

Franziska Scheibel[1], Johannes Puy[1], Adrian Guder[2], Christian Lauhoff[2], Tino Gottschall[3], Thomas Niendorf[2], Oliver Gutfleisch[1]
[1]Technical University of Darmstadt, Darmstadt, Germany. [2]University of Kassel, Kassel, Germany. [3]Helmholtz-Zentrum Dresden-Rossendorf, Dresden, Germany

Multicaloric materials like Ni-Mn-based Heusler alloys exhibit large magnetocaloric (MCE) and elastocaloric effects (ECE). However, the significant thermal hysteresis of their first-order magnetostructural transition (FOMST) limits reversibility and reduces cyclic caloric performance under moderate stimuli. Applying higher magnetic fields or uniaxial stress enables larger cyclic MCE or ECE. Alternatively, combining magnetic field and stress in a multi-stimulus cycle can reduce required stress, though mechanical stability of Ni-Mn-Sn remains challenging. Additive manufacturing (AM) offers tailoring geometry, hysteresis, and mechanical stability opportunities.

AM techniques such as laser powder bed fusion (PBF-LM) and direct energy deposition (DED) allow fine-tuning of microstructure and transformation behavior. Excellent superelasticity has been demonstrated in textured Co-Ni-Ga Heusler alloys processed by DED. We applied similar methods to Ni-Mn-Sn and investigated composition, structure, and functional properties along the full processing chain—from powder to processed components [1]. Our study highlights how functional properties can be tailored from particles to components using microstructural and geometric design via PBF-LB, DED, spark plasma sintering (SPS), and hot densification. Particle size selection enables control over thermal hysteresis and the FOMST. These particles are building blocks for tuning FOMST via process parameters and particle size. Microstructural engineering through DED, PBF-LB, or SPS improves mechanical and cyclic stability compared to casting. AM and SPS also offer better scalability and reproducibility than lab-scale synthesis.

To enable multicaloric studies, we developed a multi-stimuli test setup with pulsed magnetic fields up to 9 T and uniaxial loads up to 10 kN [2]. This serial hysteresis-based approach separates magnetic field application from heat exchange: the field induces forward transformation, while uniaxial load triggers the reverse. In Fe-Rh (28 K hysteresis), a 1.9 T field yields an irreversible -6.7 K MCE. Combining 3 T and 700 MPa achieves a reversible ±2.5 K effect, demonstrating efficient multicaloric cycling. This novel setup enables systematic optimization across various materials.

We acknowledge funding by ERC (Adv. Grant "CoolInnov"), DFG CRC/TRR 270 "HoMMage", BEsT, and HLD at HZDR (EMFL)

[1] F. Scheibel et al., Materialia 29, 101783 (2023)
[7] F. Scheibel et al., J. Appl. Phys. 137, 014901 (2025)

030_378

Additive manufacturing of metamagnetic shape memory alloys: heat exchangers for magnetic refrigeration

Daniel Salazar
BCMaterials, Basque Center for Materials, Applications and Nanostructures, Leioa, Spain

Existing societal challenges necessitate the advancement of innovative, eco-friendly technologies and the ability to manufacture 3D structures sustainably and profitably. Progress in caloric materials, such as magneto-or elasto-caloric compounds, as integral components of the next generation of energy-efficient devices, presents new opportunities for breakthroughs in additive manufacturing. Metamagnetic shape memory alloys have emerged as promising candidates for magnetic refrigeration due to their high entropy change through the first-order martensitic transformation. However, it is important to note that their crystalline phase becomes unstable at temperatures exceeding 300 ºC.

In this work, we developed novel alloys, inks and pastes specifically designed for screen-printing and cold extrusion techniques, enabling the fabrication of intricate 3D structures using NiMn-based magnetocaloric powders derived from alloy design. A sustainable matrix composed of hydroxypropyl cellulose and deionized water as a solvent was used. The printable ink, containing over 95 wt.% powder, was carefully optimized to achieve the ideal viscosity, allowing the deposition of several hundred layers with high printing resolution (0.5mm wall thickness). The post-processing for the printed structures involves a specialized thermal treatment to desiccate the printed structures, eliminating the polymer via calcination. Subsequently, sintering is performed to obtain an all-metal structure, and nickel electrodeposition is applied to enhance corrosion resistance. The final solid sections exhibit a porosity of less than 8 vol. %.

031_160

Mechanical properties of heterogeneous-structured 18Ni300 maraging steel manufactured by directed energy deposition

Jung Gi Kim[1], Jonghyun Jeong[1], Gun Woo No[1], Sang Kyu Yoo[2], In-Chul Choi[2], Hyoung Seop Kim[3]
[1]Gyeongsang National University, Jinju, Korea, Republic of. [2]Kumoh National Institute of Technology, Gumi, Korea, Republic of.
[3]Pohang University of Science and Technology, Pohang, Korea, Republic of

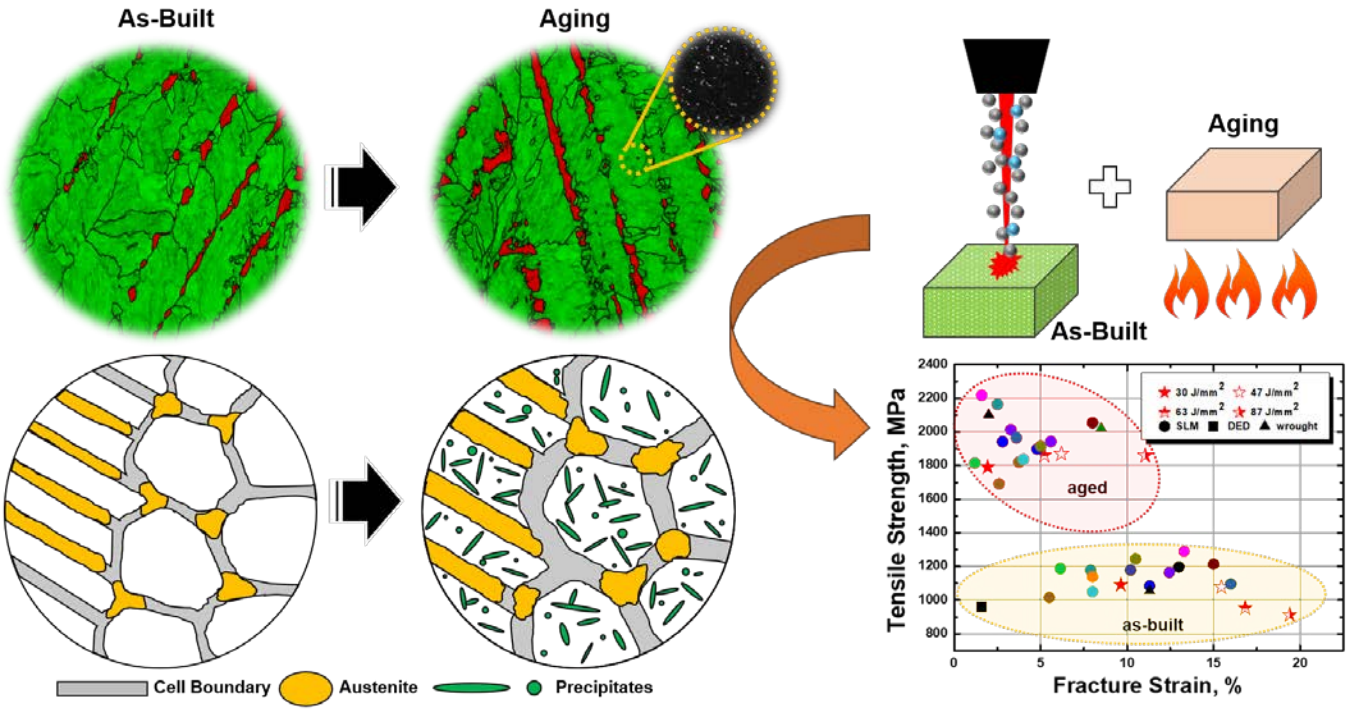

Combination of repetitive melting-solidification cycles and directional laser scanning during laser-based additive manufacturing (AM) result into the unique and heterogeneous microstructure, including chemical segregation, hierarchical defects, and metastable phases. The heterogeneous microstructure in AM-processed metallic materials effectively interrupts dislocation gliding during plastic deformation that affect their mechanical properties. Specifically, retained and reverted austenite in maraging steels allows to make a design window to enhance strength-ductility combination, so the role of metastable austenite on the mechanical properties of AM-processed maraging steel was investigated. The stripe laser scanning induced linear (Mo, Ti, Ni)-rich segregations that formed lamellar-structured austenite by reducing the martensitic transformation starting temperature in the high-Ni-content maraging steel. Both deformation-induced martensite and back-stress hardening near the austenite-martensite interface support to absorb an extra-deformation energy that results into the enhanced strain hardening capability in AM-processed maraging steel. Thus, the heterogeneous microstructure in AM-processed maraging steel allows to achieve a better strength–ductility combination compared with conventional and recently developed AM-processed maraging steels. This result implies that heterostructure design using AM is important to control a performance of metallic alloys by distributing chemical segregation, defects, and metastable phases in the matrix.

032_164

Superelastic Ti-Nb-Sn porous alloys prepared by material extrusion additive manufacturing

Tae-hyun Nam, Jinhwan Lim
Gyeongsang National University, Jinju, Gyeongnam, Korea, Republic of

In this study, a Ti-15Nb-5Sn (at. %) alloy was prepared by material extrusion additive manufacturing (MEAM) process for biomedical application. Elemental Ti, Nb and Sn powders were blended with a thermoplastic polyurethane (TPU) binder in a ratio from 40 to 50 vol. %. The filament preparation and printing process parameters were then investigated and optimized. Considering the surface roughness and extrusion speed, the optimal extrusion temperature and printing temperature of the filament were selected to be 150 °C and 225 °C, respectively. After thermal debinding, microstructures of Ti-15Nb-5Sn specimens were characterized by the coexistence of α phase, β phase, α″ martensite and TiC. α phase remained even after solution treatment (ST) due to the high oxygen levels ranging from 1.17 wt. % to 1.66 wt. %. An elastic modulus of 0.2 and 0.4 GPa was achieved at room temperature in ST45 and ST50 specimens, respectively. These elastic moduli in ST45 and ST50 specimens were similar to that of cancellous bone, helping to avoid the stress shielding effect. The compressive strength and elongation of ST45 and ST50 specimens were 7.9 MPa and 16.6 MPa, 6.9 % and 9.0 %, respectively. The maximum recoverable strains in ST45 and ST50 specimens were measured to be 0.3 % and 0.8 %, respectively. A noticeable decrease in the XRD intensity of $(110)_{\beta}$ peak and the appearance of $(020)_{\alpha''}$ XRD peak indicated that the mechanism of the recoverable strain is attributed to superelastic behavior. This study was the very first attempt to fabricate a Ti-based alloy using elemental powder by the MEAM process for biomedical applications.

033_161

The weak twins in martensite

Cyril Cayron
Ecole Polytechnique Fédérale de Lausanne, Neuchâtel, 2000, Switzerland

Martensite form complex and intricate assemblies of laths or plates that are related by the symmetries of the parent phase. Two martensite variants form a type I twin if the link between them is a mirror symmetry. They form a type II twin is the link is a 180° rotation. They form a compound twin if they are linked these two two-fold symmetries together. How can we define the twin and predict the junction plane between variants linked by a parent symmetry that is not two-fold, for example a three-fold rotation? The Phenomenological Theory of Martensite Crystallography (PTMC) have no solution for them. We propose to introduce the concept of weak plane and weak twins and will explain how to calculate them. The predictions will be compared to TKD maps obtained in martensitic NiTi alloys.

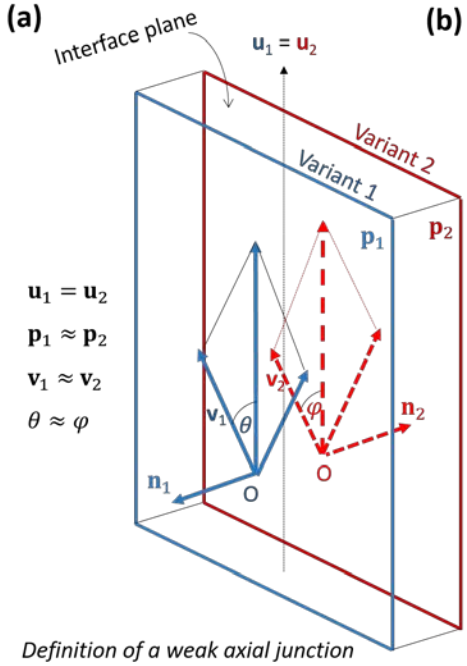

Definition of a weak axial junction between two variants

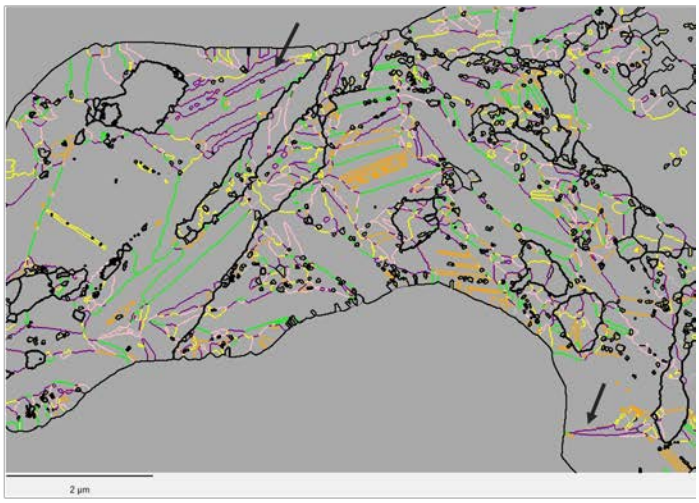

TKD map of a martensitic NiTi alloy showing only the grain boundaries (GBs). The junctions between the variants are colored according to their specific misorientations (operators). The junction planes between the variants linked by a parent 3-fold rotation (polar operator) are in purple, as indicated by the black arrows.

034_162

Beyond Martensitic Transformations: Intrinsic Orientation Relationships via Generalized Lattice Correspondences

Wenzheng Zhang
School of Materials Science and Engineering, Tsinghua University, Beijing, China. School of Materials Science and Technology, Fujian University of Technology, Fuzhou, Fujian, China

Reproducible orientation relationship (OR) and a habit plane are key characteristics of a martensitic phase transformation. Various ORs are also observed between phases related by other phase transformations, often described in various equivalent expressions. For unifying the descriptions, we propose the concept of *intrinsic OR* to characterize the OR formed during the early stage of a phase transformation. The intrinsic OR inherently relates to the low-energy interfacial structure, characterized as either one-to-one (primary preferred state [1]) or non-one-to-one matching configuration (secondary preferred state [1]). It captures the matching geometry by specifying the parallelism of a pair of matching-related vectors and a pair of matching-related planes across the two phases.

Defining an intrinsic OR requires identifying the matching correspondence in the preferred state. This correspondence can be regarded as a generalized lattice correspondence, a critical input in the PTMC. It links all pairs of matching related vectors, which may not be parallel to each other. For a secondary preferred state with a 2D structure, the intrinsic OR must be expressed through the parallelism of a pair of rational planes in the two lattices, to which the interface containing the 2D preferred state is parallel. The in-plane OR is then determined by a pair of matching-related parallel vectors in these planes.

In practice, matching-related elements are often not perfectly parallel, as in irrational ORs resulting from martensitic transformations. However, the deviation of the final OR from the intrinsic OR is generally small, ensuring the local presence of the preferred state in the habit plane. Therefore, the intrinsic OR can often be identified as a rational OR within a small angular range from the observed one. Practical guidelines are provided to find matching-related parallel planes in an intrinsic OR according to the near-matching rows in an overlapping diffraction pattern.

This presentation will demonstrate the determination of intrinsic ORs through case studies spanning martensitic and non-martensitic systems. While some expressions align with conventional OR descriptions, others offer novel perspectives. The proposed framework not only unifies the OR descriptions across diverse material systems but also assists in the elucidation of the crystallography of phase transformations.

1. W. Bollmann, Crystal lattices, interfaces, matrices, Bollmann, Geneva (1982).

035_206

Disclination-mediated twin-twin reactions in martensitic transformation of titanium

Yipeng Gao
Jilin University, Changchun, China. Max-Planck-Institute for Sustainable Materials, Dusseldorf, Germany

Disclinations, alongside dislocations, are fundamental topological defects governing deformation in metals, yet their rotational nature remains less explored due to characterization challenges. We develop a Lie-algebra-based method to quantify disclinations from EBSD data, enabling precise identification of their density and distribution. Combined with phase transition graph theory, we demonstrate how disclination dipoles at twin boundaries junctions mediate twin-twin reactions, linking mechanical twinning and phase transformations as coupled symmetry-breaking processes. The formation mechanism of unconventional twins (e.g., {332}, {5 8 11} twins) and extended twin boundary structures observed in titanium alloys has been analyzed, which suggests an intrinsic coupling between twinning and phase transformations. These findings advance the understanding of topological defect formation in martensitic transformations, offering pathways to design alloys with tailored transformation plasticity and twinning plasticity.

036_301

Texture Evolution in Transforming and Twinning Materials: A Comparison of Neutron Diffraction and MTEX-Based Simulations

Jan Čapek[1], Efthymios Polatidis[2], Manas Upadhyay[3]
[1]Charles University, Praha, Czech Republic. [2]University of Patras, Patras, Greece. [3]École Polytechnique, Palaiseau, France

The evolution of crystallographic texture during deformation plays a crucial role in defining the mechanical properties of materials, particularly those undergoing phase transformations or twinning. This study compares neutron diffraction experiments with MTEX simulations to analyze texture development under mechanical loading. By correlating experimental and simulated texture evolution, we assess the accuracy of modeling approaches in capturing grain reorientation, variant selection, and twinning behavior. The results provide insights into the microstructural mechanisms governing deformation in complex materials and highlight the predictive capabilities of computational methods.

037_217

Latent thermal energy storage driven by martensitic transformation in shape memory materials

Žiga Ahčin, Jaka Tušek
Faculty of Mechanical Engineering, University of Ljublajana, Ljubljana, Slovenia

Thermal energy storage (TES) systems are crucial for improving energy efficiency and integrating renewable energy sources into the wider energy grid. The most widely used TES technologies include sensible thermal and latent storage, where the latter primarily relies on phase transitions from solid to liquid. However, latent heat TES often faces problems such as material degradation during thermal cycling, lower charge and discharge rates, corrosion, toxicity, and significant volume changes. In contrast, shape memory alloys, which undergo a solid-to-solid martensitic phase transformation, offer an innovative alternative for TES. Shape memory alloys exhibit a wide range of transformation temperatures, which makes them an interesting solution for TES in a very wide temperature range, from cryogenic to high-temperature applications. For example, the lowest reported temperature interval for solid-to-solid phase transformation is between 45 and 85 K for $Cu_{78}Al_9Mn_{13}$ alloy, while the highest reported temperature interval is between 1360 K and 1471 K for $Ni_{50}Hf_{50}$ alloy with a latent heat of about 500 $MJ \cdot m^{-3}$. Although shape memory alloys typically have a lower latent heat than conventional phase change materials with solid-to-liquid transitions, their significantly higher thermal conductivity enables rapid thermal charging and discharging and thus superior thermal power, making them particularly suitable for applications that require highly dynamic operation. In this talk, we will discuss a comparison of different shape memory alloys and conventional phase change materials in terms of thermal capacity and output power, which has been performed using an experimentally validated numerical model. While most conventional phase change materials generally offer higher thermal capacity due to larger latent heat, some shape memory alloys (e.g., Ni-Ti-based alloys, Mn-Co-Ga-B alloys) exhibit up to 10 times higher thermal output powers [1]. These results highlight a significant potential of shape memory alloys to outperform traditional latent thermal storage systems for certain applications.

[1] Ž. Ahčin, A. Kitanovski, J. Tušek, Latent thermal energy storage using solid-state phase transformation in caloric materials. Cell Reports Physical Science, Volume 5, Issue 9, 102175

038_235

Development of Film-Based Elastocaloric Cooling Using Shape Memory Alloy Actuators

Yi-Ting Hsiau[1], Shuichi Miyazaki[2], Manfred Kohl[1], Jingyuan Xu[1]
[1]Institute of Microstructure Technology (IMT), Karlsruhe Institute of Technology (KIT), Karlsruhe, Germany. [2]Division of Materials Science, University of Tsukuba, Tsukuba, Japan

Elastocaloric cooling has emerged as a novel solid-state cooling technology with zero global warming potential and high energy efficiency. It relies on periodically applying uniaxial stress to caloric materials such as shape memory alloys (SMAs), inducing stress-driven temperature changes that can be harnessed for thermal management. However, the demands of electromechanical motors or hydraulic actuators with large force but small displacement limit practical applications. This mismatch leads to the difficulty of targeting ideal conventional actuation methods. In this work, we develop a new concept that utilizes thermally responsive SMA films as linear actuators to drive elastocaloric materials in cooling devices. Firstly, we employ one-way shape memory effect NiTi SMA films activated by Joule heating to produce linear actuation. The NiTi films are 30 µm thick and manufactured by cold rolling. The actuator film is mechanically cut into rectangular shapes to generate sufficient force and stroke. It is then annealed in a vacuum chamber to set the memory shape. Our developed thermally responsive SMA actuator unit can achieve a stroke of 180 µm and a force of 6 N when coupled with a biased superelastic SMA film. The actuation is sufficient to linearly load the superelastic SMA film to its transformation strain. Secondly, we test the performance of the cooling unit. It consists of a cold rolled 30 µm thick superelastic NiTiFe SMA film as the elastocaloric refrigerant and a pair of copper heat sink and heat source to separate the heat flows with periodic mechanical contact. The refrigerant film was shaped by ultra-short pulse laser cutting. A heat treatment process is needed to attain the superelasticity and electropolishing is followed to smoothen the surface roughness. Initial tests are performed by using two electric linear actuators, one applies tensile loading to the refrigerant film while the second one alters the thermal contact between the refrigerant film and the heat sink or heat source. The measured temperature span of the cooling unit with electric actuators is 4.9 K under 1 Hz operating frequency and 4 % strain. Currently, we are integrating the SMA actuator unit and the cooling unit to achieve a thermally responsive SMA-driven elastocaloric cooling system. Methods to shorten heating and cooling time are investigated in order to improve the overall device performance. We will present recent progress in system development and discuss its performance.

039_244

Elastocaloric effect covering wide temperature range in a Ti-Al-Cr shape memory alloy

Yuxin Song, Sheng Xu, Toshihiro Omori, Ryosuke Kainuma
Tohoku University, Sendai, Miyagi, Japan

Featuring high energy conversion efficiency, relatively cheap cost, and low environmental impact, elastocaloric cooling using shape memory alloys are promising next-generation cooling technologies to replace conventional vapor compression cooling systems. In most reported elastocaloric systems, Ni-Ti alloy is chosen as the caloric material due to its excellent cooling ability (adiabatic temperature change during phase transformation) around room temperature. However, Ni-Ti alloys typically operate within a narrow temperature range of typically less than 80 K, constrained by the strong temperature dependence of their superelastic behavior. *β*-type Ti-based alloys exhibit lower temperature dependence of superelasticity compared to benchmark Ni-Ti alloys, making them advantageous for applications requiring large temperature fluctuations, such as refrigerants for multimode elastocaloric cooling systems that leverage wide temperature spans. However, conventional β-type Ti-based shape memory alloys generally exhibit poor elastocaloric properties due to insufficient superelastic performance, characterized by low resistance to plastic deformation, which compromises the reversibility of martensitic transformation. Therefore, enhancing superelastic performance is crucial for improving elastocaloric properties. Recently, we have developed a new B2-ordered Ti-Al-Cr shape memory alloy with superior strength compared to conventional Ti-based alloys that also exhibits exceptional superelasticity across an ultra-wide temperature range. In this study, we investigated the elastocaloric properties during stress-induced martensitic transformation. The mechanical properties of the alloy were assessed through uniaxial compressive tests on [001]-oriented single-crystal samples at various temperatures. The adiabatic temperature change of the Ti-Al-Cr alloy at room temperature is approximately 10 K, which is about 1.5 times larger than the previous record for Ti-based alloys. Moreover, the functional temperature range exceeds 300 K. The adiabatic temperature change calculated from specific heat measurements agrees well with experimental values. The development of this Ti-Al-based alloy system presents a promising platform for practical elastocaloric refrigerants, with considerable potential for further optimization.

040_297

PLENARY: Development and challenges of Ni-free Ti-based biomedical superelastic alloys

Hideki Hosoda, Masaki Tahara, Naoki Nohira
Institute of Science Tokyo (Formerly: Tokyo Institute of Technology), Yokohama, Japan

Twenty years ago, Miyazaki, Kim, and I presented the development and characterization of Ni-free Ti-based shape memory and superelastic alloys at ICOMAT2005 (MSEA, vol. 438, 2006, pp. 18–24), focusing binary and ternary Ti-Nb and Ti-Mo-based alloys. At ICOMAT2025, we summarize the history of Ni-free Ti-based biomedical superelastic alloys and discuss current research directions in alloy development, particularly regarding the emergence of large superelastic strains at room temperature (RT). The β phase used in these alloys is a terminal solid solution of Ti, allowing Ti-based shape memory alloys (SMAs) to be designed without the use of toxic elements such as Ni.

The shape memory effect (SME) arises from the martensitic transformation between the body-centered cubic (bcc) parent phase (β phase) and the orthorhombic daughter phase (α" phase). The crystal structure of α" is intermediate between bcc β and hexagonal close-packed (hcp) α. This crystallographic similarity can be quantified using the axial ratio *b/a*: the α" structure is closer to bcc when *b/a* approaches √2 and closer to hcp when it nears √3 (√2 < *b/a* < √3). The lattice deformation strain between α" and β, which is essential for the shape recovery strain of Ti SMAs, increases as *b/a* value becomes larger. Thus, to achieve a large shape recovery strain, α" martensite with a crystal structure closer to hcp α is preferable. This crystal structure adjustment can be achieved by destabilizing the β phase, which is done by reducing the β-stabilizing contents. However, for RT superelasticity, the martensitic transformation temperature (M_s) must be sufficiently lower than RT. This requires the addition of an adequate amount of β-stabilizing elements. However, increasing β stability also shifts α" closer to the β phase, thereby reducing the shape recovery strain. Consequently, there is an inherent trade-off between enhancing shape recovery strain and lowering M_s. Overcoming this trade-off to develop Ti alloys with larger RT superelasticity remains a significant challenge.

Recently, instead of Nb (a continuous solid-solution-type β-stabilizer), eutectic-type β stabilizers such as Cr and Fe have attracted attention, as they can stabilize the β phase with small additions. Additionally, co-addition of large amounts of ω-phase inhibitors such as Al (an α-stabilizer) and Sn (a neutral element) has been explored. The latest researches on Ti-Cr-Sn alloys and other related systems will be presented.

041_47

PLENARY: A Multiscale Approach to the Structure and Migration of α/β Interfaces and Screw Dislocations in Titanium

Siqi Wang, Anwen Liu, Tongqi Wen, Han Wang, Jian Han, David J Srolovitz
The University of Hong Kong, Hong Kong, Hong Kong

Titanium (Ti) serves as the base material for many aerospace and biomedical applications and undergoes a martensitic transformation between a hexagonal (α) and entropy-stabilized body centered cubic (β) phase. In this presentation, we briefly outline the development of a DFT-trained machine learning potential for Ti that accurately predicts the structures, energies, elastic constants, thermal expansion, phase transition temperature, and defect properties (dislocation core structures, vacancy formation energies) of these allotropes. We then simulate the structure, thermodynamics and migration of the coherent and semicoherent Ti *α*/*β* interfaces as a function of temperature and misfit strain via molecular dynamics (MD) and thermodynamic integration. The structure of the equilibrium semicoherent interface consists of intersecting arrays of dislocation and steps (disconnection) from which we determine the habit plane. The MD simulations show the detailed interface morphology dictated by intersecting disconnection arrays. The steps facilitate *α*/*β* interface migration, while the misfit dislocations lead to interface drag; the drag mechanism is different depending on the direction of interface migration. These results are used to predict the nature of *α* phase nucleation on cooling through the *α*-*β* phase transition. Next, we combine MD simulations and kinetic Monte Carlo (kMC) methods to simulate the motion of an <a> screw dislocation in *α*-Ti. Several core structures are observed the free energy barriers for the core dissociation transitions and Peierls barriers for dislocation glide are calculated as a function of temperature (MD). This provides input to kMC simulations of dislocation dynamics as a function of temperature (which are compared with MD). On some planes, dislocations move via a locking-unlocking mechanism. Surprisingly, some dislocations glide in directions that are not parallel with the core dissociation direction. This presentation provides a picture of how defects move in Ti and a road map for multi-scale simulations of defect dynamics in complex materials.

042_179

Strain accommodation in microstructure development of lath-shaped martensite and bainite

Tadashi Furuhara, Goro Miyamoto
Tohoku University, Sendai, Miyagi, Japan

Current understanding of crystallography and interfaces of martensite and bainite in steels are summarized for discussion of uncertain problems. HRTEM observation has given good insights on transformation pathways of lath martensite, and also indicates the same atomic motion in lattice change of bainite transformation as an analogous displacive transformation. A major energetic barrier in transformation comes from accumulation of strain energy and thus, strain accommodation processes are very important to understand their transformation kinetics . It is considered that in-situ observation and advanced atomistic simulation of transformation sequences is more important in understanding natures of these displacive transformations.

043_157

The Role of Plastic Deformation in Martensitic Transformation of Low Carbon Steel

Hesham Salama, Oleg Shchyglo, Ingo Steinbach
Ruhr-University Bochum, Bochum, NRW, Germany

The complex interplay between the rapid martensitic transformation and the plastic relaxation during martensitic transformation in low-carbon steel is investigated using a combined phase-field and phenomenological crystal plasticity approach. The large transformation-induced deformations and local lattice rotations are rigorously described within the finite strain framework. The study reveals that plastic relaxation plays a crucial role in accommodating the transformation-induced deformations of martensite in the parent austenite phase. By systematically varying the plastic slip rate, imposed cooling rate, and carbon content, the simulations provide insights into the interdependence between these factors, contributing to a better understanding of the martensitic transformation process and the resulting microstructures. The phenomenological crystal plasticity model effectively relates the plastic relaxation rate to the rate of martensitic transformation with a significant time scale difference between the two processes. The findings contribute to a deeper understanding of the interplay between the rapid martensitic transformation and the requirement for plastic deformation.

044_275

In situ neutron diffraction study on the development of martensitic transformation in hydrogen-charged Type 316L steel at low temperature

Tatsuya Ito[1], Yuhei Ogawa[2], Wu Gong[1], Takuro Kawasaki[1], Akinobu Shibata[2], Stefanus Harjo[1]
[1]Japan Atomic Energy Agency, Tokai, Japan. [2]National Institute for Materials Science, Tsukuba, Japan

Elucidating the influence of hydrogen on the deformation mechanisms of steel is essential for ensuring the reliability and safety of hydrogen infrastructure. In this study, we focused on Type 316L austenitic stainless steel (Fe-17Cr-12Ni, mass%), a material widely employed in hydrogen infrastructure applications. This steel undergoes a martensitic transformation from γ (FCC) to ε (HCP) and/or α′ (BCC) phases when deformed at low temperatures. This transformation is closely associated with hydrogen embrittlement and is considered one of the key factors limiting the alloy's lower service temperature. Understanding the effect of hydrogen on this transformation is therefore crucial; however, it remains under debate whether hydrogen promotes or suppresses the transformation.

To address this issue, we employed *in situ* neutron diffraction to investigate the evolution of martensite phase fractions during low-temperature deformation of hydrogen-charged Type 316L steel. Neutrons, with their high penetration capability, enabled continuous monitoring of phase fraction changes throughout the deformation process, providing direct insight into the influence of solute hydrogen on the martensitic transformation.

Round-bar tensile specimens were prepared and exposed to hydrogen gas at 100 MPa and 543 K for 200 hours, achieving a uniform hydrogen concentration of 96 mass ppm. *In situ* neutron diffraction measurements at 177 K were conducted during tensile testing using a cryogenic loading machine equipped at TAKUMI, the pulsed neutron diffractometer at the MLF of J-PARC. The diffraction patterns of hydrogen-charged and non-charged specimens were analyzed and compared.

Before deformation, both specimens primarily consisted of the FCC matrix, with a small amount of δ-ferrite detected. As deformation progressed, diffraction peaks corresponding to ε and α' martensite phases emerged in both specimens and increased in intensity. Phase fraction analysis based on peak intensities revealed that hydrogen addition suppressed the development of α' martensite. Further details will be presented at the conference.

This study was supported by JSPS KAKENHI (JP23K19189, JP21K14045), the MEXT program (JPMXP1122684766), and the Iketani Science and Technology Foundation (0361224-A).

045_247

Sustaining the TRIP Effect in High-Strength Steels for Enhanced Mechanical Performance

Xuejun Jin
Shanghai Jiao Tong University, Shanghai, China

The TRIP (Transformation-Induced Plasticity) effect, driven by retained austenite, offers a promising pathway to mitigate the strength-ductility trade-off in high-strength steels while maintaining cost efficiency. This study systematically investigates the interplay of composition, phase/grain size, and morphology on austenite stability under external loading and thermal variations, with emphasis on thermodynamic and kinetic mechanisms. A critical challenge lies in sustaining the TRIP effect to enable delayed strain hardening, thereby achieving superior strength-ductility synergy and enhanced toughness.

By tailoring the metastability of retained austenite through composition gradients, domain dispersion, and morphology optimization, we demonstrate sustainable TRIP behavior in Quenching & Partitioning (QP) steels, medium-Mn steels, and additive-manufactured (AM) high-strength steels. Notably, AM-processed steels with finely dispersed austenite domains and heterogeneous carbon distribution exhibited exceptional work hardening, yielding tensile strength of ~1900 MPa, elongation of ~12.5%, and Charpy V-notch impact energy of ~40 J at moderate alloying levels. These results highlight the pivotal role of spatially graded austenite stabilization in balancing mechanical properties.

The proposed strategy extends beyond steels to martensitic-transformable materials, including titanium alloys, high-entropy alloys, and advanced ceramics, offering a universal framework for designing high-performance additive-manufactured components. This work underscores the potential of microstructure-engineered metastability to revolutionize multi-property optimization in structural materials.

046_274

Improving the ductility of ultrahigh-strength high-carbon martensite by prior bainitic transformation

Sien Liu, Shoichi Nambu
the University of Tokyo, Tokyo, Japan

The application of ultrahigh-strength martensite (M) is limited by its brittleness. As a solution, prior bainitic transformation along prior austenite grain boundaries (PAGBs) can enhance local deformability, which provides a route for designing bainite/martensite (B/M) steels with superior strength-ductility combinations. Studies have shown that higher carbon content and finer bainitic sheaves can improve the overall strength while, in turn, leads to slower bainitic transformation kinetic. On the contrary, prior martensite can accelerate bainitic transformation by altering bainitic nucleation sites from PAGBs to martensitic (M) interfaces. So far, various fabricating routes of B/M steels have been proposed whereas it is still hard to suggest an optimized microstructure. Moreover, the tensile deformation mechanisms of the B/M microstructure require further study.

In this study, we designed a novel high-carbon steel (0.83 wt.% C) and investigated two fabricating routes of B/M steel: either a direct bainite-to-martensite two step route (BM) or with prior martensitic transformation (MBM). The main objectives are to reveal the differences in mechanical properties and the deformation behaviors due to distinct bainitic nucleation sites.

Tensile specimens with 1 mm thickness were prepared by cold rolling. After austenization at 900ºC for 2 min, only the MBM group was oil quenched to 70ºC and held for 1h. Then both groups were isothermally held at 300ºC for various times and followed by oil quenching. Finally, both groups were tempered at 200ºC for 3 h. Uniaxial tensile tests were conducted to compare the mechanical properties and fracture mechanisms. OM, SEM and EBSD were performed to analyze and deformation behaviors.

The tensile results indicated that the BM group exhibited a superior strength-ductility combination of 2.6 GPa-10% with a transformation of 10 min. A little amount of prior lower bainite along PAGBs effectively enhances the ductility of ultra-high strength martensite. With longer bainitic transformation time, the bainite volume fraction continuously increased, leading to increased ductility and decreased tensile strength. On the other hand, the ductility of MBM specimens exhibited early fracture and poor ductility compared to those of the BM specimen with the same holding times. It is inferred that the bainite transformation site plays an important role on the overall mechanical properties.

047_171

Detwinning Elasticity of NiTi

Yuxuan Chen[1], Xiaobin Shi[2], Junsong Zhang[3], Yinong Liu[4]
[1]Hebei Vocational University of Technology and Engineering, Xingtai, Hebei, China. [2]Anhui University of Technology, Maanshan, Anhui, China. [3]Yanshan University, Qinhuangdao, Hebei, China. [4]The University of Western Australia, Perth, Western Australia, Australia

This study investigated the crystallographic and mechanical reversibility of detwinning deformation of the B19' and R phases in a nanocrystalline $Ni_{50.8}Ti_{49.2}$ alloy by means of *in-situ* X-ray diffraction analysis and crystallographic calculations. Due to the thermodynamic equivalence among different martensitic variants, reorientation and detwinning among them are generally considered irreversible. However, *in-situ* XRD measurement reveals reversible evolutions of crystallographic textures of both the B19' and the R phases during their respective detwinning deformation processes. The texture selection and evolution are confirmed by phenomenological crystallographic calculations to follow the principle of maximum macroscopic strain output in the direction of the applied stress. The reversibility of the texture evolution is explained on the basis of internal elastic stresses generated at the lattice correspondence variant pair boundaries by the detwinning process. Detwinning within a lattice correspondence variant pair jeopardizes the invariant plane criterion for the martensites, thus it incurs a crystallographic penalty in the form of local elastic lattice distortions. The local elastic stresses associated with these lattice distortions serve as the driving force for the reversal of the detwinning process (or retwinning of the lattice correspondence variant pairs) and macroscopic shape recovery. These findings provide insight into the fine deformation mechanisms of NiTi which helps to explain some unique mechanical behaviour of the alloy and to guide designs for some novel properties, such as low elastic modulus and linear pseudoelasticity.

048_370

Elastic instabilities in NiTi shape memory alloy

Petr Sedlak, Hanus Seiner, Miroslav Frost, Michaela Janovska
Institute of Thermomechanics, CAS, Prague, Czech Republic

NiTi shape memory alloy is the most commonly used shape memory material and one of the most studied in the literature. Despite significant progress in describing the properties of NiTi, some fundamental features have not been fully understood yet and are still the subject of active research. Already decades ago, it was discovered that NiTi alloy behaves very differently compared to other shape memory alloys in several aspects. Very unusual properties were observed in the elasticity of both austenite and martensite and its evolution with temperature.

In this contribution, we present an experimental study of the elastic properties of NiTi using several laser-ultrasonic techniques. Both single-crystal and fine-grained polycrystalline samples were analyzed over a wide temperature/stress range mapping the elastic properties of both pure austenite and martensite phases, as well as their evolution near and during the phase transformation. The most interesting conclusions from this analysis were:

- The martensitic transition during the cooling run is preceded by pronounced softening of the c_{44} elastic coefficient in austenite, which leads to nearly complete vanishing of its elastic anisotropy prior to the transition.
- The elastic anisotropy of martensite is large and remains large even at temperatures well below the transformation. This unusually large elastic anisotropy can be related to the theoretically predicted instability of the B19’ lattice with respect to (001)[100] slip.
- The elastic anisotropy of martensite is also transferred to polycrystalline samples with oriented martensitic microstructures. These exhibits strong elastic anisotropy with Young's moduli in different directions differing by several tens of GPa−s.
- The difference in elasticity between martensite and austenite increases with increasing temperature. This can be advantageously used to map transformation processes at elevated temperatures/stresses, where martensitic transformation is strongly coupled to plastic deformation.

[1] Bodnárová L. et al., Elastic Constants of Single-Crystalline NiTi Studied by Resonant Ultrasound Spectroscopy (2025) Shape Memory and Superelasticity.

[2] Thomasová M. et al., Evolution of macroscopic elastic moduli of martensitic polycrystalline NiTi and NiTiCu shape memory alloys with pseudoplastic straining (2017) Acta Materialia, 123, pp. 146-156.

The support of the MEYS CZ project Ferroic Multifunctionalities (CZ.02.01.01/00/22_008/0004591) is acknowledged.

049_373

Martensite Textures and Recoverable Strain Limits of NiTi: Taylor Model vs. Experiment

Luděk Heller, Petr Šittner, Lukáš Kadeřávek
Institute of Physics of the Czech Academy of Sciences, Prague, Czech Republic

The outstanding functional properties of polycrystalline NiTi are to large extent due to the ability of the monoclinic B19' martensite to accommodate constraints from neighbouring grains during stress-induced martensitic transformation or reorientation and detwinning. One explanation for this is the low symmetry of the martensite lattice, forming 12 variants. 6 of them provide linearly independent transformation deformation gradients thus fulfilling von Mises criterion for uniform deformation without failure at the grain boundary. This criterion, however, is formulated for unlimited plastic deformation via slip. In the case of NiTi, the deformation gradients are realized via twinning that has finite shear magnitudes. This impose limits on the macroscopic deformation that can be accommodated by martensite variants. These limits are obviously anisotropic and depends on the distribution of grain orientations withing the polycrystalline aggregate. For a successful NiTi application design, these deformation limits has to be determined for a NiTi component at hand. For highly textured NiTi, a single-crystal approximation has been used to date.

We have have implemented a purely kinematic Taylor model that enables to estimate the deformation limits for any initial austenite texture and macroscopic strain. Furthermore, the model helps interpret textures of deformed martensitic microstructures in terms of martensite variants distribution and available twinning systems. The physically plausible microstructures may be plugged into the model as particular sets of transformation deformation gradients. The model can simulate textures of deformed martensite thanks to its the relative simplicity, allowing to consider thousands of grains; a sufficient number to cover the whole orientation space.

We will present the model along with deformation limit predictions for representative textures and macroscopic deformations.

We will show how the model can capture texture evolutions of deformed martensites in two NiTi samples with different initial austenite texture. The model predictions of selfaccommodated textures and those induced by tension and compression will be shown to fit well measured textures obtained from dedicated ex-and in-situ synchrotron diffraction experiments as shown in Fig. 1.

Finally, morphology of detwinned microstructures in NiTi will be discussed in view of presented results as well as other experimental investigations available in literature.

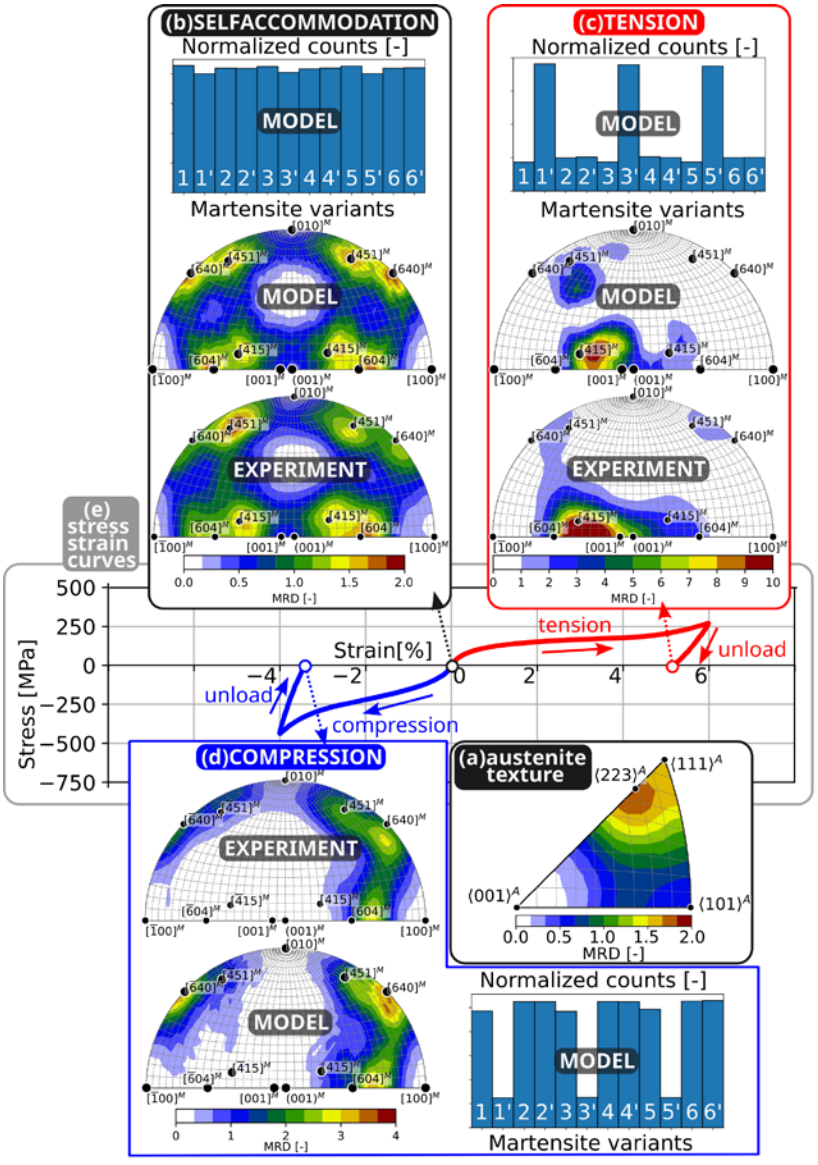

Fig. 1 Comparisons between experimentally identified and modeled martensite textures of a NiTi wire with austenite <223> fiber texture aligned with the wire axis (a). The martensite textures represented by inverse pole figures (IPFs) of the wire axis projected onto martensite (001) plane were identified and modeled in self-accommodated state after stress-free cooling from austenite (b), after tension (c) and compression (d) both applied to self-accommodated microstructures and followed by unloading as indicated by stress-strain curves in (e). IPFs in (a), (b), (c) depict martensite directions corresponding to austenite <223> fiber direction as well as martensite basal directions and (001) pole.

050_192

Energies of type II twin boundaries and martensite plates in NiTi

Meron Doar[1], Yuriy Chumlyakov[2], Eilon Faran[1], Doron Shilo[1]
[1]Technion, Haifa, Israel. [2]National Research Tomsk State University, Tomsk, Russian Federation

The martensitic transformation in shape memory alloys involves the formation of twinned martensite regions at the austenite-martensite phase boundaries. The twin boundary energy plays a significant role in determining the twinned microstructure, as well as the hysteresis and kinetics of the transformation. We present a systematic microscopy-based approach to analyze the microstructure of twinned martensite plates, enabling the identification of the twin system and extraction of the energies of twin boundaries and martensite plates. The method is applied to the abundant <011> type II twin boundaries in the B-II-1 system, in single crystals of NiTi. The obtained knowledge paves the route for modeling the macroscale evolution of the phase transformation based on material properties measured at the nanoscale.

051_367

A numerical tool to predict the dynamical behavior and the damping effect of Shape Memory Alloys: Application for design of NiTi based passive dampers.

Frédéric Thiebaud, Tarak Ben Zineb
Université de Lorraine, CNRS, Arts et Métiers Paris Tech, LEM3, F-54000, Nancy, France

It is actually well established that Shape Memory Alloys (SMAs) are highly suitable candidates for the design of damping applications. In fact, the martensitic transformation is a dissipative mechanism leading to a hysteretic thermomechanical behavior. This study concerns the development of a numerical prediction tool that characterizes the dynamic behavior of SMAs and their damping capability. The adopted approach is based on a complex modulus formulation using Valanis' endochronic theory and the harmonic balance method. Two loading conditions are investigated: mono-harmonic strain inputs without (i), and with the application of a pre-strain (ii). This numerical tool is based on the computation of key physical quantities related to the complex modulus: the storage modulus (associated with the material's ability to store and release mechanical energy), the loss modulus (quantifying energy dissipation), the loss factor (a measure of damping efficiency), and energy efficiency (defined as the ratio of dissipated to stored energy). The methodology begins with the calibration of a phenomenological macroscopic thermomechanical constitutive model to capture the specific SMA behavior with the finite element method. Then, virtual tensile tests are automatically simulated using a Python routine, by varying the vibration amplitude (case i), or both amplitude and pre-strain (case ii). A Matlab script is used to extract the complex modulus parameters and identify the optimal conditions maximizing the damping performance. Finally, the predictive capability of the numerical tool is validated through experimental DMA (Dynamic Mechanical Analysis) tests conducted on a NiTi SMA at room temperature. The results confirm the potential of this approach, which can be extended for the design of efficient passive damping systems considering other SMAs as Cu-based or Fe-based ones . The discrete characterization of the complex modulus as a function of strain amplitude (with or without pre-strain) will serve to feed into the axial vibration equation (tension-compression), enabling the prediction of the SMA's dynamic response under both free and forced vibration conditions. Additionally, all numerical simulations can be performed at various values of temperature in order to investigate the influence of thermal effects on the damping capacity.

052_238

Substructures and crystallographic features of as-quenched lath martensite in medium-carbon steel

Akinobu Shibata[1], Goro Miyamoto[2], Shigekazu Morito[3], Akiko Nakamura[1], Taku Moronaga[1], Houichi Kitano[1], Toru Hara[1]
[1]National Institute for Materials Science, Tsukuba, Japan. [2]Tohoku University, Sendai, Japan. [3]Shimane University, Matsue, Japan

Due to the growing demand for advanced high-strength steels aimed at enhancing efficiency in transportation and power generation, lath martensite structures have gained increasing attention. Although lath martensite is a common microstructure utilized in the design of high-strength steels, its structure has not been fully clarified, posing challenges to the development of novel advanced high-strength steels.

The present study investigated the substructures and crystallographic features of as-quenched lath martensite in a medium carbon steel (2Mn-0.5C steel) using focused ion beam-scanning electron microscopy (FIB-SEM) serial sectioning and automated crystallographic orientation mapping in transmission electron microscopy (ACOM-TEM).

A three-dimensional analysis reveals that the morphology of the smallest structural unit exhibits a plate-like shape rather than the ideal lath shape. The habit plane orientations determined by two-surface trace analysis are close to those predicted by the phenomenological theory of martensite crystallography with high tetragonality. Each martensite plate contains twin-related variants along with dislocations and transformation twins. The twin-related variants inside a martensite plate also exhibit a plate-like shape, with inter-variant boundaries oriented close to the $(1\ 1\ 1)_A$ // $(0\ 1\ 1)_M$ planes. Simple micromechanics calculations indicate that the formation of twin-related variants results from the low interaction energy with the stress field of austenite induced by the pre-formed martensite variant. This suggest that stress-induced variant selection could be the primary factor driving the formation of twin-related variants.

053_211

Phase-field simulation of internal stress distribution during martensitic transformation in low-carbon steel

Yuhki Tsukada, Akio Yoshida, Toshiyuki Koyama
Nagoya University, Nagoya, Japan

Internal stress and high dislocation density occur in martensite microstructure during martensitic transformation (MT) in low-carbon steel. Precise knowledge of the internal stress distribution is necessary for controlling microstructure evolution, including dislocation recovery, carbon diffusion, and carbide precipitation during the tempering process. Recent in-situ X-ray or neutron diffraction experiments have reported the change in average dislocation density and average hydrostatic stress during MT in both martensite (α′-bct) and austenite (γ-fcc) phases. In this study, a three-dimensional phase-field simulation of MT was performed to investigate the internal stress distribution during MT in Fe–0.1 mass% C alloy.

We developed a phase-field model in which the total free energy of the microstructure was formulated as the sum of chemical free energy, gradient energy, and elastic strain energy. The Gibbs energy difference between the γ-fcc phase and α-bcc phase was calculated and used as the driving force for MT. In the elastic strain energy formulation, the eigenstrain was defined by considering both the fcc-to-bct transformation strain (Bain strain) and the slip of the γ and α′ phases. The simulation of MT at 300 K was started by seeding a nucleus of the α′ phase in a γ-phase polycrystalline structure [1].

The simulation results showed that MT proceeded with the formation of clusters composed of three crystallographic orientation variants (Bain variants) of the α′ phase. When the α′ phase reached the γ grain boundary, plastic strain occurred in the adjacent γ grains, inducing further MT within the γ grains. The average dislocation density in the α′ phase rapidly increased at the beginning of MT and then became almost constant. In contrast, the average dislocation density in the γ phase gradually increased during MT. During MT, the average hydrostatic stress in the γ phase remained negative (compressive stress), whereas that in the α′ phase fluctuated slightly around zero. Notably, the average hydrostatic stress at the prior austenite grain boundary (PAGB) was continuously positive (tensile stress), and its magnitude was significantly large at the end of MT compared to that in the γ and α′ phases. It was found that the magnitude of hydrostatic stress was reduced at the PAGB in contact with the retained γ phase.

[1] Y. Tsukada *et al.*, Proceedings of the 7th International Symposium on Steel Science (ISSS 2024), pp. 49–54 (2024).

054_175

A novel observation of hcp martensite layer formed at bcc martensite lath boundaries in medium-Mn steel during quenching

Ru Ge, Haiwen Luo
University of Science and Technology Beijing, Beijing, China

Here we report the first observation of new *hcp* film phase, ε-martensite, formed at the martensite (α') lath boundaries with the width of about 10 nm in the quenched medium-Mn steel after a long diffusion annealing at high temperature, as identified by high-resolution transmission electron microscopy (HRTEM). The measured C content in ε-martensite by atom probe tomography (APT) is up to 1.7 wt%. We infer that such a high C concentration should result from the partition of supersaturated C atoms in the formed α' into the residue austenite (γ) at lath boundaries in the proceeding γ→α' transformation during quenching and the resultant C-enriched γ grains are not stable enough for being retained at the ambient temperature but transform to the *hcp* structure, the latter has an approximate 2 nm transitional layer at the α'/ε interface due to the presence of pronounced compressive stress produced during γ→α' transformation. Thermodynamic calculations on T_0 temperature indicate that such γ→ε transformation shall be due to both very high C content accumulated in the minor fraction of residue austenitic film and ultrahigh compressive stress produced on them during γ→α'. Furthermore, such a ε phase is not stable but gradually transforms to cementite during the subsequent annealing. In summary, we present the new phase transformations observed in medium-Mn steel during quenching and heating in this paper.

055_189

Deformation microstructure developed via anisotropic slip behaviour in lath martensite blocks of ultra-low carbon steel

Shohei Ueki[1], Shigekazu Morito[2]
[1]Kyushu University, Fukuoka, Japan. [2]Shimane University, Shimane, Japan

Lath martensite has a hierarchical microstructure consisting of prior austenite grains, packets, blocks, sub-blocks and laths in low-carbon steels. Although the martensite block exhibits anisotropic slip behaviour depending on the habit-plane orientation [1], the mechanism remains unknown. The misorientations between sub-blocks exhibit variety related to the habit-plane orientation [2], implying that the role of the sub-block boundary differs depending on the habit-plane orientation. Therefore, we focused on the deformed microstructures developed by the interaction between slips and sub-block boundaries. The present study examined the yielding behaviour and deformed microstructure using single-block micro-tensile specimens with different habit-plane orientations to elucidate the anisotropic slip behaviour. An ultra-low carbon steel was used to eliminate the effect of carbon and retained austenite. Two types of single-block specimens were prepared in which the angles between the loading direction and normal to the habit plane were roughly set to 0° and 45°. Tensile tests were performed at an initial strain rate of 2×10^{-3} s^{-1}, and the specimens were unloaded after the yielding. Subsequently, the deformed microstructure was characterised using electron back-scatter diffraction (EBSD) analysis. In situ observation of the yielding behaviour combined with the post-yielding EBSD analysis revealed that the shear stress required for the slip transfer across the sub-block boundary is clearly lower in the in-habit-plane direction than in the out-of-habit-plane direction. Although the in-habit-plane slip did not significantly change the misorientation within the sub-block, the out-of-habit-plane slip caused a significant change of the misorientation in the distribution related to the sub-block and lath boundaries. Furthermore, analysis of the rotation axis influencing the misorientation suggested that the edge dislocations gliding in the in-habit-plane direction easily traversed sub-block and lath boundaries, whereas the dislocations gliding in the out-of-habit-plane direction were inhibited by interaction with sub-block and lath boundaries. Therefore, it is plausible that the interaction between dislocations and low-angle grain boundaries is an important factor in the anisotropic slip behaviour of ultra-low carbon lath martensite.

[1] K. Kwak et al., Mater. Sci. Eng. A 856 (2022) 144007.

[2] T. Hayashi et al., Scr. Mater. 180 (2020) 1–5.

056_215

High-Rate Actuation of Shape Memory Alloys

Doron Shilo[1], Eilon Faran[1], Shahaf Vollach[1], Asaf Dana[2]
[1]Technion, Haifa, Israel. [2]Texas A&M University, Collage Station, Tx, USA

Actuators based on shape memory alloys (SMA) provide a unique combination of large stresses and strains that result in work per volume larger by more than two orders of magnitude than all other active material actuators. However, conventional SMA actuators suffer from slow actuation time. The question “how fast can the martensitic transformation be?” is elemental to the field of solid-solid phase transformations. However, the answer to this question remains obscure or experimentally unvalidated as in most studies the transformation rate is restricted by heat or momentum transfer and the applied driving force just slightly exceeds the threshold value required for overcoming the transformation barriers.

In the first part of the talk, I will present a study of the transformation kinetics in the large thermodynamic driving force regime by superheating a polycrystalline NiTi wire via a high-voltage heating pulse. The evolution of the transformation is tracked by microsecond-scale multi-frame, time-resolved X-ray diffraction (XRD) at synchrotron radiation with simultaneous high-bandwidth stress measurements. Our results show that the transformation in bulk actuator wires follows the heating rate, even at the microsecond scale. Further, I will discuss the effect of the microstructure and local mismatch strain on the transformation kinetics.

In the second part, we apply the knowledge presented in the first part to formulate design guidelines for high-rate SMA actuators with improved energy efficiency, larger travel per wire length, and shorter response and total actuation times, compared to slow-rate actuators. Specifically, we develop simulations of actuator response that can serve as accurate design tools; and map actuator performance into three regimes that enable users to quickly evaluate the expected output of their system.

057_343

How to transform martensite in NiTi within picoseconds

Klara Lünser[1,2], Bruno Neumann[3], Daniel Schmidt[4,5], Yuru Ge[3], Fabian Ganss[3], Daniel Hensel[4], Mariana Brede[4], Mallika Khosla[4], Sakshath Sadashivaiah[6,7], Peter Gaal[4,5], Sebastian Fähler[3]
[1]University Duisburg-Essen, Duisburg, Germany. [2]Research Center Future Energy Materials and Systems (RC FEMS), University of Duisburg-Essen, Duisburg, Germany. [3]Helmholtz-Zentrum Dresden-Rossendorf, Dresden, Germany. [4]Leibniz-Institut für Kristallzüchtung (IKZ), Berlin, Germany. [5]TXproducts UG haftungsbeschraenkt, Hamburg, Germany. [6]Helmholtz-Institut Jena, Jena, Germany. [7]GSI Helmholtzzentrum für Schwerionenforschung GmbH, Darmstadt, Germany

Most applications of shape memory alloys benefit from a fast transformation, e. g. for actuation and elastocaloric cooling, high cycle frequencies increase the power density of devices. Still, knowledge about the speed and possible speed limits of the martensitic transformation in the shape memory alloy NiTi is scarce, especially below the microsecond range.

Here, we report the fastest transformations in NiTi so far by heating an epitaxial NiTi film with a laser pulse and tracking the martensitic transition with in-situ synchrotron x-ray diffraction. When using a ns laser pulse, the martensite to austenite transition upon heating can proceed within the 7 ns pulse duration of the laser [1]. Recent experiments with a 200 fs laser pulse allowed to decrease the transformation time to around 150 ps, which is in the same range as the duration of the synchrotron pulse used to probe the transformation. We can thus conclude that the actual speed limit of the martensite to austenite transformation may not be reached yet with our experiments. The austenite to martensite transition is slower because cooling proceeds by conductive heat transfer into the substrate. With appropriate undercooling, we could decrease this part of the transformation to 10…200 ns. As we use epitaxial films, we can distinguish different variant orientations in diffraction. During cooling, we observe that some martensitic variants appear faster than others, hinting to the interplay between fast transformation and microstructure.

We compare our results to experiments on the Heusler alloy Ni–Mn–Ga [2, 3] and find similar trends, which reveal that during fast heating and cooling martensitic transformations in general behave similarly.

[1] K. Lünser et.al., J. Phys. Mater. 7, 045007, 2024

[2] S. Schwabe et.al., STAM 23(1) 633-641, 2022

[3] Y. Ge et.al., Mater Today Adv. 25, 100567, 2025

058_395

Elastic and Thermal Properties of NiTi investigated by Transient Grating Spectroscopy

Jakub Kušnír[1], Tomáš Grabec[1], Kristýna Repček[1], David Mareš[1], Klara Lünser[2], Sebastian Fähler[2], Pavla Stoklasová[1], Petr Sedlák[1], Hanuš Seiner[1]
[1]Institute of Thermomechanics, Czech Academy of Sciences, Prague, Czech Republic. [2]Helmholtz-Zentrum Dresden-Rossendorf, Institute of Ion Beam Physics and Materials Research, Dresden, Germany

NiTi and its epitaxial thin films are promising micromechanical systems with an interesting elastic and thermal properties. However, their properties are anisotropic, and there is only a limited number of methods that can be used for their comprehensive analysis. Transient grating spectroscopy (TGS) is a method that has been successfully used for the measurement of epitaxial single-crystalline thin films of NiTi.

TGS is a non-destructive, contactless and localized (spot size 500x100 μm^2) technique that can be used to determine the elastic and thermal properties of solid materials. The method uses two pulsed 1064 nm laser beams, which interfere on the sample surface, thus creating a spatially harmonic pattern acting as a thermoelastic source of acoustic waves. Probe beams of a continuous 532 nm laser are diffracted from the excited sample surface. The geometry of the TGS experiment ensures recombination with a reference beam which, thereby creating heterodyne detection. The relative phase shift between the diffracted and reference beam (the heterodyne phase) influences the information obtained. The ideal signal is obtained when the heterodyne phase is set to ($\pm\pi/2$), where the detected signal is a combination of propagating surface acoustic waves in a selected propagation direction and a gradual decline of thermal peaks due to heat homogenization.

The presented study will show advantages of the combined measurement of thermal and elastic properties of the NiTi films by TGS. The films were studied in both austenite, where epitaxial strains may affect the elasticity, and martensite, where effective elasticity depends on the obtained mixture of the martensitic variants. However, TGS allows for the in-situ characterization of the thermal and elastic behaviour across the transformation, which may provide a unique insight into the specifics of phase transformation of single-crystalline NiTi thin films.

T. Grabec et al., Ultrasonics 138, 2024

P. Stoklasová et al., Exp. Mech. 61, 2021

J. Kušnír et al., J. Appl. Phys. 133, 2023

K. Lünser et al., J. Phys. Mater. 6(3), 2023

This work was financially supported by the Ministry of Education, Youth and Sports of the Czech Republic in the frame of the project 'Ferroic multifunctionalities' (project No. CZ.02.01.01/00/22_008/0004591).

059_289

Dynamic characterisation of NiTi during martensite–austenite transformation

Carolina Guerra, Arthur Ford, Wenqi Li, Rafael Fuentes-Dominguez, Rikesh Patel, Richard J. Smith, Matt Clark
The University of Nottingham, Nottingham, United Kingdom

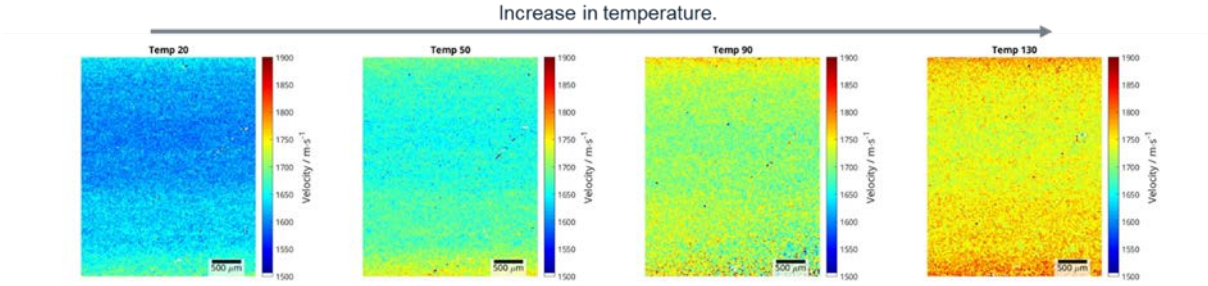

Figure 1. Velocity maps of NiTi in relation to the increase in temperature.

Characterising the visual transformation of martensite into austenite in NiTi (nickel-titanium) alloys when temperature is applied is challenging compared to existing methods. Continuous monitoring is essential for understanding the phenomena that occur in shape memory alloys, as it allows us to predict the material's properties at various transformation percentages. In this presentation, we will introduce Spatially Resolved Acoustic Spectroscopy (SRAS), which can measure the stiffness tensor of different phases at varying temperatures [1].

The SRAS technique utilises laser ultrasonics to robustly and repeatably measure the surface acoustic wave (SAW) velocity. These measurements can then be mapped to reconstruct the microstructure [2], making it a powerful tool for material characterisation, capable not only of imaging the microstructure, but also identifying the crystallographic orientation of each grain and determining the stiffness tensor of various engineering alloys. Additionally, it is a non-destructive and versatile technique, allowing for the rapid measurement of large and real components compared to other techniques like tensile stress and Electron Backscatter Diffraction (EBSD).

The results indicate that it is possible to determine the phase proportions (tetragonal and cubic structures) during dynamic transformations, as is shown in Figure 1, at different temperatures, which allows for the prediction of mechanical properties at each phase. Analysis of the SAW through velocity maps shows that the velocity increases with temperature due to phase transformation, even though, in other materials, it typically decreases due to a decline in stiffness. We will present the ability to image and identify the austenite phase starting (As) and finishing (Af) temperatures [3]. This achievement allows for real-time observation of phase change occurring under various stimuli, creating valuable research opportunities in the context of shape memory alloys.

References

[1] Paul Dryburgh et al. Acta Materialia (2022) DOI: 10.1016/j.actamat.2021.117551

[2] Rikesh Patel et al. Scripta Materialia (2017) DOI: 10.1016/j.scriptamat.2017.07.003

[3] Xi Xie et al. European Journal of Mechanics-A/Solids (2025) DOI: 10.1016/j.euromechsol.2025.105656.

060_305

Variant Selection in Polycrystalline CuAlNi and NiTi Shape Memory Alloys Investigated with In-Situ X-ray Topotomography

Janice Moya[1], Wolfgang Ludwig[2,3], Timothy Thompson[1], Jonathan Wright[2], James Ball[2], Adam Creuziger[4], Ashley Bucsek[1]
[1]University of Michigan, Ann Arbor, Michigan, USA. [2]European Synchrotron Radiation Facility, Grenoble, France. [3]INSA Lyon, Villeurbanne, France. [4]U.S. National Institute of Standards and Technology Science, Gaithersburg, Maryland, USA

Understanding habit plane variant (HPV) selection is critical for predicting and engineering the properties of materials that undergo martensitic phase transformations. In this study, we employ three-dimensional (3D) in-situ X-ray topotomography to resolve 3D martensitic microstructures during stress-induced transformation with sub-micrometer spatial resolutions and over millimeter-sized fields of view. X-ray topotomography is an X-ray diffraction imaging technique that captures a full 360-degree view of individual grains by aligning the tomographic rotation axis with the crystal's scattering vector. In this study, topotomography enables 3D imaging of the austenite parent grain and, by way of diffraction contrast, the developing martensitic domain structures. The in-situ topotomography experiments were performed at beamline ID11 of the European Synchrotron Radiation Facility. These experiments were used to investigate HPV selection criteria during stress-induced transformation in polycrystalline copper-aluminum-nickel (CuAlNi) shape memory alloys (SMAs). Building on the established single-crystal selection theories of maximum transformation work and resolved shear stress, we propose a new criterion: In addition to maximizing transformation work, the simple shear deformations introduced by the martensite should minimize the rotation of grain boundaries. Using 3D imaging, we characterize key features of this evolution, including nucleation at triple junctions, grain boundary interactions, and the formation of multiple intersecting martensite variants. These findings advance HPV selection models for polycrystalline SMAs, with future studies extending these principles to nickel-titanium (NiTi) SMAs.

061_386

3D Characterization of Austenite-Martensite Microstructures During Mechanical Loading Using In Situ Dark-Field X-Ray Microscopy and X-Ray Topotomography

Celeste Perez[1], Sangwon Lee[1], Janice Moya[1], Raqual Rodriguez-Lamas[2], Can Yildirim[2], Carsten Detlefs[2], Wolfgang Ludwig[2], Jonathan Wright[2], Othmane Benafan[3], Evan Rust[4], Adam Creuziger[4], Ashley Bucsek[1]
[1]University of Michigan, Ann Arbor, MI, USA. [2]European Synchrotron Radiation Facility, Grenoble, France. [3]NASA GRC, Cleveland, OH, USA. [4]NIST, Gaithersburg, MD, USA

This presentation explores the use of next-generation x-ray diffraction imaging techniques—dark-field x-ray microscopy (DFXM) and x-ray topotomography—to shed new light on martensitic phase transformations. By imaging in the diffraction condition, these advanced x-ray characterization techniques enable strain, orientation, and phase mapping with spatial resolutions on the order of 100 nm, resulting in the capability to resolve fine microstructure features. Moreover, DFXM and x-ray topotomography can be performed *in situ*, on bulk materials, and in three dimensions (3D). Applied to martensitic phase transformations, the result is a look into evolving martensitic microstructures in 3D during stress-induced transformation, including austenite-martensite interfaces, interfacial stress fields, and even dislocations. Here, we discuss the application of these techniques to Cu-Al-Ni and Ni-Ti-Pd shape memory alloys during tensile loading and unloading. The results reveal the nucleation behavior of martensite near triple junctions, the growth behavior of martensite in relation to local stress concentrations, the effect of granular constraints on habit plane variant selection, and the relationship between martensite volume fraction and residual stresses. Finally, we discuss differences in martensite morphology and interfacial stresses in cubic-to-orthorhombic versus cubic-to-monoclinic Ni-Ti-Pd shape memory alloys.

062_260

Application of full-field measurement techniques for the thermomechanical analysis of Ti-26Nb, Ti-25Nb-0.3O and Ti-25Nb-0.3N shape memory alloys under tension

Karol Golasiński[1], Michał Maj[2], Sandra Musiał[2], Wataru Tasaki[3], Hee Young Kim[4]
[1]Multidisciplinary Research Center, Cardinal Stefan Wyszynski University in Warsaw, Warsaw, Poland. [2]Institute of Fundamental Technological Research, Polish Academy of Sciences, Warsaw, Poland. [3]Institute of Fundamental Technological Research, Polish Academy of Sciences, Tsukuba, Japan. [4]Department of Materials Science, Institute of Pure and Applied Sciences, University of Tsukuba, Tsukuba, Japan

This work deals with the thermomechanical behavior of Ti–26Nb, Ti–25Nb–0.3O and Ti–25Nb–0.3N (at. %) shape memory alloys (SMAs) under load-unload tension. These SMAs exhibit superelasticity with recoverable strain of around 2% due to the to the stress–induced β–α″ phase transformation [1]. Recently, it was demonstrated that the deformation of this class of SMAs shows inhomogeneous features [2]. In this study, full–field measurement techniques of digital image correlation and infrared thermography were simultaneously applied to monitor load-unload tensile tests of Ti–26Nb, Ti–25Nb–0.3O and Ti–25Nb–0.3N SMAs at the strain rate of around 0.02 1/s. Based on the determined temperature and kinematic fields, global and local thermomechanical characteristics of the SMAs during tensile loading and unloading were compared. The kinematic fields demonstrated that the SMAs exhibited inhomogeneous deformation from the beginning of the loading process. It started with the appearance of thin parallel bands perpendicular to the loading axis. Upon further loading, these bands formed larger areas with higher strain and reappeared upon unloading. Furthermore, it was shown that the average temperature change can effectively serve to estimate deformation stages of the Ti–26Nb, Ti–25Nb–0.3O and Ti–25Nb–0.3N SMAs, including true elasticity accompanied by a temperature drop, as well as superelasticity with exothermic loading and endothermic unloading. Significant temperature increase and decrease exceeding 14 K were generated in all the SMAs during loading and unloading, respectively. The Ti–25Nb–0.3N SMA, demonstrated the highest temperature change per cycle (over 16 K), the highest recoverable strain and a relatively low critical transformation stress.

Acknowledgments
Karol M. Golasiński acknowledges the support of the Japan Society for the Promotion of Science (JSPS) Postdoctoral Fellowship ID No. P20812 and the National Science Centre, Poland through the Grant 2023/48/C/ST8/00038. The authors would like to express their gratitude to Leszek Urbański from IPPT PAN for conducting tensile tests.

References
[1] Miyazaki S. Shap Mem Superelasticity. 2017;3:279–314.
[2] Golasiński KM et al. Metall Mater Trans A. 2024;55:2509–2518.

063_281

Mechanical splicing of superelastic Cu-Al-Mn alloy bars with rolled threads

Sumio Kise[1], Toshihiro Omori[2], Ryosuke Kainuma[2], Minoru Nishida[1,3], Yoshikazu Araki[4]
[1]Special Metals Division, Furukawa Techno Material Co., Ltd., Hiratsuka, Kanagawa, Japan. [2]Department of Materials Science, Graduate School of Engineering, Tohoku University, Sendai, Miyagi, Japan. [3]Department of Advanced Materials Science and Engineering, Faculty of Engineering Sciences, Kyushu University, Kasuga, Fukuoka, Kasuga, Fukuoka, Japan. [4]Department of Architecture and Architectural Engineering, Graduate School of Kyoto University, Kyoto, Kyoto, Japan

In recent decades, applications of shape memory alloys (SMAs) with shape recovery properties by superelasticity to large structures such as buildings and bridges have attracted considerable attention in the fields of structural engineering and earthquake engineering to improve their resistance to earthquakes. In such applications, connecting superelastic alloy rods to steel rods is a major challenge. Mechanical splicing by means of thread ends is the most widely used technique for connecting steel bars, in which threads are usually formed by plastic deformation through the thread rolling process because of its low cost and high toughness. However, it is difficult to plastically deform SMAs with the ability of shape recovery.

Cu-Al-Mn SMAs with about 17 at%Al are characterized by high cold-workability, and its single crystals with the $L2_1$ structure can exhibit excellent superelasticity. The material is solution-heat-treated and quenched from high temperature around 1173 K and subsequently aged between 373 and 473 K. Before aging, the degree of $L2_1$ order is low [1], and therefore, it is expected that the superelasticity is insufficient and that plastic deformation is easily introduced. In this study, we attempted roll threading of single crystal Cu-Al-Mn SMA members without losing their good superelasticity that is obtained by aging.

It was demonstrated in this feasibility study that roll threading of Cu-Al-Mn SMA bars is possible in the as-quenched condition. Since additional heat treatment from the ordinary manufacturing process is unnecessary, roll threading of Cu-Al-Mn SMA bars is as easy as that of steel bars. After aging at 423 K for 0.5 h, the threaded bars showed superelasticity. Moreover, it was found that the roll threads have significantly superior fatigue resistance without fracture up to 500 cycles compared to the cut threads which showed brittle or fatigue fracture. These results suggest that the mechanical splicing of superelastic Cu-Al-Mn SMA bars with rolled threads is feasible for structural and earthquake engineering applications.

[1] R. Kainuma et al., Metall. Mater. Trans. A 27 (1996) 2187.

064_195

Enhancement of Shear-Band Formation During Bending through Tempering and Its Influence on Crack Suppression in Low-Carbon Martensitic Steel

Naoki Maruyama[1], Yoshiaki Honda[2], Shinichiro Tabata[2], Shigeru Yonemura[2], Tomohito Tanaka[2]
[1]The University of Osaka, Suita, Osaka, Japan. [2]Nippon Steel Corporation, Futtsu, Chiba, Japan

High-strength martensitic steel is increasingly being used in vehicle body frames and reinforcements to achieve lightweight structures and improve crash performance. During automotive crashes, structural components fold and bend, resulting in severe tight-radius bending in the folding regions. Because crash performance deteriorates when cracks form in these severely bent areas, understanding the relationship between the failure mechanisms and microstructure during bending is necessary. This study investigated the microstructural factors that govern the formation of shear bands and surface cracks during three-point bending tests in low-carbon lath martensitic steel, with a focus on the tempering effect. The deformation behavior of the outer surface was mainly characterized *in situ* using scanning electron microscopy with a three-point bending apparatus.

During bending, finely striated steps and elongated notches formed on the surface, which were attributed to the block boundary sliding along the $\{110\}_\alpha$ in-habit-plane slip systems and the formation of shear bands, respectively. Boundary plasticity dominated the subsurface deformation in the as-quenched martensite, while shear-band formation was enhanced by tempering at ≥200 °C, with a more pronounced effect at higher tempering temperatures. The activation of shear banding in tempered martensite is likely due to the enhanced simultaneous activation of multiple slip systems, including out-of-habit-plane slip systems. In AsQ martensite, surface cracks are often initiated near less-deformed hard martensite packets, which are assumed to sustain higher stresses during bending. Tempering at temperatures of ≥200 °C retarded the initiation and growth of the surface cracks. The promotion of shear bands by tempering reduces the area of less-deformed hard martensite packets. The suppression of crack initiation and growth by tempering is also attributed to the increased local formability at the shear bands and crack tips, which is primarily due to the enhanced activation of multiple slip systems. The formation of shear bands is often considered to be harmful to surface cracking because they are accompanied by surface notches or grooves that function as crack initiation and propagation sites. However, the present results indicate that the positive effect of the microscopic and macroscopic stress reduction at the bend apex by shear banding surpasses the negative effect, particularly for quenched lath martensite.

065_381

Competing effects of grain refinement and $Cr_{23}C_6$ carbide precipitation on martensitic transformation behavior in low-Ni austenitic stainless steel

Yeonggeun Cho[1], Hyung-Jun Cho[1], Han-Seop Noh[2], Sung-Ho Kim[1], Sung-Joon Kim[1]
[1]POSTECH, Pohang, Gyeongsangbuk-do, Korea, Republic of. [2]POSCO, Pohang, Gyeongsangbuk-do, Korea, Republic of

Low-Ni (less than 3 wt.%) austenitic stainless steels with varying C contents were designed and heat treated to compare the effects of grain refinement and $Cr_{23}C_6$ carbide precipitation on deformation-induced martensitic transformation (DIMT) behavior. High yield strength (>600 MPa) with good tensile elongation (>45 %) was achieved through both grain refinement and $Cr_{23}C_6$ carbide precipitation, but the DIMT behavior was markedly different. Grain refinement to 2~3 μm suppressed DIMT by increasing austenite stability, resulting in a reduced strain hardening rate. In contrast, the formation of fine, homogeneously distributed $Cr_{23}C_6$ carbides within austenite grains promoted DIMT by depleting Cr and C concentrations, thereby destabilizing austenite and enhancing the strain hardening rate. The competing effects of grain refinement and $Cr_{23}C_6$ carbide precipitation on DIMT led to an overall increase in strain hardening rate, as the destabilizing effect of carbide precipitation dominated. Further Olson-Cohen analysis revealed that stacking fault energy and thermodynamic driving force for the γ → α' transformation varied with C content and annealing conditions. These findings demonstrate an effective strategy for tailoring martensitic transformation behavior in high-performance low-Ni austenitic stainless steels.

066_256

Plastic Deformation Mechanism of Low-Carbon Steel Lath Martensite by Multiscale Deformation Analysis

Shuang Gong, Junya Inoue
The University of Tokyo, Tokyo, Japan

This study investigates the dislocation dynamics involved in the plastic deformation of lath martensite in low-carbon steel, by employing a synergistic approach combining in-situ tensile Electron Channeling Contrast Imaging (ECCI) analysis and Molecular Dynamics (MD) simulation. The hierarchical structure of lath martensite results in anisotropic deformation behavior, critically affecting its mechanical properties. By directly observing dislocation motion and performing computational modeling, the key mechanisms of plastic deformation are analyzed.

In-situ ECCI analysis during tensile testing reveals dislocation activity within lath interiors. Analysis of dislocation motion identifies intra-lath crystallographic slip and boundary sliding as the primary deformation modes. Dislocations start moving at relatively low stress and, as stress increases, gradually overcome obstacles within the lath, leading to macroscopic yielding. In-lath-plane dislocations travel farther than out-of-lath-plane dislocations, contributing to the anisotropy in slip system activity. For boundary sliding, lath boundary sliding initiates after a certain extent of deformation within the lath.

MD simulations further provide insight into the evolution of dislocation networks at grain boundaries. For low-angle twist grain boundaries, the critical resolved shear stress (CRSS) is closely correlated to the ratio of <111> screw dislocations to <100> screw dislocations within the dislocation network. The motion of in-out edge dislocations plays a crucial role in modifying the dislocation network structure. For high-angle twist grain boundaries, specific variant pair boundaries exhibit enhanced sliding behavior due to their unique atomic arrangements.

067_268

Variant selection in deformation-induced martensitic transformation during tensile deformation of ultrafine grained metastable austenitic steel

Yuanhong Liu, Si Gao, Myeongheom Park, Nobuhiro Tsuji
Kyoto University, Kyoto, Kyoto, Japan

This study has investigated variant selection in deformation-induced martensitic transformation (DIMT) and resultant microstructure changes during tensile deformation of ultrafine grained (UFG) Fe-24Ni-0.3C metastable austenitic steel. UFG specimens with a mean grain size of 0.8 *μm* were deformed to different strains in tension at room temperature, during which identical area observations were carried out. In tensile deformation, DIMT from austenite (FCC) to martensite (BCC) occurred, where martensite exhibited progressive growth with tensile strain increased. Mobile martensite/austenite interphases and twinned substructures were observed, both of which were characteristic features of thin-plate martensite. It was confirmed that the martensite maintained Kurdjumov-Sachs (K-S) orientation relationship with austenite with small deviation angles. Compared to coarse-grained specimens, UFG specimens exhibited significantly fewer K-S martensite variants within each prior austenite grain. A strong texture of $<110>_{bcc}$ parallel to tensile axis (TA) developed in martensite during deformation, indicating a variant selection during DIMT. The variant selection was analyzed in terms of accommodation of transformation strain based on the phenomenological theory for martensitic transformation. It was found that the shape strain of pre-formed martensite variants was rarely reduced by the formation of new neighboring variants, and even twin-related variants showed no significant accommodation of shape strain. Furthermore, within each micro-scale region, the total transformation strain of multiple variants formed in adjacent austenite grains remained comparable to that of a single variant, suggesting limited self-accommodation among martensite variants. Instead, the selected variants predominantly exhibited high transformation strain components along TA, aligning under the applied stress/strain field. Statistical analysis revealed that grain refinement intensified such an interaction, further enhancing the variant selection. These findings highlight the crucial role of local strain states in triggering DIMT and determining the transformation pathways including the formation of specific crystallography variants.

068_263

Fatigue crack growth in metastable austenitic stainless steels related to martensitic transformation-induced hydrogen embrittlement

Yuhei Ogawa[1], Osamu Takakuwa[2]
[1]National Institute for Materials Science, Tsukuba, Japan. [2]Kyushu University, Fukuoka, Japan

Strain-induced transformation to BCC (BCT) martensite from metastable austenite (FCC) in Fe-Cr-Ni-based stainless steels is a promising way to enhance their strength-ductility balance. However, despite its usefulness in a wide range of engineering applications, such FCC-to-BCC martensitic transformation during mechanical loading becomes, in reversal, harmful phenomenon that triggers embrittlement under the presence of solute hydrogen (*i.e.*, hydrogen embrittlement). The present study specifically focuses on the martensitic transformation occurring in the local zone around a fatigue crack in metastable 300-series austenitic stainless steels and related changes in the crack propagation rate.

AISI Type304 and 316L stainless steels having diverse austenite stabilities were subjected to fatigue crack growth (FCG) experiments under hydrogen pre-charged condition (internal hydrogen of ~95 mass ppm) and in a pressurized gaseous hydrogen environment (external hydrogen of 90 MPa at ambient temperature). Due to its lower phase stability, significant hydrogen-induced acceleration of FCG rate was confirmed in Type304 steel, while the acceleration was minute in 316L. Nevertheless, the Type304 steel exhibited an abnormally slower FCG rate under internal hydrogen than external hydrogen although the estimated crack-tip hydrogen concentration was greater for the former situation. In the presentation, this newly found anomaly will be interpreted based on the hydrogen-related alteration of deformation character inside the plastic zone surrounding the fatigue crack. In particular, inhibition of dislocations cross-slip (*i.e.*, planar dislocation glide) or enhanced deformation twinning play the vital roles in determining the propensity for strain-induced phase transformation. The importance of the sequence between hydrogen absorption and phase transformation in the crack-tip zone will also be highlighted.

069_317

Complex Thermomechanical Loading Paths for High Temperature Shape Memory Alloys

Dimitris C Lagoudas, Adrien Cassagne, Jean-Briac Le Graverend
Texas A&M University, College Station, Texas, USA

This work studies the impact of complex thermomechanical loading paths on the response of a NiTiHf High Temperature Shape Memory Alloy (HTSMA). Two types of loadings were performed: out-of-phase loadings involving a simultaneous increase of stress and decrease of temperature and in-phase loadings involving a simultaneous increase of stress and temperature. Various maximum stress levels were studied for a given temperature range. 3D Digital image correlation (DIC) and thermal imaging allowed a detailed analysis of the nucleation and evolution of martensite and irrecoverable strains. Experimental results showed differences in the phase transformation and irrecoverable strains along with transformation temperatures, depending on the type of the loading path. A crystal plasticity approach was adopted to model the different responses observed. A continuum thermodynamics approach guided a phenomenological modeling for austenite-martensite transformation and transformation induced plasticity strains. A mean field-based framework was developed to represent the macro-micro scale modeling and scale transitions that also incorporate interaction among grains and intergranular hardening. Overall, the proposed modeling provided a satisfying description of the strain evolutions witnessed in the experimentally conducted complex thermomechanical loading paths.

070_323

Shape memory behavior of additively manufactured Ti-Ta high-temperature shape memory alloy lattice structures

Christian Lauhoff[1], Mikkel Nobach[1], Alexander Medvedev[2], Shudong Luo[2], Tingting Song[2], Bettina Seiler[3], Eslam Abdelhady[4], Melanie Stenzel[5], Markus Weinmann[5], Mehrshad Mehrpouya[4], Ma Qian[2], Wei Xu[6], Andrey Molotnikov[2], Thomas Niendorf[1]
[1]University of Kassel, Kassel, Germany. [2]RMIT University, Melbourne, Australia. [3]Chemnitzer Werkstoffmechanik GmbH, Chemnitz, Germany. [4]University of Twente, Enschede, Netherlands. [5]Taniobis GmbH, Goslar, Germany. [6]Deakin University, Geelong, Australia

In light of current ecological and economic challenges, the development of resource and energy efficient components and processes is paramount. Shape memory alloys (SMAs), a class of smart materials, are high-potential candidates for fulfilling these requirements. Their unique shape memory behavior is the result of a thermoelastic solid-state phase transformation between a high-temperature austenitic parent phase and a low-temperature martensitic product phase. As SMAs can provide very high work output per unit volume, for instance, design concepts based on these materials allow for the realization of compact solid-state actuators with extraordinary lightweight potential. To date, binary Ni-Ti is the most widely employed SMA system. However, the inherent application temperature limit of about 80 °C hinders its technological breakthrough in fields like the aerospace and energy sectors, where operating temperatures often exceed 100 °C. Hence, alloy systems with increased martensite start temperatures ($M_s \geq 100$ °C), so-called high-temperature (HT-)SMAs, have been designed and introduced in the last decades in order to extend the application temperature range. Among the numerous HT-SMA systems introduced so far, Ti-Ta alloys are seen as promising candidates due to their relatively high M_s temperatures combined with excellent workability and transformation strains in polycrystalline state of up to ~4%.

In the present work, filigree near-net shaped parts (also referred to as lattice structures) have been fabricated from pre-alloyed Ti-30Ta (at.%) HT-SMA powder feedstock employing laser beam powder bed fusion (PBF-LB/M). Microstructural features and their evolution along the entire process chain, i.e. from powder material to additively manufactured structures in both as-built and post-processed heat-treated conditions, were characterized in depth employing optical microscopy (OM), computed tomography (CT) as well as scanning electron microscopy (SEM). Furthermore, for the first time, superior shape memory behavior with recovery strains of around 2% at temperatures well above 100 °C is shown for Ti-Ta HT-SMA lattice structures. Thermal cycling under superimposed tensile stresses was conducted accompanied by digital image correlation (DIC), allowing for deep insights into the local strain distribution and the evolution of functional degradation.

071_357

Effects of Chemistry and Annealing Treatments on HTSMA Ni-Ti-Hf-Nb Alloys

Alberto Coda, Jannis Nicolas Lemke, Carlo Alberto Biffi, Jacopo Fiocchi, Ausonio Tuissi
CNR-ICMATE, Lecco, Italy

In the field of high-temperature shape memory alloys (HTSMA), Ni-Ti-Hf system has been extensively investigated to achieve higher transformation temperatures than standard binary NiTi. Steady progress has been made on specific systems, like Ni-rich NiTi-20Hf, and thermo-mechanical treatments have been elaborated to tailor the high temperature transformation behavior. On the other hand, the development of ternary Ni-Ti-Hf alloys is still far from a wide commercialization due to their low processability and sometimes poor functional properties despite many efforts. In order to optimize the desired HTSMA characteristics, adding a fourth element has been demonstrated to be a promising route for improving key issues of these materials.

Among several investigated systems, Ni-Ti-Hf-Nb quaternary system was recently explored and emerged as particularly promising for a sustainable development of HTSMA components, due to superior mechanical properties of its alloys compared to those of the ternary Ni-Ti-Hf system. The ductility of Ni-Ti-Hf increases significantly by adding Nb, allowing the formation of a soft eutectic network composed of shape memory matrix phase and a not transforming β-Nb phase at the grain boundaries. But the impact of annealing treatments on the microstructure, workability, and high temperature martensitic transformation of the system has not been investigated yet.

In this work, small vacuum arc melted ingots of eight different Ni-Ti-Hf-Nb chemistries, respectively Ni-rich and Ti-rich, with two Hf contents (15 and 20 at. % Hf) and different Nb content (4,0 and 8,0 at. %) were prepared and benchmarked against ternary NiTi-15Hf and 20Hf reference alloys. Samples of 2 mm thickness were EDM cut, cleaned, and homogenized at 1273K for 24 hours under vacuum followed by furnace cooling. An annealing campaign consisting of solution (1173K for 30 min, followed by quenching in water) and aging (823K for 3 h) heat treatments was then carried out.

The microstructure of homogenized, solution treated and aged samples was investigated by scanning electron microscopy (SEM) and by X-ray diffraction (XRD). The martensitic transformation of these alloys before and after heat treatments was explored by differential scanning calorimetry (DSC), while the workability properties were assessed by hot rolling tests.

The impact of chemistry and annealing parameters on microstructure and martensitic transformation will be presented and discussed.

072_212

On designing Aging of Stress-Induced Martensite in Order to Produce High Temperature Shape Memory Alloys

D.L. Beke[1], Asmaa A. Azim[1,2]
[1]Solid State Physics Deprtment, University of Debrecen, Debrecen, Hungary. [2]Faculty of Science, Ain Shams University, Cairo, Egypt

Production of shape memory alloys, SMAs, with high martensitic transformation temperatures, MT, is important for industrial applications using sensors and actuators. One effective way to increase the transformation temperatures is aging of stress-induced martensite under stress, called SIM-aging, based on symmetry conforming short rage ordering in martensite. It requires high temperatures enough for effective diffusion resulting the requested short range ordering. Two factors are considered as necessary conditions for effective SIM aging in the literature: i) large T_0/T_m ratio (T_0 and T_m are the equilibrium transformation temperature and the melting point, respectively) ii) small value of the slope of the Clausius-Clapeyron relation: $d\sigma_0/dT=-\Delta s/\Omega\varepsilon^{tr}$ (>0) ($\Delta s(<0)$ *i*s the entropy of the austenite to martensite transformation, Ω is molar volume and ε^{tr} is the transformation strain). We demonstrate, in the dimensionless stress, $\sigma^*(=\sigma\Omega/kT_m)$ versus temperature $T^*(=T_0/T_m)$ phase diagram (k is the Boltzmann constant), that the change of $d\sigma_0/dT$ is more important in design of SIM aging. In this diagram the area available for SIM aging is given by the area between the σ_0^* versus T^*curve and the σ_y^* versus T^* straight line (where σ_y^* is the reduced yield stress of the martensite which is a decreasing function of temperature) [1,2]. If ε^{tr} increases the $d\sigma_0^*/dT^*$ slope decreases and the crossing point with the $\sigma_y^* \sim T^*$ straight line is shifted to higher temperatures increasing the above area. ε^{tr} can increase i) with increasing temperature, due to different values of the elastic modulus, E_i ($i=M, A$) of the martensite and austenite [3], if $E_M<E_A$, or ii) if the transformation strain is more and more "complete" [3] (i.e. if ε^{tr} approaches to its theoretical maximum value ε_{maxt}). This can be a typical case for single crystalline samples along certain direction or in specially textured polycrystals. In addition, the $d\sigma_0/dT$ slope can be different for compression and tension. Thus, in designing of SMAs, capable of showing high temperature applications, the values of ε^{tr} and the level and slope of the σ_y^* versus T^* function should be optimized.

[1] P. Sittner, et al. Mat. & Design, 226 (2023) 111638
[2] Yu. Chumljakov et al. J Alloys and Comp. 5775 (2013) S393
[3] Y. Liu, H. Yung, Smart. Mater Struct. 16 (2007) S22

073_369

Effect of Fast Laser Shape Setting on Functional Performances of Thin NiTiHf based Shape Memory Alloy for High Temperature Applications

Carlo Alberto Biffi, Alberto Coda, Jannis Nikolas Lemke, Jacopo Fiocchi, Ausonio Tuissi
CNR, Lecco, Italy

In recent years, the interest in shape memory alloys with high transformation temperatures (HTSMAs) has significantly increased for some sectors, like aerospace, automotive, and robotics. Among different HT SMA systems, the Ni-Ti-Hf has been selected for offering a good balance between mechanical properties and high transformation temperatures. It can offer brittle behavior during its processing, but the role of its chemistry can solve this issue.

In this work, rapid shape setting, carried out using laser technology, was explored on thin HT SMA wires. The functional performances of laser treated wires were assessed through differential scanning calorimetry (DSC) and thermos-mechanical testing. The main laser parameters were selected for reaching stable phase transformation at high temperatures, and these results were compared to those ones of furnace annealed wires.

074_314

Acoustic emission-a promising tool to study the functional stability of superelasticity of shape memory alloys

Anja Weidner[1], Robert Lehnert[1], Moritz Müller[1], Christian Lauhoff[2], Viktor Remich[2], Philipp Krooss[2], Thomas Niendorf[2], Horst Biermann[1]
[1]TU Bergakademie Freiberg, Freiberg, Germany. [2]Universität Kassel, Kassel, Germany

The shape memory effect (SME), discovered in 1932 by Olander for the alloy system Au-Cd, is the result of a thermoelastic, martensitic (diffusionless) phase transformation from a high-temperature phase (austenite) to a low-temperature phase (martensite) in a characteristic temperature interval. Shape memory alloys (SMAs) may show the “one-way” SME, the “two-way” SME and/or superelasticity depending on their chemical composition and microstructure. Whereas the one-way SME is characterized by a one-time change in shape when heating a sample that was previously pseudoplastically deformed in the martensitic state allowing only a one-off change in shape, the two-way SME offers the ability of a material to remember one shape at a low temperature and one at a high temperature. The superelasticity is the ability for a reversible shape change at a constant temperature at an external load up to “unusually” high strains. In contrast to martensitic phase transformation (MPT) occurring in steels, the MPT in SMAs is of thermoelastic nature, which causes its high reversibility. The reversibility of the MPT is crucial for the functionality of SMAs. The easier the martensite/austenite interface is pinned by dislocations or a martensite stabilization occurs due to interaction of multiple martensite variants and dislocations, the faster occurs the degradation of the SME during repeated loading, which is also known as functional fatigue. To shed some light on to the understanding of different degradation mechanisms and their kinetics, in situ acoustic emission (AE) measurements are applied during mechanical loading of the shape memory alloys. Thus, dislocations as well as detwinning mechanisms were discovered as important mechanisms enhancing the irreversibility of the martensitic phase transformation.

The presentation gives an overview on the application of AE on different types of shape memory alloys (Fe-based SMAs, CoNiGa) focusing on their superelastic behavior and cyclic stability. For example, a pronounced functional fatigue was studied on a <001> oriented single crystal of Fe-Mn-Al-Ni under compressive loading in combination with acoustic emission showing a significant decrease in the activity of acoustic emission with an increase in number of loading cycles.

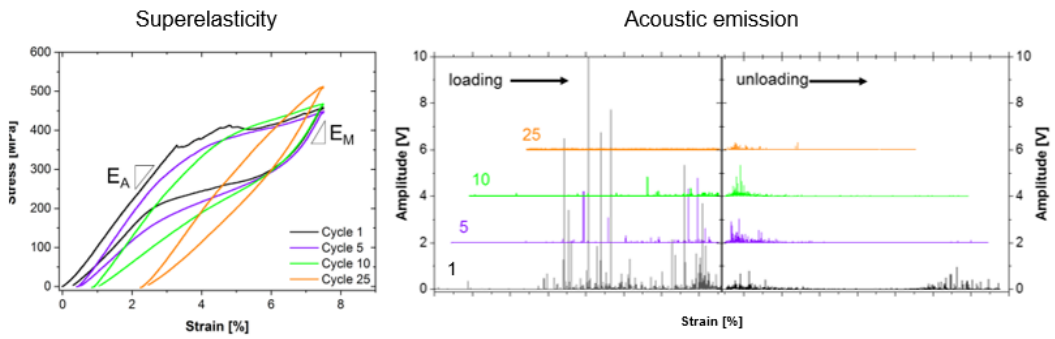

Figure 1: Functional fatigue of superelasticity and acoustic emission activity studied on a <001> oriented Fe-Mn-Al-Ni single crystal under compressive loading..

075_158

Investigation of TiNi Shape Memory Alloy, Polymer and TiNb Ni -free High Elastic Alloys by using Digital Image Correlation, Infrared and Acoustic Emission Techniques

Elżbieta Pieczyska[1], Karol Golasiński[2], Michał Maj[1], Maria Staszczak[3], Hisaaki Tobushi[4]
[1]Institute of Fundamental Technological Research Polish Academy of Sciences, Warsaw, mazowieckie, Poland. [2]Multidyscyplinar Research Center of WKU, Warsaw, mazowieckie, Poland. [3]Institute of Fundamental Technological Research Polish Academy of Sciences, Warsaw, Mazowieckie, Poland. [4]AICHI Institute of Technology (AIT), Toyota-city, AICHI, Japan

The goal of the research was to compare and discuss the behavior of new multifunctional materials under cyclic loading conditions. To this end, the TiNi SMA produced by Furukawa [1], the Gum Metal provided by the Toyota Central Research & Development Labs, Japan, as well as the Shape Memory Epoxy 3D-printed at the Technical University of Madrid [2], were subjected to loading on a smart Instron Testing Machine. For the Ti-based alloys, stress-induced martensite/reverse transformations that nucleate and develop during the loading process were analyzed based on the obtained mechanical, infrared (IR) and acoustic emission (AE) data. The digital image correlation (DIC) system with its own algorithm was used. The fast and sensitive Infrared Camera Phoenix Flir Co. evaluated the temperature changes during the deformation process. The obtained experimental data (an example is presented in Fig. 1), correlated with the microstructure of the materials, expand our understanding of these novel materials and provide valuable input for modeling.

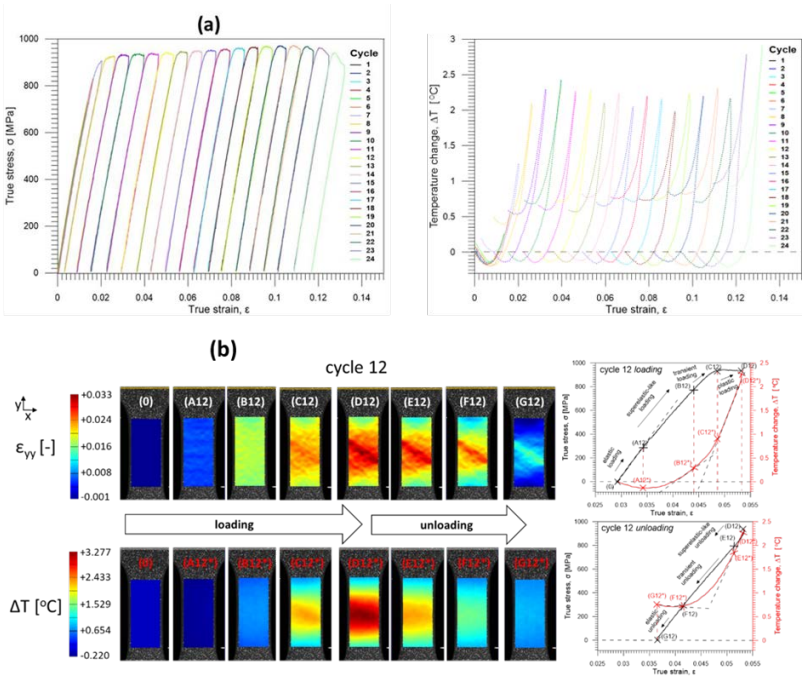

Fig. 1. (a) Stress σ vs. strain ε curves and the related average temperature change ΔT vs. strain ε curves obtained for Gum Metal under loading-unloading 1-24 tensile cycles.

(b) Evolution of strain ε_{yy} obtained by DIC and temperature ΔT fields obtained by IRT of Gum Metal specimen at selected stages of loading-unloading cycle No. 12 [3].

Acknowledgements: The research has been supported by the National Science Centre, Poland NCN under project UMO-2024/53/B/ST8/03931.

1. Pieczyska E.A, Tobushi H, Kulasiński K., Development of transformation bands in TiNi SMA for various stress and strain rates studied by fast and sensitive infrared camera, *Smart Mater. Struct*, 2013
2. Nabavian Kalat, M.; Staszczak, M.; Urbański, L.; Fernandez, C.; Vega, C.; Cristea, M.; Ionita, D.; Lantada, A. and Pieczyska, E.A., Investigating a shape memory epoxy resin and its application to engineering shape-morphing devices empowered through kinematic chains and compliant joints, *Mater. Des.* 2023
3. Golasiński K., Maj M., Urbański L., Staszczak M., Gradys A. and Pieczyska E.A., Experimental study of thermomechanical behaviour of Gum Metal during cyclic tensile loadings: the quantitative contribution of IRT and DIC, *Quant. Infrared Therm. J.*, **2023.**

076_408

On experimental parameters characterizing functional fatigue performance of NiTi alloys

Lukáš Kadeřávek, Petr Šittner, Luděk Heller
Institute of Physics of the CAS, Department of Functional Materials and Composites, Na Slovance 1992/2, Prague, Czech Republic

NiTi based shape memory alloy components (wires, sheets, tubes) utilized in engineering applications presumably display recoverable stress-strain-temperature responses in cyclic thermomechanical loads due to thermomechanically driven martensitic transformation and possibly martensite reorientation deformation processes. A complication is that forward and reverse martensitic transformations, anytime they proceed under external stress above certain thresholds tend to generate plastic strains and permanent lattice defects that accumulate upon thermomechanical cycling [1], giving rise to cyclic instability of stress-strain-temperature responses (functional fatigue).

Various NiTi components display various propensities to functional fatigue degradation, which is a kind of material characteristics that depends on chemical composition, material state (grain size, precipitates, lattice defects, and texture). It is frequently characterized by the accumulated unrecovered strain determined in cyclic superelastic tests at room temperature up to selected number of cycles. However, only such material parameter is not suitable to treat components made from NiTi based alloys with different transformation temperatures. There is a need to characterise the predisposition of various NiTi based alloys to functional fatigue degradation by set of material parameters (evaluated in defined testing procedures) that will be applicable to NiTi-based alloys having various transformation temperatures (-200C-400C).

In this work, we propose to perform thermal actuation tests on NiTi based alloy components to determine material parameters that characterise the predisposition of NiTi based alloys to functional fatigue degradation from the recorded cyclic strain-temperature actuation responses. The predisposition of various commercially available superelastic and shape memory NiTi wires towards functional fatigue degradation will be evaluated and compared. The advantages of the proposed approach over the use of conventional accumulated unrecovered strain as well as the reasons for integrating cyclic thermal actuation testing to isothermal superelastic testing will be discussed.

[1] Šittner, P., et al. Generation of Plastic Strains by the Martensitic Transformations under Stress via Dislocation Slip in Martensite as the Origin of Functional Fatigue. *Shap. Mem. Superelasticity* (2025)

077_330

Growth kinetics and property tuning in magnetic shape memory alloys prepared by optical floating zone growth

Denys Musiienko[1], Ross Colman[2], Petr Veřtát[1], Alexej Perevertov[1], Ladislav Straka[1], Oleg Heczko[1]
[1]FZU-Institute of Physics of the Czech Academy of Sciences, Prague, Czech Republic. [2]Charles University, Prague, Czech Republic

Ni-Mn-Ga ferromagnetic shape memory alloys (FSMAs) are valued for their unique magneto-mechanical coupling, enabling applications in actuators, energy harvesters, and adaptive devices. Realising these properties requires high-quality single crystals, which are difficult to grow due to the alloy's incongruent melting and associated chemical segregation. We study the crystal growth process and employ finite element modelling to optimise magnetic and magneto-mechanical properties of Ni-Mn-Ga FSMAs grown using a modified optical floating zone (OFZ) technique. The modification involved the use of single-crystalline sapphire crucibles to improve molten zone stability and to mitigate Mn evaporation, a key challenge in Mn-containing Heusler alloys.

Crystals were grown at speeds ranging from 2 to 80 mm/h. Higher speeds (40-80 mm/h) led to cellular morphologies and increased micro-segregation, Fig. 1, while slower rates promoted planar growth and chemical uniformity. At intermediate speeds (around 20 mm/h), irregular instabilities appeared without fully cellular or planar structure. Finite element modelling in COMSOL Multiphysics was used to simulate transient temperature fields and molten zone profiles, enabling accurate predictive estimation of chemical segregation during growth and aiding process optimisation, Fig. 2.

Magnetic and magneto-mechanical properties were characterised in both as-grown and annealed states. Heat treatment significantly improved functional performance by promoting homogenisation-eliminating the micro-segregation observed in as-grown crystals at high growth speeds. The resulting crystals matched or exceeded the quality of those grown by conventional Bridgman methods. These findings demonstrate that the modified OFZ approach is a viable and scalable method for growing functional Ni-Mn-Ga single crystals, offering new insights into the relationship between processing, structure, and performance in FSMAs.

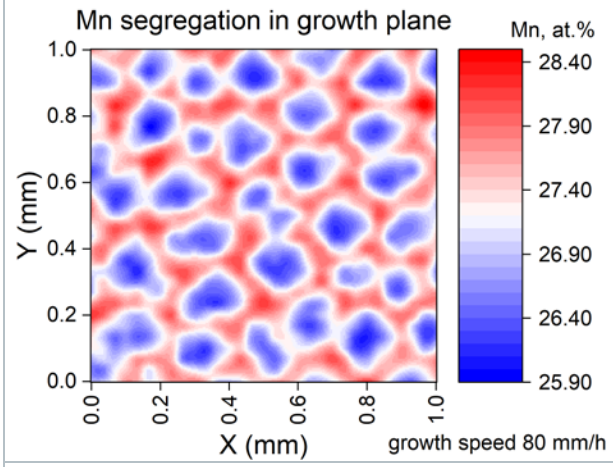

Figure 1. Measured variation of Mn content in plane, perpendicular to the growth direction, demonstrating the cell structure.

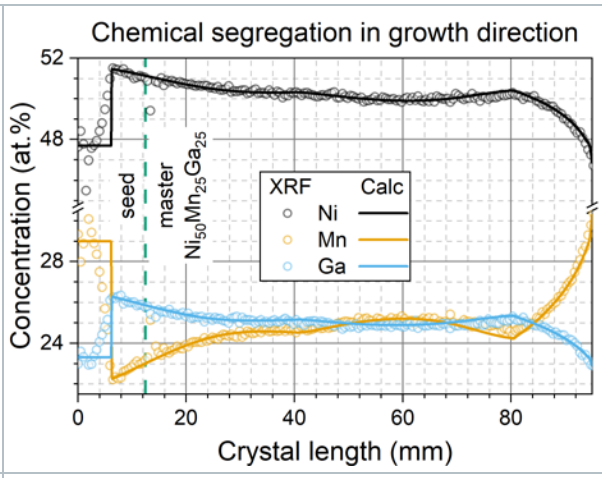

Figure 2. Comparison of measured vs calculated chemical composition evolution along the growth direction of the grown crystal.

The authors acknowledge the support of OP JAK project No. CZ.02.01.01/00/22_008/0004591 and CSF grant No. 22-22063S.

078_398

Microstructural features of NiMnGa polycrystalline alloys manufactured by rapid solidification methods

Anna Wojcik[1], Robert Chulist[1], Arkadiusz Szewczyk[1], Wojciech Maziarz[2]
[1]Faculty of Metals Engineering and Industrial Computer Science, AGH University of Krakow, Krakow, Poland. [2]Institute of Metallurgy and Materials Science, Polish Academy of Sciences, Krakow, Poland

Melt-spinning and laser powder bed fusion (LPBF) are two of the most promising rapid solidification techniques, offering control over the texture and microstructural features that directly affect the magnitude of magnetic-field-induced strain (MFIS). In this study, we produced alloys with three different compositions using both melt-spinning and LPBF, combined with various heat treatment conditions. Key microstructural features, including atomic order, grain size, and texture, were tailored through thermal treatments and characterized using a range of techniques. The evolution of microstructure and texture in both types of NiMnGa materials was investigated using SEM, TEM, and synchrotron radiation diffraction. For both fabrication methods, the processing and annealing conditions facilitated the development of micostructures with preferred <100> fiber orientations along the growth/build direction. It was also demonstrated that chemical composition—strongly affected by Mn evaporation during the LPBF and melt-spinning processes—has a significant influence on the resulting crystal structure (ternary Ni-Mn-Ga: 10M for melt-spun ribbons; 14M for LPBF). Furthermore, internal stresses introduced during both fabrication processes were found to impact the crystal structure, promoting the formation of multi-modulated metastable phases that could be stabilized via heat treatment.

Appropriate heat processing enabled the growth of nearly single austenitic orientations within each column, forming two structural variants that yielded MFIS values of 1.15% and 0.5% in untrained polycrystalline ribbons and 3D-printed samples, respectively. Moreover, mechanical training of the ribbons increased MFIS to as much as 3% making the material very promising for microactuation applications.

Acknowledgement
The work was carried out within the project 2021/42/E/ST5/00367 of the National Science Centre of Poland.

079_204

Suppression of transformation-induced dislocations in supercompatible martensite microstructure satisfying the triplet condition in Ti-Ni based alloys

Tomonari Inamura[1], Akira Heima[1], Francesco Della Porta[2], Hikari Inoue[1], Ryutaro Matsumura[1], Yuri Shinohara[1], Hiroshi Akamine[3], Minoru Nishida[3], Fumiyoshi Yamashita[4], Sumio Kise[4]
[1]Institute of Science Tokyo, Yokohama, Japan. [2]Max Planck Institute for Mathematics, Bonn, Germany. [3]Kyushu University, Kasuga, Japan. [4]Furukawa Techno Material, Hiratsuka, Japan

We propose a new geometrical condition that enables the formation of a supercompatible martensitic microstructure and investigate how it suppresses transformation-induced dislocations. Addressing the issue of functional fatigue in shape memory alloys, including improving the stability of thermal cycling properties, has remained a significant challenge in the field. Therefore, controlling the compatibility of martensitic structures represents a groundbreaking approach to alloy design. The cofactor condition (CC) is a well-established geometrical condition that simultaneously removes incompatibility at both parent/martensite and martensite/martensite interfaces. However, achieving CC places strict constraints on alloy composition, making it difficult to satisfy in practical applications. In our research, we have identified another condition that gives rise to a distinctive martensitic microstructure resembling the one obtained under CC. We term this the triplet condition (TC), which represents an alternative path to achieving supercompatible martensite microstructure. Unlike CC, which is satisfied along curves in the eigenvalue space of lattice deformation, TC is satisfied on two-dimensional surfaces, suggesting that it is more feasible to find alloys that satisfy TC. To demonstrate the effectiveness of TC in suppressing dislocation generation, we measured the yield stress caused by dislocation slip at the martensitic start temperature (Ms) and compared the microstructure and dislocation accumulation behavior of alloys with similar yield stress but different deviations from TC. We present detailed observations of the unique martensitic microstructure and clarify how satisfying TC reduces dislocation accumulation in Ti-Ni-based alloys.

080_307

Analysis of complex microstructures in $Ti_{76}Nb_{22}Al_2$

John Ball[1], Francesco Della Porta[2], Tomonari Inamura[3]
[1]Heriot-Watt University, Edinburgh, United Kingdom. [2]formerly at Max Planck Institute, Leipzig, Germany. [3]Institute of Science, Tokyo, Japan

We describe attempts [1] to understand the remarkable microstructures observed in experiments of the third author resulting from the cubic to orthorhombic phase transformation in $Ti_{76}Nb_{22}Al_2$. The middle eigenvalue $\lambda_2(\mathbf{U})$ of the corresponding transformation strain $\mathbf{U}$ is very close to one. Assuming $\lambda_2(\mathbf{U}) =1$ there are then exactly 12 matrices $\mathbf{A}_i$ on the 6 martensitic energy wells that are rank-one connected to the identity matrix $\mathbf{1}$ (corresponding to the undeformed austenite), but *there are no rank-one connections between the* $\mathbf{A}_i$. The observed fractal-like microstructure appears to be an approximation to a deformation gradient taking only the values $\mathbf{A}_i$, with the distribution of martensitic plates of different sizes following a power law similar to those predicted by probabilistic models of martensitic transformations [2,3]. As part of the analysis we note that the set $K=\{\mathbf{A}_1,...,\mathbf{A}_{12}\}$ forms a degenerate T_{12} configuration, and we discuss its corresponding set of macroscopic gradients, the quasiconvex hull K^{qc}.

Reference

[1] J.M. Ball, F. Della Porta, T. Inamura, *Complex Martensitic Microstructures in $Ti_{76}Nb_{22}Al_2$*, In preparation.

[2] J. M. Ball, P. Cesana, B. Hambly, *A probabilistic model for martensitic avalanches*, MATEC Web of Conferences, 33, 02008, 2005.

[3] P. Cesana, B. Hambly, *A probabilistic model for interfaces in a martensitic phase transition,* Journal of Applied Probability, 59(4), 1081-1105*,* 2022.

081_169

Crystallographic and morphological changes during successive stress-induced martensitic transformations in single crystal Cu-Al-Mn shape memory alloys

Hiroshi Akamine[1], Ryo Takamatsu[1], Sheng Xu[2], Toshihiro Omori[2], Ryoshuke Kainuma[2], Sumio Kise[3], Kakeru Ninomiya[2], Maiko Nishibori[2], Minoru Nishida[1]
[1]Kyushu University, Kasuga, Japan. [2]Tohoku University, Sendai, Japan. [3]Furukawa Techno Materials Co. Ltd., Hiratsuka, Japan

Single-crystal Cu-based shape memory alloys (SMAs) have attracted attention for their excellent superelasticity and lower cost compared to widely used Ti-Ni alloys [1]. Recently, Kise et al. [2] reported the crystal orientation dependence of the deformation behavior in Cu-Al-Mn single crystals produced by cyclic heat treatment [3], revealing that rods with specific tensile orientations exhibit excellent shape recovery due to successive stress-induced martensitic transformation (SSIMT) [4]. In this study, the crystallographic and morphological evolution during SSIMT was investigated using transmission electron microscopy, scanning electron microscopy and synchrotron X-ray diffraction. A Cu-16.8Al-9.6Mn (at.%) alloy, initially in the 6M martensitic phase at room temperature, exhibited a 6M→2M transformation after reorientation from multiple variants to a single variant suitable for the tensile axis in the 6M phase. At the 6M and 2M interface, partial dislocations running every three layers within the 6M structure were observed, suggesting that the 6M→2M transformation progresses through the motion of partial dislocations along the basal planes. Similarly, a Cu-17Al-11Mn (at.%) alloy, which is in the $L2_1$ parent phase at room temperature and exhibits superelasticity, underwent an SSIMT of $L2_1$→6M→2M, resulting in a shape recovery exceeding 16%. During the reverse transformation, the 2M→6M→$L2_1$ sequence occurred at the boundary region, characterized by a complex multiple variants structure of the 2M and 6M phases. The 6M→2M transformation expanded the stress-strain hysteresis loop, thereby enhancing the energy dissipation capability. The large stress-strain hysteresis highlights the potential of single-crystal Cu-Al-Mn SMAs for seismic applications.

[1] R. Kainuma et al., Metall. Mater. Trans. A 27 (1996) 2187. [2] S. Kise, et al., J. Mater. Civ. Eng. 33 (2021) 04021027. [3] T. Kusama, et al., Nat. Commun. 8 (2017) 354. [4] Otsuka et al. Acta Metall. 27 (1979) 585.

082_173

Reorientation Behavior of Martensitic Variants and Mechanical Response in Aged Ti–Mo–Al Shape Memory Alloys

Naoki Nohira, Masaki Tahara, Hideki Hosoda
Institute of Science Tokyo (Formerly: Tokyo Institute of Technology), Yokohama, Kanagawa, Japan

β-Ti shape memory alloys (SMAs) are promising for biomedical and actuator applications due to their biocompatibility and excellent functional properties. However, the formation of the ω phase, which often happens during aging or thermal exposure, is a serious problem. This phase reduces ductility and degrades the shape memory effect. Recent studies have shown that increasing aluminum content in the Ti–Mo–Al alloys can effectively suppress ω phase formation, enabling both room-temperature superelasticity and high-temperature (HT) shape memory effects. In HTSMAs, the material is often used in the martensite phase even at elevated temperatures. However, it is still not clear how aging affects deformation behavior of martensite.

Our recent work revealed that the yield stress of the Al-rich Ti–Mo–Al alloys increased with aging time. Since the yield stress reflects the stress required to initiate variant reorientation, that suggests the reorientation is hindered by aging. To clarify the mechanism, this study investigates microstructural changes responsible for aging-induced changes in deformation behavior of the martensite phase.

Ti–4Mo–11Al (mol%) alloys were prepared by Ar arc melting, followed by homogenization, hot rolling, solution treatment (ST) at 1273 K for 1.8 ks, and aging at 573 K up to 100 ks, below the reverse transformation temperature. X-ray diffraction (XRD), scanning and transmission electron microscopy (SEM and TEM) confirmed a single α″ martensite (orthorhombic) phase was retained throughout aging, with no ω phase detected and no change in lattice parameters.

Tensile testing showed that the yield stress increased with aging. Two-stage yielding behavior, associated with variant reorientation, was present in ST specimens but diminished or disappeared after aging. SEM observations revealed that reorientation occurred in the ST samples but it was suppressed in aged ones, which preserved their original microstructure. Since the phase and lattice constants remained unchanged, aging likely suppresses reorientation via localized changes near twin boundaries rather than macro-scale structural alterations.

These results offer new insights into the mechanical behavior of metastable martensite in β-Ti based HTSMAs and the aging-induced suppression of variant reorientation.

083_366

Supercompatibility and nucleation in martensite

Mohd Tahseen, Vivekanand Dabade
Indian Institute of Science, Bengaluru, Karnataka, India

Functional fatigue and transformation hysteresis remain significant hurdles in the effective design of shape memory alloys for a range of advanced applications. These limitations arise primarily from plastic deformation caused by the motion of highly stressed interfaces during repeated phase-transformation cycles. Previous studies have shown that alloys that satisfy the cofactor conditions exhibit remarkable reversibility and minimal hysteresis. This enhanced performance is attributed to the elimination of transition layers at phase interfaces through the formation of triple junctions involving Type I or Type II twins and austenite. These triple junctions enable zero elastic energy interfaces between the phases and facilitates seamless phase transformation. This mechanism enhances both the functional life and reversibility of the material. Motivated by the success of cofactor conditions, this work explores the possibility of extending such compatibility to compound twins. We examine whether transition layers can be eliminated in the case of compound twins as well, and whether the simultaneous elimination in Type I/II and compound twins is possible. Such a configuration may unlock a degree of reversibility that surpasses what is currently achieved through existing cofactor conditions. Furthermore, this enhanced compatibility could pave the way for the emergence of new microstructures that facilitate easier and more efficient phase transformations. The analysis is rooted in the geometrically non-linear theory of martensite, which explains microstructural formation as a result of the material's tendency to minimize elastic energy. We study the commutation properties of the stretch tensors of martensitic variants, which reveals an interesting connection to their ability to form triple junctions with austenite. By utilizing this connection, we propose new compatibility conditions, which enable the simultaneous elimination of the transition layer in Type I/II as well as compound twins. Furthermore, the analysis can be extended to analyze the formation of triple junctions in non-conventional twins as well. We present novel microstructures that emerge from the interplay of Type I/II and compound triple junctions. These configurations introduce a new self-accommodating nucleation mechanism, which is further expected to enhance the reversibility of the transformation. The next generation of highly reversible SMAs can be designed used the idea presented in this work.

084_371

NiTi-Hf Shape Memory Alloys via Binder Jet Printing: Materials Insights and Process Strategies

Mohammad Elahinia[1], Vidura R.S. Kanakaratne[1], Daniel B Mahoney[1], Mohammad Pourshams[1], Alireza Behvar[1], Ahu Celebi[1], Ausonio Tuissi[2], Carlo Biffi[2]
[1]UToledo, Toledo, Toledo, USA. [2]CNR ICMATE Lecco, Lecco, Italy

NiTi-Hf shape memory alloys (SMAs) are gaining increasing attention due to their elevated transformation temperatures, enhanced thermal stability, and potential for high-temperature actuation in aerospace, energy, and automotive applications. The partial substitution of Hf for Ti in NiTi alloys enables tailored phase transformation behavior, but also introduces challenges such as elemental segregation, sluggish diffusion, and embrittlement during conventional and fusion-based additive manufacturing (AM) processes. Binder Jetting (BJ) enables the fabrication of Hf-added NiTi alloys without melting, minimizing phase segregation and thermal stress-induced defects. This results in a more homogeneous microstructure and enhanced high-temperature stability. This study presents a comprehensive assessment of the opportunities and challenges in fabricating NiTi-Hf SMAs via BJ. The effects of Hf concentration on microstructure evolution, phase transformation sequence (B2 → B19′), and sintering behavior are critically examined. Special focus is given to key process parameters such as powder characteristics, binder saturation control, and optimized sintering profiles to ensure homogenous phase distribution, high densification, and suppression of secondary brittle intermetallics. This work identifies current gaps in BJ-based NiTi-Hf research, including the lack of experimental validation and optimization of post-sintering treatments. A forward-looking research roadmap is proposed, outlining strategies for alloy development, debinding and sintering protocols, and surface finishing techniques to realize high-performance, high-temperature SMA components. The findings provide a foundation for the scalable, defect-tolerant manufacturing of NiTi-Hf driving innovation in smart structures and extreme-environment devices.

Keywords: NiTi-Hf alloys, Binder Jet Additive Manufacturing, Shape Memory Alloys, Powder Sintering, Thermal Hysteresis, Alloy Design, Additive Manufacturing

085_329

Microstructure Evolution of Ni-Ti-Hf Shape Memory Alloys Manufactured via Additive Manufacturing Processes

Philipp Krooss, Mikkel Nobach, Julia Richter, Thomas Niendorf
University of Kassel, KASSEL, Germany

Ni-Ti-based Shape memory alloys (SMA) represent promising candidates for actuation and damping applications due to their good functional properties. Ternary additions of Hf are known to increase the transformation temperatures and therefore the application temperature range. However, Hf additions may also lead to an increase of brittleness and thus, limit thermomechanical processing. Additive manufacturing (AM) processes may help to overcome this issue, due to the possibility of realizing near-net shaped functional materials. The present study focuses on a Ni-Ti-Hf SMA processed via different powder bed fusion processes. The impact of process induced defects on the functional properties is discussed in view of the chemical composition and microstructural findings.

086_181

Effect of Hf on the martensitic transformation behavior and self-accommodation in Ti-Ni-Hf and Ti-Pd-Hf alloys

Mitsuhiro Matsuda[1], Hiroshi Akamine[2], Minoru Nishida[2]
[1]Kumamoto University, Kumamoto, Japan. [2]Kyushu University, Kasuga, Fukuoka, Japan

Shape-memory effect and superelasticity are strongly affected by the microstructure of thermoelastic martensite. The transformation strain originating from the change of shape is accommodated through combination of crystallographically equivalent multiple habit plane variants (HPVs) (i.e., self-accommodation). We investigated the microstructure and crystallography of martensite variants in $Ti_{50-x}Ni_{50}Hf_x$ and $Ti_{50-x}Pd_{50}Hf_x$ alloys by EBSD analysis and TEM observation. In the $Ti_{50-x}Ni_{50}Hf_x$ alloys, each transformation temperature decreases when less than 10 at% Hf is substituted for Ti, whereas they increase when more than 10 at% Hf is substituted for Ti. The crystal structures of martensite in $Ti_{50-x}Ni_{50}Hf_x$ alloys substituted with Hf at concentrations less than 25 at% and greater than 35 at% were the B19' and B33 structures, respectively. In the $Ti_{25}Ni_{50}Hf_{25}$ alloy, the lattice invariant shear (LIS) was the $\{001\}_{B19'}$ compound twin; a pair of HPVs with plate-and polygonal-like morphologies were bounded by the $\{011\}_{B19'}$ Type I twin formed around each of the $<100>_{B2}$ axes of the B2 parent phase. In the $Ti_{15}Ni_{50}Hf_{35}$ alloy, no twin existed in the martensite variants with plate-and polygonal-like morphologies, providing that the LIS was $(010)_{B33}$ basal stacking faults. A pair of HPVs were bounded by the $\{021\}_{B33}$ compound twin formed around each of the $<100>_{B2}$ axes of the B2 parent phase. As the martensitic transformation proceeds, each HPV pair should contact and impinge on the $\{110\}_{B2}$ plane, resulting in a mosaic-like microstructure.

In the $Ti_{50-x}Pd_{50}Hf_x$ alloy, the martensitic transformation temperature decreased with increasing amount of Hf. No indication of a martensitic transformation was observed in the as-quenched $Ti_{25}Pd_{50}Hf_{25}$ and $Ti_{10}Pd_{50}Hf_{40}$ alloys, even when the samples were cooled to 150 K. The $Ti_{40}Pd_{50}Hf_{10}$, $Ti_{35}Pd_{50}Hf_{15}$, and $Ti_{30}Pd_{50}Hf_{20}$ alloys were composed of a B19 phase having plate-like habit-plane variants. LIS of these alloys was a $\{111\}_{B19}$ Type I twin. A solution-treated sample of the $Ti_{25}Pd_{50}Hf_{25}$ alloy consisted of a B2 cubic matrix with local atomic displacement and lattice distortions. The as-quenched $Ti_{10}Pd_{50}Hf_{40}$ alloy contained rounded H-phase particles several tens of nanometers in diameter embedded in a B2 matrix. The martensitic transformation temperature was drastically decreased by both the fully coherent nanosized H-phase particles and the short-range order originating from clustering of solute atoms.

087_391

Exploring Crack Dynamics and Actuation Fatigue in NiTiHf High-Temperature Shape Memory Alloys with High Hf Content

Benat Kockar, Merİc Ekiciler
HACETTEPE UNIVERSITY, MECHANICAL ENGINEERING DEPT., ANKARA, Turkey

Shape Memory Alloys (SMAs) are unique materials capable of recovering their original shape through phase transformation triggered by mechanical or thermal stimuli [1]. This characteristic enables them to perform mechanical work against loads, making them suitable for actuator applications. Among SMAs, NiTi alloys are widely used due to their excellent shape memory behavior, but their low transformation temperatures (TTs) limit their use at elevated temperatures. To overcome this, NiTiHf alloys have emerged as promising High Temperature Shape Memory Alloys (HTSMAs), offering improved strength and higher TTs but they face challenges such as thermal and thermomechanical instability, fatigue, and crack growth during high-temperature actuation cycles. This study focuses on evaluating the actuation fatigue and crack propagation behavior of Ni50Ti30Hf20 (at.%) alloys through thermal cycling under constant load. Tests were conducted on three sample types: non-notched, pre-notched (HE-PN), and annealed pre-notched (HE-PN-AN). HE-PN-AN samples demonstrated slower and more stable crack growth and actuation fatigue behavior, attributed to stress relief and improved microstructure from annealing [2, 3]. Crack growth rates and fatigue performance varied significantly in HE-PN samples, while HE-PN-AN samples showed consistent trends and minor crack formation due to lower induced stresses. The effect of Upper Cycle Temperature (UCT), applied stress magnitude, and Hf content was also explored. Higher UCT led to surface oxidation, promoting crack formation and reducing fatigue life. For example, Ni50Ti30Hf20 samples tested at 600°C under 200 MPa exhibited higher strain than Ni50Ti25Hf25 under the same conditions, but were more prone to crack propagation due to oxidation. Furthermore, a higher stress level (300 MPa) applied at a lower UCT (440°C) caused shorter fatigue life with sudden fracture. These findings highlight the importance of balancing actuation strain, material composition, and operational parameters for reliable use of NiTiHf HTSMAs in high-temperature actuator applications, where durability and stability are critical.

[1] O. K., C.M. Wayman, Shape memory materials, Cambridge University Press, (1998).

[2] M. Ekiciler, B. Kockar, Crack growth behavior during actuation cycling of hot extruded and annealed $Ni_{50}Ti_{30}Hf_{20}$high temperature shape memory alloys, Smart Mater. Struct. 31 (2022).

088_412

Tensile actuation using NiTiHf HTSMA fabricated via LPBF additive manufacturing

Hongwei Ma[1], Haizhou Lu[2], Weisi Caia[1], Chao Yang[1], Orsolya Molnárová[3], Eduardo Alarcón[3], Petr Šittner[3]
[1]National Engineering Research Center of Near-net-shape Forming for Metallic Materials, Guangdong Provincial Key Laboratory for Processing and Forming of Advanced Metallic Materials, South China University of Technology, Guangzhou, China. [2]School of Mechatronic Engineering, Guangdong Polytechnic Normal University, Guangzhou, China. [3]Institute of Physics of the CAS, Na Slovance 1992/2, 18200, Prague, Czech Republic

$Ni_{50.4}Ti_{29.6}Hf_{20}$ (at. %) High Temperature Shape Memory Alloys (HTSMA) fabricated via Laser Powder Bed Fusion (LPBF) suffer from poor tensile strength preventing their use in actuator applications. We managed to fabricate NiTiHf HTSMA with capable of tensile actuation in the temperature range 250-350 °C via LPBF additive manufacturing. Tensile strength 821 MPa, actuation strain 2.34% under 300 MPa tensile stress with negligible irrecoverable plastic strain fracture upon cooling under tensile stress 600 MPa are best values reported so far in the literature for LPBF fabricated NiTiHf. The tensile strength reaching half of the strength of the conventional cast and thermomechanically processed NiTiHf alloys is high enough to allow for tensile actuation under stress up to 600 MPa. The enhanced strength of the LPBF fabricated NiTiHf alloy was attributed to the lack of micropores (porosity 0.02%) and the tensile actuation performance is claimed to be facilitated by the strengthening effect from homogeneously distributed oxide nanoparticles introduced naturally into the microstructure of the alloy by the LPBF process.

089_354

Nanotwinning and magnetoelastic coupling in Ni-Mn-based Heusler compounds from first principles

Markus Gruner, Olga Miroshkina, Mike Bruckhoff
University of Duisburg-Essen, Duisburg, NRW, Germany

Functional ferroic properties in Ni-Mn-based Heusler compounds such as magnetic shape memory and magnetocaloric effect are linked to the presence of hierarchically modulated structures in martensite. Starting from a band-Jahn-Teller-type reconstruction of the Fermi surface of cubic $L2_1$ austenite softens the [110] transversal acoustic phonons, modulations can evolve into adaptive, self-organized arrangement of [110]-aligned nanotwins consisting of non-modulated tetragonal building blocksas shown previously for the paradigmatic case of stoichiometric Ni_2MnGa. First-principles calculations in the framework of density functional theory (DFT) suggest further that frustrated antiferromagnetic coupling between neighboring Mn atoms give rise to competing repulsive and attractive interactions in the nonmodulated $L1_0$ martensite stabilize the twin interfaces. Off-stoichiometric compounds, in particular with In and Sn frustrated magnetic interactions between Mn atoms, lead to an effective decoupling of the magnetic order on the two sublattices occupied by Mn atoms and result in substantial positional reconstruction. Based on DFT calculations, we will elucidate the interplay of electronic structure, magnetic frustration and partial chemical disorder on the stability of nanotwinned microstructures, in particular 10M, 14M and 4O. In addition, we discuss the perspective of DFT-based machine-learning force fields to include the intricate cross-coupling between electronic, magnetic and lattice degrees of freedom to simulate the evolution of modulated and nanotwinned microstructures.

090_190

Investigation on the electronic structure of modulated martensite phase of magnetic shape memory alloy Ni_2MnGa via quasi-particle self-consistent GW approach

Masao Obata[1], Takao Kotani[2], Tatsuki Oda[1]
[1]Kanazawa University, Kanazawa, Japan. [2]Tottori University, Tottori, Japan

The magnetic shape memory alloy Ni-Mn-Ga exhibits both magnetic field-induced strain (MFIS) effects and shape memory properties [1]. The MFIS effect arises from the high mobility of macroscale twin boundaries formed in the martensite phases, which emerge upon cooling from the austenite phase. This high mobility of twin boundaries is observed in modulated martensite phases with nanoscale twin boundaries. Conversely, the non-modulated martensite phase does not exhibit any MFIS effect. Therefore, nanoscale structural modulation may be related to the MFIS effect, underscoring the importance of understanding its modulation and physical properties. Experimental studies have reported various modulated martensitic phases in Ni-Mn-Ga-based alloys, such as the 10M (5-period) and 14M (7-period) structures, depending on composition and temperature [2].

We have analyzed the electronic states of Ni-Mn-Ga alloys using the quasi-particle self-consistent GW (QSGW) approach, which can account for the effects of electron localization that are difficult to handle using density functional theory calculations with generalized gradient approximation (GGA). Using the QSGW approach [3], we have suggested that the appearance of such modulated martensitic structures can be attributed to the instability of the electronic structure in the high-temperature phase [4,5]. This study also investigates the electronic structure of modulated martensite phases of 10M and 14M by QSGW. Due to the presence of 20 (10M) or 28 (14M) atoms in the unit cell, the high computational cost of QSGW was a significant challenge. However, we overcame this issue by utilizing computational accelerators (GPUs). We found that the minority spin density of states near the Fermi level of Ni forms a valley structure. It is suggested that the modulated structure is electronically stabilized by positioning the Fermi level at the minimum of this valley. Such a structure was not observed in GGA calculations, which relates to the GGA estimation of the 10M phase as meta-stable, contrary to experimental facts [6].

[1] K. Ullakko et al., Appl. Phys. Lett. 69, (1996) 1966
[2] L. Righi et al., Acta Mater. 55, (2007) 5237
[3] M. van Schilfgaarde et al., Phys. Rev. Lett. 96, (2006) 226402
[4] M. Obata et al., Phys. Rev. Mater. 7, (2023) 024413
[5] M. Obata et al., Proceedings of 34th IUPAP Conference on Computational Physics, in press
[6] M. Zelený et al., Mater. Des. 209, (2021) 109917

091_345

Predictions of modulation and structural stability of Ni-Mn-X (X = Al, Ga, In) from first-principles

Jakub Luštinec[1,2], Masao Obata[3], Petr Sedlák[4], Jaroslav Hamrle[2], Oleg Heczko[1], Tatsuki Oda[3]
[1]FZU-Institute of Physics of the Czech Academy of Sciences, Prague, Czech Republic. [2]Department of Solid State Engineering, Faculty of Nuclear Science and Engineering, Czech Technical University in Prague, Prague, Czech Republic. [3]Division of Mathematical and Physical Sciences, Graduate School of Natural Science and Technology, Kanazawa University, Kanazawa, Japan. [4]Institute of Thermomechanics of the Czech Academy of Sciences, Prague, Czech Republic

The magnetic shape memory (MSM) effect observed in ferromagnetic Heusler alloy Ni-Mn-Ga is unique due to the magnetically induced strain, reaching up to 11 %. This huge strain has motivated intensive experimental and theoretical research on the effect. However, the essence of the effect is still not fully understood. Although the effect was observed in some other materials, Ni-Mn-Ga remains the most studied and promising one. If the essential properties of the electronic structure for MSM are identified, the search for new candidate materials will be enabled via first-principles calculations. One of the key requirements is the presence of the modulated martensitic phases since the MSM effect is observed only for 10M and 14M in Ni-Mn-Ga. These phases also appear in Ni-Mn-Al and Ni-Mn-In, but the MSM effect is not present there.

In this contribution, we show that the formation of modulation in martensite and the resulting modulation vector can be theoretically predicted from the generalized susceptibility $\chi(\mathbf{q})$ calculated in austenite. We demonstrate this by calculating the electronic structures of several Heusler alloys Ni_2MnX (X = Al, Ga, In) using the density functional theory (DFT) and quasiparticle self-consistent *GW* (QSGW) methods [1,2]. The QSGW method shows the best agreement between the predicted and experimentally observed modulation vectors. This suggests that the formation of modulated martensites is intrinsic to the electronic states of austenite. However, differences among the studied compounds were apparent, supporting the unique experimental behavior of Ni-Mn-Ga. Additionally, the generalized susceptibility was calculated for FM and spin non-polarized configurations of Ni_2MnGa to investigate the role of magnetic ordering. The peak of the generalized susceptibility present for the FM calculation disappears for the spin non-polarized calculations for both DFT and QSGW methods, highlighting the role of the magnetic ordering for the formation of the modulated phases which also agrees well with experimental results.

[1] Obata, M. et al., *Physical Review Materials*, 2023
[2] Luštinec, J. et al., *Journal of the Magnetics Society of Japan*, 2024

092_227

Ab initio study of long-period commensurate structures of Ni_2MnGa modulated martensite

Martin Zelený[1], Petr Veřtát[2], Ladislav Straka[2]
[1]Faculty of Mechanical Engineering, Brno University of Technology, Brno, Czech Republic. [2]FZU-Institute of Physics of the Czech Academy of Sciences, Prague, Czech Republic

The five-layered modulated martensite phase of the Ni-Mn-Ga magnetic shape memory alloy (10M) is widely studied for its high twin boundary mobility, originating from a significant shear elastic instability in the lattice [1]. Previous studies suggest an interplay between lattice modulation and twin boundary mobility [2,3]. Neutron diffraction measurements reveal an anharmonic, incommensurate modulation evolving from a commensurate state near the martensitic transformation, with an initial modulation vector $q = 0.4$, which increases with decreasing temperature [4]. This evolution leads to two key microstructural features: i) periodic a/b-nanotwin domains and ii) long-period commensurate structures (34O, 24O, 14O) where multiple modulation periods combine to achieve lattice alignment [6]. These orthorhombic unit cells inherently incorporate a/b-nanotwins as 2-2-like faults in a $(2\text{-}3)_2$ sequence of plane shifts describing commensurate modulation.

We performed ab initio calculations on long-period commensurate structures in Ni_2MnGa to examine their stability, energy landscape, and elastic properties. The effect of the electron localization correction parameter U was studied for 0–1.8 eV [5]. Regardless of U, all structures are stable with respect to structural relaxation and exhibit modulation comparable to experimental measurements. However, the energy profiles—including structures 10M and 4O alongside long-period structures—vary with U: (i) for $U = 0$–1 eV, energy decreases with increasing q (i.e., decreasing modulation periodicity); (ii) for $U > 1$ eV, the energy profile becomes nearly flat, exhibiting shallow minima corresponding to long-period structures. Even at $U = 0$ eV, energy differences among modulated structures remain within 3.5 meV, indicating that the long-period commensurate structures exhibit energies comparable to that of the 10M phase. Thus, the ab initio calculations confirm the stability of long-period commensurate structures. Finally, computed elastic constants do not reveal the expected shear elastic instability, likely due to the model's exclusion of a/b twin boundary motion.

[1] K. Repček et al., Adv. Mater. 36, e2406672 (2024).
[2] M. Vronka et al., Scr. Mater. 242, 115901 (2024).
[3] R. Chulist et al., Adv. Funct. Mater. 34, 2307322 (2024).
[4] P. Veřtát et al., Scr. Mater. 252, 116251 (2024).
[5] M. Zelený et al., Mater. Des. 209, 109917 (2021).
[6] P. Veřtát et al., https://doi.org/10.48550/ARXIV.2503.04379.

093_397

Antiphase boundaries in Ni_2MnGa: an atomistic perspective

Jan Zemen[1,2], František Máca[1], Václav Drchal[1], Martin Veis[3], Oleg Heczko[1]
[1]FZU-Institute of Physics of the Czech Academy of Sciences, Prague, Czech Republic. [2]Faculty of Electrical Engineering, Czech Technical University in Prague, Prague, Czech Republic. [3]Faculty of Mathematics and Physics, Charles University, Prague, Czech Republic

Antiphase boundaries (APBs) are planar crystallographic defects intrinsic to ordered alloys that play an important role in tuning mechanical and magnetic properties. Thermal APBs in magnetic shape memory alloys (MSMAs) affect magnetic coercivity through magnetic domain wall (DW) pinning [1], which was ascribed to antiferromagnetic coupling of local magnetic moments across APBs in Cu_2MnAl alloys as early as 1973 [2]. In Ni-Mn-Ga the investigation of APB is complicated as there is no transmission electron microscopy (TEM) contrast on APBs [3] and the only visualization is due to magnetic contrast which does not provide sufficient level of detail [3,4].

Moreover, magnetic force microscopy (MFM) [1] and Lorentz TEM [4] studies of Ni_2MnGa have shown a clear difference between signals generated by a thermally induced APB and by a single magnetic DW. A change of sign of the out-of-plane component of magnetic flux (B_z) measured across the interface is a signature of APB in an in-plane magnetized sample, whereas a simple but much stronger peak of B_z indicates a single DW.

In order to understand the character of APBs at the nanoscale, we perform density functional theory (DFT) calculations of supercells accommodating one or two APBs in cubic austenitic Ni_2MnGa. Our total energy analysis reveals that the lowest-energy APB configuration is formed by two parallel planes with antiphase configuration in the same supercell with only one Mn-Ga atomic layer between them (see Figure 1). This results in an antiphase domain less than 2 nm wide with magnetic moments oriented antiparallel to the neighbouring domains. Despite its narrowness the generated magnetic contrast simulated using the finite element method (FEM) is very broad and corresponds to the contrast measured by MFM [1]. The atomically sharp magnetic domain wall located at each APB arises from the interplay of strong ferromagnetic exchange within bulk and antiferromagnetic coupling across the APB due to shorter Mn–Mn distances at the boundary.

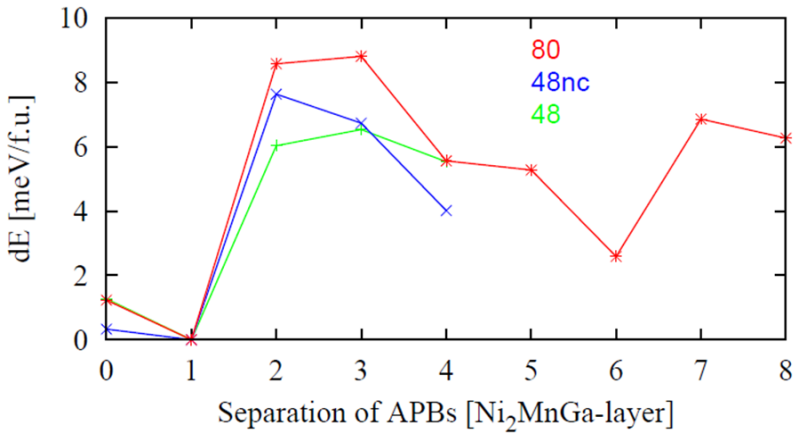

Fig. 1. Total energy calculated by DFT as a function of number of Mn-Ga layers separating two APBs in one supercell of 48 or 80 atoms; collinear and non-collinear (nc) VASP simulations in agreement;

References:

[1] L. Straka, et al., Appl. Phys. Lett. 113, 172901 (2018)
[2] A. J. Lapworth & J. P. Jakubovics, Philosophical Magazine, 29:2, 253-273 (1973)
[3] S.P. Venkateswaran, et al., Acta Materialia 55, 2621–2636 (2007)
[4] M. Vronka, et al., Acta Materialia 184, 179–186(2020)

094_380

Crystallographically compatible ceramic shape memory materials

Justin Jetter[1], Ashutosh Pandey[2], Hanlin Gu[3], Richard D. James[2], Eckhard Quandt[1]
[1]Kiel University, Kiel, Germany. [2]University of Minnesota, Minneapolis, Minnesota, USA. [3]Peking University, Beijing, China

The systematic tuning of crystal lattice parameters to achieve improved kinematic compatibility between different phases-referring to the fitting together of the phases-is a broadly effective strategy for improving the reversibility and lowering the hysteresis of solid–solid phase transformations.

The theory of mechanical compatibility was used to predict promising ceramic candidates in the system $(Y_{0.5}Ta_{0.5}O_2)_{1-x}(Zr_{0.5}Hf_{0.5}O_2)_x$, $0.6<x<0.85$. When these compatibility conditions are met, a reduction in thermal hysteresis by a factor of 2.5, a tripling of deformability, and a 75% enhancement in strain recovery within the shape-memory effect was found [1]

On the other hand, an apparently paradoxical example will be presented in which tuning to near perfect kinematic compatibility results in an unusually high degree of irreversibility. Specifically, when cooling the kinematically compatible ceramic $(Zr/Hf)O_2(YNb)O_4$ through its tetragonal-to-monoclinic phase transformation, the polycrystal slowly and steadily falls apart at its grain boundaries or even explosively disintegrates. If instead the lattice parameters are tuned to satisfy a stronger ‘equidistance’ condition, the resulting material exhibits reversible behavior with low hysteresis. These results show that a diversity of behaviors—from reversible at one extreme to explosive at the other—is possible in a chemically homogeneous ceramic system by manipulating conditions of compatibility in unexpected ways. These concepts could prove critical in the current search for a shape-memory ceramic [2].

In this search many synthetic compositions were generated, and a promising composition, 31.75Zr-37.75Hf-14.5Y-14.5Ta-1.5Er was identified, which closely satisfies all the design criteria based on predictions from machine learning. Furthermore, reducing tetragonality of the austenite phase by addition of Er_2O_3 was investigated by this approach. The underlying idea is to tune the lattice parameters of austenite phase towards a cubic structure that will increase the number of martensite variants, thus, allowing more flexibility for them to accommodate high strain during transformation [3].

[1] Jetter, J.; Gu, H.; Zhang, H.; Wuttig, M.; Chen, X.; Greer, J.R.; James, R.D.; Quandt, E.: Phys. Rev. Materials 3 (2019), 093603.
[2] Gu, H.; Rohmer, J.; Jetter, J.; Lotnyk, A.; Kienle, L.; Quandt, E.; James, R. D.: Nature 599 (2021), 4963
[3] Pandey, A.; Jetter, J.; Gu, H.; Quandt, E.; James, R. D.: (2025), arXiv:2504.01896.

095_262

An EBSD Study of Crystallographic Correspondences and Variant Selection in Zirconia-Based Shape Memory Ceramics

Alejandra Slagter[1], Christopher Schuh[2]
[1]Department of Materials Science and Engineering, Northwestern University, Evanston, Il, USA. [2]Department of Materials Science and Engineering, Northwestern University, Evanston, IL, USA

Lattice engineering has recently been shown to reduce the hysteresis and cracking susceptibility of zirconia ceramics, via controlled alloying. One key aspect of such engineering is the improved martensite-austenite interface compatibility that is achieved when lattice parameters are such that λ_2, the second eigenvalue of the stretch tensor describing the martensitic transformation, is as close as possible to one. Unfortunately, a distinctive aspect of the martensitic transformation in zirconia materials is the slight tetragonality of the austenitic phase, which leads to three different values of λ_2 instead of one; three lattice correspondences are possible depending on whether the tetragonal c axis becomes the monoclinic a, b, or c axis. This places an onus upon the lattice engineering efforts in zirconia ceramics, requiring some knowledge of the correspondences that are being formed.

Previous studies of the martensitic transformation in zirconia ceramics have suggested a preference for specific lattice correspondences based on lattice invariant shear minimization. However, these conclusions have largely been drawn from small datasets, primarily obtained via transmission electron microscopy. In this work, we employ advanced Electron Backscatter Diffraction (EBSD) methods to statistically analyze the distribution of martensite variants in ZrO_2-CeO_2 alloys. By leveraging novel techniques that resolve the long-standing pseudosymmetry problem in tetragonal zirconia, we demonstrate the simultaneous presence of all twenty-four possible martensitic variants, encompassing three lattice correspondences and two distinct orientation relationships. Our findings challenge the conventional assumption that a single dominant correspondence governs the transformation, and reveal a significant role for self-accommodation mechanisms in variant selection. These results offer new insights into the crystallographic factors governing martensitic transformations in zirconia and open new pathways for microstructural design in shape memory ceramics.

096_372

Martensitic phase transformations in a compositionally graded thin film

Ole Martin Løvvik[1,2], Marit Stange[1], Lars Bumke[3], Eckhard Quandt[4], Jakub Kušnír[5], Tomas Grabek[5], Hanuš Seiner[5]
[1]SINTEF, Oslo, Norway. [2]University of Oslo, Oslo, Norway. [3]University of Kiel, Kiel, Germany. [4]University of Kiel, Oslo, Germany. [5]Czech Academy of Sciences, Prague, Czech Republic

Elastocaloric cooling represents an innovative refrigeration method utilizing solid-state technology, leveraging shape-memory alloys that experience martensitic phase transitions within a defined thermodynamic cycle. This relies on materials that possess a high enthalpy of transformation and robust structural integrity, attainable by satisfying the cofactor conditions. These conditions define the compatibility between the austenite and martensite phases, enabling super-reversible transformations.

In our research, we focused on quaternary TiNiCuZr alloys to identify materials with optimal elastocaloric properties. We employed a combinatorial thin-film deposition technique using magnetron sputtering, with a target composition of $Ti_{44.5}Ni_{40.5}Cu_{10}Zr_5$. By using a non-rotating substrate, we produced films with a graded composition, suitable for high-throughput analysis.

To assess the films' properties, we applied various characterization methods. Energy-dispersive X-ray spectroscopy (EDS) was used to determine the chemical composition. The elemental concentrations within the films exhibited variations of 2–4 atomic percent compared to the sputtering target. Transient grating spectroscopy (TGS) measured the elastic and thermal properties across a range of compositions. This provided elastic constants that helped identify regions with austenite and martensite crystal structures. Combining these findings with theoretical investigations allowed us to pinpoint specific areas of the films as promising for elastocaloric applications, with the compatibility criteria satisfied. Differential scanning calorimetry (DSC) was employed to evaluate temperatures and enthslpies of a series of martensitic phase transformations. This was validated by temperature-dependent X-ray diffraction, which indicated a cubic B2 phase at high temperatures (austenite) and a lower-symmetry phase at low temperatures (martensite).

While microscopic tensile testing on selected compositions revealed that the mechanical properties of the thin films were insufficient for testing, the diverse methodologies employed in this study provided a comprehensive understanding of the interactions between composition, microstructure, and the thermal and mechanical properties of TiNi-based quaternary alloys.

097_401

Supercritical martensitic phase transformations in NiFeGaCo ferromagnetic shape memory alloys

Ashley Bucsek[1], Timothy Thompson[1], Abdulhamit Sarac[1], Seunghee Oh[2], Amlan Das[3], Fei Xiao[4]
[1]University of Michigan, Ann Arbor, MI, USA. [2]Argonne National Laboratory, Lemont, IL, USA. [3]Cornell High Energy Synchrotron Source, Ithaca, NY, USA. [4]Shanghai Jiao Tong University, Shanghai, China

Many multiferroics from shape memory alloys to ferroelectrics owe their unique functionality to a reversible martensitic phase transformation, the advantages of which include an ability to switch between distinct electrical/magnetic properties via thermal or mechanical biasing, and, conversely, convert the energy of electric/magnetic fields to high-frequency actuation. Normally, martensitic phase transformations take place via the nucleation and propagation of sharp phase interfaces, and energy barriers associated with these processes lead to hysteresis and functional fatigue. However, new research suggests that, when the material exists in a supercritical state, the transformation takes place via a gradual transformation of the lattice, i.e., without any sharp interfaces. As a result, these “supercritical martensitic phase transformations” exhibit exceptional reversibility for thousands to millions of cycles and low hysteretic or even anhysteretic behaviors—despite more than 10% recoverable strains. In this presentation, we present experimental observations of "subcritical" versus "supercritical" martensitic phase transformations in NiFeGaCo ferromagnetic shape memory alloys using in-situ differential interference contrast (DIC) optical microscopy and far-field high-energy diffraction microscopy (ff-HEDM). We discuss how the results mimic well-known characteristics of phase transformations in subcritical versus supercritical fluids. Finally, we discuss the outlook for capturing supercritical martensitic phase transformations in other multiferroic materials, such as $BaTiO_3$ ferroelectrics.

098_294

Functional behaviour of shape memory alloys at the nanoscale: An overview.

Jose M. San Juan, Jose F. Gómez-Cortés, Maria L. Nó
Universidad del Pais Vasco, UPV/EHU, Bilbao, Spain

Shape memory alloys (SMA) constitute the family of smart materials offering the highest work-output per unit of volume, which could represent an intrinsic advantage for their use as actuators in micro electro-mechanical systems (MEMS). Recent techniques associated to the development of the nanotechnology have allowed the production and characterization of small features of SMA, which allow testing the functional properties of shape memory and superelasticity. This last decade has witnessed outstanding advances in the characterization of the SMA at small scale, with the determination of an important size effect on the critical stress for the stress-induced martensitic transformation [1], the observation of a very stable superelastic behaviour along thousands of cycles in nanopillars [2], or the ultra-high damping of micro/nano bridges in bending [3].

In this work an overview of the functional behaviour of SMA at micro and nano scale will be presented. Although our pioneering research activity in this field was mainly focused in Cu-Al-Ni SMA, we will overview the state of the art in the different SMA families, such as those of Ti-Ni-based and Cu-Al-based SMA, as well as Ni-based magnetic SMA and other less-known SMA, which are being studied at small scale.

In addition, although the worldwide experiments to characterise the SMA at small scale have been mainly focused on nano-compression tests, using the nano-indenters technology, our review will also include other kind of working modes like tension or bending, in order to draw a complete scenario of the potential performances of SMA at nanoscale.

It will be concluded that SMA exhibit an exceptional behaviour at micro/nano scale and could offer new unforeseen applications with enhanced capabilities for sensors and actuators in small systems for MEMS, health-care devices or flexible and wearable electronic. It is time to face these challenges.

[1] J.F. Gómez-Cortés et al., Nature Nanotechnology 12 (2017) 790-796.
[2] J.F. Gómez-Cortés et al., Acta Materialia 166 (2019) 346-356.
[3] J.M. San Juan et al., J. Alloys & Compounds 929 (2022) 167307.

099_322

Magnetic Manipulation of Spatially Confined Multiferroic Heuslers by Martensitic Microstructure Engineering

Milad Takhsha[1], Vipin Kumar Singh[2], Julian Ledieu[2], Simone Fabbrici[1], Francesca Casoli[1], Francesco Mezzadri[3], Michal Horký[4], Vincent Fournée[2], Vojtěch Uhlíř[4], Franca Albertini[1]
[1]IMEM-CNR, Parma, Italy. [2]Institut Jean Lamour, Nancy, France. [3]University of Parma, Parma, Italy. [4]CEITEC BUT, Brno, Czech Republic

Magnetic shape-memory (MSM) Heuslers show a strong coupling between magnetic and structural degrees of freedom, evidencing a correlation between magnetic, thermal, and mechanical characteristics of the material through a magnetostructural phase transformation. In particular, epitaxial Ni-Mn-Ga thin film systems are the benchmark for possible integration in smart micro/nanodevices such as sensors, energy harvesters, and actuators [1].

The ability to control the martensitic microstructure, which rules the magnetic characteristics of these films at different length scales, is the key point for the optimization of their magnetic functional properties. The low-temperature martensite phase of epitaxial Ni-Mn-Ga films, having film(001)//underlayer(001)//substrate(001) crystallographic relation, evolves either of both or one of the differently oriented hierarchical twinning configurations, where magnetic domain direction is alternatively out of plane and in-plane (X-type) or in-plane (Y-type) [2-4]. Different arrangements of these twinning configurations give rise to various magnetic properties. Controlling these twinning configurations in a film is a subtle process depending on many parameters such as composition, thickness, underlayer/substrate, growth conditions, and post-growth treatments [2].

Here, we report a strategy for manipulating magnetic properties of spatially confined epitaxial Ni-Mn-Ga films grown on Cr(001)//MgO(001) by martensitic microstructure engineering. We show how the twinning configurations in the continuous films, as well as the micropatterned structures, can be switched from Y-type (showing negligible magnetic stray field) into X-type (presenting significant magnetic stray field) by a post-annealing process. Advanced characterization techniques enable us to analyze the atomic structure as well as the surface quality of the annealed samples and to disentangle the “twin-switching” phenomenon. The martensitic microstructure engineering reported in this study introduces a simple method for promoting the magnetic stray-field contribution at the surface of Ni-Mn-Ga epitaxial thin films and micropatterns initially showing negligible magnetic stray field.

[1] L. Fink *et al.* Adv. Funct. Mater. **33** (2023), 2305273.
[2] M. Takhsha Ghahfarokhi *et al.* Acta Mater. **187** (2020), 135-145.
[3] R. Niemann *et al.* Acta Mater. **132** (2017): 327-334.
[4] A. Diestel *et al.* J. Phys. Condens. Matter. **25** (2013): 266002.

100_242

Martensitic transformation in Ni_2FeGa Glass-Coated Microwires

Lucia Frolova[1], Zuzana Vargova[2], Ondrej Milkovic[3], Tomas Ryba[4], Oleg Heczko[5], Rastislav Varga[4]
[1]CPM UPJS, Kosice, Slovakia. [2]IoC UPJS, Kosice, Slovakia. [3]IoEP SAS, Kosice, Slovakia. [4]RVmagnetics, Kosice, Slovakia. [5]IoP CAS, Prague, Czech Republic

Wire shape introduces additional functionality into the shape memory alloys behavior [1]. Due to the shape anisotropy, their straining in axial direction is strongly enhanced. Moreover, magnetic nature allows for sensing ability that can be used for precise detection of structural transformation.

Ni_2FeGa glass-coated microwires presented here were produced by Taylor-Ulitovski method, which is inexpensive methods that allows for production of large volume of wires in short time [2]. They show martensitic transformation within 240-290 K with, straining up to 2% directly after wire production without necessity of post-production thermal treatment or training [3].

Ni_2FeGa composition show good miscibility and workability-the alloys with very precise chemical composition can be produced. This allows for wide range of transformation temperature (100-400K) that can be obtained [2]. Fine tuning of the transformation temperature can be performed by application of pre-stress. Pre-stress of 260MPa in axial direction increases the transformation temperatures to 330K, while simultaneously increases the strain due to martensitic transformation to 4%.

1. J. Alam, C. Bran, H. Chiriac, N. Lupu, T. A. Óvári, L. V. Panina, V. Rodionova, R. Varga, M. Vazquez, A. Zhukov, J. Magn. Magn. Mater. 513 (2020), 167074.
2. M. Hennel, M. Varga, L. Frolova, S. Nalevanko, P. Ibarra-Gaytán, R. Vidyasagar, P. Sarkar, A. Dzubinska, L. Galdun, T. Ryba, Z. Vargova, R. Varga, Phys. Status Solidi A 2022, 2100657N. P. Author1, Phys. Rev. A **70**, 013603 (2004).
3. L. Frolova, T. Ryba, J. Gamcova, O. Milkovic, P. Diko, V. Kavecansky, J. Kravcak, Z. Vargova, R. Varga, Materials Science and Engineering B **263** (2021) 114891

101_411

Coherent electron imaging of magnetic nanoparticles

Marco Beleggia[1,2], Frederik Durhuus[3], Cathrine Frandsen[2]
[1]University of Modena and Reggio Emilia, Modena, MO, Italy. [2]Technical Uniiversity of Denmark, Kgs. Lyngby, DK, Denmark.
[3]Technical University of Denmark, Kgs. Lyngby, DK, Denmark

Magnetism of nanoparticle superstructures, in the forms of clusters and chains of varying dimensionality, is fundamentally driven by dipolar interactions. For example, a self-assembly process that starts from a colloidal suspension of individual particles, evolves and settles under the influence of the dipole-dipole interactions between particles, terminates with the formation of superstructures where the internal anisotropy configuration is set by the *dipolar ground state*. Additionally, once a superstructure is formed, the internal arrangement of particles governs its magnetic properties, leading to the concept of *configurational anisotropy*, which is a mesoscopic manifestation of dipole interactions.

In some ranges of sizes and temperatures, the individual particles of the colloid might be superparamagnetic. Even in this case, dipolar interactions cannot be ignored, as they lead to a statistical net force, similar to a magnetic Van der Waals force, that is a fundamental ingredient in controlling particle dynamics.

This talk will describe how to access experimentally, with coherent electron imaging, some of the key physical quantities characterizing a magnetic nanoparticle superstructure: the magnetic moment of each individual particle, and the fields present within and around it, including a direct view on the dipolar fields established among particles that is controlling the degree of interaction between them.

Applications include the dynamic study of martensitic and austenitic tranformations in various shape memory alloy nanoparticles by in-situ coherent electron imaging to unveil the important role of finite size effects.

102_375

Simulating the early stages of martensite band formation in pseudoelastic wires

Maximilian Hinze, Martin Wagner
Institut für Werkstoffwissenschaft und Werkstofftechnik / Technische Universität Chemnitz, Chemnitz, Saxony, Germany

Pseudoelastic NiTi shape memory alloys deformed in tension exhibit localized deformation by the formation and growth of stress-induced martensite bands. The initial stages of this Lüders-like deformation mode are characterized by a well-known nucleation peak in the stress-strain curve, but the underlying mechanisms-i.e., the nucleation of the martensite bands themselves-have still not been characterized in detail. Here we provide a careful analysis of the early stages of martensite band formation based on a continuum level constitutive model implemented in the Finite Element Analysis software Abaqus. The strain-softening model is capable of capturing effects such as localized deformation and the tension/compression asymmetry often observed in NiTi. In the present study, we consider the formation of a symmetric martensite nucleus and its radial growth in a NiTi SMA wire under uniaxial stress conditions. By analyzing the energy functional in the transition zone from martensite to austenite during band initiation, we gain insights into the underlying energetics of this macroscopic feature. In particular, we attribute the shape of the macroscopically observed interface between both phases to this analysis. We finally observe excellent agreement between our simulation results and high-resolution surface strain field data from DIC measurements on NiTi tensile samples.

103_396

Constitutive modeling of martensite plasticity and TRIP in polycrystalline shape memory alloys

Miroslav Frost[1], Petr Sedlák[1], Alexej Moskovka[1], Hanuš Seiner[1], Barbora Benešová[2], Martin Kružík[3], Petr Šittner[4]
[1]Instutute of Thermomechanics, Czech Acad Sci, Prague, Czech Republic. [2]Faculty of Mathematics and Physics, Charles University, Prague, Czech Republic. [3]Institute of Information Theory and Automation, Czech Acad Sci, Prague, Czech Republic. [4]Institute of Physics, Czech Acad Sci, Prague, Czech Republic

Experimental studies of martensitic transformation in NiTi SMA have revealed that i) martensite can undergo large plastic deformation, ii) forward martensitic transformation is affected by martensite plasticity even at moderate stresses, and iii) reverse martensitic transformation can result in plastically deformed austenite even though it occurs at macroscopic stresses well below the corresponding yield stress of either phase. The latter phenomenon is therefore essentially 'transformation induced plasticity'.

Constitutive models implemented in finite element methods are used as an efficient analytical tool for design and optimization of applications. In order to include the above phenomena, we have extended a well-established continuum thermodynamics-based constitutive model [1]. It features a refined description of inelastic processes via an extended set of internal variables and a complex dissipation (rate) function. The time evolution of the material response is recovered by a combination of minimization problems, which allows the mutual influence of the inelastic processes to be taken into account [2]. Finally, numerical homogenization allows the influence of microscale heterogeneity to be effectively incorporated into the macroscale response. The model has been implemented in a lightweight finite element software capable of finite-strain calculations [3]. After validation on an extensive experimental dataset, we have performed several simulations to demonstrate the predictive capabilities of the model. The possible adaptation of the approach to β-Ti SMA is also touched upon.

The authors acknowledge the support provided by the Ferroic Multifunctionalities project, supported by the Ministry of Education, Youth, and Sports of the Czech Republic. Project No. CZ.02.01.01/00/22_008/0004591, co-funded by the European Union.

[1] P. Sedlák et al., Thermomechanical model for NiTi-based shape memory alloys including R-phase and material anisotropy under multi-axial loadings (2012), Int. J. Plasticity 39, 132-151.
[2] M. Frost et al., Thermomechanical model for NiTi-based shape memory alloys including plasticity, in preparation
[3] A. Moskovka et al., Finite-strain constitutive model for shape memory alloys formulated in the logarithmic strain space, submitted to Shape Mem. Superelasticity

104_389

High-resolution strain-field mapping during nucleation and propagation of martensite bands in pseudoelastic NiTi

Martin Wagner, Maximilian Hinze
TU Chemnitz, Institute of Materials Science and Engineering, Chemnitz, Germany

While the propagation phase of martensite bands in pseudoelastic NiTi samples subjected to tensile loading is well appreciated, the early stage of martensite band nucleation has hardly been studied in detail. The present study addresses this topic by performing a dedicated analysis of high-resolution strain-field data captured experimentally by digital image correlation. Pseudoelastic NiTi rods as well as thin wires are subjected to pseudoelastic loading-unloading cycles, and the nucleation and propagation of distinct martensite bands are carefully monitored with high spatial and temporal resolution. We specifically focus on the nucleation phase, where our results show that a wide-spread disturbance in the uniaxial strain field (covering a width of more than one sample diameter) already occurs in the nominally elastic deformation regime of austenite, clearly preceding the nucleation peak in the stress-strain curve. We show that this strain disturbance is directly associated with the non-linear part of the “elastic” loading regime prior to the onset of the transformation plateau. Integrating uniaxial strains on the sample surface, we estimate the size of a small martensite nucleus forming simultaneously in the center of the sample. The comparison of rod and wire results shows that in both cases, martensite band formation is governed by the same meso-scale processes, scaling with sample diameter. Our results on the evolution of local surface strain fields during martensite band nucleation provide a detailed view particularly on the onset of pseudoelastic deformation. They additionally form the basis for modeling of martensite band nucleation in the framework of finite element analysis investigations, and for an analytical model of martensite nucleation and radial growth from the center line of the sample towards the outer surface, further completing our understanding of stress-induced martensite formation and localized pseudoelastic deformation.

105_298

Shell-based finite element modelling for predicting buckling stability of superelastic SMA tubes

Luka Porenta, Adam Plantarič, Jaka Tušek, Miha Brojan
Faculty of Mechanical Engineering, University of Ljubljana, Ljubljana, Slovenia

Superelastic shape memory alloys (SMA) have shown fatigue-resistant operation when loaded in compression, which is crucial for various practical applications such as elastocaloric cooling [1]. However, to facilitate heat transfer and assure efficient operation elastocaloric devices require thin-walled elements, which can collapse due to buckling during compressive loading. To computationally predict buckling behavior during compressive loading, either 3D solid finite elements coupled with 3D SMA constitutive equations (which are accurate but time consuming), or shell finite elements coupled with simplified SMA constitutive models (which are usually faster but have limited accuracy) can be used. Here, we will present a new numerical approach to predict buckling behavior based on highly accurate 7-parameter shell formulation and full 3D constitute equations that account for the phase transformation between austenite and martensite [2, 3]. To initiate buckling in the numerical simulations of the thin-walled structures, random geometric imperfections are forced into the mesh of finite elements in radial direction. Results of the numerical simulations are verified with experimental observations [4] and good agreement in stress-strain behavior and buckling modes was obtained (see Fig. 1) [3]. Phase diagrams of the buckling modes are numerically determined for NiTi tubes with an outer diameter between 2 and 3 mm and a diameter-to-thickness ratio in the range between 5 and 25, which appear to be promising candidates for use in elastocaloric technology. We have demonstrated the potential of the proposed computational model as a fast and reliable tool to simulate the buckling behavior of SMA elements not only for elastocaloric technology but also for other applications where superelastic SMA elements are used.

[1] Ž. Ahčin et al., Joule 6 (2022)
[2] L. Porenta et al., Communications in Nonlinear Science and Numerical Simulation 101 (2022)
[3] L. Porenta et al., Thin-Walled Structures 208 (2025)
[4] L. Porenta et al., International Journal of Solids and Structures 256 (2022)

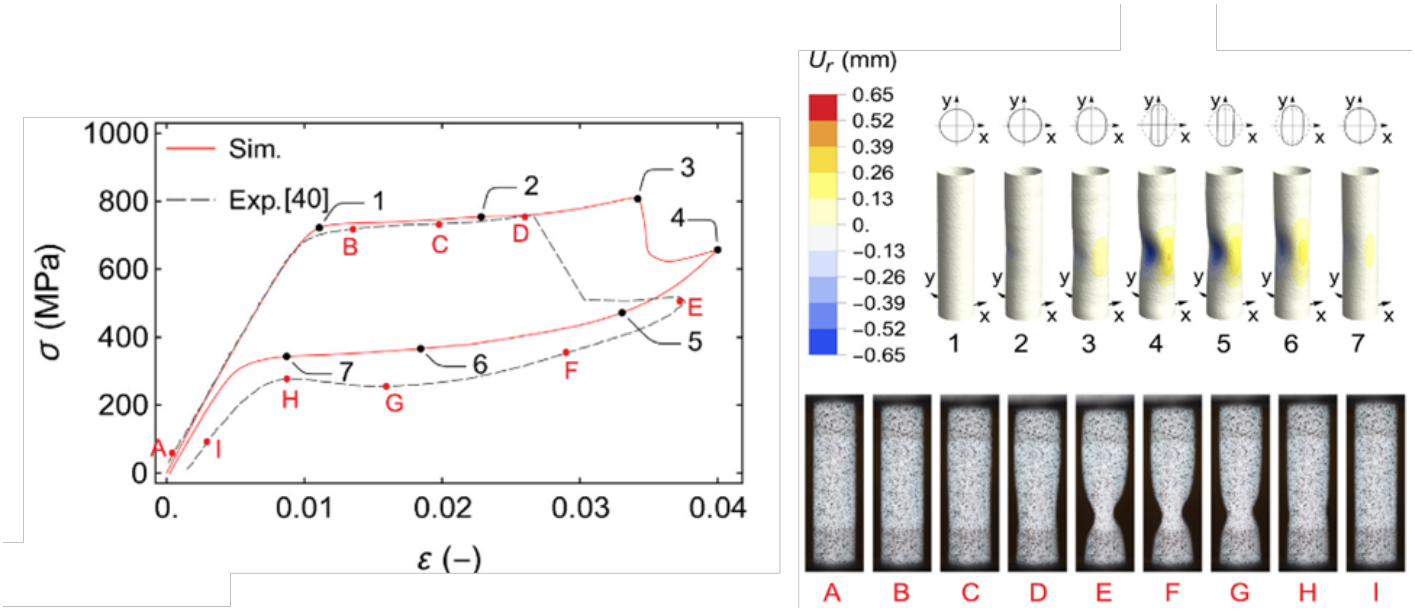

Figure 1: Comparison of numerically calculated (shell-based finite element model) and experimentally obtained stress-strain response (left) and buckling mode (right) of thin-walled superelastic NiTi tube.

106_224

PLENARY: Probing theory of martensite by epitaxial films

Sebastian Fähler
Helmholtz-Zentrum Dresden-Rossendorf, Dresden, Saxony, Germany

Martensitic twin-within-twins microstructures are beautiful and often look like modern art. Understanding their formation is decisive for applications since this microstructure controls most of the functional properties of shape memory alloys. There are various theoretical concepts to describe these microstructures, but often it is difficult to recognize at which type of length scale they can be applied. In polycrystalline materials, this is additionally hampered by incompatible grain boundaries, which affect spacing and orientation of twin boundaries.

To avoid these complications, here we use epitaxial films as model systems. We show that the hierarchical martensitic microstructure consists of five levels of nested building blocks, which are connected by different types of twin boundaries. Starting from the atomic scale, we show that each of this level solves a particular complication of a martensitic transformation. We sketch the relevant energies, which decrease with each level. This approach gives a scale-bridging understanding of all features within the three-dimensional martensitic microstructure. [1]

In this talk, we mostly focus on Ni-Mn-Ga, where all levels of twinning fit seamingless together, but show also recent experiments on NiTi films. Despite the different crystallography, NiTi also exhibits a hierarchical microstructure. However, we identify incompatible regions, which illustrate that the 3D puzzle for NiTi is not completely solved yet. [2]

Films are often considered as fundamentally different compared to bulk and thus we discuss the limits of our model system. We show that that indeed spacings of twin boundaries differ strongly between bulk and films, but both exhibit the same key microstructural features. The suitability of films as model system, however, only holds for films constrained by substrate. Freestanding films can exhibit a fundamentally different microstructure. In this case the microstructure is governed by an invariant *line*, in contrast to bulk, where an invariant *plane* between austenite and martensite occurs. Thus, these freestanding films represent the transition from 3D bulk to 2D films. [3]

[1] S. Schwabe et al, Adv. Funct. Mat. 31 (2020) 2005715
[2] K. Lünser et al, Mat. Today Advances 20 (2023) 100441
[3] S. Kar et al, Adv. Funct. Mater. (2024) 2416638

107_406

PLENARY: Development of high-performance shape memory alloys for elastocaloric refrigeration technology

Qingpin Sun
Department of Mechanical and Aerospace Engineering Hong Kong University of Science and Technology, Hong Kong, China

Elastocaloric cooling/heating by harvesting latent heat from phase transition of shape memory alloys (SMAs) attracted considerable interest as a greenhouse-gas-free alternative to conventional vapor-compression refrigeration. Developing this disruptive technology involves multidisciplinary interaction and collaborations among the fields of material science and engineering, heat transfer, design and manufacturing, solid and fluid mechanics. So far, many different SMA materials have been developed and kilowatt-scale elastocaloric cooling prototypes have been built based on cyclic phase transition of NiTi shape memory alloy under compression. Large specific heat transfer area of NiTi SMA tubular structure and heat transfer nano-fluid have enabled a giant cooling power density of 12.3 W g^{-1}, a total cooling power of 1284 Watt and a temperature lift of 31.6 K, demonstrating great potential in commercializing this novel technology for future space cooling and heating. This talk will present, from an experimental and theoretical point of view, recent progress and challenging issues in developing elastocaloric refrigeration, especially the impacts of high-performance shape memory alloys on this disruptive technology.

Keywords: elastocaloric refrigeration technology, high-performance shape memory alloys, cyclic stability, fatigue life, transformation stress, latent heat, material energy efficiency.

108_187

Microstructure refinement of 0.1C-4Mn martensitic steel utilizing heterogeneous Mn distribution

Ji Hoon Kim[1], Masayoshi Akaishi[2], Goro Miyamoto[2], Yongjie Zhang[2], Wu Gong[3], Stefanus Harjo[3], Tadashi Furuhara[2]
[1]Pusan National University, Busan, Korea, Republic of. [2]Tohoku University, Sendai, Japan. [3]J-PARC, Tokai, Japan

Microstructure refinement is an effective method to enhance the mechanical properties of metallic materials. In martensitic steels, refining the prior austenite grain (PAG) size is the most widely adopted method for the refinement, as PAG boundaries act as barriers to martensite growth. Cyclic heat treatment, which involves repeated austenitization and quenching, is applied to refine PAG size to about 5–10 μm. However, as the demand for high-strength steels increases, achieving an even finer microstructure is essential to meet these requirements. Therefore, a new method for the refinement of martensitic steel is needed.

Recently, chemically heterogeneous steels have gained significant attention as a new approach to microstructure design. These steels exhibit substantial variations in initial chemical composition across different regions, introducing chemical boundaries (CB) where composition changes significantly without altering crystal orientation. Such chemical heterogeneity creates localized differences in the driving force for phase transformation, allowing CBs to function similarly to grain boundaries. Moreover, the scale of chemical heterogeneity can be refined to the sub-micron level through intercritical annealing, potentially overcoming the limitations of conventional PAG size refinement methods. This study aims to explore the feasibility of utilizing chemical boundaries to refine martensitic microstructures.

In this study, microstructures with heterogeneous and homogeneous Mn distributions were compared in Fe-0.1C-4.0Mn (mass%) steel. For homogeneous martensitic steel, specimens were conventionally austenitized at 850–1000°C for 1 min to vary PAG size, followed by cooling to room temperature at rates ranging from 50°C/s to 12.5°C/s. For chemically heterogeneous steel, specimens underwent pre-annealing in the two-phase region (635°C for 24 hrs) before being subjected to the same heat treatment as the homogeneous specimens to obtain a martensitic microstructure. The results revealed that introducing chemical heterogeneity effectively refined the martensitic microstructure. This refinement was particularly pronounced under low austenitization temperatures and slow cooling rates, conditions in which chemical heterogeneity was more pronounced. The refinement mechanism is attributed to the lower transformation temperature in Mn-and C-enriched regions, which promotes the formation of additional variants to accommodate transformation strain

109_177

Effect of microstructure on hole expansion ratio of advanced high strength steel

Jin Sung Hong, Seong Kyung Han, Tae Woo Kwon
Hyundai Steel R&D Center, Dangjin, Korea, Republic of

One of the biggest issues in the recent automotive steel sheet market is to make a hard and light steel to raise passenger stability and fuel efficiency. A commonly used method to achieve both goals simultaneously is to increase the strength of the steel sheet used in automotive part. However, since the strength and formability of steel generally has a trade-off relationship, development of advanced high strength steel with improved formability is necessary.

Hole expansion ratio (HER) is one of the indices of the formability, quantifying the edge stretching capability of the steel sheet. HER can be obtained by measuring the maximum size of the hole that can be expanded without cracking. In the present study, we investigated the effect of microstructure on the HER of advanced high strength steel, using steels with similar strength level but with different microstructures.

Although both HER and post-uniform elongation are representative indices of local formability, HER did not have a strong relationship with post-uniform elongation in the present study. Rather, HER has a strong positive correlation with yield strength; As yield strength increases, HER also increases. HER has a linear inverse relationship with hardness difference between hard and soft phases. Increase in the hardness difference between two phases raised the amount of deformation for the formation of void, resulting in the increase of the HER. Therefore, decreasing the hardness of hard phase, such as martensite, by optimizing microstructure is key factor in developing multi-phase advanced high strength steel with high HER. Through the optimization of microstructure, we developed an advanced high strength steel with TS of ~870MPa and HER of ~94%.

110_248

Effect of microstructure on mechanical properties of 1.0G TRIP steels produced by quenching and partitioning process

Wontae Cho
POSCO, Kwangyang, Korea, Republic of

Influence of microstructure on tensile properties and stretch-flangeability of TRIP steels with tensile strengths higher than 1.0 GPa has been investigated under various Quenching and Partitioning (Q&P) conditions. Lowering the quenching stop temperature (QT) from 300°C to 190°C after intercritical annealing increased the volume fraction of tempered martensite (TM), decreased that of bainite, and maintains that of ferrite and retained austenite constant in the final microstructure. 300°C was Ms temperature, thus, QT 300°C sample consisted of negligible TM and 36% bainite. So, as the QT was reduced to 190°C, the TM phase was integrated into the bainite up to 13.8%. The yield strength (YS), tensile strength (TS), and hole expansion ratio (HER) of QT 300°C steel were inferior compared to that of QT 190°C steel; however, the total elongation was improved by 2.9% for QT 300°C steel. The elevated YS and TS of the QT 190°C steel were attributed to the increased micro hardness caused by the increased TM fraction. Furthermore, the high HER of the QT 190°C steel was elucidated by the reduced micro void formation compared to the QT 300°C steel under the same reduction ratio. That was because QT 300°C steel, comprised mainly of bainite, has a higher fraction of blocky retained austenite that, when subjected to deformation, transforms into mechanically induced blocky martensite, acting as a significant source of micro voids.

111_311

Effect of the manufacturing method and heat treatment on martensite formation in maraging 250 steel

Thaissa Sampaio Nunes[1], Julianna Magalhães Garcia[1], Andersan dos Santos Paula[1], Talita Gama de Sousa[2], Luiz Paulo Brandao[1]
[1]Instituto Militar de Engenharia, Rio de Janeiro, Rio de Janeiro, Brazil. [2]Centro Brasileiro de Pesquisas Físicas, Rio de Janeiro, Rio de Janeiro, Brazil

The martensitic transformation in maraging steels is essential for their mechanical properties, playing a key role in structural and aerospace applications. This study investigated the phase fraction in maraging 250 steel samples manufactured by both conventional methods and Wire Arc Additive Manufacturing (WAAM), before and after heat treatments. The preforms were produced using Mig Marval 18S wire (1.2 mm) on an ASTM A36 substrate. The WAAM process employed near-immersion active cooling (NIAC), with condition 1 using a current of 160 A and a contact tip-to-work distance (CTWD) of 22 mm, while condition 2 used 196 A and a CTWD of 12 mm. Phase fraction quantification was performed using ferritoscopy with a FISCHER FMP30 device, calibrated with ferrite standards. The results showed that conventionally hot-rolled maraging 250 steel (MC) exhibited a martensite fraction ranging from 88.3% to 98% (average of 91.6%). For WAAM, condition 1 (M1) varied between 86.7% and 92.3% (average of 88.87%), while condition 2 (M2) ranged from 83.3% to 88.7% (average of 86.93%). After heat treatment at 800°C for 1 h, followed by aging at 520°C for 4 h, a significant reduction in martensite fraction was observed, indicating microstructural stabilization. The heat-treated conventional material (MCTT) ranged from 29.6% to 34.9% (average of 32.15%), while WAAM condition 1 (M1TT) varied from 26.8% to 30.6% (average of 27.8%), and condition 2 (M2TT) ranged from 37.3% to 41.4% (average of 39.78%).The comparison between manufacturing processes showed that WAAM deposition alters the martensitic fraction, impacting mechanical properties. Condition 2 retained a higher martensite fraction after heat treatment, highlighting the influence of deposition parameters. CTWD affects heat transfer and martensite formation. An increased CTWD reduces welding current, accelerating cooling and favoring martensite formation, while a reduced CTWD increases welding current, leading to higher heat input and a lower martensite fraction. Heat treatment promoted the partial reversion of martensite into austenite due to matrix enrichment with nickel and the precipitation of intermetallic compounds. The formation of reversed austenite, stable at room temperature, can enhance the balance between strength and ductility. Ferritoscopy proved effective in microstructural characterization, enabling a non-destructive phase transformation analysis.

112_258

Fatigue performance of low-temperature aged NiTi filaments

Ondřej Tyc[1], Petr Šittner[1], Yuchen Chen[1,2]
[1]Institute of Physics of the Czech Academy of Sciences, Prague, Czech Republic. [2]Xi'an Aeronautical University, Xi'an, China

It is well known that the superelastic deformation of NiTi tends to be accompanied by plastic deformation, which gives rise to the accumulation of unrecovered strains upon cycling and instability of cyclic stress-strain response. One of the important factors affecting both functional and structural fatigue is precipitation of Ni_4Ti_3 phase in Ni-rich NiTi. In this work, a nonconventional method of pulse heating by electric current was employed to recover cold-worked NiTi filaments (100 µm in diameter) and set the initial microstructure without precipitation. The impact of recovery processes and precipitation on mechanical properties can be separated, owing to the ultrafast electric current annealing. Afterwards, some NiTi filaments were subjected to aging at 250-400 °C for 1-5 h followed by tensile fatigue tests to determine how functional and structural fatigue are affected by grain size and aging.

It is shown that the homogenous distribution of ~5nm Ni_4Ti_3 precipitates created by low-temperature aging (250-300°C) yields much higher functional stability even at elevated temperatures. This is notable, especially for samples with larger grain sizes. Furthermore, samples with larger grain sizes exhibit higher fatigue life in the tested range of grain sizes (d~75-1000nm). The experiments also show that aging at low temperatures does not significantly change transformation temperatures and stresses compared to aging at the higher temperature of 400°C allowing better comparison of fatigue lives between samples that were subjected to aging and samples with recrystallized microstructure only. This improved functional stability results in higher fatigue life at elevated temperatures (transformation stresses). However, the fatigue life is lower near Af temperatures compared to samples without Ni_4Ti_3 precipitates suggesting a detrimental effect of precipitates on fatigue life and ductility likely due to internal stresses in crystal lattice around Ni_4Ti_3 precipitates.

113_252

Third element diffusion induced amorphization of NiTi

Sam Bakhtiari[1,2], Arpit Agrawal[3], Yinong Liu[1], Hong Yang[1]
[1]The University of Western Australia, Perth, WA, Australia. [2]Curtin University, Perth, WA, Australia. [3]Indian Institute of Technology Delhi, New Delhi, India

This study investigated the amorphization of NiTi. The study was focused on two main aspects: (i) amorphization of NiTi induced by third element diffusion through its the B2 matrix and (ii) comparative tendency of amorphization of four different B2 alloys caused by anti-site defects. The first aspect was studied experimentally using a NiTi-Nb alloy, which forms a nanowire *in-situ* composite. Upon heat treatment the Nb nanowires spheroidize and agglomerate via diffusion though the NiTi B2 matrix, causing its amorphization along the diffusion path. This is attributed to the effect of Ni-Ti atomic swapping within the B2 matrix, i.e., the formation of anti-site defects in the B2 lattice, caused by the substitutional diffusion of Nb. The second aspect was studied by means of molecular dynamics simulation on the effect of anti-site defect concentration. The B2 systems studied include AlFe, CuZr, FeTi and NiTi. It was found that anti-site defects cause severe random lattice distortions to the B2 structures, lowering their crystalline ordering. Among the four B2 systems studied, equiatomic AlFe and FeTi cannot be fully amorphized by anti-site defects, but NiTi and CuZr can become fully amorphous at above a threshold concentration of the defects, with NiTi being the easier one to be amorphized. These findings also help us to understand the amorphization of NiTi caused by cold working.

114_400

Aging effect on orientation dependent superelastic behavior of NiTi Shape Memory Alloy by multicycle nanoindentation

Akhil Bhardwaj[1], Luděk Heller[2], Petr Šittner[3], Ondřej Tyc[2], Jaromír Kopeček[2], Elizaveta Iaparova[2]
[1]FZU, Institute of Physics of the Czech Academy of Sciences, Prague, Prague 8, Czech Republic. [2]FZU, Institute of Physics of the Czech Academy of Sciences, Prague, praha 8, Czech Republic. [3]FZU, Institute of Physics of the Czech Academy of Sciences, Prague, Praha 8, Czech Republic

This study examined the impact of aging on functional fatigue performance of superelastic NiTi by cyclic nano indentation. The B2 austenite in grains of NiTi polycrystal was loaded in <111>,<110> and <100>directions by cyclic nano indentation in force control mode with force limits of 1mN and 20 mN. A spherical tip with 10 µm diameter was used for 200 loading-unloading cycles. The NiTi polycrystal was investigated in two conditions: i) solution annealed (SA), ii) solution annealed with subsequent aging at 350 °C for 15 minutes (SA+AG350). Ni_4Ti_3 nano precipitates were observed in the microstructure of SA+AG350 by TEM. Note that the aging did not induce the premartensitic R-phase transformation or shift substantially the transformation temperatures, according to DSC measurements. The recovered and unrecovered deformation along with hysteresis energy was evaluated before and after aging for <111>, <110> and <100> loading directions. The recovered deformation along <111>, <110> and <100> loading directions remains almost same as it was before aging. However, aging results in an increase in recovered deformation along all loading directions (increase 14% to 16%).

The recovered and unrecovered deformation and hysteresis energy were evaluated after 1^{st}, 2^{nd}, 10^{th}, 100^{th} and 200^{th} cycles. Before aging, the cumulative unrecovered deformation found to be minimal along the <110> direction and maximal along the <111> loading direction. However, after aging, minimal unrecovered deformation was observed along the <111> loading direction. The cumulative unrecovered deformation tends to decrease after aging by 8.6%, 16.3% and 50.0% along <100>, <110> and <111> loading direction respectively indicating very efficient stabilization of superelastic response along <111> loading direction after aging. Hysteresis energy after 100^{th} cycle was found to 65 ± 5 pJ along <100>, 80± 5 pJ along <110> and 95 ±5 pJ along <111> loading direction and changed by 117% in <100>, 91% in <110>, 35% in <111> loading direction after aging.

The present study indicates that cyclic nano indentation can be used to evaluate orientation dependent instability of cyclic superelastic deformation (functional fatigue) of NiTi-i.e substitute single crystal or nanopillar experiments.

115_213

Standard and repetitive load-unload nanoindentation studies on superelastic and shape memory NiTi

Sneha Samal[1], Lukáš Kadeřávek[1], Jan Tomáštík[2], Lukáš Václavek[2], Orsolya Molnárová[1], Petr Šittner[1]
[1]FZU-Institute of Physics of Czech Academy of Science, Prague, Czech Republic. [2]Institute of Physics of the Czech Academy of Sciences, Joint Laboratory of Optics of Palacký University and Institute of Physics of the Czech Academy of Sciences, Olomouc, Czech Republic

Standard and repetitive load-unload nanoindentation was performed on superelastic (SE) and shape memory (SME) NiTi alloy. The mirror-like surface of the NiTi sheets was prepared by electro chemical polishing. A spherical indenter of 10 µm radius was used with various indent loads on the surface of SE and SME alloys. Elastic and thermal recovery of indentation depths were measured through evaluation of residual indents. The maximum recovery of 95 % of indent depts was revealed at lower loads of 25 and 50 mN in SE alloy in Fig. 1 (a). SME samples show a maximum recovery after heating on residual imprints of indent depth of 79 % at 250 mN load in Fig. 1 (b). Elastic recovery in SE NiTi sample during unloading results from the reverse phase transformation, while in case of SME NiTi, it results from spring back twinning. On subsequent heating, the SME NiTi shows indentation depth recovery twice as large as the SE samples. In case of repetitive load-unload indentation tests a maximum load of 10 mN with dwell time of 1s was applied. SE NiTi shows response that quickly stabilizes, while SME NiTi displays ratcheting in Fig. 1 (c-f) and (g-j).

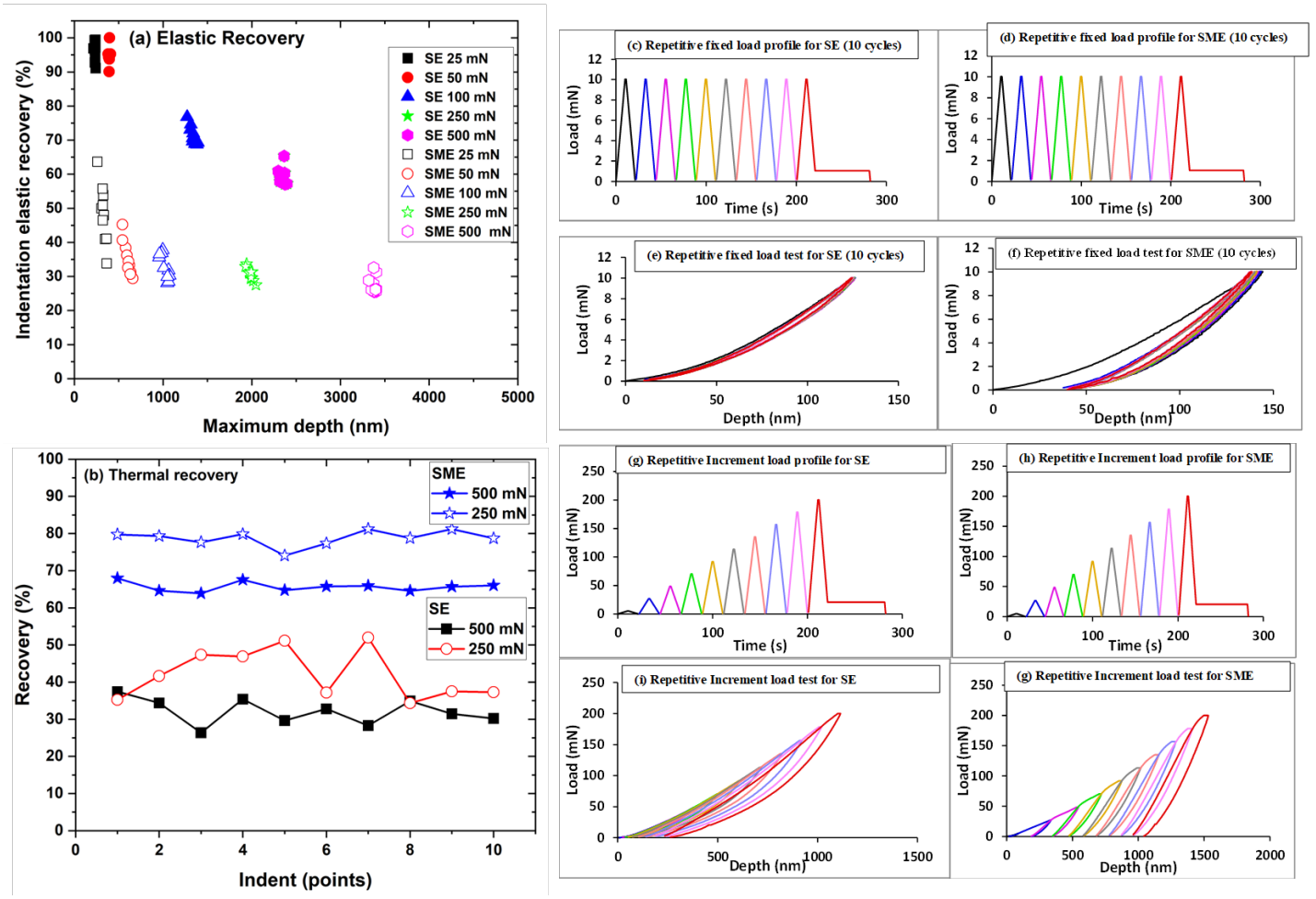

Fig. 1: Nanoindentation test results with (a) Elastic Recovery and (b) Thermal recovery for SE and SME NiTi at various loads. Repetitive load-unload indentation tests at (c-f) fixed load and (g-j) increment load in SE and SME NiTi.

Ref: Recovery of deformation surface of superelastic and shape memory NiTi alloy, Applied Surface Science Advances, Volume 25, 2025, 100684, ISSN 2666-5239, https://doi.org/10.1016/j.apsadv.2024.100684.
(https://www.sciencedirect.com/science/article/pii/S2666523924001120)

116_319

Hydrogen Outgassing from FCC Metal Surfaces under Thermal Treatment

Avadh Saxena[1], A. Karkash[2], L. Diaz[2,3], R. C. Albers[1], M. Sanati[1,2]
[1]Theoretical Division, Los Alamos National Laboratory, Los Alamos, New Mexico 87545, USA. [2]Department of Physics and Astronomy, Texas Tech University, Lubbock, Texas 79409, USA. [3]Sandia National Laboratories, Albuquerque, New Mexico 87185-1322, USA

The existing macroscopic models are not adequate for explaining experimentally observed hydrogen outgassing processes from metallic surfaces. To address this, we performed electronic-structure calculations and molecular dynamics simulations on hydrogen diffusing through FCC metal surfaces. Hydrogen absorption sites. We then carried out a systematic analysis of various stages of outgassing by studying diffusion and energetics and found excellent agreement with experimental measurements. Our atomistic methods revealed the direct impact of the hydrogen potential energy surface on hydrogen surface mobility and recombination. Our approach is quite general, applicable to other hydrogen outgassing systems and is important in the context of hydrogen-based economy.

117_347

Development of neural network interatomic potentials for molecular dynamics: Application for martensitic nickel titanium

Petr Jaroš[1], Petr Sedlák[1], Petr Šesták[1], Jörg Behler[2]
[1]Institute of Thermomechanics, Czech Acad Sci, Prague, Czech Republic. [2]Ruhr-Universität Bochum, Bochum, Germany

Molecular dynamics (MD) simulations can offer entirely new insights into microstructure evolution, however, their accuracy critically depends on the quality of the interatomic potential. Traditionally, empirical potentials such as EAM and MEAM have been used to model atomic interactions. While these approaches capture basic properties of simple systems, they often fall short when applied to more complex materials. Recent advances in computer science have enabled the use of machine learning algorithms to develop interatomic potentials that aim to achieve density functional theory (DFT)-level accuracy in MD simulations.

In this study, we present a high-dimensional neural network potential (HDNNP) methodology, which utilizes atom-centered symmetry function descriptors [1]. We apply this approach to the extensively studied shape-memory alloy NiTi, which poses significant challenges at both experimental and theoretical levels. Our focus is on developing a neural network potential for the martensitic B19’ phase, capable of simulating complex microstructure evolution involving both twinning and plastic slip [2]. We demonstrate that the developed potential accurately captures the strong plastic slip anisotropy and that the HDNNP approach is well-suited for modeling the evolution of martensitic microstructures. In particular, we address the well-known discrepancy between the DFT-predicted ground state BCO structure and the experimentally observed B19’ phase by investigating the temperature-dependent stability of the BCO phase through molecular dynamics simulations using the newly developed NN potential.

Ref.
[1] Behler, J., 2011. Neural network potential-energy surfaces in chemistry: A tool for large-scale simulations. Physical Chemistry Chemical Physics 13, 17930–17955. https://doi.org/10.1039/c1cp21668f

[2] Seiner, H., Sedlák, P., Frost, M., Šittner, P., 2023. Kwinking as the plastic forming mechanism of B19′ NiTi martensite. International Journal of Plasticity 168, 103697. https://doi.org/10.1016/j.ijplas.2023.103697

This work was financially supported by the Ministry of Education, Youth and Sports of the Czech Republic in the frame of the project 'Ferroic multifunctionalities' (project No. CZ.02.01.01/00/22_008/0004591).

118_270

Reversible domain switching induced by gradient precipitation with high dissipative superelasticity at low temperature

Dong Wang, Chuanxin Liang, Tianjiao Dong
Xi'an Jiaotong University, Xi'an, Shaanxi, China

Shape memory alloys have various specialized applications due to their ability to recover original shape after deformation. These alloys maintain martensite at low temperatures and exhibit detwinning behavior and ferroelasticity, losing their superelasticity under loading. We present a new mechanism of reversible domain switching to achieve superelasticity at low temperatures through phase field simulations. This mechanism allows for the adjustment of dissipation and recoverable strain during loading and unloading. By utilizing a system with gradient-distributed, variant-selective precipitation conditions, we address the challenge of achieving both superelasticity and high dissipation in traditional martensitic transformations at low temperatures. Further simulations show that the critical stress for superelasticity at low temperatures does not conform to the Clausius-Clapeyron relationship, which can be attributed to the recoverable domain switching between different martensitic variants. These findings are highly desirable for various space-based applications and open new possibilities for designing novel shape memory alloys.

119_231

Grain boundary network-induced martensitic transformations in polycrystals at finite strains: Multiphase-field approach and scale-effect

Newton ., Anup Basak
Indian Institute of Technology Tirupati, Tirupati, Andhrapradesh, India

Martensitic phase transformation (PT) in polycrystalline materials, induced by grain boundaries(GBs) and their triple junctions (TJs), is studied using a thermodynamically and physically consistent nanoscale multiphase-field (MPF) approach of the Ginzburg-Landau type at large strain considering the interfacial stresses. The present model employs N order parameters (OPs) to describe the N grains in the sample and M + 1 OPs to describe the austenite (A) ↔ martensite (M) transformation and M martensitic variants. Unlike the previous MPF models, our model considers distinct energy and intrinsic size of the dry GBs and TJs energies, providing a more realistic representation. GB energies are assumed to be isotropic and vary due to PTs. A double-obstacle potential for the grains and a double-well potential for the MTs are assumed, ensuring no ‘spurious phases’ within the GBs and phase boundaries appear. The strong effect of intrinsic length scales, including dry GB widths and grain size, on the temperature of barrierless phase transformations, kinetics, and complex microstructural evolution is studied during the forward (A → M) and reverse (M → A) transformations. The simulation results show that an intermediate stationary state between A and M, called premartensite (PM), nucleate barrierlessly within the GB network at a temperature well above the critical temperature for A → M PT. As the temperature of the sample decreases, more volume fraction of the twinned microstructures evolves within the grains. The forward and reverse transformation paths differ, indicating the transformations involve hysteresis. The elastic and structural stresses within the samples are also studied.

120_312

Analysis of Variant Pair Formation on Σ3 Boundaries in Lenticular Martensite Microstructures

Yuri Shinohara[1], Satomu Akabane[2], Tomonari Inamura[2]
[1]The University of Electro-Communications, Chofu, Japan. [2]Institute of Science Tokyo, Yokohama, Japan

Introduction: Variants in steel martensite microstructures exhibit specific pairing tendencies. Our group has analyzed variant pairs formed intragranularly in lenticular martensite microstructures based on the rank-1 connection and crystallography. The rank-1 connection gives information about incompatibility at the variant/variant junction plane (JP). This study analyzed lenticular martensite microstructures formed on specific prior austenite grain boundaries, namely Σ3 grain boundaries; variant pairs also form straddling them.

Materials and Methods: An alloy with a nominal composition of Fe-30Ni-0.3C (wt%) was used. The microstructures were examined using electron backscatter diffraction (EBSD) analysis. Variants were identified using crystal orientations measured by EBSD and midrib traces. The rank-1 connection at the JP with normal **m** for the V*i*/V*j* (*i*,*j* = 1,2,…,24) variant pair was evaluated by the following equation: $\mathbf{QRP}_{Vj}\mathbf{R}^{T}\text{-}\mathbf{P}_{Vi} = \mathbf{b}\otimes\mathbf{m}$. **Q** is the rigid body rotation (magnitude: θ) required for the variant V*j*, and θ corresponds to the degree of incompatibility at the JP. **R** is the matrix representing the orientation difference between the two prior austenite grains that form Σ3 boundaries. We set **R** as the 60° rotation about [111]. $\mathbf{P}_{Vi}$ and $\mathbf{P}_{Vj}$ are total shape strains of two variants given by the invariant plane condition at the habit planes. A $(112)_{\alpha'}$ twin was adopted as the lattice invariant deformation.

Results and Discussion: The solutions of the rank-1 connection are labeled in decreasing order of θ. This labeling is reasonable because variant pairs with small θ are preferential in the case of intragranular formation. The top six solutions with small θ are listed in Table 1. EBSD analysis revealed that types *II* and *VI* were formed preferentially on Σ3 boundaries; they theoretically have a (111) JP. Some Σ3 boundaries were further examined using two-surface trace analysis. It was found that these Σ3 boundaries have (111) twinning planes, and the JPs were on these twinning planes. Type *II* and *VI* formations are considered favorable because these types share (111) planes as both the twinning planes and JPs, exhibiting small θ.

Table 1 Solution of rank-1 connection. The variant pairs shown are representative examples.

	Variant pair (in the K-S variant notatnion)	**JP**	**θ (°)**
I	V7/V19	(0.61, -0.77, 0.16)	0.13
II	V1/V5	(111)	1.26
III	V9/V18	(0.07, -0.64, 0.77)	1.45
…	…	…	…
VI	V10/V22	(111)	2.11

121_198

Martensitic Transformation-Dominated Lüders Deformation in Ultrafine-Grained 304 Steel at 77K

Stefanus Harjo[1], Wenqi Mao[2], Si Gao[3], Tatsuya Ito[1], Wu Gong[1], Takuro Kawasaki[1]
[1]Japan Atomic Energy Agency, Tokai-mura, Ibaraki, Japan. [2]Northeastern University, Shenyang, China. [3]Kyoto University, Kyoto, Japan

304 stainless steel is known as a metastable austenitic stainless steel, and when deformed, in addition to dislocation slip, the introduction of stacking faults, deformation twins, and martensitic transformation occurs. As the deformation temperature decreases, martensitic transformation becomes more likely, significantly increasing the tensile strength due to the presence of the martensitic phase; however, it has been reported that the yield strength remains largely unchanged.

Recently, a combination of multi-step cold rolling and heat treatment successfully refined the grain size of SUS304 to 0.3 μm (UFG-304 steel). At room temperature, this UFG-304 steel exhibited a high yield strength of approximately 1 GPa, followed by a stress drop and significant Lüders deformation, then underwent uniform deformation with minimal work hardening before fracturing. During Lüders deformation, traces of extensive martensitic transformation were observed.

To investigate how deformation behavior at low temperatures changes with ultrafine grain refinement and the mechanisms involved, in-situ neutron diffraction experiments were conducted on the low-temperature tensile deformation of UFG-304 steel.

The yield strength of UFG-304 steel increased as the deformation temperature decreased, reaching approximately 1.4 GPa at 77 K. However, the amount of stress drop after yielding was larger compared to room temperature. Lüders deformation occurred even at low temperatures, but the strain associated with it decreased as the deformation temperature decreased. At low temperatures, uniform deformation was observed after Lüders deformation, accompanied by significant work hardening, resulting in considerable elongation before necking. The work-hardening rate during uniform deformation increased with decreasing temperature. At 77 K, the maximum strength during uniform deformation reached 1.9 GPa.

The mechanism behind this behavior will be explained using in-situ neutron diffraction data. Further details will be presented on the day of the report.

This study was supported by JST CREST (JPMJCR1994) and the MEXT program (JPMXP1122684766).

122_324

Revisiting γ-ε martensitic transformation: sluggish plate growth and significant TRIP effect.

Kaneaki Tsuzaki
National Institute for Mateterials Science, Tsukuba, Ibaraki, Japan

This study has been conducted to develop a new type of ε-TRIP steel with high yield strengh, and the paper consists of two parts: one is in-situ observation of ε martensite growth and the other is deformation-induced transformation of prior warm-rolled plate.

[1] In-situ observation of ε martensite growth:
γ-ε martensitic transformation during cooling in Fe15Mn10Cr8Ni (wt.%, Ms=250 K) was observed with SEM equipped with a cold stage available to around 215 K. Electron channeling contrast imaging (ECCI) was utilized for the in-situ observations during cooling. Discontinuous lengthening and thickening of hcp martensite plates were confirmed during not only cooling to 222 K but also isothermal holding at 238K for 8 min, indicating that ε (hcp) martensite grows slowly and sluggishly unlike very fast growth of lenticular and thin-plate a' (bcc or bct) martensite. This indicates that the control of transformation kinetics is fairly easy in the γ-ε martensitic transformation.

[2] Deformation-induced transformation of prior warm-rolled plate.

Tensile tests at room temperature were conducted in Fe30Mn10Cr10Co (at.%) that had been 50% warm-rolled at 573K (above A_f). Postmortem X-ray diffraction (XRD) and electron backscatter diffraction (EBSD) analyses were performed to investigate transformation behavior. In an annealed sample without the warm-rolling, the Ms temperature was 328 K and the volume fraction of ε martensite at room temperature was 10%. On the other hand, athermal ε martensite was completely suppressed in the warm-rolled sample and the volume fraction of ε martensite at room temperature was zero. Stress-assisted γ-ε martensitic transformation at room temperature was also suppressed in the warm-rolled sample, but significant strain-induced transformation after austenite yielding by slip was confirmed. More that 70% volume fraction of ε martensite was observed after failure both in the annealed and warm-rolled samples. Combination of work-hardened austenite and ε-TRIP effect exhibited a threefold increase in yield strength while retaining substantial uniform elongation.

123_333

Effects of Cryogenic Rolling and Metallographic Preparation on Martensitic Transformation and Residual Stress in 304L TRIP Steel

Juciane Alves[1,2], Marcelo Bittencourt[3], Andersan dos Santos Paula[1], Luiz Paulo Brandão[1]
[1]Instituto Militar de Engenharia, Rio de Janeiro, RJ, Brazil. [2]Centro Brasileiro de Pesquisas Físicas, Rio de Janeiro, RJ, Brazil. [3]Instituto de Engenharia Nuclear, Rio de Janeiro, RJ, Brazil

We investigated the effects of cryogenic rolling on martensitic transformation and the influence of metallographic preparation through mechanical, chemical, and electrolytic polishing on phase quantification and residual stresses of the 304L austenitic stainless steel. Cryogenic rolling led to fully martensitic samples after 60% and 80% thickness reductions. The results showed that the sample preparation method affected the phase content identified by X-ray diffraction (XRD) and ferritescopy measurements, the residual stresses measured by XRD, and the quality of the EBSD patterns. On the other hand, the residual stresses determined by ultrasound did not show significant variations among the different preparation methods. Based on results, electrolytic polishing proved to be the most effective method for removing the modified surface layer generated during the cryogenic rolling and grinding of the samples. X-ray diffraction and ultrasound techniques revealed microstructural changes from plastic deformation. The residual stresses associated with the martensitic transformation, measured by these techniques, showed dependence on the nature of the phases present, their relative proportions, and the intensity of the diffracted peaks. These results indicated a trend from tensile to compressive residual stresses. Ultrasonic testing clearly showed limitations in detecting the martensitic transformation in samples with thicknesses close to 1 mm. The results obtained by this technique indicated an increase in the magnitude of compressive residual stresses with the phase transformation increment. The microstructural analyses by XRD and ultrasound revealed changes related to the plastic deformation induced by cryogenic rolling and the resulting martensitic transformation. However, their results are not directly comparable due to the different methodologies. While X-ray diffraction analyzes only the surface layer, ultrasound involves a larger volume of the material.

Keywords: 304L steel, cryogenic rolling, metallographic preparation, residual stresses, detection limitations.

124_280

Cyclic Transformation Strengthening in Fine-Grained Fe-24Ni-0.3C Metastable Austenitic Steel Studied by In-Situ Synchrotron XRD

Mayu Dono, Si Gao, Myeong-Heom Park, Nobuhiro Tsuji
Kyoto University, Kyoto, Kyoto, Japan

TRIP (Transformation-Induced Plasticity) steels exhibit both high strength and good ductility owing to deformation-induced martensitic transformation (DIMT). However, their yield strength tends to be low because of the parent phase, metastable austenite with FCC structure. Grain refinement can effectively increase yield strength of TRIP steels. However, it also stabilizes the austenite phase against DIMT by hindering shear deformation in martensitic transformation within fine-grained austenite, which usually results in less TRIP effect and decreasing strain hardening. Recently, it has been reported that cyclic transformation process which involves repeated martensitic transformation and reverse transformation to austenite through thermal cycling treatments, greatly improves both yield strength and strain hardening in an Fe-24Ni-0.3C metastable austenitic steel [1]. Therefore, it is expected that ultrafine-grained Fe-24Ni-0.3C subjected to the cyclic transformation can exhibit both high yield strength and good tensile elongation.

In this study, the effect of cyclic transformation on mechanical properties of an ultrafine-grained Fe-24Ni-0.3C(wt%) metastable austenitic steel was investigated using the in-situ synchrotron X-ray diffraction (XRD). Specimens with recrystallized austenite microstructures of average grain size 0.67 μm were prepared and then subjected to the cyclic transformation up to 5 cycles.

Microstructural observations revealed that austenite grains retained nearly the same crystallographic orientation and grain size as the initial austenite grains even after the cyclic transformation. However, it was also found that intergranular misorientations in austenite significantly increased. The yield strength was enhanced by 100 MPa by one cyclic transformation treatment and the work-hardening ability was simultaneously increased. The effects of the cyclic treatment on the yield strength and transformation rate of DIMT were quantitatively evaluated using microstructural information, i.e., phase composition, phase stress, and dislocation densities obtained from the in-situ XRD measurements during tensile deformation. These findings will be shown and discussed in the presentation.

References
[1] Alaei A, Jafarian H, Eivani AR. Mater Sci Eng A Struct Mater 2016;676:342.

125_293

Prospects and challenges in Fe-based shape memory alloys

Thomas Niendorf
University of Kassel, Kassel, Hesse, Germany

Shape memory alloys (SMAs) often suffer high cost and, thus, cannot be applied in mass production where huge components of high weight are required. A group of SMAs being characterized by relatively low cost for alloying elements and processing contain iron as the base element. The Fe-based SMAs gained a lot of attention in recent years. Very interesting microstructures and functional properties were reported. Three different groups of Fe-based SMAs are in focus: Fe-Mn-Al-Ni-X; Fe-Ni-Co-Al-X and Fe-Mn-Si-X (where X denotes different potential alloying elements depending on the base alloy).

The present paper highlights most important findings elaborated in recent years. Focus will not only be on apt thermo-mechanical processing routes to establish specific microstructures, but also on functional properties (shape memory effect and superelasticity) and functional/structural degradation. Furthermore, novel combined effects will be introduced. Based on the results presented future prospects and prevailing challenges, respectively, will be thoroughly discussed.

126_228

Crystal structure and superelasticity in novel Fe-Mn-Al-Si alloy

Toshihiro Omori, Kimika Edagawa, Sheng Xu, Makoto Nagasako, Xiao Xu, Ryosuke Kainuma
Tohoku University, Sendai, Miyagi, Japan

Fe-based superelastic alloys have been attracting attention for potential applications including as large components in the civil engineering field owing to their low cost. Although Fe-Mn-Al ternary alloys show non-thermoelastic martensitic transformation from the α (A2) parent phase, the Ni addition results in the nano-size NiAl precipitates with the B2 structure in the disordered A2 matrix and Fe-Mn-Al-Ni alloys exhibit thermoelastic martensitic transformation and superelasticity. However, Fe-Mn-Al-Ni alloys suffer from poor functional fatigue of superelasticity, which is presumably related to the disordered structure of the matrix. It is known that Si promotes atomic ordering of the α phase in Fe alloys. Therefore, in this study, Si was added to Fe-Mn-Al alloy and the microstructure, martensitic transformation, and superelasticity were investigated.

Microstructure of Fe-Mn-Al-Si was observed by optical microscopy, TEM, and STEM. It was found from the TEM, STEM, and STEM-EDS analyses that the $L2_1$ phase precipitates in the B2 matrix. It was also found that martensite can be stress-induced and that the crystal structure is tetragonal with fine twins, which is different from the nano-twinned fcc or 8M in Fe-Mn-Al-Ni alloys. The tetragonality is probably caused by the ordered B2 and $L2_1$ structures in the parent phase. Superelasticity of Fe-Mn-Al-Si was evaluated by compression tests and the single crystal near <100> showed superelasticity. The temperature dependence of the critical stress for transformation was small, which results in the superelasticity in a wide temperature range from 4.2 K to 297 K.

127_254

Ordering and Martensitic Transformation in Fe-Mn-Al-Ga Alloys

Ji Xia, Keita Watanabe, Toshihiro Omori, Ryosuke Kainuma
Tohoku University, Sendai, Miyagi, Japan

Fe-Mn-Al alloys show martensitic transformation from the ferromagnetic α parent phase with the A2 structure to the antiferromagnetic γ' martensite phase with the 2M (fcc) structure [1]. Similarly, Fe-Mn-Ga alloys exhibit martensitic transformation from the paramagnetic α parent phase with the $L2_1$ structure to the ferromagnetic γ' martensite phase with the 2M ($D0_{22}$) structure [2]. These two alloy systems show similar phase transformation in terms of crystal structure, yet the order structure is different. Moreover, Fe-Mn-Al alloys with the disordered structure shows non-thermoelastic martensitic transformation, and thus no superelasticity can be obtained. Although Fe-Mn-Ga alloys exhibit thermoelastic martensitic transformation and superelasticity due to the ordered structure, the problems are high cost of Ga and low cold-workability. Since Al and Ga, which belong to the same group in the periodic table, are bcc stabilizers, it is expected to obtain thermoelastic martensitic transformation by substitution of Al by Ga. In this study, systematic investigations were conducted to reveal the change in the crystal structure, martensitic transformation, and magnetic properties in Fe-40Mn-xGa-(15-1/3x)Al (at%) alloys.

With the substitution of Al by Ga, the microhardness gradually increased due to the $L2_1$ ordering of the parent phase, which was confirmed by the XRD and TEM. Meanwhile, the cold workability drastically decreased with increasing Ga content between 6 and 9 at% Ga. As for magnetic properties, the magnetization of the parent phase decreased with the Ga substitution. In the in situ optical microscopy observation, the surface relief resulted from forward martensitic transformation in the cooling process remained after heating to the 373 K in low Ga alloys, which indicates the martensitic transformation may be non-thermoelastic. Similar to Fe-Mn-Al alloys, this can be explained by the low strength and the disordered structure of the parent phase. However, the transformation became reversible with increasing Ga content, changing to thermoelastic martensitic transformation.

REFERENCES

1. K. Ando, T. Omori, I. Ohnuma, R. Kainuma, K. Ishida, Appl Phys Lett, **95** (2009), 212504.
2. T. Omori, K. Watanabe, R. Y. Umetsu, R. Kainuma, K. Ishida, Appl Phys Lett, **95** (2009), 082508.

128_315

In situ studies on the functional stability of a polycrystalline highly textured Fe-Ni-Co-Al-Ti-B shape memory alloy using synchrotron X-ray diffraction and acoustic emission measurements

Anja Weidner[1], Cesar Sobrero[2], F. Napolitano[3], Robert Lehnert[1], Viktor Remich[4], Philipp Krooss[4], Thomas Niendorf[4], Horst Biermann[1]
[1]TU Bergakademie Freiberg, Freiberg, Germany. [2]Institute of Physics Rosario, Rosario, Argentina. [3]Centro Atómico Bariloche, San Carlos de Bariloche, Argentina. [4]Universität Kassel, Kassel, Germany

Iron-based shape memory alloys (SMAs) are promising alternatives to conventional SMA candidates such as Ni-Ti or Co-Ni-Ga, particularly regarding cost-efficiency. Majority of studies on these SMAs are performed in single crystalline material conditions. However, the industrial application of these materials in particular using the superelastic properties, requires the manufacture of large-scale components and, therefore, a polycrystalline microstructure with a pronounced texture. For this purpose a Fe-Ni-Co-Al-Ti-B alloy was cold rolled to 94 % of thickness reduction and subjected to recrystallization and aging. As a consequence of this thermo-mechanical processing, a coarse-grained polycrystalline material (300 µm grain size) with a pronounced <001> texture parallel to the rolling direction (see Fig. 1a) and fine g' precipitates were achieved enabling full reversibility under thermal (extrinsic two-way shape memory effect) and mechanical loading (superelasticity). However, despite the strong texture and the presence of the g' precipitates, a low functional stability was observed for the superelastic behaviour (see Fig. 1b). To understand the reasons for this functional degradation, in situ experiments using a combination of acoustic emission and synchrotron X-ray diffraction (S-XRD) measurements were conducted under mechanical loading in tension at RT. The martensite evolution during 13 cycles (cycles 1 to 8 to a nominal strain of 5.5 %, cycles 9 to 13 as incremental strain tests up to a maximum nominal strain of 8.5 %) was evaluated from XRD measurements. The analysis of the AE data revealed at least two different sources of acoustic emission: (i) the stress-induced martensitic phase transformation and (ii) the movement of dislocations. Thus, the martensite evolution was also evaluated form the progression of the cumulative AE energy of signals belonging to the cluster of the martensitic phase transformation. Finally, the amount of retained, stabilized martensite after the 13th cycle correlated well with the results obtained from S-XRD and AE.

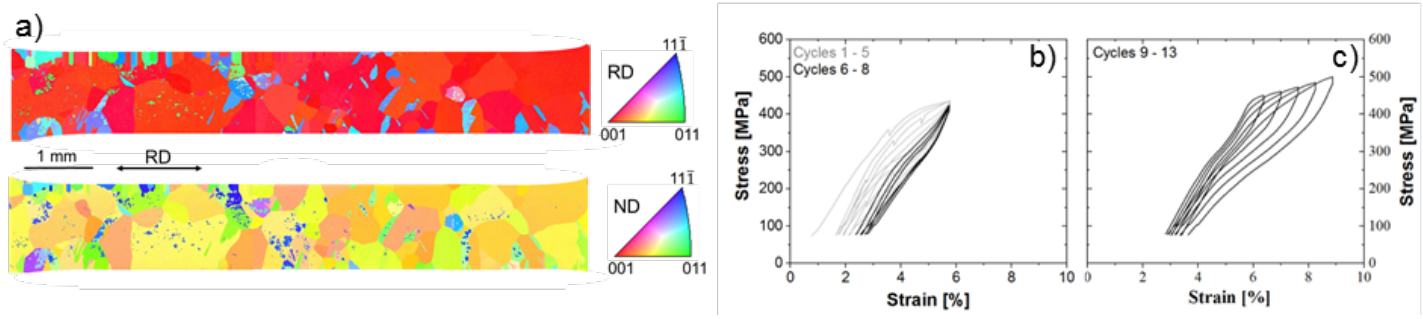

Figure 1: Polycrystalline microstructure of a Fe-Ni-Co-Al-Ti-B alloy obtained after thermo-mechanical processing showing large grain size (300 µm] and pronounced <001> texture parallel to the rolling direction (a) and superelastic stress-strain responses obtained under tensile loading at RT (b,c). (b) Constant nominal strain tests for cycles 1-8. (c) Incremental strain tests for cycles 9 to 13.

129_272

Change in Reverse Transformation Start Temperatures of Fe-33%Ni and Fe-28%Ni-20%Co Alloys by Shot-Peening

Hisashi Sato, Sayaka Sakurai, Yoshimi Watanabe
Nagoya Institute of Technology, Nagoya, Aichi, Japan

When the shot-peening (SP) is subjected to the Fe-33%Ni alloy with large amount of martensite (α'), reverse transformation from α' to austenite (γ) occurs [1]. Although this reverse transformation would come from the decrease in reverse transformation start temperature (A_s) due to the compressive residual stress induced by the SP, the amount of the change in the A_s by the SP is not clear. Moreover, since this change of the A_s occurs thermodynamically by inducing the compressive residual stress, the volume change caused by the phase transformation also would influence on the A_s. According to previous study [2], at the martensitic transformation, the volume of the Fe-28%Ni-20%Co alloy shrinks while that of the Fe-33%Ni alloy expands. In this study, using the Fe-33%Ni and Fe-28%Ni-20%Co alloys with large amount of α', the change in the A_s by the SP is investigated. Furthermore, the effect of the compressive residual stress by the SP on the A_s is discussed.

Fe-33%Ni and Fe-28%Ni-20%Co alloy specimens were austenitized at 1100 °C for 30 min and subsequently water-quenched. Then, these specimens are subzero-treated in liquid nitrogen for 30 min to occur martensitic transformation. The subzero-treated specimens were SPed at 0.2 MPa and 0.6 MPa in blast pressure for 30 min. The blast particle is $ZrSiO_2$ particle with 210 ~ 300 μm in diameter. After that, the SPed specimens were heat-treated at arbitary temperature from 120 °C to 200 °C, and the γ volume fraction were measured using X-Ray diffraction. The A_s were determined from the change in the g volume fraction.¨

Figs. 1 (a) and (b) show the γ volume fraction around the surface of the SPed Fe-33%Ni and Fe-28%Ni-20%Co alloy specimens as a function of heat-treatment temperature, respectively. The A_s of the Fe-33%Ni and Fe-28%Ni-20%Co alloy specimens without SP are 200 °C and 270 °C, respectively. In the case of the Fe-33%Ni alloy specimen, the γ volume fraction starts to increase at lower than 200 °C. This means that the A_s of this SPed specimen is decreased by the SP. But, the γ volume fraction of the SPed Fe-28%Ni-20%Co alloy specimen start to increase at higher than 270 °C, and its A_s is increased by the SP. This change of the A_s can be explained by the compressive residual stress due to the SP.

[References]
1. H. Sato, T. Nishiura, T. Moritani, Y. Watanabe, Surf. Coat. Technol., 462 (2023) 129470.

2. A. Shibata, H. Yonezawa, K. Yabuuchi, S. Morito, T. Furuhara, T. Maki, Mater. Sci. Eng. A, 438-440 (2006) 241.

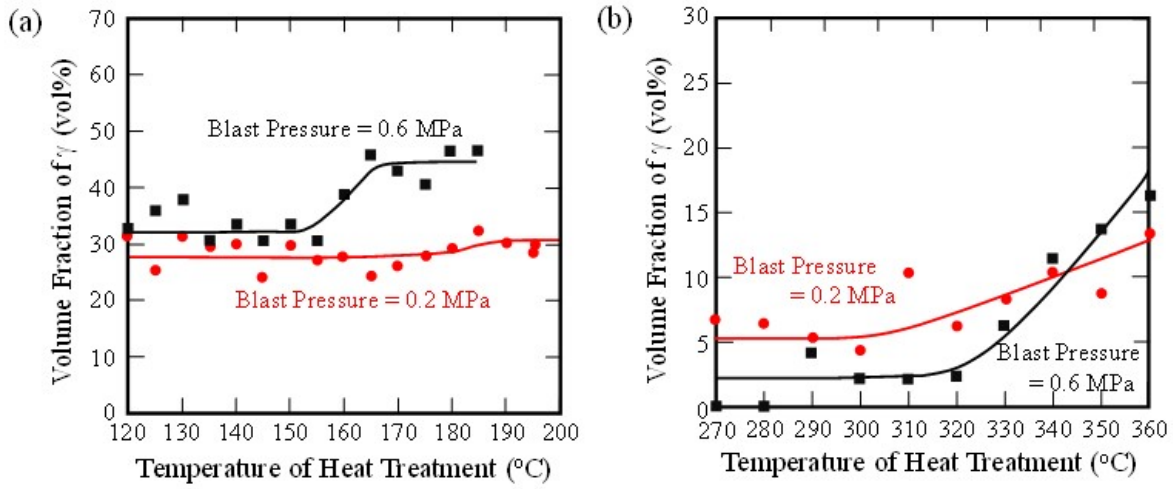

Fig. 1 Volume fractions of γ around SPed surface of (a) Fe-33%Ni and (b) Fe-28%Ni-20%Co alloy specimens as a function of heat-treatment temperature.

130_342

Bridging Fundamental Crystallography and Magnetic Shape Memory: Minor Diffraction Features Reveal Anharmonic Incommensurate Modulation in Ni-Mn-Ga Single Crystals

Petr Veřtát[1], Milan Klicpera[2], Oscar Fabelo[3], Oleg Heczko[1], Ladislav Straka[1]
[1]FZU-Institute of Physics of the Czech Academy of Sciences, Prague, Czech Republic. [2]Faculty of Mathematics and Physics, Charles University, Prague, Czech Republic. [3]Institut Laue-Langevin, Grenoble, France

The structure of magnetic shape memory martensites is often viewed from two distinct perspectives: that of a fundamental crystallographer and that of an applied physicist. The crystallographer constructs complex, diffraction-based structural models described in specialized language, often challenging for applied physicist to interpret. Conversely, the applied physicist—in our case, a magnetic shape memory specialist—focuses on tangible bulk material and its functionality, occasionally overlooking nuanced diffraction features due to simplified interpretations (such as “four satellites between main peaks equals five-layered” rule of thumb). In this talk, we bring the both perspectives together and show how accessible crystallographic findings bring novel insights into Ni-Mn-Ga and its extraordinary functionality.

Through high-resolution, high-statistics diffraction experiments on bulk Ni-Mn-Ga single crystals exhibiting supermobile twin boundaries, we revealed previously overlooked features, identifying multiple high-order satellite reflections. By tracking the temperature evolution of the satellite-rich diffraction patterns (**Fig. 1**), we uncovered an anharmonic incommensurate modulation within the 10M martensite [1]. Our proposed model not only precisely reproduces the evolution of the diffraction pattern from 300 K to 10 K using a single parameter but also explains that the observed, seemingly distinct crystal structures at different temperatures are merely variations of the same universal structure.

Our findings pave the way toward understanding how incommensurate modulation relates to the fine features in twinned microstructure and the resulting supermobility of martensite twin boundaries.

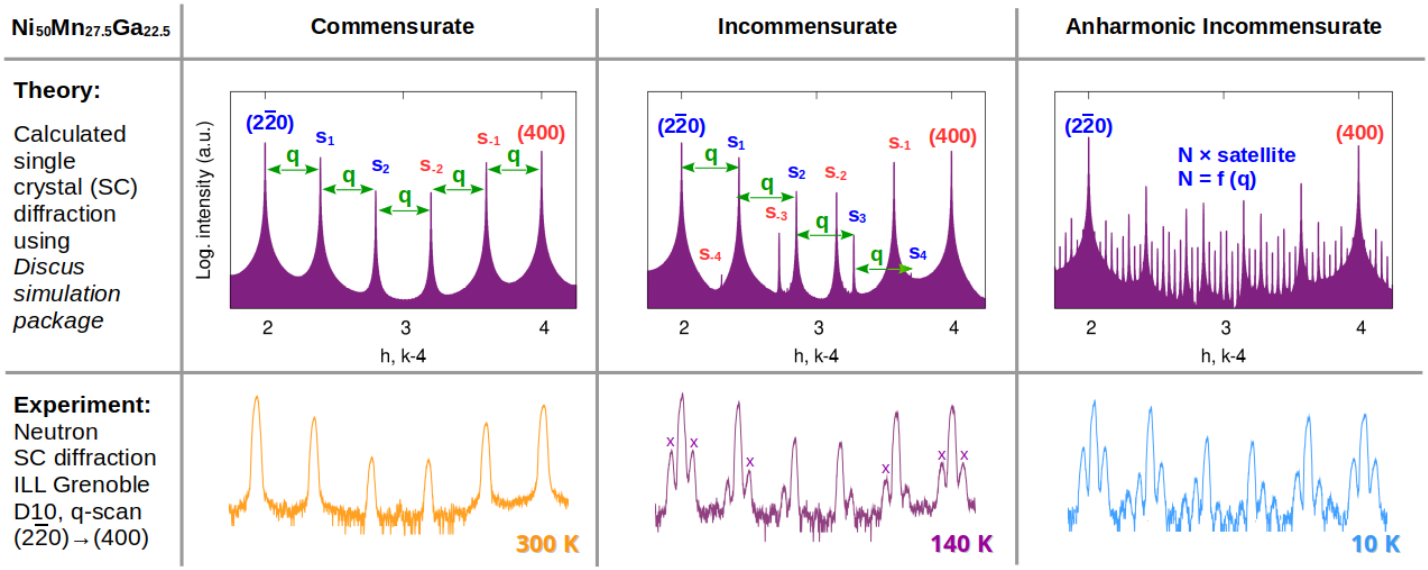

Fig. 1: Weak high-order satellite reflections (marked by “x” in the lower part of the figure) revealed only on a logarithmic scale are a fingerprint of anharmonic incommensurate structural modulation in $Ni_{50}Mn_{27.5}Ga_{22.5}$. Illustration of commensurate, (harmonic) incommensurate and anharmonic incommensurate modulation. [1]

[1] Veřtát et al., Scr. Mater. 252 (2024) 116251. doi: 10.1016/j.scriptamat.2024.116251

131_382

Modulated structures & Elasticity: On the road towards understanding the supermobility in Ni-Mn-Ga

Tomáš Grabec[1], Kristýna Repček[1], Pavla Stoklasová[1], Martin Ševčík[1], Petr Sedlák[1], Petr Veřtát[2], Ladislav Straka[2], Oleg Heczko[2], Hanuš Seiner[1]
[1]Czech Academy of Sciences, Institute of Thermomechanics, Prague, Czech Republic. [2]Czech Academy of Sciences, Institute of Physics, Prague, Czech Republic

There is something special about Ni-Mn-Ga alloys. Not only are they notable for their magnetic shape-memory behavior, which opens diverse applications, but they also exhibit supermobility-twin boundaries moving under extremely small mechanical or magnetic loads, producing large reversible strains. It is understood that this supermobility stems from a mechanical instability of the modulated crystal lattice, but the character and origin of this instability remains unexplained (despite two decades of research). And yet, it is this knowledge gap that hinders the search for materials with similar properties but more favorable transformation temperatures offering higher application potential.

A large step towards understanding this phenomenon came recently through extensive X-ray and neutron diffraction research and novel laser-ultrasonic methods. The diffraction methods revealed that temperature-induced changes in the modulation vector—from 2/5 (10M) to 3/7 (14M)—are gradual, not discrete switches between these states. Moreover, the modulation was found to be anharmonic, allowing for dynamic faulting of the modulation sequence. These modulation changes dramatically affect the shear elasticity of the martensite. For the commensurate 10M structure, one shear elastic constant nearly vanishes, indicating extraordinary softness to specific shearing forces perpendicular to the modulation vector. Interestingly, atomistic calculations predict a nearly ten-times higher value for this elastic constant, while accurately predicting other elastic properties. Once the modulation becomes incommensurate, this extraordinary softness quickly disappears, with the shearing stiffness matching the theoretical predictions.

This discrepancy points to mechanisms beyond atomistic simulations. A promising explanation involves phasons-quasi-particles representing phase fluctuations of the modulation wave. While phasons cannot be captured by atomistic simulations, phason-phonon coupling in the commensurate structure likely explains the observed extreme softness. This interplay between modulation characteristics, phason dynamics, and elastic properties offers a framework for understanding supermobility and its persistence across wide temperature ranges.

K.Repček et al., Adv Mater 36 (2024);
P.Veřtát et al., J Phys: Condens Matter 33 (2021);
S.M.Shapiro et al., EPL 77 (2007)

Financially supported by MEYS-CZ and co-funded by the EU (CZ.02.01.01/00/22_008/0004591)

132_339

Long-period Commensurate States in Ni-Mn-Ga Modulated Martensite

Petr Veřtát[1], Martin Zelený[2], Oleg Heczko[1], Ladislav Straka[1]
[1]FZU-Institute of Physics of the Czech Academy of Sciences, Prague, Czech Republic. [2]Faculty of Mechanical Engineering, Brno University of Technology, Brno, Czech Republic

A precise understanding of the martensitic crystal structure in magnetic shape memory alloys (MSMAs) is essential for explaining their extraordinary functional properties, including twin boundary supermobility and giant magnetic field-induced strain. One structural feature that has remained largely unnoticed—despite long-standing observations of temperature-evolving modulation—is the formation of long-period commensurate (LP–C) states, in which a rational modulation period locks with the lattice periodicity. In this work, we systematically determine and characterize all LP–C structural states that can arise as the modulation wave vector *q* shifts away from 2/5 upon cooling. Several of these LP–C superstructures—such as 14O, 24O, and 34O—are identified experimentally and emerge as stable, energetically favored ground states, supported by neutron/X-ray diffraction [1] and *ab initio* calculations [2]. Their unit cells inherently realize *a/b*-nanotwinning and explain the observed transition from monoclinic to orthorhombic symmetry. The findings clarify the structural evolution in five-layer modulated martensite, unify previous interpretations based on continuous modulation and nanotwinning, and establish LP–C states as key elements in the formation and stabilization of the low-temperature crystal structure.

References

[1] P. Veřtát et al., https://doi.org/10.48550/ARXIV.2503.04379.
[2] M. Zelený, et al., this conference.

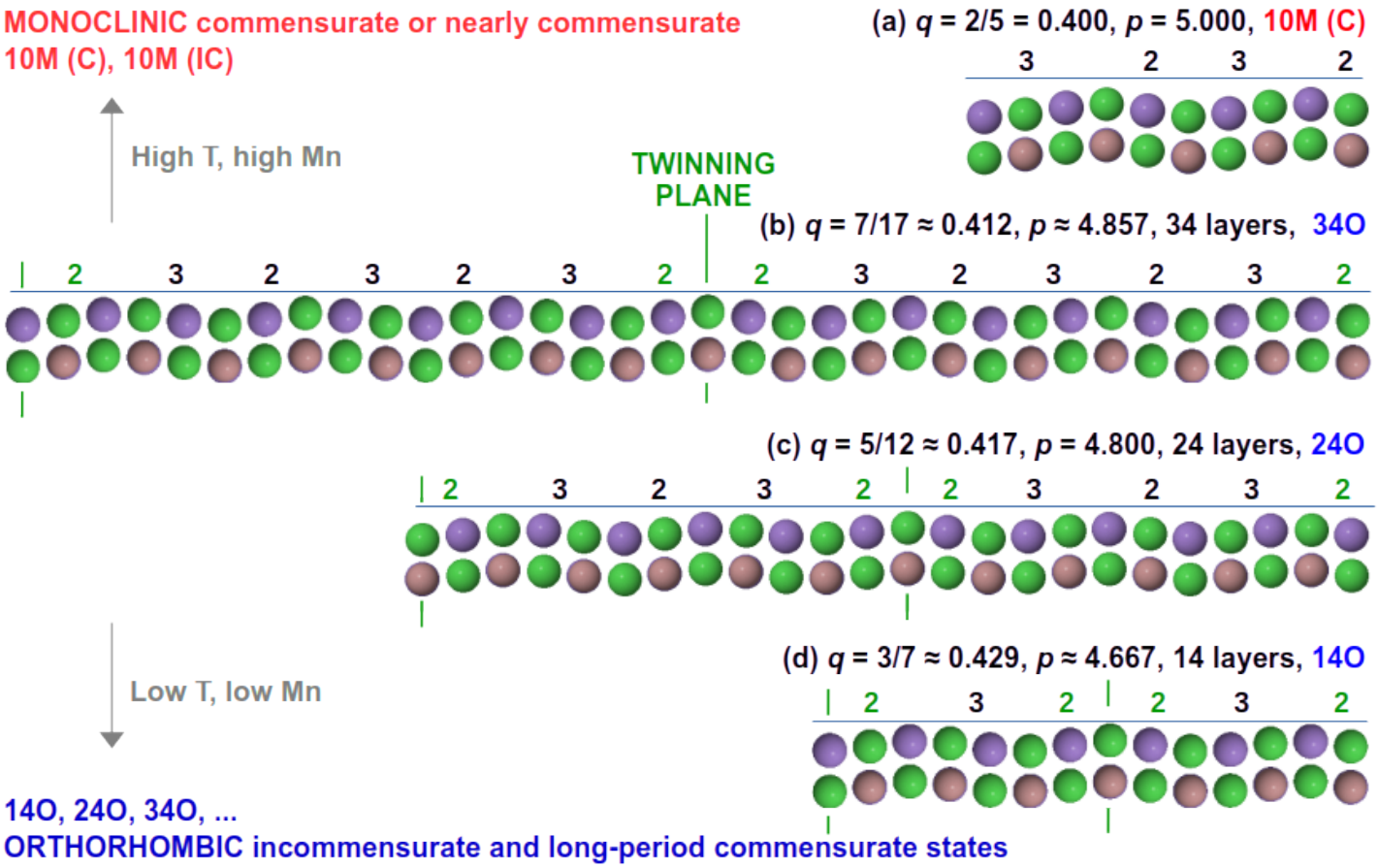

Fig. 1. *Overview of selected long-period commensurate (LP–C) states in Ni–Mn–Ga martensite: 14O, 24O, and 34O supercells, each forming via rational modulation periods that inherently realize a/b-nanotwinning. These structures are favored at low temperatures and arise from lock-in transitions as q departs from 2/5, with trends driven by alloy composition and temperature.*

133_310

Temperature and stress induced structural transformations in $Ni_{50}Mn_{27}Ga_{22}Fe_1$ alloy

Mariia Vinogradova[1], Alexei Sozinov[2], Ladislav Straka[3], Martin Zelený[4], Robert Chulist[5], Kari Ullakko[1]
[1]LUT University, Lappeenranta, Finland. [2]Tikomat Oy, Savonlinna, Finland. [3]FZU, Prague, Czech Republic. [4]Faculty of Mechanical Engineering, Brno University of Technology, Brno, Czech Republic. [5]AGH University of Krakow, Krakow, Poland

This study investigates temperature-and stress-induced structural transformations in the $Ni_{50}Mn_{27}Ga_{22}Fe_1$ magnetic shape memory alloy. First, we examine temperature-induced intermartensitic transformations. The large thermal hysteresis allows us to compare the lattice parameters of the five-layered modulated (10M), seven-layered modulated (14M), and non-modulated (NM) phases at the same temperature. Based on our results, we introduce a constant plane shift (CPS) model to accurately describe the continuous and discontinuous changes in lattice parameters with temperature. The CPS model addresses the limitations of the previous tetragonal building block model for the 10M lattice and accounts for the jump in the *c*-lattice parameter during the intermartensitic transition. The CPS model proposes an equal shift *dx* of the nearest (110) planes along the [-110] or [1-10] directions. The plane shift *dx* (Figure 1) varies significantly between different martensites, being the smallest in 10M martensite, increasing approximately threefold during the 10M–14M transformation, and further increasing by 30% during the 14M–NM transformation.

Within the 10M phase, temperature hysteresis also exists between the commensurate (C) and incommensurate (IC) structures. We show that the thermally induced C–IC transition coincides with a change in the average lattice symmetry from monoclinic to orthorhombic. The IC structure is stable under uniaxial tensile stress along the *a*-axis for deformations $\varepsilon < 0.16\%$ (Figure 2). A mixture of IC and C structures appears for $\varepsilon > 0.16\%$, leading to irreversible changes. Further increasing the deformation above $\varepsilon = 0.43\%$ results in a transformation to the 14M martensite. Given the stress stability of the IC structure, we investigate its elastic properties, present the free energy as a function of the monoclinic angle in diagonal coordinates (Figure 3), and extend the CPS model to describe the IC structure.

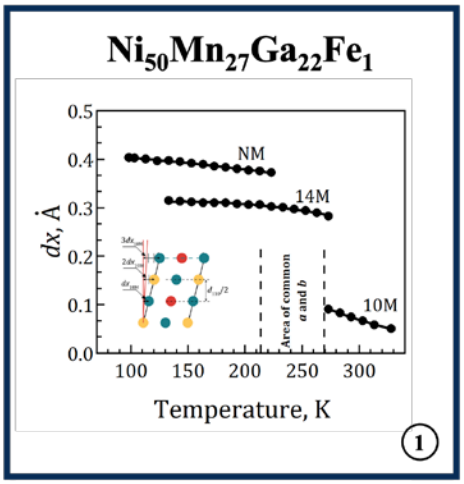

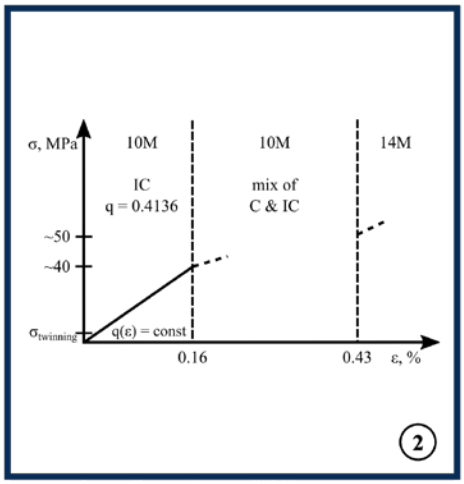

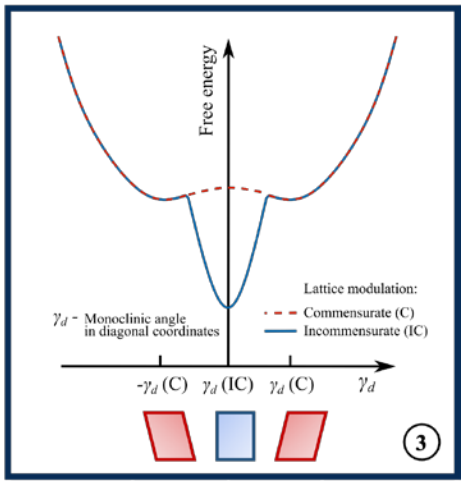

134_207

Austenite-Martensite interface propagation in Ni-Mn-Ga single crystal

Xingke Gao[1], Chengguan Zhang[2], Xue Chen[3], François Brisset[4], Olivier Hubert[1], Yongjun He[2]
[1]LMPS, Université Paris-Saclay, CentraleSupélec, ENS Paris-Saclay, CNRS, 91190 Gif-sur-Yvette, France. [2]LMI, UME, ENSTA Paris, Institut Polytechnique de Paris, 91120 Palaiseau, France. [3]Faculty of Engineering and Environment, Northumbria University, Newcastle Upon Tyne, United Kingdom. [4]ICMMO, Université Paris-Saclay, CNRS, Institut de chimie moléculaire et des matériaux d'Orsay, 91405 Orsay, France

The martensitic phase transformation of Shape Memory Alloys (SMAs) occurs via the nucleation and propagation of an Austenite-Martensite interface (A-M interface), whose morphology/configuration determines the driving force of the phase transformation and governs some key material behaviors such as energy dissipation and hysteresis [1-8]. In this paper, we develop an experimental setup to control the temperatures at the two ends of the Ni-Mn-Ga single crystal to observe the A-M interface propagation under different loading conditions. For example, in attached Fig. 1, during the heating-induced M⟶A transformation, the A-M interface is not always the planar habit-plane but can be a non-planar interface consisting of numerous wedges/needles that contain different martensite twins forming compatible internal structures (like self-accommodation configuration). The different forms of the interface propagation imply complicated interface kinetics. These results not only provide insights into the physical mechanism of the phase transformation, but also encourage the improvement of the theoretical modeling to better predict the material behaviors.

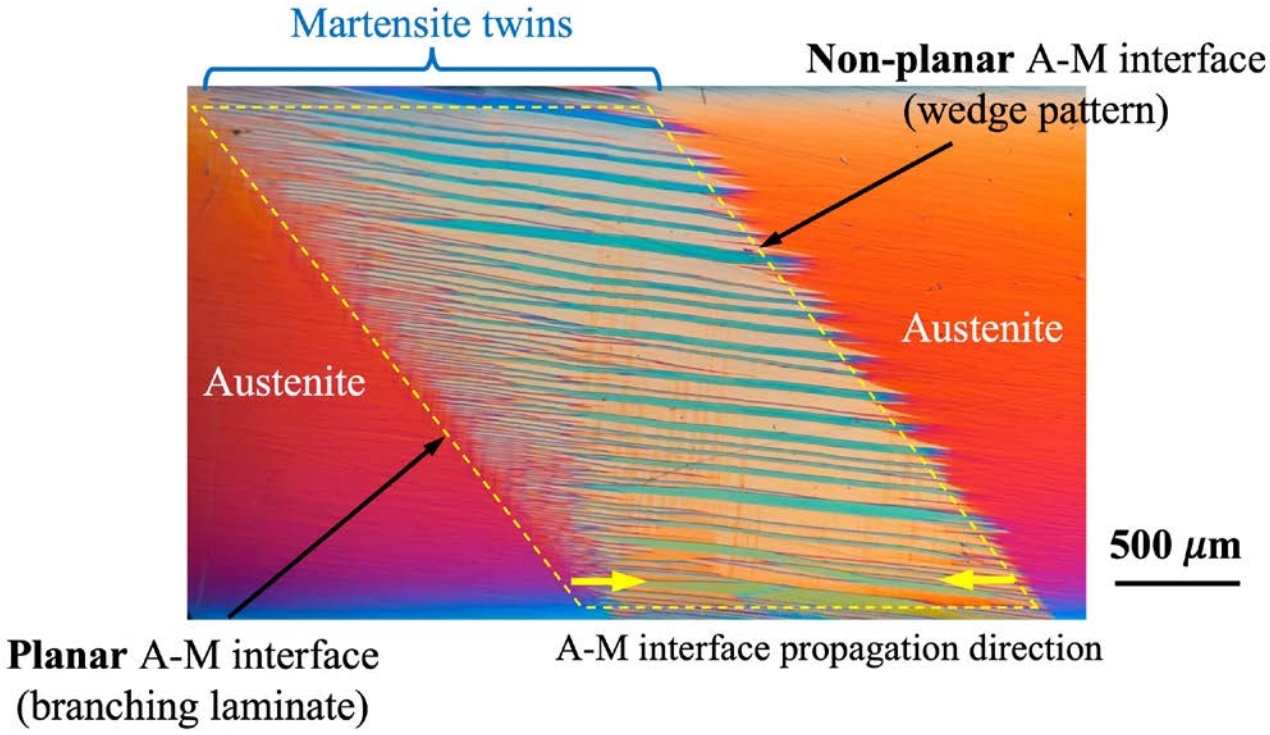

Fig. 1. Two different forms of the propagating Austenite-Martensite interface in Ni-Mn-Ga single crystal during heating-induced M➔A phase transformation.

References:
[1] Z. Zhang, R.D. James, S. Müller, Acta Mater. 57(15) (2009) 4332-4352.
[2] S. Stupkiewicz, G. Maciejewski, H. Petryk, Acta Mater. 55(18) (2007) 6292-6306.
[3] K. Tůma, S. Stupkiewicz, H. Petryk, J. Mech. Phys. Solids 95 (2016) 284-307.
[4] H. Seiner, P. Plucinsky, V. Dabade, B. Benešová, R.D. James, J. Mech. Phys. Solids 141 (2020) 103961.
[5] E. Bronstein, E. Faran, D. Shilo, Acta Mater. 164 (2019) 520-529.
[6] C. Zhang, X. Chen, X. Gao, F. Brisset, O. Hubert, Y.J. He, Acta Mater. 281 (2024).
[7] C. Zhang, X. Balandraud, Y.J. He, J. Mech. Phys. Solids 183 (2024) 105481.
[8] Y.J. He, Scripta Mater. 230 (2023) 115420.

135_276

Variant selection in deformation-induced martensite transformation

Manabu Takahashi[1], Yuichi Kinoshita[1], Shunkei Park[1], Kohtaro Hayashi[2]
[1]Kyushu University, Kasuga-shi, Fukuoka, Japan. [2]Nippon Steel Corporation, Futtsu-shi, Chiba, Japan

Transformation-induced plasticity is known to be the most promising method for enhancing the ductility of high-or very-high-strength steels for automotive applications. Low-alloy TRIP-type multiphase steels are produced by heat treatment at a temperature typically in the ferrite and austenite two-phase region, followed by rapid cooling to a temperature at which bainite forms, enriching the carbon in untransformed austenite. The microstructures of deformation-induced martensite in the Fe-C-Si-Mn and -Ni alloys were analyzed using SEM-EBSD observations to understand the nature of the deformation-induced martensite transformation. It should be noted that there are two phases of shear transformation in the individual processes. One is bainite transformed during heat treatment at bainite-transformation-treatment temperatures. The other type is martensite, formed during deformation, usually at ambient temperature. And these two species form from the same austenite grain.

Bainite forms at 400°C show either N-W or K-S orientation relationships with retained austenite. It is noted that twin-related austenite grains are frequently observed in the Fe-C-Si-Mn alloy studied. It is necessary to consider the 24 symmetries of cubic crystals to discuss the variants and their selection rule for shear transformation products. An austenite grain transforms into bainite or martensite with 24 different variants as defined by Morito et al.. As a result, a bainite or martensite grain transformed from austenite could select one of the 576 combinations. Furthermore, when a twin plane is parallel to the plane for K-S or N-W relations, we have to select an appropriate equivalency matrix for the austenite grains with which parallelism could be maintained. Using this method, deformation-induced martensite grains were found to select restricted variants where the (011) plane of martensite is parallel to one of the {111} planes of austenite, with which the (011) plane of bainite is parallel. Moreover, in particular cases, the plane of austenite was found to be parallel to the TWIN plane of two twin-related austenite grains. Naturally, in this case, bainite and martensite that share the same {111} plane of an austenite grain also share the {111} plane of another austenite grain, which is twin-related to the first one. The possible rules of variant selection are discussed.

136_210

Microstructure and bending fatigue behavior of martensite steel with 0.4%C subjected to different heat treatments

Jiaqiang Dang, Ryuji Yabutani, Sien Liu, Shoichi Nambu
The University of Tokyo, Tokyo, Japan

High strength martensite steels have been extensively utilized in various structures owing to their distinguished mechanical properties. Fatigue failure is one of the major concerns for structural parts served in harsh environment, which is closely related to the involved material. It has been reported that carbon content exerts an influence on the deformation of martensite. However, most previous papers were focused on the low carbon martensite steels while there are limited studies that address the fatigue behavior of martensite steel with medium carbon, which restricts the application of such materials in the industry. Therefore, this work aims to analyze the microstructure evolution of martensite steel with 0.4C (in mass%) under different heat treatments marked as OQ900 and OQ1000, and its effect on bending fatigue behavior. A crystal plasticity finite element method (CPFEM) was developed to analyze the role of multi-scale lath martensite structures on fatigue crack initiation, and the fatigue lives of the materials with varying substructures were quantitatively compared. The numerical simulation was verified by fatigue tests where special attention was paid on the peculiarity of crack initiation and early propagation exposed to the microstructural effect.

The results showed that OQ900 sample hold a smaller size in equivalent prior austenite grain, packet and block length than OQ1000 sample. Both inclusions and slipping fractures were found as the origins of fatigue crack initiation in the martensite steels with 0.4C, and especially the latter played a dominant role in high-cycle fatigue (HCF) regime. The block morphology and its orientation affected the strain localization in an obvious way, where lower fracture indicator parameters (FIPs) value and longer crack initiation life were obtained in OQ900 sample. The EBSD analysis indicated that the block boundaries tended to be the most preferred initiation sites of fatigue cracks for both samples, which were characterized as persistent slip bands. However, the length of slip bands was larger in OQ1000 sample, which agreed with the simulation results. The crack propagation path was distributed in a deflected manner owing to the inhibition effect of boundaries. Overall, the fatigue resistance of OQ900 sample is higher compared with OQ1000 sample in HCF regime as also supported by the S-N data.

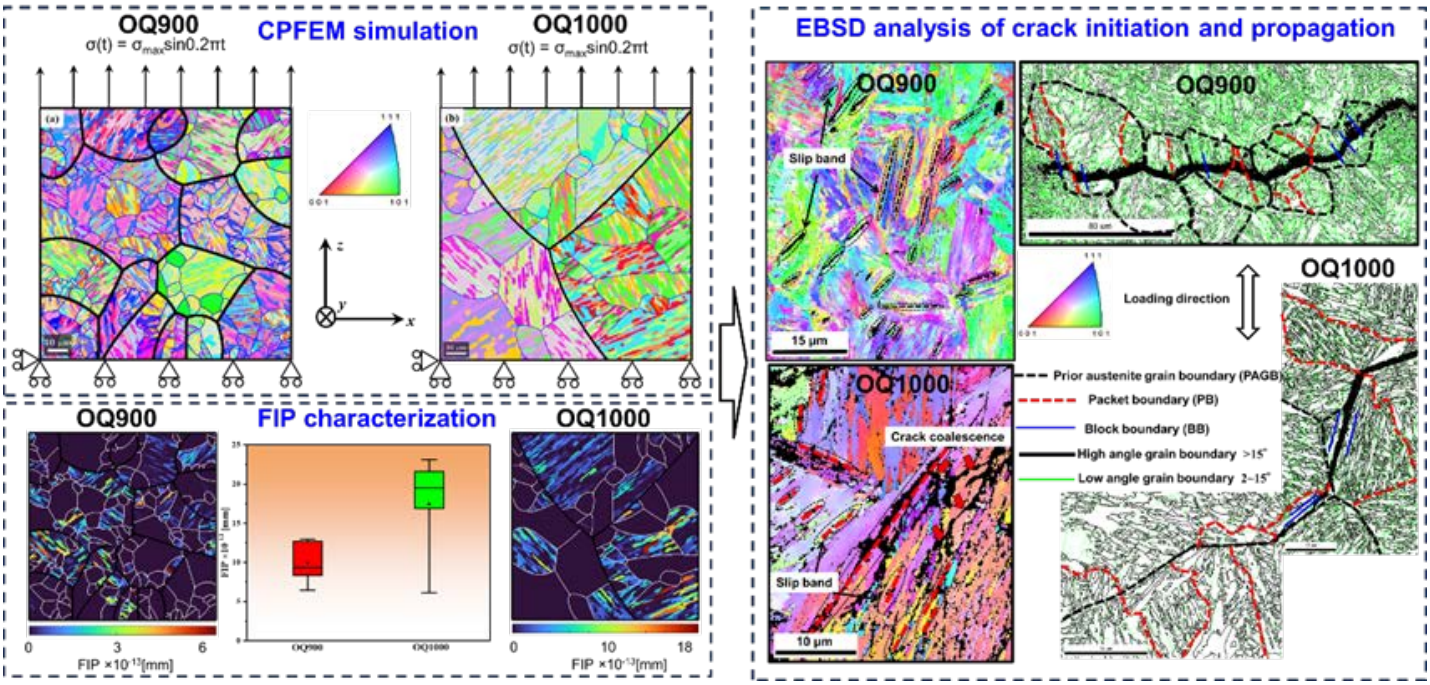

Reference:

[1] Okada K, Shibata A, Takeda Y, Tsuji N. International Journal of Fatigue 2021, 143: 105921.

137_208

In-situ 3D characterization of deformation-induced martensitic transformation in metastable austenitic alloy by synchrotron X-ray micro-and nano-tomography

Tatsuya Iwano[1], Osamu Takakuwa[2], Kyosuke Hirayama[3], Hiroyuki Toda[2]
[1]Graduate School of Mechanical Engineering, Kyushu University, Fukuoka, Japan. [2]Department of Mechanical Engineering, Kyushu University, Fukuoka, Japan. [3]Faculty of Engineering and Design, Takamatsu, Japan

Metastable austenitic steels exhibit excellent mechanical properties due to the deformation-induced martensitic transformation (DIMT). Several attempts have been made to investigate the DIMT process and the resultant improvement of mechanical properties by employing various observation and analysis methods in previous research. However, the DIMT process has scarcely been unveiled on spatial and temporal scales owing to the complicated three-dimensional (3D) structure of the martensite phase, which changes drastically during deformation. In this research, the progressive DIMT process was investigated in 3D through each deformation step by in-situ characterization employing two types of synchrotron X-ray CT, projection-type tomography (micro-CT), and imaging-type tomography (nano-CT).

The material used was a commercially available JIS-SUS304 stainless steel (Fe-18Cr-8Ni). A specimen with a cylindrical gage section of φ0.25×0.70 mm was prepared. A tensile test was conducted under a crosshead speed of 0.2 mm/min, and then the micro-CT and nano-CT were performed at several deformation steps, strain, ε = 0.14, 0.23, and 0.40, with an X-ray energy of 37.7 keV at the BL20XU beamline at SPring-8. The newly formed martensite phase was visualized by detecting the phase contrast between the austenite and martensite phases.

Figure 1 shows the cross-sectional images at each deformation step detected by the micro-CT and nano-CT, and reconstructed 3D images of the martensite phase. The results of the micro-CT demonstrated that a contrast in gray values was generated at the strain, ε = 14%, and the darker portion was presumed to be the deformation-induced martensite phase, stemming from the difference in density between the austenite and martensite phases. As for the nano-CT, the martensite phase was visualized in more detail than that of the micro-CT. The 3D structures of the martensite phase indicated that the martensite products appeared along specific habit planes, and the products developed along these habit planes. In this way, the progressive DIMT process was tracked in 3D through each deformation step by nano-CT.

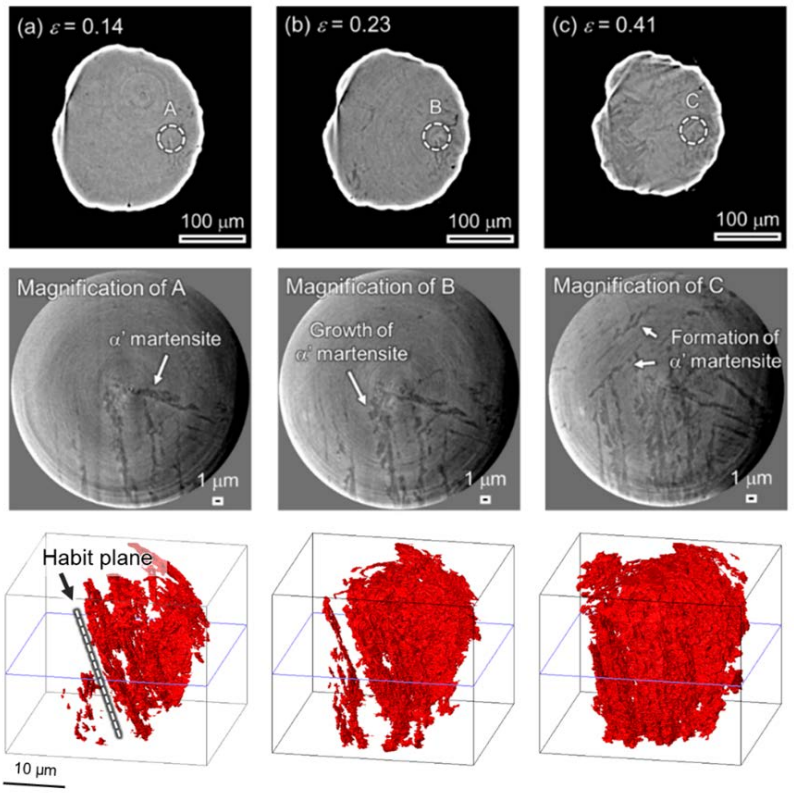

Figure 1. Deformation-induced martensitic transformation during tensile deformation detected by micro-CT (top images) and nano-CT (middle images), and 3D images of the martensite phase reconstructed by the cross-sectional images of the nano-CT.

138_174

Hydrogen Cation-Induced Martensitic Transformation During Electrochemical Hydrogen Charging in Metastable Austenitic Stainless Steel

Junyoung Chae[1], Guihyung Lee[1], Hyukjae Lee[1], Yeonggeun Cho[2], Dameul Jeong[3], Young-Kyun Kwon[3], In-Ho Jung[1], Sung-Joon Kim[2], Heung Nam Han[1]
[1]Seoul national University, Seoul, Korea, Republic of. [2]Pohang University of Science and Technology, Pohang, Korea, Republic of. [3]Kyung Hee University, Seoul, Korea, Republic of

The martensitic transformation was observed during electrochemical cathodic hydrogen charging in metastable austenitic stainless steel. When the charging conditions exceeded the critical current density and duration, a significant amount of martensitic transformation occurred due to the absorbed hydrogen, as confirmed by EBSD analysis. To determine the polarity of the absorbed hydrogen, an external magnetic field was applied to induce a Lorentz force along the specimen's longitudinal direction during cathodic charging. Microstructural analysis and hardness measurements revealed a gradient in martensitic transformation and hardness along the Lorentz force direction, which remained consistent under reversed force conditions. This finding indicates that electrochemically introduced hydrogen interacts electromagnetically and exists in a positively charged state. Furthermore, EBSD, XRD, and ferritescope measurements confirmed that the martensitic transformation was confined to the extreme surface of the specimen. To elucidate the transformation mechanism, finite element modeling (FEM) was employed to calculate the hydrogen cation concentration near the specimen's surface during cathodic charging, and first-principles calculations were conducted to assess the mechanical effects of hydrogen cation accumulation on the lattice. The results demonstrated that the accumulation of hydrogen cations induces substantial internal stress, potentially triggering a mechanically induced martensitic transformation (MIMT). These findings suggest that hydrogen, when introduced electrochemically via cathodic charging, can enter as cations and influence the martensitic transformation kinetics of metastable austenitic stainless steel before being neutralized by free electrons.

139_296

Enhanced Mechanical Properties by FCC-HCP Martensitic Transformation in Co-Cr-Mo-Ni Medium Entropy Alloys

Koichi Tsuchiya[1], Bikash Tripathy[1], Wataru Tasaki[2]
[1]National Institute for Materials Science, Tsukuba, Ibaraki, Japan. [2]University of Tsukuba, Tsukuba, Ibaraki, Japan

FCC high/medium alloys often exhibit enhanced mechanical properties by the formation of nano-twinning or by the FCC-HCP martensitic transformation. Thus the property of the alloys strongly depends on the stacking their fault energy, which is closely related to the free energy difference between the metastable FCC phase and the HCP phase.

In the present study, $Co_{51-x}Cr_{23}Mo_6Ni_{20+x}$ (x = 0–15) medium entropy alloys (referred to as CCMN alloys) were designed based on the FCC-HCP phase stability using Calphad method. Room temperature tensile tests revealed markedly high work-hardening rate and good strength–elongation balance of the alloys.

X-ray diffraction (XRD) and Electron Backscattered Diffraction (EBSD) analysis revealed that the dominant deformation modes gradually shift from the FCC-HCP martensitic transformation to deformation twinning and dislocation slip with the Ni content, x. The observed good strength–elongation balance may be due to the TRIP and TWIP. In the tensile deformed samples of the x = 3~9 alloys, HCP phase and twins coexist.

The low-cycle fatigue (LCF) behavior was investigated with a total strain amplitude of 0.01. The highest LCF lives were observed for the x = 6 alloy (6537 cycles). They are much higher than those of alloys currently used for coronary stents, such as L605 or MP35N. These findings suggests that the formation of epsilon-twin bundles may be an important factor to obtain high LCF resistance.

The developed alloys also exhibit excellent plastic workability. Thin-wall tubes (1.6 mm OD, 0.1 mm thick) and thin wires (down to 0.2 mmφ) was produced by cold-drawing. The prototype stent laser-cut from the CCMN tubes exhibit much higher radial force than the one made from conventional Co-Cr alloy.

Rat Back Subcutaneous Implantation Study revealed that the developed CCMN alloys have weaker biological response and inflammatory properties than SUS316L.

These results support the CCMN alloys are strong candidate materials for the medical devices for endovascular treatment.

140_257

Structure formation in high entropy shape memory alloys

Georgiy Firstov[1], Vira Filatova[1], Yuri Koval[1], Andrei Timoshevskii[1], Valerii Odnosum[1], Gregory Gerstein[2], Hans Jurgen Maier[2]
[1]G.V. Kurdyumov Institute for Metal Physics of the National Academy of Sciences of Ukraine, Kyiv, Ukraine. [2]Institut fur Werkstoffkunde (Materials Science) Leibniz Universitat Hannover, Hannover, Germany

Shape memory alloys (SMA) exhibit the number of functional properties due to the structural peculiarities along structural phase transformations of high temperature phase including so-called martensitic. In fact, the structure formation starting from crystallization down to reversible martensite transformation (MT) provides the conditions for shape memory, superelasticity and high damping capacity in a number of conventional SMA like industrial NiTi, Cu-based and others.

A decade ago high entropy shape memory alloys (HESMA) emerged against the background of existing industrial shape memory materials. Superiority of these multi-component alloys in resistance to plastic deformation, functional fatigue in combination with the possibility of MT and perfect shape memory behavior in a wide temperature range is strongly related to their specific crystal and electronic structure (lattice distortion, cocktail effect etc.). First successful attempt to design TiZrHfCoNiCu multiple principal element high entropy shape memory alloy has been accomplished using NiTi intermetallic compound as a prototype [1,2]. Our own view on a subject depends not only on compositional complexity of these alloys but on their peculiar structure also [3].

The present report intends to show how structure formation in emerging HESMA is different comparing to conventional SMA. It will be argued that the approach towards production and treatment of these novel materials might be different also due to their multi-component design. In particular, some details of multi-component structure formation that might become useful for 3D printing of these materials will be discussed.

[1] G.S. Firstov, T.A. Kosorukova, Yu.N. Koval, V.V. Odnosum, *Mater. Today Proc.* 2S: S499–S504 (2015); https://doi.org/10.1016/j.matpr.2015.07.335
[2] G.S. Firstov, T.A. Kosorukova, Y.N. Koval, P.A. Verhovlyuk, *Shape Memory and Superelasticity*, 1(4): 400–407 (2015); https://doi.org/10.1007/s40830-015-0039-7
[3] G. S. Firstov, Yu. M. Koval, V. S. Filatova, V. V. Odnosum, G. Gerstein, and H. J. Maier, *Progress in Physics of Metals*, 24, No. 4: 819–837 (2023); https://doi.org/10.15407/ufm.24.04.819

141_291

Fe-based near HEA with shape memory effect: microstructure and quantitative characterization of the martensitic transformation

Lucia Del-Río[1,2], Mikel Pérez-Cerrato[2], Takanobu Hiroto[1], Raul Gómez[3], Leire García-Sesma[3], Maria Luisa Nó[2], Koichi Tsuchiya[1], Jose Maria San Juan[2]
[1]National Institute for Materials Science (NIMS), Tsukuba, Ibaraki, Japan. [2]Dep. of Physics, University of the Basque Country UPV/EHU, Leioa, Bizkaia, Spain. [3]LORTEK-Basque Research Technology Alliance, Ordizia, Gipuzkoa, Spain

Among the different ferrous shape memory alloys (SMA), the family of Fe-Mn-Si-based alloys has attracted a renewed interest in the last decade, because of its low cost, good corrosion resistance and high strength during shape memory behavior. They can be considered as a new kind of stainless steel and exhibits a martensitic transformation (MT) from the cubic austenite γ (FCC) to the hexagonal martensite ε (HCP), which is responsible for a shape memory effect. Although the ε martensitic transformation is non-thermoelastic, and do not exhibit superelastic effect, these alloys found several industrial applications due to the high strength during the shape memory recovery, and are being currently used in various applications, such as coupling systems, self-healing composites or seismic damping in civil engineering [1]. Additionally, the new technologies of additive manufacturing offer unforeseen possibilities for this family of SMA.

In the present work, the reversible γ − ε MT, responsible for the shape memory effect, was investigated in two alloys with different chemical composition; high 20Mn and low 16Mn (wt%) manganese content, produced by the conventional route of casting and rolling. In addition, a third alloy, with a balanced intermediate composition, was produced by gas atomization and additive manufacturing through Laser Poder Bed Fusion (LPBF) [2], and was also studied in comparison with the former ones.

Along with the microstructure characterization by electron microscopy (SEM and TEM), the forward and reverse γ − ε MT is studied by mechanical spectroscopy through the internal friction spectra and the dynamic modulus variation. These data are then compared and completed by in situ X-Ray diffraction as a function of temperature, in order to determine the transformed fraction throughout the thermal transformation. Furthermore, the behavior of the MT and the evolution of the transformed fraction are evaluated and followed along thermal cycling in all three alloys.

[1] T. Sawaguchi, I. Nikulin, K. Ogawa et al., Low-cycle fatigue life and plasticity mechanisms of a Fe-15Mn-10Cr-8Ni-4Si seismic damping alloy under cyclic loading at various temperatures, Acta Mater. 220 (2021) 117267.

[2] L. Del-Río, M. L. Nó, R. Gómez et al., Additive Manufacturing of Fe-Mn-Si-Based Shape Memory Alloys: State of the Art, Challenges and Opportunities, Materials 16 (2023) 7517.

142_184

A polymer-like ultrahigh-strength metal alloy

Yuanchao Ji[1], Zhizhi Xu[1], Xiaobing Ren[2]
[1]Xi'an Jiaotong University, Xi'an, Shaanxi, China. [2]Yongjiang Laboratory, Ningbo, Zhejiang, China

Futuristic technologies such as morphing aircrafts and super-strong artificial muscles depend on metal alloys being as strong as ultrahigh-strength steel yet as flexible as a polymer. However, achieving such 'strong yet flexible' alloys has proven challenging because of the inevitable trade-off between strength and flexibility. Here we report a Ti–50.8 at.% Ni strain glass alloy showing a combination of ultrahigh yield strength of $\sigma_y \approx 1.8$ GPa and polymer-like ultralow elastic modulus of $E \approx 10.5$ GPa, together with super-large rubber-like elastic strain of approximately 8%. As a result, it possesses a high flexibility figure of merit of $\sigma_y/E \approx 0.17$ compared with existing structural materials. In addition, it can maintain such properties over a wide temperature range of −80 °C to +80 °C and demonstrates excellent fatigue resistance at high strain. The alloy was fabricated by a simple three-step thermomechanical treatment that is scalable to industrial lines, which leads not only to ultrahigh strength because of deformation strengthening, but also to ultralow modulus by the formation of a unique 'dual-seed strain glass' microstructure, composed of a strain glass matrix embedded with a small number of aligned R and B19′ martensite 'seeds'. In situ X-ray diffractometry shows that the polymer-like deformation behaviour of the alloy originates from a nucleation-free reversible transition between strain glass and R and B19′ martensite during loading and unloading. This exotic alloy with the potential for mass producibility may open a new horizon for many futuristic technologies, such as morphing aerospace vehicles, superman-type artificial muscles and artificial organs.

143_229

Sharp Atomic Structure of Highly Mobile Type I and Type II Twin Boundaries in Ni-Mn-Ga Magnetic Shape Memory Single Crystal

Marek Vronka, Ladislav Straka, Petr Veřtát, Oleg Heczko
FZU-Institute of Physics of the Czech Academy of Sciences, Prague, Czech Republic

The exceptionally high mobility, or even supermobility, of Type I and Type II twin boundaries in the five-layered modulated structure of Ni-Mn-Ga martensite plays a crucial role in magnetically induced reorientation resulting in a giant magnetic field-induced strain. Understanding the atomic structure of these twin boundaries—whether diffuse or faceted—is essential for elucidating the mechanisms governing supermobility and the distinctly different behaviors of these two boundary types.

Using transmission electron microscopy (TEM) and high-resolution TEM (HRTEM), we investigated and compared the atomic-scale structures of Type I and Type II twin boundaries in a 10M Ni-Mn-Ga single crystal, both of which have been experimentally confirmed to be highly mobile. TEM foils were prepared by focused ion beam (FIB) milling across individual Type I and Type II twin boundaries. Contrary to earlier reports suggesting diffuse interfaces, our findings reveal that both boundary types exhibit atomically sharp features.

These results highlight the significance of topological models in understanding twin boundary formation and evolution. Furthermore, our findings indicate that the supermobility of Type II twin boundaries appears to be closely linked to their faceted, step-like interface, which accommodates lattice mismatch.

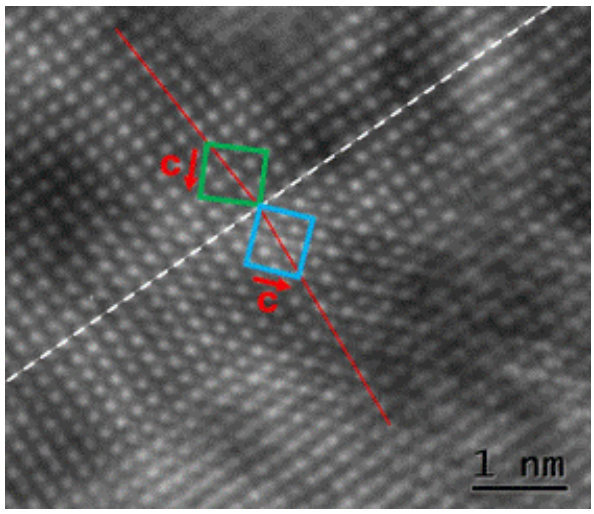

Figure: *High resolution transmission electron microscopy (HRTEM) micrograph of an atomically sharp Type I twin boundary in a 10M Ni-Mn-Ga single crystal.*

144_374

Demagnetization tensor for a parallelepiped with a mirror symmetry in the xy plane and its use for magnetically induced reorientation in Ni-Mn-Ga crystal sample.

David Vokoun[1], Marco Beleggia[2], Oleg Heczko[1]
[1]FZU-Institute of Physics of the Czech Academy of Sciences, Prague, Czech Republic. [2]University of Modena and Reggio Emilia, Modena, Italy

The demagnetization tensor quantifies the reduction of the internal magnetic field in a material due to its shape and geometry. In this study, we apply a cross-correlation function approach to derive the nonzero components of the demagnetization tensor for a parallelepiped with a mirror symmetry in the xy plane —N_{xx}, N_{yy}, N_{zz}, and N_{xy} — expressed as single definite integrals dependent on geometric parameters. This formulation helps to avoid cumbersome mathematical expressions.

The motivation for examining the parallelepiped shape arises from the need to estimate the demagnetizing field in a Ni-Mn-Ga crystal undergoing transformation from a cubic to a monoclinic system and to assess the effect of magnetostatic interactions on the crystal's switching field [1], i.e. the field inducing twin boundary motion and structure reorientation. Additionally, the analytical expression of demagnetization factors for the parallelepiped may have further applications in related fields.

When the parallelepiped simplifies to a rectangular prism, the Fourier space transformation method provides accurate estimates of the demagnetization tensor, particularly when one edge length is a multiple of the other two. However, for edge lengths of similar magnitude, the accuracy of this estimation decreases.

Reference

[1] Heczko, O., Vokoun, D., Kopecký, V., Beleggia, M. (2015). Effect of magnetostatic interactions on twin boundary motion in NiMnGa Magnetic Shape Memory Alloy. *IEEE Magnetics Letters*, *6*, 1-4.

145_390

Elastic moduli measurements in 10M martensite of Ni-Mn-Ga-based alloys with commensurate and incommensurate lattice modulation

Andrey Saren[1], Mariia Vinogradova[1], Alexei Sozinov[2], Sergey Kustov[3], Kari Ullakko[1]
[1]LUT University, Lappeenranta, Finland. [2]Tikomat Oy, Savonlinna, Finland. [3]University of the Balearic Islands, Palma, Spain

Apparent elastic moduli measurements in 10M martensite of Ni-Mn-Ga alloys are influenced by highly mobile twin boundaries (TBs). The existing data on the elastic properties are limited to measurements in commensurate (C) state using ultrasonic oscillatory method [1], and transient grating spectroscopy [2]. According to [1], the effective modulus E_{100} does not represent lattice elasticity but is dominated by contribution of additional strain due to stress-induced motion of a/b TBs. In [3], a very soft modulus E_{100} was estimated under tension from the measured lattice constants: the initial modulus was 0.3 GPa, and an average modulus in the whole 20 MPa stress range was about 0.7 GPa.

In the present work, we employed direct measurements of the elastic moduli E_{001} and E_{100} in 10M martensite of $Ni_{50}Mn_{28}Ga_{22}$ and $Ni_{50}Mn_{27}Ga_{22}Fe_1$ alloys up to a strain of 5×10^{-4}, using a piezo-actuator for loading and laser interferometry for strain measurements. XRD was used to reveal the crystal structure. a/c twins' contribution was excluded by preparation of a single-variant state and loading up to 20-35 MPa in a direction which did not allow a/c twins' nucleation. Loading in the opposite direction was studied up to a stress of 1.6 MPa.

The results show that in C state both alloys demonstrate Young's modulus softening and hysteretic behavior near zero stress when loaded along [100] direction, due to the highly mobile a/b TBs with twinning stress of about 0.1 MPa. Outside the a/b twins' redistribution region, a strong modulus hardening up to tens of GPa was observed. In [001] direction there was no hysteresis as expected. In the incommensurate (IC) state of Ni-Mn-Ga-Fe alloy, there was no Young's modulus softening in both directions. This result, along with the XRD data, points to the absence or immobilization of a/b twins. An elasticity matrix for Ni-Mn-Ga-Fe alloy is provided in [4].

Stress-strain response for [100] and [001] directions was measured at RT in both C and IC states of Ni-Mn-Ga-Fe alloy. Preliminary results show nearly same moduli values in correspondent directions in C and IC states. We aim to compare Young's moduli in C and IC states in both alloys having different modulation vector values (the Ni-Mn-Ga alloy has a reduced IC modulation vector at RT, close to the vector in C state).

[1] Kustov et al., Scr. Mat. 178 (2020) 483
[2] Repček et al., Adv. Mater. 36 (2024) 2406672
[3] Cejpek et al., Acta Mat. 257 (2023) 119133
[4] Sozinov et al. ICOMAT2025, poster

146_348

Magnetic anomalies in Ni-Mn-Ga-x austenite and premartensite

Alexej Perevertov[1], Ross Colman[2], Oleg Heczko[1]
[1]Institute of Physics of the Czech Academy of Sciences, Prague, Czech Republic. [2]Charles University, Faculty of Mathematics and Physics, Prague, Czech Republic

We measure magnetization curves of MSMA alloys by the traditional for steels method-using the magnetizing yoke. The field measurement error is reduced by several orders of magnitude comparing to VSM and even the differential susceptibility curves can be studied. Thanks to that we were able to observe a number of magnetic anomalies in Ni-Mn-Ga and Ni48Mn22Ga25Cu5 austenitic phase. Assuming single crystal austenite with simple cubic structurea a normal sigmoidal shape of the *M(H)* curve can be expected with one-peak differential susceptibility. We discovered that a single crystal austenite Ni-Mn-Ga-X sample exhibits a constricted *M(H)* at certain temperatures. The first example is the switch of the magnetic easy axis in Ni-Mn-Ga with temperature from [100] to [100] and back [1]. Then the magnetic easy axis is [100]-45º away from the field direction, there is a magnetic domains reorientation similar to that in the Goss-textured Fe-3% transverse strips. Moreover, the magnetic strain at the premartensitic temperature reaches large values up to 550 ppm. The second example is the vibration-induced constricted *M(H)* curves with up to four additional peaks on the differential susceptibility curves

We found that some compositions are unstable and additional thin peaks can appear at any time and later in several minutes disappear. The instability cannot be ascribed to particular temperature, in the second heating cycle it may appear at different temperature or disappear entirely.

The observation can be tentatively explained that for certain compositions of Ni-Mn-Ga-x the austenite is not a simple homogeneous material with the cubic symmetry. Different strain/phonon domains can appear in the material [2] and all these broken symmetries is clearly visualized in DS curve. In addition to that a strain glass state can exist for Ni-Mn-Ga-X samples [3].

References

[1] A. Perevertov et al., Spin reorientation in premartensite and austenite Ni-Mn-Ga, Appl. Phys. Lett. 125, 021903 (2024).
[2] Jin, Y. M., Wang, Y. U. & Ren, Y. Theory and experimental evidence of phonon domains and their roles in pre-martensitic phenomena, npj Comput. Mater. 1, (2015).
[3] Y. Wang et al., Premartensite serving as an intermediary state between strain glass and martensite in ferromagnetic Ni-Fe-Mn-Ga, Mater. Des. 152, 102-109 (2018).

147_196

Transformation behaviors and microstructur aspects in hydrogen-charged Ti-Ni alloys

Alimzhan Kalbekov[1], Hiroshi Akamine[2], Minoru Nishida[2]
[1]Interdisciplinary Graduate School of Engineering Sciences, Kyushu University, Kasuga, Fukuoka, Japan. [2]Department of Advanced Materials Science and Engineering, Faculty of Engineering Sciences, Kasuga, Fukuoka, Japan

In many applications, especially in dentistry and medicine, Ti-Ni alloys are exposed to corrosive environments, including hydrogen. In research on mechanical properties, hydrogen embrittlement and its mechanism have attracted considerable interest. Many reports have investigated the effect of hydrogen on transformation behavior using thermal analysis and resistivity measurements. Although it has been reported that hydride forms upon hydrogen charging, we recently found that a hydrogen-induced phase with an orthorhombic structure, distinct from hydride, forms on the top surface of the hydrogen-charged specimen. This phase exhibited martensitic properties induced by cooling and stress-loading and was characterized as exceptionally hard, with a Vickers hardness of approximately 700 HV. Therefore, it was defined as hydrogen-induced martensite (HIM). Through in situ SEM observations, we also revealed that an untransformed layer exists between the HIM layer and the interior region. Meanwhile, the interior region transforms into B19’ martensite upon cooling. We refer to this untransformed layer as the hydrogen-affected layer (HAL), which corresponds to the area where the B19’ martensitic transformation is suppressed in the hydrogen-charged specimen. It has been reported that hydrogen suppresses the thermoelastic martensitic transformation from the B2 structure to the B19’ structure both experimentally and theoretically, using first-principles calculations. However, the hydrogen-induced microstructural modifications, including the HIM and the HAL, and their interaction with thermoelastic transformation behaviors remain unclear.

In this study, we experimentally investigate the transformation behaviors and microstructural aspects of hydrogen-charged Ti-Ni and Ti-Ni-Fe alloys. This investigation is conducted with in-situ SEM observations. We also discuss the effects of aging at temperatures below and above room temperature on the transformation behavior, which is thought to be related to delayed fracture. Notably, the transformation temperature from B2 to R is hardly affected; however, those from B2 to B19’ and from R to B19 are significantly altered, in the hydrogen-charged specimens. Furthermore, the transformation behavior changes dramatically with slight variations in the aging temperature, even around room temperature.

148_159

EBSD and TKD Study of Microstructure Evolution in NiTi Alloys

Junfeng Xiao, Cyril Cayron, Roland Loge
EPFL, Neuchatel, Neuchatel, Switzerland

NiTi alloys are of great interest due to their exceptional mechanical properties, such as superelasticity and the shape memory effect, driven by reversible phase transformation between the parent B2 phase and monoclinic B19' martensite. Understanding the microstructural evolution during martensitic transformation is vital for enhancing the functional performance of NiTi alloys. Compared to transmission electron microscopy (TEM) and X-ray diffraction (XRD), electron backscatter diffraction (EBSD) and transmission Kikuchi diffraction (TKD) offer direct orientation mapping and global analysis of martensitic variants.

This study utilizes EBSD and TKD, integrated with the theoretical framework of Interaction Work (IW), to explore the microstructural evolution of martensite in NiTi alloys. IW quantifies the mechanical work during transformation, favoring variants with high positive IW. EBSD analysis reveals variant selection, texture evolution, and deformation twinning in superelastic NiTi. All of these changes are explained by the IW criterion. In shape memory NiTi, martensite morphology evolves from needle-like to block-like structures, with orientations of remaining martensite aligning along the loading direction, consistent with IW predictions. The IW framework is particularly effective in explaining complex microstructure changes under multi-dimensional stresses, such as those introduced by laser shock peening, including reorientation and texture formation. Fine-scale TKD observations further demonstrate that reorientation initiates with detwinning, followed by transformation twinning under applied strain. These findings suggest that the martensitic microstructure evolves with strains following a trajectory with increasing maximum IW of different deformation modes. These insights into microstructural evolution are crucial for guiding the design and optimization of next-generation shape memory alloys.

150_331

Unraveling the precipitation-controlled martensite self-accommodation and shape memory effect in NiTi alloy across atomic scale and microscale

Shanshan Cao[1], Shi-Ping Wu[1], Qiu-Shu Wang[1], Shuai Liu[1], Xiao-Feng Chen[1], Yuan Li[2], Chang-Bo Ke[1], Xiao Ma[1], Xin-Ping Zhang[1]
[1]South China University of Technology, Guangzhou, China. [2]Wuhan University of Science and Technology, Wuhan, China

The metastable Ni_4Ti_3 precipitates has significant contribution to the martensite self-accommodation behavior via as-induced coherent stress/strain field and spatial partitioning in the NiTi B2 matrix and thus governs both type and magnitude of the shape memory effect in NiTi alloys. In stress-assisted aged $Ni_{50.6}Ti_{49.4}$ stripes containing parallel Ni_4Ti_3 precipitates, triangular B19´ self-accommodation morphology (SAM) can be observed in the ones exhibiting two-way shape memory effect (TWSME). The dimension of the triangular SAM initially increases with the size of Ni_4Ti_3 precipitates, but subsequently decreases as the precipitates coarsen to lose coherency. The recovery ratio of TWSME exactly follows the same trend. Particularly, the stripe stress-assisted aged at 450 ºC for 5h containing the largest self-accommodated triangles of around 13 mm^2 aligned in the matrix displays the highest recovery ratio of 96%. Parallel Ni_4Ti_3 precipitates with an average length of 81.3 nm and spacing of 59.7 nm are responsible for the SAM and TWSME by introducing strong overall strain field with band-like distribution in the B2 matrix. Furthermore, as the parallel precipitates completely lose coherency, the triangular SAM vanishes together with the TWSME. On the other hand, in the stress-free aged stripes without TWSME, crossing Ni_4Ti_3 precipitates of multi-variants introduce nondirectional block-like strain field in the B2 matrix. Triangular SAM only appears in the ones containing precipitates smaller than 70 nm, and its size decreases with the size of Ni_4Ti_3. Additionally, V shape SAM can be observed in all aged stripes, as the basic unit of SAM.

To further investigate the underlying mechanism, molecular dynamics (MD) simulation was employed to investigate the martensitic transformation in NiTi containing Ni_4Ti_3 of different spatial configurations. Results show that at the onset of the martensitic transformation, B19´ preferentially nucleates in the regions of relatively strong strain field and sufficient space. By the end of the transformation, the coherent strain field induced by Ni_4Ti_3 of different arrangements determine the SAM. Only triangular SAM composed of the corresponding variants (CVs) of (2´)/(4´)/(6´) forms in the model containing parallel and step-like arranged Ni_4Ti_3, while various SAMs involving more CVs are found with the presence of intersecting Ni_4Ti_3. The number of the SAM types depends on the sites of strain concentration.

151_222

In situ neutron diffraction examination of anomalous hysteresis behavior in Co-Cr-Al-Si superelastic alloys

Xiao Xu[1], Raiki Shimizu[1], Tatsuya Ito[2], Wu Gong[2], Stefanus Harjo[2], Toshihiro Omori[1], Ryosuke Kainuma[1]
[1]Department of Materials Science, Tohoku University, Sendai, Japan. [2]J-PARC Center, Japan Atomic Energy Agency, Tokai, Japan

Shape memory alloys (SMA), especially the NiTi-based alloys, have been widely used as biomedical devices such as self-expanding vascular stents and orthopedic bone staples. However, the large amount of Ni content of NiTi raises the concern about Ni allergy. Recently, we developed Ni-free Co-Cr-Al-Si (CCAS) SMAs. By using <001> single crystals, a maximum recoverable strain up to about 17.0% was obtained, which is twice that of NiTi. However, the CCAS alloys suffer from an anomalous phenomenon related to the hysteresis of superelasticity. For the process of stress-induced martensitic transformation by tensile tests, upon the formation of martensite, i.e., the martensitic transformation starting stress (σ_{Ms}), a clear sudden decrease of stress appears. Unfortunately, this behavior is reproducible, and it does not disappear after training. Moreover, the samples seem to be damaged by this behavior, and for the worst case, the sample may fracture only after several full cycles of superelasticity. In this research, we examined the superelasticity behavior of <001> single-crystal CCAS alloys over a wide temperature range of 100 K to 300 K. Interestingly, it was revealed that the sudden decrease of stress upon the formation of martensite was remarkably alleviated at low temperatures. *In situ* measurements including neutron diffraction for the investigation of crystal structures and digital image correlation (DIC) for the observation of microstructure evolution were conducted during tensile tests. At low temperatures, an extra peak was found on the boundary between the parent and martensite phases, whereas no such peak was seen at higher temperatures. Thus, we consider the hypothesis of the appearance of an intermediate phase at low temperatures, which may attribute to an easier nucleation of martensite and result in an alleviated decrease of stress upon the formation of martensite during tensile tests.

152_379

Elastic behavior of Co-Cr-Ga-Si: Resonant ultrasound spectroscopy at Weyl's asymptote and giant negative magnetoelastic coupling

Hanuš Seiner[1], Petr Sedlák[1], Michaela Janovská[1], Jakub Lustinec[2], Xiao Xu[3], Ryosuke Kainuma[3]
[1]Institute of Thermomechanics, Czech Acad Sci, Prague, Czech Republic. [2]FzÚ-Institute of Physics, Czech Acad Sci, Prague, Czech Republic. [3]Tohoku University, Sendai, Japan

Shape memory alloys typically exhibit phonon softening in the vicinity of the transition temperature, manifesting itself as a decrease in shear elastic coefficients in both phases close to their stability limits. In Co-Cr-based alloys with the so-called re-entrant transition [1], the phonon-mediated instability couples with magnetism-induced stabilization of the cubic phase. As a result, the cubic-tetragonal-cubic pathway cannot be simply related to elastic constants evolution, and, at the same time, several unique features are observed.

The first is the transition from austenite to martensite with heating, which is the transition between two stable phases, that is, it is a martensitic transition not associated with any phononic instability. The second occurs when the forward transition is blocked by chemical stabilization and the paramagnetic austenite transforms directly into the ferromagnetic half-metal cubic phase.

The talk will report on in-situ experimental observations of all these features using laser-based resonant ultrasound spectroscopy. This required performing the measurements on fine mixtures of tetragonal martensite (utilizing a the Weyl-limit behavior in the experiments) and utilizing first-principles calculations to explain the extreme stiffening of the cubic lattice with the magnetic transition after the chemical stabilization.

[1] X. Xu, T. Kihara, A. Miyake, M. Tokunaga, T. Kanomata, R., Kainuma, Magnetic-field-induced transition for reentrant martensitic transformation in Co-Cr-Ga-Si shape memory alloys (2018) Journal of Magnetism and Magnetic Materials, 466, pp. 273-276.

This work was financially supported by the Ministry of Education, Youth and Sports of the Czech Republic in the frame of the project 'Ferroic multifunctionalities' (project No. CZ.02.01.01/00/22_008/0004591), co-funded by the European Union.

153_220

Realization of tensile plasticity and shape memory effect in NiMnGa shape memory alloys by constructing a unique dual-phase configuration

Jiaxi Meng, Jingmin Wang, Chengbao Jiang
Beihang University, Beijing, China

NiMn-based shape memory alloys have attracted significant attentions for decades due to their excellent functional properties, including the shape memory effect, magnetoelastic effect, magnetocaloric effect and elastocaloric effect. However, their severe brittleness, particularly their inability to be tensed, has remained a bottleneck, hindering the development and applications. It has been revealed the severe brittleness primarily originates from the grain boundary brittleness. Previously, introducing a large amount of a second phase can effectively improve the ductility of NiMn-based alloys, while the functionalities are simultaneously deteriorated. Recently, we developed a strategy for NiMnGa alloys by constructing a unique dual-phase configuration with a small amount of the second phase distributed along grain boundaries. This strategy was investigated in $Ni_{30}Cu_{20}Mn_{40+x}Ga_{10-x}$ (x=0-10) alloys. We found that substituting Mn for Ga induces the precipitation of a FCC γ phase, which is a disordered solid solution. Quenching from 850℃, a large amount of the γ phase forms, and the shape memory effect is negligible, similarly. Interestingly, after a two-step annealing process (850℃ followed by 650℃), a unique dual-phase configuration where a small amount of thin-layered γ phase just distributed along grain boundaries can form. Along with the microstructure, tensile deformation is realized with a strain of 13%, and a remarkable tensile shape memory effect with the recoverable strain of 3.2% is detected. Microstructural analysis confirms the high plasticity originates from the cooperative deformation of martensite and γ phase, facilitating with their crystallographic orientation relationship. Dislocations can slip across the martensite/γ phase interface, reducing stress concentration at grain boundaries. The observed composite fracture characteristics reveal a cooperative deformation mechanism. Transgranular cleavage in martensite phase directly correlated with stress-induced reversible martensitic transformation, governing the shape memory effect. Ductile fracture in γ phase is responsible for the high tensile plasticity. Thus, the γ phase act as a "glue effect" during tensile deformation, eliminating the grain boundary brittleness. The developed strategy of constructing the unique dual-phase configuration to significantly improve plasticity of NiMnGa alloys will also be suitable for the other NiMn-based alloys, such as NiMnIn, NiMnSn, NiMnSb and so on.

154_214

The origin of the β-relaxation phenomenon in strain glass: a phase field modeling

Chuanxin Liang[1], Dong Wang[1], Yunzhi Wang[2]
[1]Xi'an Jiaotong University, Xi'an, Shaanxi, China. [2]The Ohio State University, Columbus, Ohio, USA

Strain glass state in ferroelastic systems is the counterpart of relaxor in ferroelectric systems and cluster spin glass in ferromagnetic systems, all of which are collectively referred to as ferroic glasses. Different from other glasses such as metallic glasses, polymer glasses, glass-ceramics, etc., which show the frozen process into an amorphous state from a liquid state by rapid cooling or pressurizing, a ferroic glass is structurally still in a crystalline state; and it is the corresponding order parameter (e.g., polarization, magnetization or strain) that is “frozen” into a disordered state from a para ferroic state by charge-or stress-carrying defects (including point defect, dislocations, nano-precipitates, etc.).

The β-relaxation phenomenon in glasses has shown important effects on toughness, ductility, and creep. However, such a β-relaxation has not been reported yet in an important class of glassy materials, ferroic glasses. Here, we report the existence of a β-relaxation anomaly and its physical origin in strain glass systems by combining molecular statics calculation and phase field simulation. The resolved β-relaxation is observed below the strain glass transition temperature at a critical composition accompanied with spontaneous strain glass to normal martensitic phase transformation, and the internal friction for this β-relaxation anomaly fits well with the Arrhenius equation. The superelasticity with β-relaxation has shown low modulus with high recoverable strain over a wide temperature range. Calculated microstructural evolution and the local stress field caused by point defects suggest that the formed percolation-like metastable suppression field under cooling could be the physical origin of the β-relaxation in strain glass systems and is correlated with crystallization.

155_328

Effect of solidification rate on martensitic transformation behavior of Cu-doped Ni-Mn-Ga metamagnetic shape memory ribbons

Patricia Lázpita[1,2], Natalia A. Río-López[1], David Mérida[1], Mariana Ríos[2], Jon Gutiérrez[1,2], Joan Torrens-Serra[3], Jaume Pons[3], Rubén Santamarta[3]
[1]University of the Basque Country (UPV/EHU), Leioa, Spain. [2]BCMaterials, Leioa, Spain. [3]University of the Balearic Islands (UIB), Palma, Spain

Cu-doped Ni-Mn-Ga Heusler magnetic shape memory alloys have become the focus of intense research due to the observation of a metamagnetic phase transformation from a high magnetization martensite phase to a low magnetization austenite phase, with reduced hysteresis. Associated with this behaviour, some interesting properties such as large magnetocaloric, giant magneto-strain and giant magnetoresistance effects have been reported, which make these alloys excellent candidates for multifunctional applications. In our previous work, Cu-doped Ni-Mn-Ga alloys were investigated concluding that the Cu addition up to 6 % merged the martensitic transformation and magnetic one resulting in an increment of the magnetization change (ΔM), and as result of the entropy change across the martensitic transformation (MT), and reducing its hysteresis.

Based on these results, in this work we present a study concerning the fabrication of melt spun ribbons of $Ni_{50}Mn_{19}Ga_{25}Cu_6$ nominal composition alloy and the effect of the ribbon wheel speed fabrication rate on the structure, microstructure, martensitic transformation and magnetic properties, as well as on functional properties. Samples have been elaborated at different melt-spinning wheel speeds ranging from 15 m/s to 30 m/s. Our results show a reduction of the grain size and thickness of the ribbon accompanied by a decrease on the martensitic and magnetic transformation temperatures with increasing cooling rate (Figure 1). Moreover, the observed ΔM change is maximum for the 15 m/s wheel speed fabricated sample showing a value of almost 60 $A \cdot m^2/kg$ for 2 T and a maximum entropy change of 8 J/kg·K (Figure 2).

We will discuss the role of the composition, structure, microstructure and magnetic coupling in these alloys, essential for a better understanding of the increase of the observed ΔM change when the magnetic field induced MT occurs.

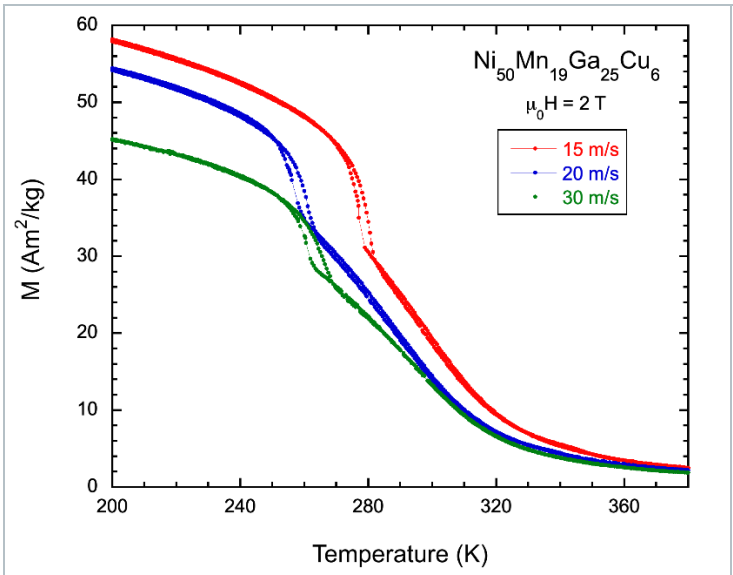

Figure 1. Thermo-magnetization curves showing the MT for ribbons fabricated at 15, 20 and 30 m/s wheel speed values.

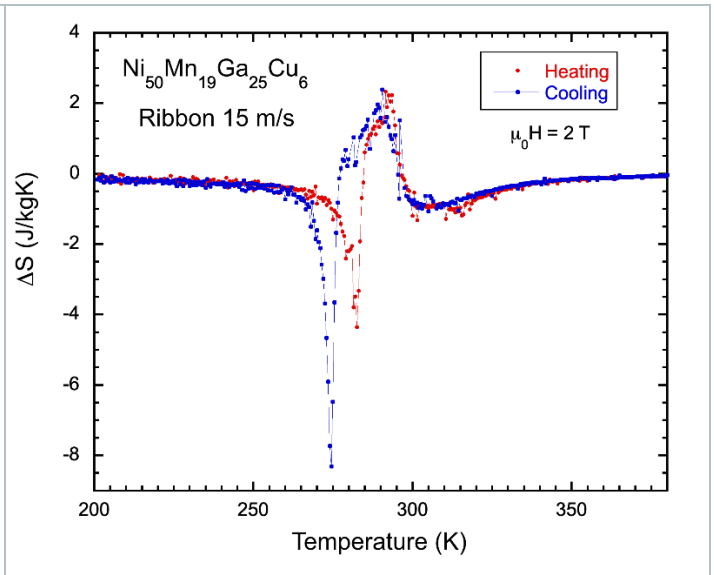

Figure 2. Magnetic entropy change as a function of temperature for the ribbon fabricated at 15 m/s upon cooling and heating at 2 T applied field.

156_250

Magnetic-field-induced martensitic transformation with small hysteresis in Mn_3Ga alloys

Daisuke Imatomi[1], Masashi Tokunaga[2], Yuto Kinoshita[2], Kohki Takahashi[3], Xiao Xu[1,4], Toshihiro Omori[1], Ryosuke Kainuma[1]
[1]Department of Material Science, Graduate School of Engineering, Tohoku University, Sendai, Japan. [2]The Institute for Solid State Physics, The University of Tokyo, Kashiwa, Japan. [3]Institute for Materials Research, Tohoku University, Sendai, Japan. [4]Organization for Advanced Studies, Sendai, Tohoku University, Sendai, Japan

When a martensitic transformation occurs between the parent and martensite phases with different magnetization, the martensitic transformation temperatures shift on the application of a magnetic field, because the phase with a higher magnetization is stabilized due to the Zeeman energy. Thus, at a fixed temperature with a strong magnetic field, magnetic-field-induced (MFI) forward/reverse martensitic transformation and its associated MFI strain can be achieved. Ni–Mn based alloys have been intensively investigated since Kainuma *et al*. first reported MFI shape recovery in the Ni–Co–Mn–In system [1]. However, a relatively large magnetic-field hysteresis appears during the first-order martensitic transformation. Recently, Ito *et al.* reported a small magnetic-field hysteresis of 7 kOe in the Pd_2MnGa alloy [2]; however, the high cost of Pd may limit its practical application. In this study, we focused on Mn_3Ga alloys which exhibit a transformation from a high-temperature paramagnetic $D0_{19}$ phase to a low-temperature ferromagnetic orthorhombic phase with a small thermal hysteresis [3,4]. First, the crystal structures were analyzed down to low temperatures by in-situ XRD and the change of crystal structure was confirmed to agree with the previous reports. The microstructure was also observed using in-situ optical microscopy; surface relief was detected upon the transformation, indicating the martensitic nature of the transformation in this alloy. Thermomagnetization measurements were performed using a SQUID magnetometer, revealing the fact that the transformation temperature increases with increasing magnetic field, which also suggests the possibility of MFI forward martensitic transformation. Therefore, we observed the change of microstructure using an optical microscope under a high pulsed magnetic field. When the magnetic field was applied on the parent phase, surface relief was observed, indicating the MFI martensitic transformation. Additionally, the magnetization measurements were conducted by the application of high pulsed magnetic fields on the parent phase, and a small hysteresis was confirmed for the MFI martensitic transformation. Furthermore, by using a strain gauge, the MFI strain was also evaluated.

[1] Kainuma *et al.*, *Nature,* 439 (2006) 957–960.

[2] Ito *et al*., *Adv. Sci.,* 10 (2023) 2207779.

[3] Niida *et al.*, *J. Phy. Soc. Jpn.*, 52 (1983) 1512–1514.

[4] Boeije *et al.*, *J. Magn. Magn. Mater.,* 433 (2017) 297–302.

157_265

Correlation of Crystallographic and Magnetic Domain Structures in Fe-61.8at%Pd Alloy

Yuto Tomita[1,2], Yongmei M. Jin[3], Takehiro Tamaoka[2], Yasukazu Murakami[1,2]
[1]The Ultramicroscopy Research Center, Kyusyu University, Nishi-ku, Fukuoka, Japan. [2]Department of Applied Quantum Physics and Nuclear Engineering, Kyushu University, Nichi-ku, Fukuoka, Japan. [3]Department of Materials Science and Engineering, Michigan Technological University, Houghton, Michigan, USA

Fe-61.8 at.% Pd alloy undergoes a crystallographic phase separation, in which tetragonal $L1_0$ (FePd-based) phase and cubic $L1_2$ ($FePd_3$-based) phase coexist [1]. Following the electron microscopy studies by Savovici [1], the $L1_0$ phase shows a well-defined polytwin structure, while the $L1_2$ phase exists as thin plates at the positions of $L1_0$ twin boundaries. Observations of the magnetic domain structure provide a key for deeper understanding of the complex microstructure of ferromagnetic shape memory alloys and compounds. However, the magnetic domain observation remains yet to be a challenge. The aim of this study is to reveal the correlation between the magnetic domain structure and the complex crystallographic microstructure in an Fe-61.8 at.% Pd alloy by using transmission electron microscopy (TEM), Lorentz microscopy (LM), and electron holography (EH).

Figure 1(a) provides a typical TEM image showing twin plates produced in an Fe-61.8at.%Pd alloy. As a high-resolution STEM image in Fig. 1(b) demonstrates, thickness of the $L1_2$ plates is only a few atomic layers: see the bright region (representing the Pd-rich region) at the positions of $L1_0$ twin boundaries as indicated by arrowheads. Another bright region in Fig. 1(b) (labelled by “perpendicular boundary”) represents an antiphase boundary by which the geometric phase in the $L1_0$ structural order was changed. A LM image in Fig. 1(c) revealed the positions of magnetic domain walls, most of which are placed in the twin boundaries. These walls were identified to be a type of 90-degree walls, as indicated by the zig-zag contour lines in the EH observation of Fig. 1(d): that is, a plot of the phase shift of incident electrons. In addition to these magnetic domain walls, a 180-degree wall across many $L1_0$ plates was introduced as shown in Figs. 1(c) and 1(d). The antiphase boundaries did not provide appreciable pinning sites for the magnetic domain walls.

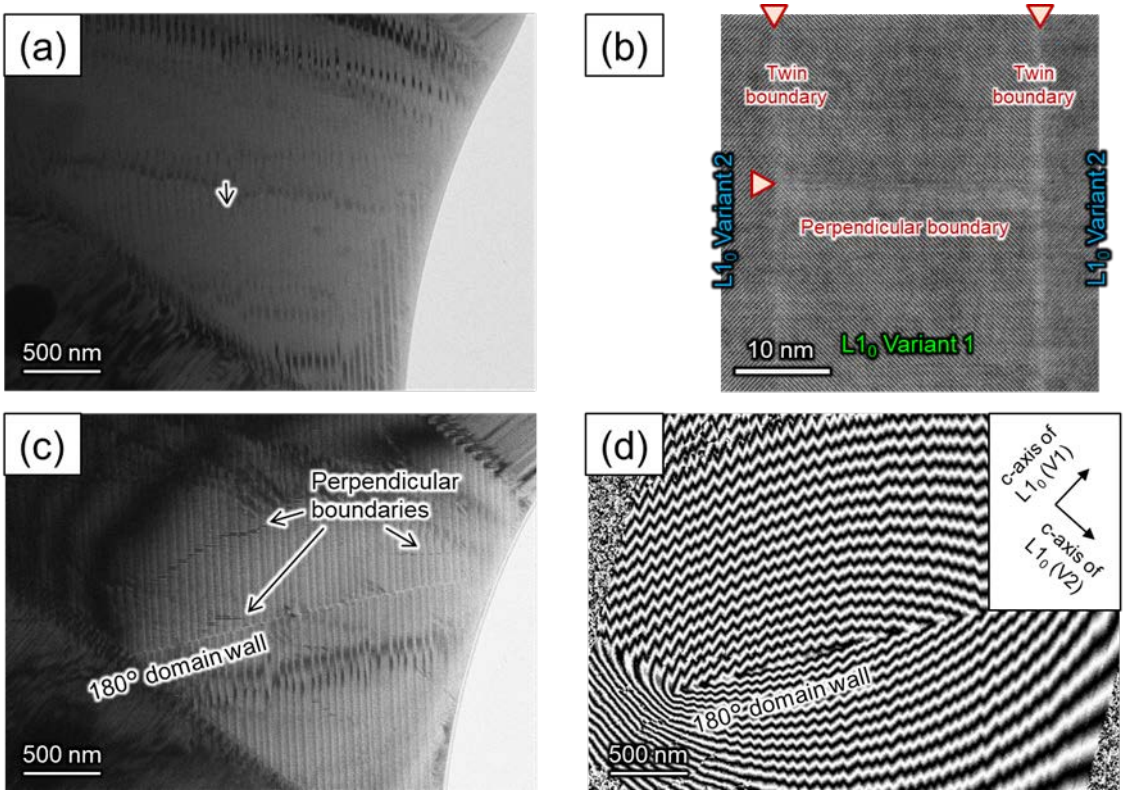

Figure 1 (a) TEM image and (b) STEM image of with $L1_0$ plates and $L1_2$ layers. (c) LM image and (d) phase contour image retrieved by EH.

1. A. Savovici et al., Scr. Mater. 2024, 246, 116067.
2. The authors would like to acknowledge support from the FY2022 JSPS Invitational Fellowships for Research in Japan under ID no. L22503. This study was partly supported by the program “Advanced Research Infrastructure for Materials and Nanotechnology in Japan (ARIM)” from the Ministry of Education, Culture, Sports, Science and Technology (MEXT) under proposal no. JPMXP1222KU0105.

158_303

Magnetostructural behaviour of Ni35Co13Mn35-xFexTi17 melt spun-ribbons

Mariana Ríos Naranjo[1], Patricia Lázpita Arizmendiarreta[2], Daniel Salazar Jaramillo[1]
[1]Basque Center for Materials, Applications, and Nanostructures-BCMaterials, Leioa, Biscay, Spain. [2]University of the Basque Country UPV/EHU, Electricity & Electronics Department, Leioa, Bizcay, Spain

All-d-metal Heusler alloys show an enhancement of the magnetocaloric response when it is compared with the conventional Heusler alloys, especially at low temperature ranges [1, 2]. The hybridization of d-d orbitals play a crucial role in enabling the martensitic transformation, which is fundamental to the emergence of shape memory behavior and magnetically controlled thermal effects [3]. In this work, a series of $Ni_{35}Co_{13}Mn_{35-x}Fe_xTi_{17}$ (x = 0-6) ribbons were prepared using the melt-spinning technique. Macroscopic magnetic measurements indicate that the change in magnetization (ΔM) during the martensitic transformation strongly depends on the alloy composition (see Figure 1, left). The Curie temperature and the direct and reverse martensitic transformation (MT) temperatures were determined using the first-order derivative and slope methods (see inset Figure 1 right), and the values of magnetic entropy change were calculated under an applied field of 2 T by the indirect method (see figure 1 , right). The inclusion of Fe atoms in the structure shifts MT to lower temperatures up to 60 K, which makes these compounds potential candidates for solid-state refrigeration at low temperatures. Microstructural analysis using SEM-EDX revealed surface grains, which correlate with anomalous behavior in some of the samples (see Figure 2). X-ray and neutron diffraction studies confirmed the presence of the austenitic B2 cubic phase as an important feature of this new type of Heusler Alloys.

Keywords: All-d-metal Heusler alloys, Martensitic transformation, Magnetocaloric effect.

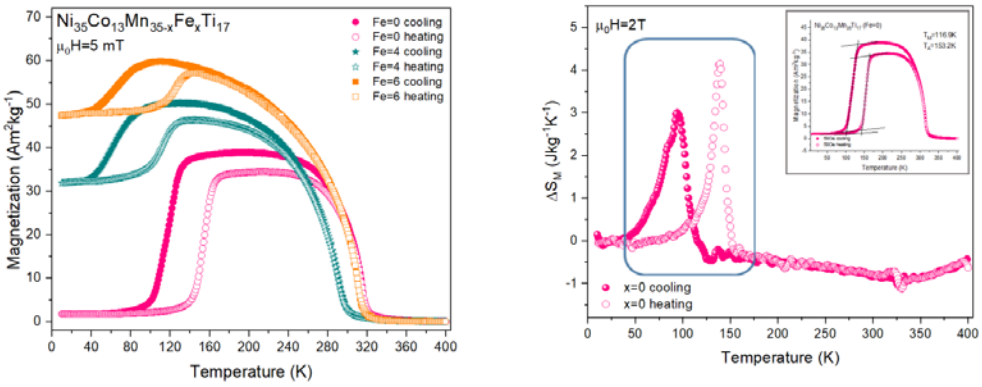

Figure 1. (Left) Thermomagnetization for some representative ribbons. (Right) Isothermal magnetic entropy change curve when x= 0, inset shows the conventional method for martensitic transformations.

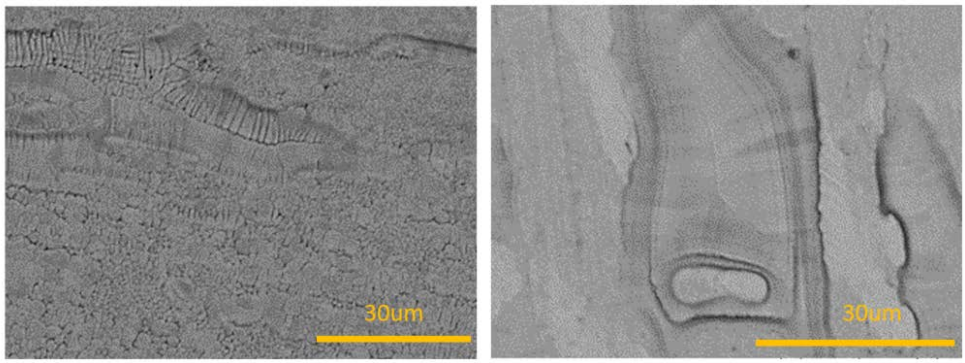

Figure 2. SEM images of the free surface for the ribbons with x=0 and 2 at% respectively.

Acknowledgements
This work has been carried out with the financial support of the Spanish Ministry of Science, Innovation and Universities (PID2022-138256NA-C22 and PID2022-138108OB-C33 funded by MCIN/AEI/10.13039/501100011033). M. Ríos wants to thank the Basque Government (Department of Education) for providing funding under the specific program IKUR-Neutronics.

References
1. B. Beckmann et al., Acta Materialia 246 (2023) 118695
2. H. Neves Bez., et al., Acta Materialia 173 (2019) 225-230
3. G. de Paula Vinicius, M. Reis., Chem Mater 33 (2021) 5483 -5495.

159_359

In-situ DMA studies during thermomechanical loading of NiTi wires

Elizaveta Iaparova, Petr Šittner, Luděk Heller
Institute of Physics of the Czech Academy of Sciences, Prague, Czech Republic

Stress-strain responses of NiTi shape memory wires to oscillatory loading in in-situ DMA tests can be used to track down activity of martensitic transformation (MT) processes during thermomechanical loads. In this work, we investigate the stress-strain responses of NiTi SME wires (Fort Wayne Metals NiTi #5) subjected to various thermomechanical loads in tension. As an example, results of in-situ DMA tests during heating under constant applied stress (strain-temperature and storage modulus-temperature) are shown in Fig. 1. NiTi wires were deformed at low temperature -125 °C in the martensite state up to various tensile stresses and then heated either under the same constant applied tensile stress (Fig. 1a,c) or unloaded and heated under 20 MPa stress (Fig. 1b,d) up to 200 °C.

When analyzing the results, several phenomena are observed. First, the stress-free (under 20 MPa) heated martensitic wires shorten and their storage moduli E' decrease reflecting strong elastic and thermal expansion anisotropies of the B19' martensite. Second, E' of martensite is significantly higher when heated under stress, though its magnitude decreases with increasing stress (Fig. 1b,d). Third, the evolution of E' upon heating under stress reflects the progress of reverse MT and plastic deformation of martensite by kwinking. When the oriented martensite is heated under elevated applied stresses (Fig. 1a,c), it transforms into plastically deformed B2 austenite. The higher the applied stress, the larger is the generated plastic deformation. In response to heating under the highest 1000 MPa stress, the oriented martensite in the wire deforms plastically via kwinking up to failure instead of reverse transforming into austenite. When the oriented martensite is heated stress-free (under 20 MPa), reverse MT occurs as usual (Fig. 1b.d), only Af temperatures are shifted upwards due to the stabilization of martensite by deformation. The evolution of E' upon heating (Fig. 1c,d) provides complementary information to the strain-temperature responses recorded in thermal cycling tests (Fig. 1a,b). The in-situ DMA tests can thus be used to detect and analyze coupled MT and plastic deformation proceeding in thermomechanical loading tests.

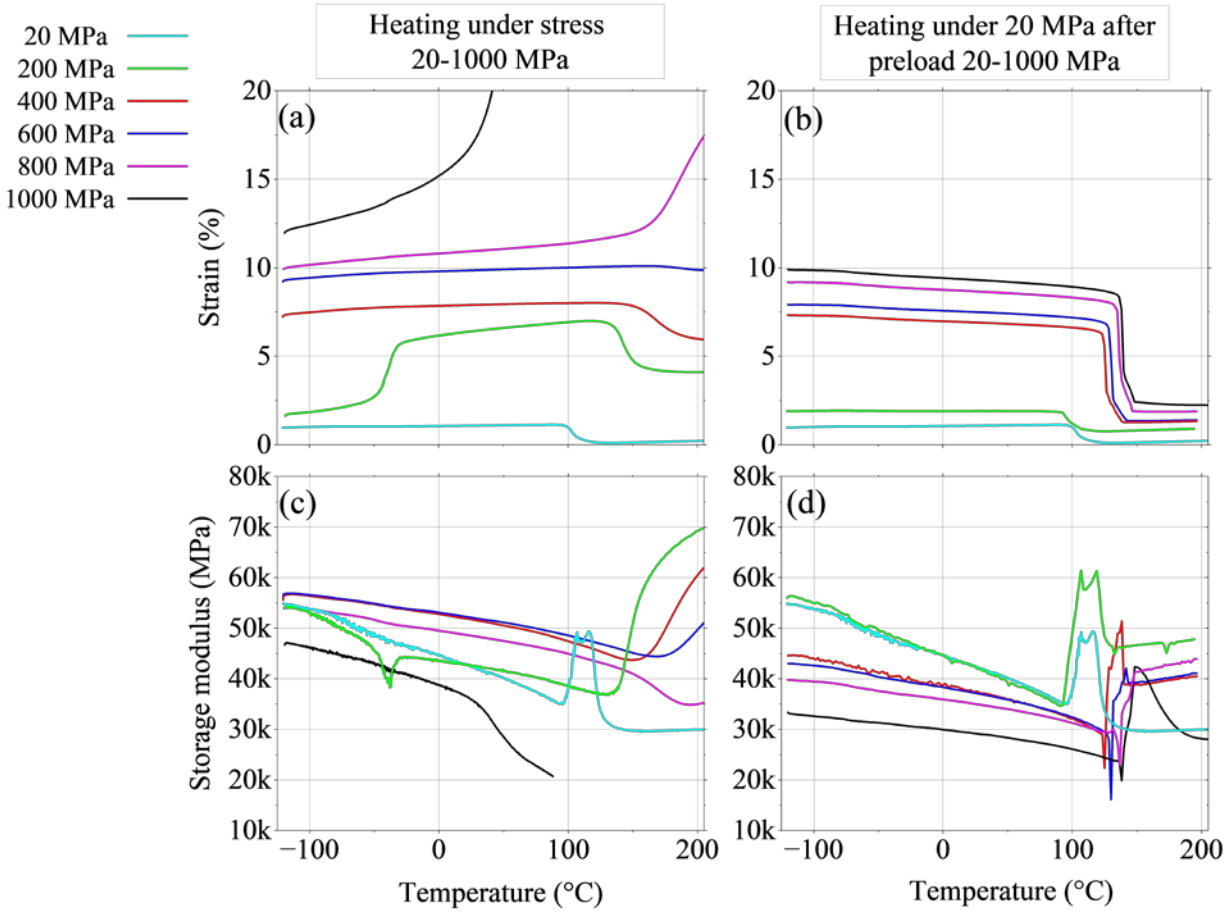

Figure 1 Evolution of tensile strain (a, b) and storage modulus (c, d) in NiTi wires during heating under constant stress (a, c), and in stress-free conditions following preliminary deformation in the martensitic state (b, d) with oscillatory loading applied.

159_393

Influence of Ni-content and Precipitates on the Mechanical and Actuation Fatigue Crack Growth of NiTiHf High-Temperature Shape Memory Alloys

Roberto Orrostieta[1], Theocharis Baxevanis[2], Kadri Atli[1], Dimitirs Lagoudas[1], Ibrahim Karaman[1]
[1]Texas A&M University, College Station, Texas, USA. [2]University of Houston, Houston, Texas, USA

Nitinol has been most successfully implemented in the biomedical field, where the majority of a device's lifespan is spent during a crack nucleation phase, followed by a relatively brief crack propagation phase. On the other hand, NiTiHf high-temperature shape memory alloys (HTSMAs), which operate at actuation temperatures above 100°C, are being considered for use in aerospace, defense, and energy industries. In these applications, a longer steady crack propagation phase may be permissible before retiring actuation components.

Unfortunately, Ni-rich NiTiHf alloys are highly sensitive to nickel content, with variations of less than 1 atomic percent causing transformation temperature shifts exceeding 100°C. Precipitates and microcleanliness also impact structural degradation and fatigue crack propagation during martensitic transformation in HTSMAs. This study examines the effects of minor Ni-content variations within 1 at.% in precipitate-free specimens with Hf20 (at.%) compositions and evaluates the role of precipitates in pseudoelastic mechanical fatigue and thermal cycling fatigue crack growth. Moreover, mechanical and actuation experiments, using the same materials and conditions, aim to determine whether actuation crack growth rates can be predicted through the faster and cost-efficient mechanical fatigue crack growth testing

Key findings reveal that inclusions and precipitates decrease the stress intensity threshold, ΔJ_{th}, during mechanical fatigue experiments, while compositional and microstructural features do not affect the steady crack growth regime. Attempts to predict actuation crack growth rates using mechanical fatigue testing were unsuccessful. Instead, a secondary threshold associated with a maximum stress intensity shielding ($\Delta J_{s,\,max}$) was found. Actuation cycling beyond $\Delta J_{s,\,max}$ yielded unstable crack growth, while cycling below $\Delta J_{s,\,max}$ led to crack arrest. Small coherent precipitates were found to increase $\Delta J_{s,\,max}$, whereas larger precipitates reduced it.

Based on these observations, the study suggests shifting the focus from crack growth rate predictions to determining $\Delta J_{s,\,max}$ during actuation crack growth. Establishing safety factors based on stress intensity levels that ensure crack arrest and stable actuation functionality is proposed as a more reliable approach to preventing failure during actuation crack growth.

160_362

Micro crack growth in NiTi based shape memory alloys

Jan Frenzel, Mustafa Rahim, Gunther Eggeler
Ruhr University Bochum, Bochum, NRW, Germany

NiTi based shape memory alloys (SMAs) show fascinating functional properties. They are able to re-establish their initial geometries after deformations which significantly exceed conventional elastic strains. The service lives of SMAs are limited by functional and structural fatigue. Functional fatigue refers to the transformation-induced formation of defects and results in a degradation of exploitable shape memory strains and changes in transformation temperatures. In contrast, structural fatigue describes the formation of cracks during dynamic loading. Today, a good understanding on surface-and microstructure-related effects on fatigue lives, crack formation and macro-crack growth of SMAs has been established. However, the present knowledge on micro crack growth is very limited. In the present work, we study short crack growth in pseudoelastic NiTi SMA wires using interrupted bending rotation fatigue (BRF) experiments. After specific number of BRF cycles, the wires surfaces were investigated in the scanning electron microscope to track the growth behavior of specific individual cracks using quantitative image analysis. Our results show that only a small number of cracks manages to evolve into macroscopic cracks which shoe Paris-type crack growth. For the first time, we document how individual micro cracks interact with microstructural constituents and other cracks.

161_182

On the origin of functional fatigue of nanocrystalline NiTi wires

Petr Šittner, Elizavieta Iaparova, Orsolya Molnárová, Luděk Heller
Institute of Physics of the Czech Academy of Sciences, Prague, Czech Republic

The instability of cyclic thermomechanical responses of NiTi, known as functional fatigue, represents one of the unsolved problems of NiTi technology. It is intuitively understood that it originates from the incremental plastic deformation by dislocation slip accompanying the cyclic martensitic transformation (MT) proceeding under external stress, but it is not known, whether the dislocation slip occurs in the austenite or martensite phase, during the forward and/or reverse MT and how it is related to the observed instability of cyclic thermomechanical responses.

Motivated by these questions, we have systematically investigated martensitic transformations in nanocrystalline NiTi wires subjected to closed loop thermomechanical loading in tension [1-6]. We evaluated the incremental plastic strain generated separately by the forward and reverse MTs in closed loop thermomechanical cycling under external stress [1-3], reconstructed martensite variant microstructures in grains of deformed wires by nanoscale orientation mapping in TEM [2-4], analyzed permanent lattice defects generated by forward and reverse MT under stress [5] and evaluated textures in oriented martensite [2,6]. In this talk, I will overview key results of this research and introduce our view on the mechanism by which the forward and reverse MTs taking place under stress above certain thresholds generates the incremental plastic strains and causes functional fatigue of nanocrystalline NiTi.

References:

1. P. Sittner, E. Iaparova, O. Molnarova, O. Tyc, X. Bian, L. Kadeřávek, L. Heller, Materials & Design 244 (2024) 113188, https://doi.org/10.1016/j.matdes.2024.113188
2. O. Tyc, X. Bian, O. Molnárová, L. Kaderavek, L. Heller, P. Šittner, Applied Materials Today, 2024, https://papers.ssrn.com/sol3/papers.cfm? id=4889650
3. O. Tyc, E. Iaparova, O. Molnarova, L. Heller, P. Sittner, Acta Materialia, 2024, https://papers.ssrn.com/sol3/papers.cfm? id=4870133
4. O. Molnarova, O. Tyc, M. Klinger and P. Sittner, Materials Characterisation, 214(2024)114084 https://doi.org/10.1016/j.matchar.2024.114084
5. O.Molnarova, E. Iaparova, L. Heller, P.Sittner, Analysis of plastic strains and permanent lattice defects created by forward and reverse martensitic transformation in nanocrystalline NiTi wire thermally cycled under stress
6. X. Bian, L. Heller, L. Kaderavek, P. Sittner, Appl Mater Today 26 (2022) 101378, https://doi.org/10.1016/j.apmt.2022.101378

162_325

Characterization and influence of Ni_3Ti precipitates on functional properties of All-*d*-Metal Ni-Mn-Ti Magnetic Shape Memory Alloys

Joan Miquel Vaquero-Crespí, Joan Torrens-Serra, Daniel Salas, Jaume Pons, Rubén Santamarta
University of the Balearic Islands, Palma, Spain

Magnetic shape memory alloys (MSMAs) are considered as promising candidates for solid-state magnetic refrigeration due to their remarkable magnetocaloric and elastocaloric properties. Their ability to undergo reversible martensitic transformations under external magnetic or stress fields enables efficient refrigeration cycles without the need for conventional gas compression. Among MSMAs, Ni-Mn-based systems have shown outstanding caloric effects, positioning them as excellent candidates. However, conventional Ni-(Co)-Mn-(In,Ga) alloys, which have been extensively studied, suffer from intrinsic brittleness, poor mechanical performance, and rapid degradation under cycling, which are critical drawbacks for refrigeration applications where long-term cycling is essential.

To overcome these limitations, two strategies have been explored. On the one hand, recent studies have shown that Ni-(Co)-Mn-Ti alloys, composed exclusively of 3*d* transition metals, may exhibit improved mechanical properties compared to alloys containing *p*-orbital metals, while preserving suitable transformation characteristics and significant caloric effects. On the other hand, thermal treatments have been proved to be effective not only tailoring the martensitic transformation characteristics but also enhancing their mechanical properties by promoting the formation of coherent precipitates. In this regard, several authors have reported the presence of micrometric Ni_3Ti precipitates in Ni-(Co)-Mn-Ti MSMAs after high-temperatures treatments (above 600 ºC).

In this work, several Ni-Mn-Ti alloys are subjected to aging treatments at lower temperatures (below 600 ºC) and for different durations to promote the formation of nanoprecipitates and to investigate their influence on functional properties. The structure and microstructure of both precipitates and the matrix are analyzed using transmission electron microscopy (TEM), energy dispersive X-ray spectroscopy (EDX), and X-ray diffraction (XRD). The effects on thermal and mechanical properties of alloys with different precipitate distributions are characterized through differential scanning calorimetry (DSC) and mechanical testing. The results will reveal whether controlled precipitation in Ni-Mn-Ti can effectively improve the mechanical performance of polycrystalline Ni-Mn-based MSMAs, enhancing their potential for reliable solid-state refrigeration applications.

163_277

Observation of strain-spin dual-glass state in all-d-metal Heusler alloy Ni_2MnTi

Qiusa Ren, Yibo Wang, Enke Liu
Beijing National Laboratory for Condensed Matter Physics, Institute of Physics, Chinese Academy of Sciences, Beijing, China

Glassy state is a common state in solid materials. For ferroic materials, the corresponding glassy states are named as spin glass, strain glass and relaxor ferroelectrics. As an important form of glassy state, strain glass characterized by nano-martensitic domains and frequency dependence of dynamical mechanical properties has been extensively studied, due to its intriguing performance on application [1, 2]. Combined with magnetism, more functional properties are found in ferromagnetic strain glass [3, 4]. It is of great interest to discover diverse physical phenomena and novel functional properties in different magnetic strain glass states.

Here, we observed a dual-glass state consisting of strain glass and spin glass in all-d-metal Heusler alloys Ni_2MnTi for the first time [5]. As shown in Figure 1, the existence of strain glass is confirmed by transmission electron microscopy (TEM) and dynamical mechanical analysis (DMA), with clear lattice distortion as nano-domains and glassy relaxation dynamic character. On the basis of antiferromagnetic (AFM) nano-domains, the existence of cluster spin-glass (CSG) is revealed by AC and DC magnetic measurements, with a long relaxation time of $T^*=5.45\times10^{-6}$ s. In addition, based on the structure of strain glass, the exchange bias effect is observed with a bias field of 900 Oe under a cooling field of 20 kOe. It is proposed that this effect can be attributed to the interaction of AFM nano-domain clusters and the disordered-ferromagnetic (FM)-layer on their interfaces. As a result, a new material design strategy can be indicated by modulating the strain glass to design larger exchange-bias materials for spintronics application or phase-transition functional materials for energy conversion. Our work not only provides new insights into the dual glassy dynamics, but also benefits the potential development of new ferroic functional materials.

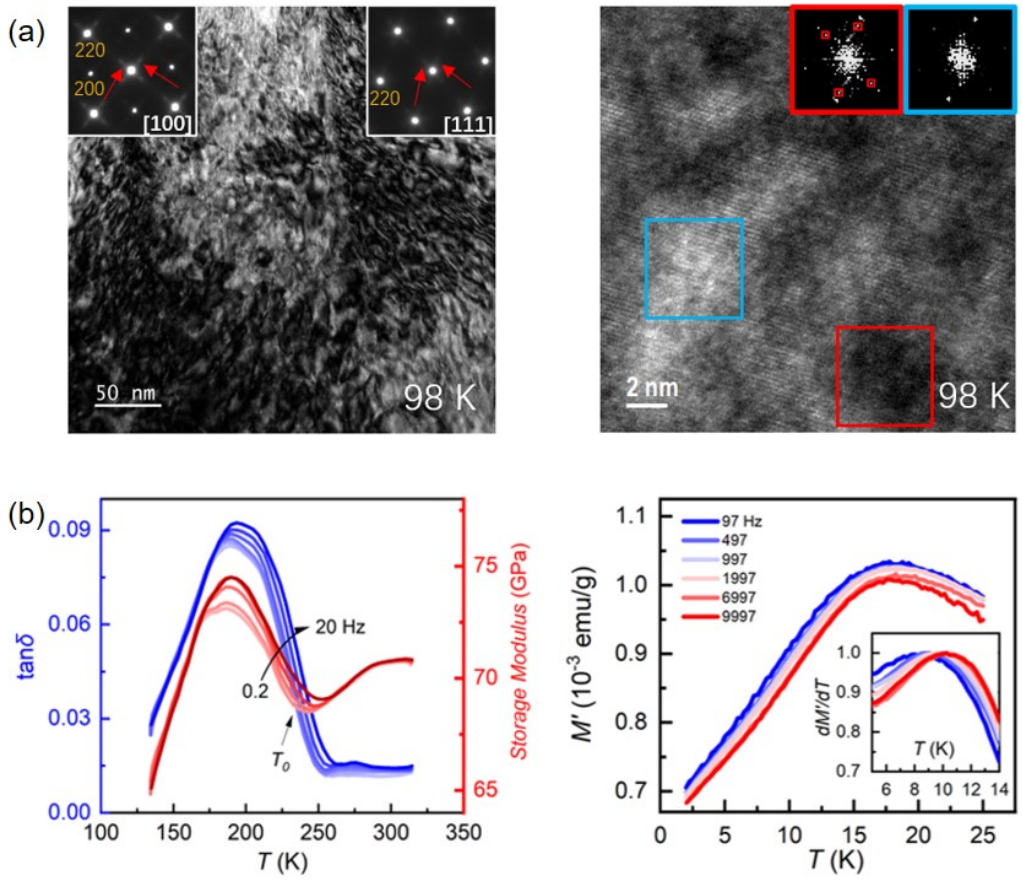

Figure 1. (a) Microstructural characterization at 98 K. (b) Results of dynamical mechanical analysis and ac susceptibility. The inset shows the normalized result of the first derivative of the real part.

References:
[1] Z. Xu, Y. Ji, C. Liu, et al., Nature, 633 (2024) 575.
[2] D. Wang, S. Hou, Y. Wang, et al., Acta Mater., 66 (2014) 349.
[3] S. Ren, D. Xue, Y. Ji, et al., Phys. Rev. Lett., 119 (2017) 125701.
[4] F. Qin, W. Xiao, F. Lu, et al., J. Mater. Sci. Technol., 35 (2019) 396.
[5] Q. Ren, C. Yuan, Z. Du, et al., Acta Mater., DOI:10.1016/j.actamat.2025.121032.

164_341

Development of Cu-doped Ni-Mn-Ga metamagnetic shape memory alloy powders

Daniel Salas[1], Joan Torrens-Serra[1], Miquel-LLuís Corró[1], Patricia Lázpita[2,3], Mariana Ríos[2,3], Boris Kustov[1], Rubén Santamarta[1], Concepció Seguí[1], Jon Gutiérrez[2,3], Jaume Pons[1]
[1]Physics Department, University of the Balearic Islands, Palma, Spain. [2]Faculty of Science and Technology, University of the Basque Country, Leioa, Spain. [3]BCMaterials, Leioa, Spain

The importance of powder metallurgy in functional alloys is growing with the rapid advancement of additive manufacturing technologies. These technologies offer innovative ways to transform powder materials into custom-shaped solid parts or, particularly relevant to this work, into composites where functional powder is embedded within a printable matrix.

Among potential candidates for functional materials, Ni_2MnGa Heusler alloys with approximately 6 at.% of Cu substituting Mn exhibit a room-temperature metamagnetic martensitic transformation between a paramagnetic austenite and a ferromagnetic martensite, with a high entropy difference exceeding 30 J/kg·K and low thermal hysteresis of about 10 K. These properties make this pseudo-Heusler composition a promising candidate for magnetic field-assisted solid-state refrigeration. However, the inherent brittleness of Ni-Mn-based shape memory alloys poses challenges in fabricating complex geometries that could further enhance their performance in refrigeration applications. To address this drawback, the development of composite materials that incorporate Ni-Mn-based alloys as micron-sized particles is proposed, enabling fabrication into custom parts using additive manufacturing techniques. Achieving this goal requires the production of metamagnetic shape memory alloy powders of suitable particle size and enhanced caloric properties.

In this study, quaternary Ni-Cu-Mn-Ga bulk alloys were subjected to mechanical and thermal treatments for pulverization and subsequent recovery of the transformation, yielding functional magnetocaloric powders. The influence of various processing parameters on the material's microstructure and martensitic transformation behavior was examined using X-ray diffraction and transmission electron microscopy for structural analysis, and differential scanning calorimetry and magnetometry to evaluate the thermal and magnetocaloric effects and magnetic field-induced transformation behavior. The results will be discussed in the context of crystalline deformation during pulverization, degree of recovery and oxidation during recrystallization, particle size, variations in $B2/L2_1$ atomic order, and the coupling between elastic and magnetic degrees of freedom.

165_304

Origami-Inspired Reprogrammable Shape Memory Alloy Microactuator System

Vincent Gottwald[1], Lena Seigner[1], Makoto Ohtsuka[2], Lars Bumke[3], Eckhard Quandt[3], Manfred Kohl[1]
[1]Institute of Microstructure Technology, Karlsruhe Institute of Technology (KIT), Karlsruhe, Germany. [2]Institute of Multidisciplinary Research for Advanced Materials, Tohoku University, Sendai, Japan. [3]Department of Materials Science, Kiel University, Kiel, Germany

We present the design, fabrication, and characterization of a SMA microactuator system that can be reconfigured without manual intervention. The system consists of antagonistic shape memory alloy (SMA) microactuators for bidirectional folding of miniature-scale tiles following the principle of origami. Integrated heatable soft-magnetic NiMnGa pads with low ferromagnetic transition temperature allow for control of magnetic latching forces. To date, only a limited number of reprogrammable origami-inspired systems have been investigated.[1] Thereby, reconfigurable SMA-based systems with multiple tiles have been constrained to macro-scale dimensions due to limitations in fabrication technology and thermal design.[2] Fig.1A shows the layout of the device consisting of four triangular tiles with an edge length of 500 µm. For selective control by Joule heating, the strongly coupled thermo-mechanical and thermo-magnetic properties of the TiNiCu bending microactuator and magnetic subsystems are taken into account. A microfabrication process is developed that considers the specific requirements for processing of the various materials and structures. In particular, a procedure for local shape setting of the SMA microactuators is presented to adjust their memory shape at either maximum or minimum bending angle and, thus, to functionalize their performance as protagonists or antagonists. Tensile stress-strain experiments in Fig. 1B show that the maximum recovery stress upon heating to 80 °C at 2% strain is about 230 MPa. Fig. 1C reveals a maximum torque of about 122 µNmm that is determined at a bending angle of 0° and electrical power of 38 mW. A demonstrator system is depicted in Fig. 1D that is programmed to adopt the shape of a pyramid and later reprogrammed to self-unlatch, self-unfold and subsequently to self-fold in downwards direction to adopt the shape of a table. In the presentation, we address the issue of thermal cross-coupling and show how coupled finite element simulations are used to cope with this issue. We also present a solution to further enhance the bidirectional angular range using a cascaded configuration of antagonistic SMA bending microactuators.

1. Hernandez, E. A. P., Hartl, D. J. & Lagoudas, D. C. Active Origami: Modeling, Design, and Applications. (Springer, 2019)

2. Hu, K., Rabenorosoa, K. & Ouisse, M. A Review of SMA-Based Actuators for Bidirectional Rotational Motion: Application to Origami Robots. Frontiers in Robotics and AI 8, 678486 (2021)

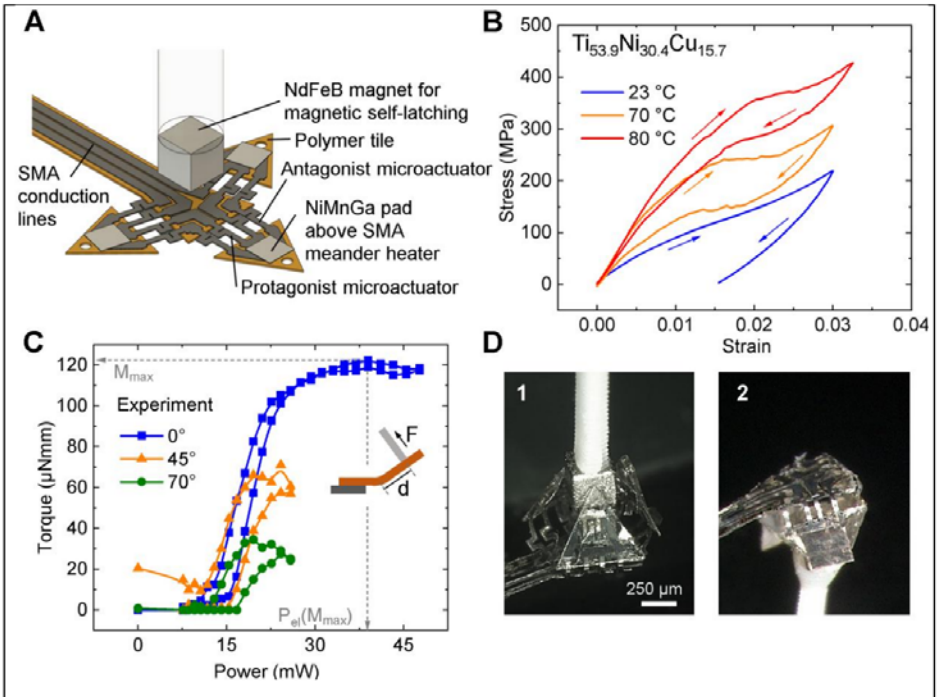

Fig. 1: (A) Layout of the reprogrammable SMA microactuator system. (B) Stress–strain characteristics of a dogbone-shaped TiNiCu tensile test specimen of 10 µm thickness at different temperatures in the range from 23 to 80 °C determined at a strain rate of $10^{-4}s^{-1}$. (C) Experimentally determined torque versus power characteristics of a protagonist microactuator at three different angles. (D) Demonstrator of the origami-inspired reprogrammable SMA microactuator system: (1) in pyramid configuration, (2) table configuration.

166_202

Interlocking Metasurfaces: A New Paradigm for Adaptive and Reconfigurable Joining

Abdelrahman Elsayed[1], Taresh Guleria[2], Kadri C. Atli[1], Ophelia Bolmin[3], Benjamin Young[3], Philip J. Noell[3], Brad L. Boyce[3], Alaa Elwany[2], Raymundo Arroyave[1], Ibrahim Karaman[1]
[1]Department of Materials Science and Engineering, Texas A&M University, College Station, TX, USA. [2]Department of Industrial and Systems Engineering, Texas A&M University, College Station, TX, USA. [3]Sandia National Laboratories, Albuquerque, NM, USA

Interlocking Metasurfaces (ILMs) are architected interfaces composed of periodic, interlocking geometries engineered to achieve reversible mechanical engagement without the need for adhesives or fasteners. This study presents the design, fabrication, and characterization of ILMs constructed from nickel-titanium (NiTi) shape memory alloys (SMAs), leveraging both the Shape Memory Effect (SME) and Superelasticity (SE) to enable active and reconfigurable mechanical locking. Two classes of ILMs are demonstrated: SME-driven ILMs that undergo thermal actuation for shape recovery and engagement, and SE-driven ILMs that utilize stress-induced phase transformations for reversible locking. All ILMs were fabricated via Laser Powder Bed Fusion (L-PBF) using optimized processing parameters to ensure high density, minimal porosity, and precise geometrical fidelity. A systematic additive manufacturing (AM) workflow was implemented, incorporating process parameter tuning, porosity minimization, and crystallographic texture control to enhance functional performance. Finite Element Analysis (FEA) guided ILM design by predicting localized strain distributions during engagement and disengagement, maintaining maximum strains below 5% for SME-based ILMs and under 3% for SE-based ILMs to ensure full recoverability. Experimental validation using Digital Image Correlation (DIC) confirmed the FEA predictions, demonstrating high locking forces, full strain recovery, and close agreement with the simulated behavior. Thermomechanical testing revealed over 95% strain recovery and excellent cyclic stability in all ILM variants. SE-driven ILMs withstood eight engagement cycles without performance degradation, achieving locking forces up to ~620 N. The integration of L-PBF with FEA and in-situ experimental characterization establishes a robust framework for the development of high-performance ILMs.This work demonstrates that NiTi SMAs, when processed through an optimized L-PBF pathway, enable ILM designs capable of high-load, reversible engagement suitable for advanced adaptive systems. The findings provide a foundation for ILM deployment in aerospace, robotics, and biomedical applications, with future work focusing on fatigue resistance and the integration of multi-functional geometries.

167_226

Proof-of-concept of superelastic active mechanical metamaterials using Cu-Al-Ni shape memory alloys.

Ander Abadín, José F. Gómez-Cortés, Luis Corcuera, Maria L. Nó, Jose M. San Juan
Department of Physics, Faculty of Science and Technology, University of the Basque Country, UPV/EHU, Bilbao, Spain

Mechanical metamaterials (MM) represent an area of research and innovation that explores new ways to employ motion, deformation, stress, and mechanical energy across various length scales, from nanometers to meters. These materials are designed and structured in regular patterns of building blocks or cells, enabling them to display a wide range of properties and functionalities beyond what would be expected from their bulk constitution; the honeycomb-like hexagonal cellular structures are the most widely studied patterns in MM.

Shape memory alloys (SMA) are active materials exhibiting shape memory effect and superelasticity, and these properties make them an excellent option for researching and developing a new active mechanical metamaterials (AMM) category. This work explores the concept of AMM and develops a proof-of-concept of superelastic AMM using a Cu-Al-Ni single-crystal SMA slide as the active starting material. For this purpose, honeycomb-like hexagonal cellular patterns were manufactured on [001]-oriented single-crystal samples using femtosecond laser micro-cutting technology. First, the different parameters of laser processing were tested and optimized, like the laser power or the scan speed for instance. Then, sample's thickness and the hexagons' lateral dimensions were set at about one hundred fifty and three hundred micrometers, respectively for the further production of AMM. Samples with different number of hexagonal cells were tested at room temperature along the [001] direction, using a tensile stage under an optical microscopy to simultaneously observe and follow the stress-induced martensitic transformation and the microstructure during the loading-unloading cycles. The load-displacement curves exhibited a characteristic closed hysteretic profile of superelasticity that was analyzed and compared to the superelastic response of the reference bulk single crystal. In parallel, a finite element analysis was conducted using COMSOL Multiphysics software to determine the evolution of strain and stress in the different sample's geometry and the numerical analysis was compared with the observed in-situ behavior. This proof-of-concept demonstrates that the design and development of new superelastic AMMs is feasible, showing a great potential to serve as the foundation for new advanced technologies.

168_241

Introduction to 3D in-situ characterization technique for deformation-induced martensitic transformation using synchrotron X-ray

Osamu Takakuwa[1], Tatsuya Iwano[1], Kyosuke Hirayama[2], Hiroyuki Toda[1]
[1]Kyushu University, Fukuoka, Japan. [2]Kagawa University, Takamatsu, Japan

Synchrotron radiation, characterized by high brightness, directionality, and parallelism, can accurately collect information within metallic materials in three dimensions. Imaging using absorption contrast derived from density differences between materials is widely applied across various fields, from medical to industrial applications. While absorption contrast enables the visualization of voids, damage, precipitated phases, and other features inside metallic materials using X-ray CT, it is challenging to identify substances (phases) with small density differences. To address this issue, a method has been developed to detect phase shifts resulting from the refraction of synchrotron radiation at interfaces between different phases, and to recover the distribution of these phase shifts. This approach enhances the interfaces and enables imaging of microstructures with relatively low density differences, such as duplex stainless steels [1]. The authors applied this technique to visualize and track deformation-induced martensitic transformation in three dimensions continuously by detecting small density changes between the parent austenite phase and the transformed phase (α' martensite) caused by the phase transformation, and demonstrated it [2].

It is widely recognized that deformation-induced martensitic transformation exhibits unique mechanical properties, including an enhanced strength-ductility balance, shape memory effect, and superelastic effect. However, the origin of these effects remains unclear, and many related studies are still ongoing. The presenters successfully identified the austenitic phase and martensitic phase at each deformation stage of metastable austenitic stainless steel using refraction contrast imaging. By complementing X-ray diffraction and 3D CT images, they were able to determine the {111} habit planes of each martensite phase. In addition to a detailed description of these results, we will show the high-resolution 3D visualization of the austenite phase (FCC) → ε-martensite phase (HCP) → α' martensite phase (BCC) transformation by X-ray microscopy using high-resolution nanotomography.

Reference
[1] H. Toda, A. Takijiri, M. Azuma, S. Yabu, K. Hayashi, D. Seo, M. Kobayashi, K. Hirayama, A. Takeuchi, K. Uesugi, Acta Mater. 126 (2017) 401–412.
[2] O. Takakuwa, T. Iwano, K. Hirayama, H. Toda, A. Takeuchi, K. Uesugi, Sci. Rep. 14 (2024) 14445.

169_261

A novel quench cracking characterisation method for induction-hardened steels with different thermal histories

Aysel Aysu Catal Isik[1], Enrique Galindo-Nava[1], Lizeth Johana Sanchez Camacho[2], Mangesh Vyankat Pantawane[2], Vikram Bedekar[2]
[1]University College London, London, United Kingdom. [2]Timken Company, Canton, Ohio, USA

The fast growth in the wind energy market requires stronger and more fatigue-resistant bearings due to larger mechanical loads on power transmission components. High-performance induction-hardened high-carbon steels can meet such demands, however, these alloys are prone to quench cracking during manufacturing, resulting in a need for improving steel processability. Such requires understanding key physical processes in the microstructure controlling microcracking during quenching. Traditional methods for examining microcracks have not provided enough insights to unveil the main features in martensite evolution that affect the nucleation and growth of cracks, and new characterisation methodologies are needed. This work introduces a new microcrack quantification method using optical microscopy by assessing the main features of microcracks, including crack distance from the induction hardened surface, crack length, crack angle to the martensite midrib, crack location on the martensite plate and the midrib length of corresponding martensite plates. Microcracks are classified as forming inside a martensite plate (internal) or at the austenite/martensite interface (interfacial cracks). Our results show that microcrack severity is affected by the distance from the induction hardened surface and peaked at ~1 mm depth. A possible reason for this can be changing local thermal history with distance from the induction hardened surface. Internal cracks outnumber interfacial cracks vastly, and they were found to be almost perpendicular to the martensite midrib. Interfacial cracks are observed to be common in smaller martensite plates and located around the mid-point of the interface rather than the tip of the martensite plate. This is attributed to the larger strain at the mid-point of the interface as it is the thickest section of a plate. Additionally, the novel characterisation method is employed to study steels following different annealing temperatures between 1173 K and 1293 K to explain possible effects of the initial microstructure on crack severity. The experimental outcomes are used to connect the thermal history with different microcracking behaviours by considering the local changes in the martensite microstructure. Overall, our microcrack quantification method provides detailed information about microcracking and its connection to thermal history and martensite microstructure, which will greatly support the design and optimisation of novel bearing steels.

170_170

Anisotropic cleavage fracture caused by transformation-induced internalstress in an as-quenched martensite

Daisuke Fukui[1,2], Yuki Kawahito[1], Ryota Nagashima[1], Nobuo Nakada[1]
[1]Institute of Sciencce Tokyo, Yokohama, Japan. [2]Deloitte Touche Tohmatsu, Tokyo, Japan

The effect of microscopic internal stresses (Type-II) generated via martensitic transformation from austenite (A) to martensite (M) on $\{001\}_M$ cleavage fracture was investigated in an as-quenched 0.1C–5.0Mn steel (mass%). Crystallographic orientation analysis using the electron backscatter diffraction technique revealed that cryogenic $\{001\}_M$ cleavage fracture was promoted predominantly in mode I fracture by Charpy impact testing, and that the Bain group, where martensite variants belong to the same Bain variants, acted as an effective unit to prevent fracture. It was also discovered that the cleavage crack preferentially propagates on $(001)_M$ rather than on $(100)_M$ in the Bain group, where $(001)_M$ was nearly parallel to $(001)_A$ in the Bain lattice correspondence ($[-110]_A$ // $[100]_M$, $[110]_A$ // $[010]_M$, $(001)_A$ // $(001)_M$). In addition, by using a combination of a micro-scale focused ion beam and high-precision digital image correlation techniques, it was found that microscopic internal stresses were anisotropically developed in each Bain group. The principal axes of the internal stresses corresponded to the $<001>_M$ coordinate axes in the Bain lattice correspondence, and the principal stress parallel to $[001]_M$ is much higher than that of the other two. After the measurement of the internal stresses, it was proved that the cleavage fracture behavior obeyed the effective normal stress in the normal direction of $\{001\}_M$ consisting of the resolved bending stress in the impact test and the anisotropic internal stress generated via martensitic transformation. This suggests that the transformation-induced internal stress originating from the Bain strain leads to the anisotropy of the cleavage fracture in lath martensite.

171_178

Development of Cold-rolled Martensitic Steels with excellent flatness and resistance to hydrogen delayed fracture

Min-Ho Jang, Bong June Park, Seong Pil Jung, Seong Kyung Han, Tae Woo Kwon
Hyundai Steel R&D Center, Dangjin, Korea, Republic of

Martensitic steels are generally manufactured using the water cooling process, and the water cooling method has three major disadvantages. First, the martensitic steels, which are fabricated, show a poor shape and flatness because the cooling rate is very fast and cannot be controlled. Second, it is very difficult to make Zn coated martensitic steel sheets using a continuous galvanizing process, they are generally manufactured using an electrogalvanizing process(EG). Finally, it is well known that it is vulnerable to hydrogen delay fracture due to its high strength. In this study, martensitic steels were developed by gas cooling to overcome these shortcomings, and their characteristics would be introduced. In the case of gas cooling, unlike water cooling, the cooling rate can be adjusted to the desired level, and this allows it to have a martensite structure without significantly distorting the shape of the steel sheet. In addition, alloying elements such as Mn, Cr, and Mo were added to avoid a large amount of bainite deformation at a temperature of about 460°C in the molten zinc bath. And then tempering process was applied to improve the yield strength and toughness of galvannealed steel(GA). Finally, Cu elements were added to ensure resistance to hydrogen-delayed fracture, which also achieved good results in various hydrogen-delayed fracture evaluation methods. Based on the concepts, coated and un-coated martensitic steel sheets with a tensile strength above 1.5 GPa were produced in factory. The mechanical properties, flatness, surface quality and hydrogen embrittlement resistance of these sheets were satisfactory for applying as automotive parts.

172_191

A lightweight yet strong Ti-Al-based superelastic alloy operating across a wide temperature range

Sheng Xu[1], Yuxin Song[1], Shunsuke Sato[1], Inho Lee[1], Xiao Xu[1], Toshihiro Omori[1], Makoto Nagasako[1], Takuro Kawasaki[2], Ryoji Kiyanagi[2], Stefanus Harjo[2], Wu Gong[2], Tomáš Grabec[3], Pavla Stoklasová[3], Ryosuke Kainuma[1]
[1]Tohoku University, Sendai, Japan. [2]J-PARC Center, Tokai, Japan. [3]Institute of Thermomechanics of the CAS, Prague, Czech Republic

Shape memory alloys exhibit superelasticity with large recoverable deformation due to the stress-induced reversible martensitic transformation. This property makes them promising in various application fields such as medical, aerospace, and civil engineering. Notably, NASA has recently conceptualized a superelastic tire made of shape memory alloys for rovers to traverse extreme environments like lunar surfaces. However, most shape memory alloys, including the benchmark Ni-Ti alloy, have limitations in operational temperature range and lightweight characteristics, both critical for advanced space exploration applications. For instance, Ni-Ti superelastic alloys typically operate from 0 °C to 80 °C, constrained by Clausius-Clapeyron relation-based thermodynamic principles and susceptibility to plastic deformation. Certain lightweight Mg-Sc-based shape memory alloys possess an even narrower operational temperature window due to their tendency toward plastic deformation. Guided by the well-established Ti-Al binary phase diagram, we have developed a new Ti-Al-Cr shape memory alloy with robust properties. The alloy, predominantly composed of Ti and Al with a chemical composition of Ti-20Al-4.75Cr (at%), exhibits a low density (4.36 g/cm³) and high strength exceeding 800 MPa at room temperature. Additionally, the alloy demonstrates excellent superelasticity, achieving a recoverable strain of over 7% at room temperature, enabled by a stress-induced B2⇔B19 martensitic transformation—a phase transformation unique among Ti-based alloys. Remarkably, this superelasticity persists across an extensive temperature range, from −269 °C to 127 °C, due to an unconventional temperature dependence of transformation stresses. Below a certain threshold during cooling, the critical transformation stress inversely correlates with temperature, contradicting traditional Clausius-Clapeyron relation-based principles. This unexpected behavior may be attributed to a temperature-dependent anomalous lattice instability in the parent phase, where the shear modulus *C*' stiffens during cooling, making martensite nucleation more difficult at lower temperatures. The exceptional properties of this alloy suggest its potential for applications requiring flexible strain accommodation, including everyday appliances, as well as components designed for extreme environmental conditions such as deep-space exploration and liquefied gas storage.[1]

[1] Y. Song, S. Xu et al. *Nature* **638**, 965-971 (2025).

173_269

Tunable High Contrast Changes in Transport Properties of Metamagnetic Phase Change Materials

Serdar Torun[1], Daniel Salas[2], Doguhan Sariturk[1], Elena Cimpoiasu[3], Joseph H Ross[4], Adam A. Wilson[5], Raymundo Arroyave[1], Ibrahim Karaman[1]
[1]Department of Materials Science and Engineering, Texas A&M University, College Station, TX, USA. [2]Department of Physics, The University of the Balearic Islands, Palma, Spain. [3]Department of Physics, United States Naval Academy, Annapolis, MD, USA. [4]Department of Physics and Astronomy, Texas A&M University, College Station, TX, USA. [5]U.S. Army Research Laboratory, Adelphi, MD, USA

Ni-Co-Mn-In magnetic shape memory alloys (MSMAs) demonstrate a magneto-structural transformation (MST) connecting a ferromagnetic cubic austenite to a weak magnetic tetragonal or modulated martensite. This uncommon phase change is accompanied by a high magnetization change, leading to a large associated magnetocaloric effect. Additionally, the phase stability of these alloys is sensitive to the application of magnetic fields, and their key properties present a complex dependence on thermal processing conditions, which altogether enables different strategies to adapt the performance of these materials to the applications' requirements. In this work, we investigate the transport properties of Ni-Co-Mn-In MSMAs and demonstrate that their MST is associated with a high-contrast change — up to a threefold jump — in thermal and electrical conductivities. We also show how variations in chemical composition and microstructure influence this contrast. Moreover, by comparing these alloys with Fe-Mn-Ga alloys, which undergo MST with a reverse magnetization change from paramagnetic austenite to ferromagnetic martensite, we will discuss how modifications in the density of states (electron concentration) near the Fermi level and concurrent changes in magnetic ordering (spin-dependent transport) ultimately drive the observed high-contrast changes in electrical and thermal conductivities. These findings reveal the complex interplay between magnetism, electronic structure, and microstructure in controlling transport properties in MSMAs, potentially paving the way for innovative applications such as magnetically controlled thermal diodes.

174_245

Effect of Composition on the Degree of B2 Ordering in Ti-Al-Cu Shape Memory Alloys

Hirobumi Tobe, Riki Takahashi, Shinji Saito, Masayuki Mizumoto
Iwate University, Morioka, Iwate, Japan

The martensitic transformation temperature of β-type Ti-based shape memory alloys such as Ti-Nb and Ti-Ta can be widely adjusted by varying the concentration of β-stabilizing elements. Additionally, their disordered crystal structure provides excellent workability, allowing for cold rolling with a reduction ratio of over 90%. However, they have a low critical stress for slip deformation, and dislocations are easily introduced during the martensitic transformation, leading to degradation of shape memory and superelastic properties. Moreover, Nb and Ta are rare metals and thus expensive, leading to high material costs. On the other hand, these alloys have been expected to be used as Ni-free superelastic alloys for medical applications or as high-temperature shape memory alloys with transformation temperatures above 100°C. As a result, extensive research has been conducted to improve their shape memory and superelastic properties to date. In this study, we aimed to enhance resistance to slip deformation by promoting the ordering of the disordered bcc parent phase through the addition of Al. Additionally, Cu was selected as a β-stabilizing element due to the recent attention given to the antibacterial properties of Cu-containing Ti-based alloys. Based on these considerations, we investigated the effects of Al and Cu concentrations on the B2 ordering in Ti-Al-Cu alloys. Furthermore, for the first time in this alloy system, we confirmed both the shape memory effect and superelasticity to be present.

175_290

Design and characterization of a new quaternary Cu-Al-Ni-Ga shape memory alloy

Mikel Pérez-Cerrato, Lucia Del-Río, José F. Gómez-Cortés, Isabel Ruiz-Larrea, Jose M. San Juan, Maria L. Nó
Universidad del Pais Vasco (UPV/EHU), Bilbao, Spain

Shape memory alloys (SMA) exhibit the exclusive properties of superelasticity and shape memory thanks to a thermoelastic martensitic transformation. The design of the alloys allows to adapt the SMA properties to the required application, through the control of the composition and the microstructure. In particular, the Cu-Al-Based SMA exhibit a remarkable versatility and can be designed for high-temperature (HTSMA) applications [1] or for very low-temperature in cryogenic applications [2].

In the present work, the design and characterization of a new family of Cu-Al-Ni-Ga SMA is approached. The alloys were designed to cover two areas of the phase diagram, in the Al-rich and Al-poor regions, adding different Ga amounts in each case. After producing the alloys by double-step induction melting and centrifugal casting, oriented [001] single crystals were grown by Bridgman method.

The microstructure was studied through scanning electron microscopy with microanalysis (EDX) and electron back-scatter diffraction (EBSD) to determine the homogeneity of the alloys, and the crystalline orientation of the final single crystals, including in each case the determination of the formed martensite. The martensitic transformation temperatures were measured by differential scanning calorimetry (DSC) and the influence of Ga on the transformation temperatures was stablished. To optimize the thermal treatments, the atomic order was studied by high-resolution transmission electron microscopy (HRTEM). Finally, the superelastic behaviour was studied at different temperatures and the Clausius-Clapeyron slope was determined, and it is worthy of remark the exceptionally large superelastic window exhibited by these new Cu-Al-Ni-Ga SMA.

The designed alloys exhibit a superelastic behaviour above 8% fully recoverable strain during hundred of cycles and similar shape memory behaviour is observed.

It can be concluded that this new family of Cu-Al-Ni-Ga SMA offers outstanding performances in terms of functional properties, and it is expected that they would fulfil the requirements for many practical applications.

[1] I. López-Ferreño et al., High-temperature shape memory alloys based on the Cu-Al-Ni system…, J. Materials Research & Technology 9 (2020) 9972-9984.

[2] J. San Juan, M.L. Nó, P. Lorenzo, New single crystalline shape memory alloy for cryogenic applications…, Patent nº P153344ES. Priority date: October 19, 2021.

176_225

An Implantable Device Based on Shape Memory Alloys

Israel Alexandron, Tony Andrey Jubran, Gal deBotton
Ben-Gurion University of the Negev, Beer-Sheva, Israel

Shape Memory Alloys (SMAs) possess the unique ability to return to their original shape after apparent plastic deformation when heated. This property enables their use as temperature-responsive actuators. Among SMAs, Nitinol stands out due to its high force-to-weight ratio, functionality in wet environments, and biocompatibility, making it ideal for biomedical applications.

One application that has received little research attention is an implantable device based on Nitinol. Potential uses include an implantable syringe capable of delivering precise doses of chemotherapy directly into affected tissues or administering pain relief medication to the spinal cord. The advantage of this targeted injection approach is the reduction of systemic drug distribution, thereby minimizing side effects.

To explore the feasibility of such a device, we developed and constructed a proof-of-concept prototype demonstrating the ability of a Nitinol actuator to drive a micro-syringe mechanism. The prototype consists of a Nitinol coil and a steel coil, both connected in parallel to a syringe plunger. When an electric current heats the Nitinol spring, it contracts, pulling the plunger and drawing liquid from a subcutaneous drug reservoir into the syringe chamber through a one-way inlet valve. As the spring cools to body temperature, it returns to its original state, pushing the liquid through a one-way outlet valve and into the body. These valves ensure controlled, unidirectional flow, preventing backflow and maintaining precise drug delivery.

The dimensions of the prototype are 12 × 30 mm. Further miniaturization is feasible, with the expected final device dimensions being approximately 25 × 45 mm.

While our prototype successfully demonstrates the Nitinol-driven actuation mechanism and integrates one-way valves for fluid control, the drug reservoir and rechargeable battery were not included in this initial proof-of-concept.

Once fully realized, such a system could operate long-term within the patient’s body, requiring only periodic check-ups for battery recharging and drug reservoir refilling. This would reduce the strain on healthcare facilities while improving patient quality of life by eliminating the need for repeated intravenous drug administration and its associated side effects. Additionally, the envisioned device is expected to be MRI-compatible, allowing patients to undergo imaging procedures without removing the implant.

177_163

Recovery stress and tensile behavior under recovery stress of cold-drawn superelastic SMA wires

Eunsoo Choi, Seong-Jun Park, Jasesung Byung, Min-Kyung Jang, Kiyeon Kim
Hongik University, Seoul, Korea, Republic of

This study investigates inducing of recovery stress of cold-drawn superelastic shape memory alloy (SMA) wires. It is well known that the cold-drawn martenstic SMA wires show recovery stress, which can be used for inducing prestressing in cementitious materials. The cold drawing work introduces tensile strain in the martensitic SMA wire as well as reduces the cross-sectional area. The heating transforms phase state of the cold-drawn martensitic SMA wire resulting in inducing recovery stress. This study tries this cold drawing work on a superelastic SMA wire and then obtains the recovery stress by heating. Therefore, after the cold drawing work, it is conjectured that the superelastic SMA wire is transformed to the similar state of the cold-drawn martensitic SMA wire. The cold-drawn superelastic SMA wire shows a similar recovery stress to that of the cold-drawn martenstici SMA wire. However, it shows flag-shaped tensile behavior under the recovery stress; this indicates that the cold-drawn superelastic SMA wire provides more energy dissipation and displacement recovery capacities than the corresponding one of the martensitic SMA wire. This is very meaningful to apply it on civil structures. Therefore, more studies are required for applying the cold-drawn superelastic SMA wires on civil members and structures.

178_318

Recycling of NiTi shape memory alloys-effects of melting methods and processing conditions

Sakia Noorzayee, Jan Frenzel, Gunther Eggeler
Ruhr University Bochum, Bochum, Germany

Shifting from a linear to a circular economy is essential to reduce resource consumption and greenhouse gas emissions. While recycling strategies are well established for most common materials like steel and aluminum, NiTi shape memory alloys (SMAs) provide special challenges. The production of Nickel and Titanium is highly energy-intensive (Ni: 0.25 EJ/yr; Ti: 0.07 EJ/yr) and associated with significant CO_2 emissions (Ni: 26 MT/yr; Ti: 6.7 MT/yr). This encourages increased efforts to investigate recycling approaches in NiTi ingot metallurgy. However, NiTi SMAs are particularly sensitive to impurities that alter their martensitic transformation behavior and functional properties, even at levels that are almost irrelevant for most other engineering materials. The present study investigates the potential for recycling NiTi SMAs, combining theoretical considerations and recycling experiments. We examine how factors such as melting method, alloy composition, surface state, and other processing conditions affect impurity incorporation and phase transformation behavior. To evaluate recycling feasibility, we conduct experiments using vacuum induction melting (VIM) and arc melting (AR) of NiTi samples, assessing impurity pick-up after different surface preparation approaches. Microstructural and compositional analysis is performed using scanning electron microscopy (SEM), differential scanning calorimetry (DSC), and atom probe tomography (APT). Our findings contribute to a better understanding of processes related to recycling of SMAs including phase chemistry and phase transformation behavior. We provide information how NiTi SMAs can be recycled with no significant changes in chemistry, transformation behavior and functional behavior.

P01_282

Changes of martensitic transformation temperature by adding Mn into 68Cu-16Al-16Zn alloys

Ayaka Ibato, Takuro Dazai, Kenjiro Fujimoto
Tokyo University of Science, Noda, Chiba, Japan

The 68Cu-16Al-16Zn (CAZ) alloy has good workability, and the martensitic transformation can occur with less critical stress. It is also known to exhibit elastocaloric effects. Therefore, CAZ alloy has attracted attention as a promising material for solid-state refrigerants. However, there are several issues to be solved for the practical use of this alloy. One of which is the control of the transformation temperature (TT), which depends on the composition. Previous studies on other ternary Cu-based alloys have shown that the addition of a fourth element changes the TT[1,2]. In this study, we investigated the effect on the TT and latent heat by adding the fourth element, Mn, into CAZ.

Ingots of Cu-Al-Mn alloys were first produced using a vacuum melting furnace, and then Zn was melted together with the ingots. Finally, two types of Cu-Al-Zn-Mn alloys were prepared. Ones are alloys with 1~3 at% of Mn substituted for all elements on CAZ. Others are alloys with 1 at% of Mn substituted for each element on CAZ. Composition analysis was measured by ICP-AES. As heat treatments, alloys were held at 1173 K for 1 hour, then quenched in ice water. Some samples were applied the aging which was treated at 423 K for 0.5 hours after quenching, then cooled to room temperature. The TT and latent heat of heat-treated alloys was estimated from DSC curves.

From DSC curves of (100-*x*) CAZ -*x*Mn alloys as shown in Fig.1, martensitic transformations were found, except for *x*=3. As the amount of Mn substitution increased, the TT and latent heat decreased. When each element was substituted, the TT was changed the most by substitution of Cu for Mn. Fig. 2 shows the correlation between A_f (the finish temperature of reverse transformation) and Cu concentration in this study. Copper concentration was observed to affect A_f. On the other hand, the TT after aging treatment did not change for some compositions. It has been reported that aging treatment increases the TT of CAZ alloys by 6 K.[3]. Our result indicates that the increase in TT due to aging treatment was suppressed by Mn additions. Therefore, Mn additions may lead to increase the degree of order on Austenite phase.

References:
1) İ. Özkul *et al*., *J. Mater. Res* **37** (2022) 2271.
2) P. Kumar *et al*., Matéria **20** (2015) 284.
3)Y. Kawarda *et al*., *J. Phys*. *Energy* **5** (2023) 024012.

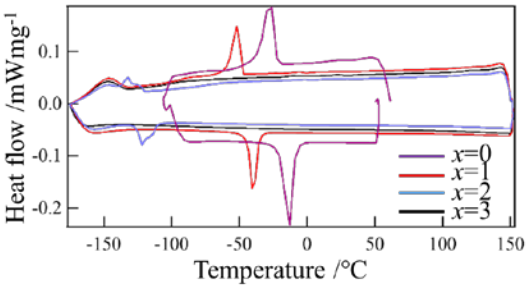

Fig. 1. DSC curves of (100-*x*)(68Cu-16Al-16Zn)-*x*Mn (*x*=1~3)

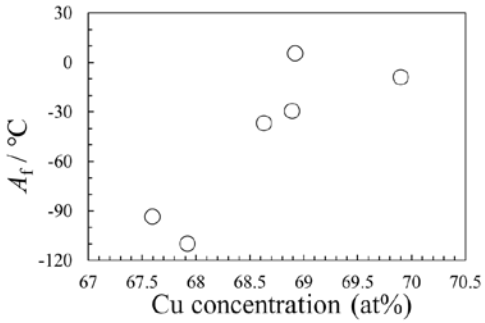

Fig. 2. Correlation between A_f and Cu concentration

P02_266

The relationship between degree of order and martensitic transformation behavior in 68Cu–16Al–16Zn

Megumi Takayama[1], Takuro Dazai[1], Akihisa Aimi[2], Ichiro Takeuchi[3], Kenjiro Fujimoto[1]
[1]Tokyo University of Science, Noda, Chiba, Japan. [2]National Defense Academy of Japan, Yokosuka, Kanagawa, Japan. [3]University of Maryland, College Park, Maryland, USA

Cu–Al–Zn alloys, particularly the 68Cu–16Al–16Zn, are promising candidates for solid-state refrigerants due to their excellent elastocaloric effect[1)]. However, several challenges remain for their practical application, one of which is the difficulty in controlling the martensitic transformation temperature. This temperature is influenced by factors such as composition, the presence of lattice defects, and the degree of order in the parent phase. In Cu-based alloys, the parent phase adopts a disordered A2 structure at high temperatures and transitions to an ordered B2 or $L2_1$ structure as ordering occurs. In this study, we focused on the degree of order and investigated its relationship with martensitic transformation behavior by varying the heat treatment temperature.

68Cu–16Al–16Zn alloy was prepared in an induction melting furnace with controlled Ar atmosphere. The prepared alloys were heated at 873–1173 K for 1 h and then quenched in ice water. The transformation temperatures were measured using DSC, and the degrees of order in the samples were evaluated by XRD measurements.

Austenite finish temperatures of the samples heated at 873–1173 K ranged from 228.4 to 246.3 K. The transformation temperatures increased with increasing heat treatment temperature. Figure 1 shows the XRD patterns for the samples heated at 873 and 1173 K, respectively. Two ordered structures, $L2_1$ and B2, exist in ordered Cu–Al–Zn alloys. The degrees of order S for these structures were obtained from the diffraction intensity ratios R of the corresponding superlattice diffractions: 111 diffraction relative to the fundamental lattice diffraction of 444 peak for $L2_1$ ordering. In Table 1, R_{1173} and R_{873} represent the intensity ratios, and S_{1173} and S_{873} indicate the degrees of order, for samples heated at 1173 and 873 K, respectively. Both S_{873}/S_{1173} for $L2_1$ and B2 ordering are greater than 1. This indicates that the sample heated at 873 K is more ordered compared to the sample heated at 1173 K. In Cu–15.935Zn–16.13Al, the ordering temperature from A2 to B2 is 1084.5 K, and from B2 to $L2_1$ is 907.9 K[2)]. Given these ordering temperatures, it is likely that the sample heated at 873 K underwent sufficient ordering into the $L2_1$ structure. These results suggest that the transformation temperatures vary with heat treatment temperature due to changes in the degree of order.

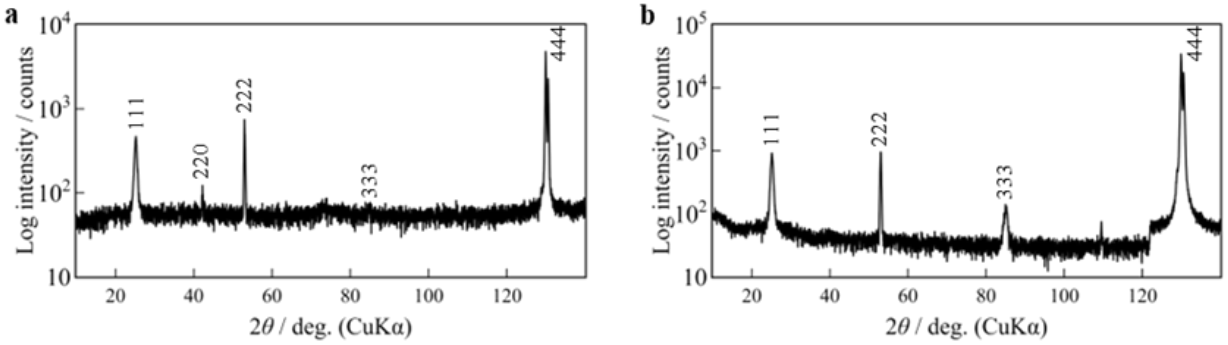

Fig. 1 XRD patterns for the samples heated at 873(a) and 1173 K(b)

Table 1 The intensity ratios and the degrees of order for samples heated at 1173 and 873 K

	R_{1173}	R_{873}	R_{873}/R_{1173}	S_{873}/S_{1173}
$L2_1$(hkl=111)	2.4×10^{-2}	1.4×10^{-1}	5.7×10^{-2}	2.4
B2(hkl=222)	1.1×10^{-2}	8.6×10^{-2}	7.5×10^{-2}	2.7

R_{1173}, R_{873}: Diffraction intensity ratios for samples heated at 1173 and 873 K
S_{1173}, S_{873}: Degrees of order for samples heated at 1173 and 873 K

Ref. 1) E. Bonnot *et al.*, *Phys. Rev. Lett.* **100** (2008) 125901. 2) F. Lanzini *et al.*, *Phys. Rev. B* **77** (2008) 134207.

P03_199

In-situ crystallographic analysis of habit plane in stress-induced martensitic transformation of Ti-Ni alloy single crystals

Kosei Ono, Chihiro Mori, Naoki Nohira, Masaki Tahara, Hideki Hosoda
Institute of Integrated Research, Institute of Science Tokyo, 4259 Nagatutacho, Midori-ku, Yokohama, Japan

In many shape memory alloys, the crystallographic features of thermally induced martensite are generally in good agreement with the phenomenological theory of martensite crystallography (PTMC). However, in Ti-Ni alloys, the discrepancy has been reported between PTMC predictions and the experimentally observed habit planes of stress-induced martensite. One possible explanation for this discrepancy is that the values of lattice constants used in the PTMC calculations may differ from their actual values under applied stress. In this study, we performed in-situ X-ray diffraction (XRD) measurements under stress using Ti-Ni alloy single crystals. And compared the crystallographic features calculated from the obtained lattice constants with those observed in-situ under stress.

Ti-51 mol% Ni single crystal with the B2 parent phase were obtained by the optical floating zone melting method, followed by homogenization at 1273 K for 604.8 ks. The crystal orientation was identified by the back-reflection Laue method. The specimens were cut with the $[1\ 3\ \text{-}3]_{B2}$ direction as the tensile direction. Solution treatment was performed at 1223 K for 3.6 ks in an Ar atmosphere. The sample surfaces were polished to mirror surfaces by mechanical polishing and electropolishing, and the sample sides were polished by focused ion beam machining. In-situ optical microscopy, in-situ scanning electron microscopy, and in-situ XRD measurements were performed under tensile stress.

During tensile deformation was applied to the sample along $[1\ 3\ \text{-}3]_{B2}$, two types of habit plane variants formed via stress-induced martensitic transformation, accompanied by internal twins as lattice invariant deformation. The habit planes, identified by the two-surface trace method, were found to be $(0.88\ 0.24\ \text{-}0.41)_{B2}$, $(0.42\ 0.23\ \text{-}0.88)_{B2}$ respectively. A comparison between the habit planes calculated by PTMC using lattice constants of thermal-induced martensite, and those determined by in-situ observation revealed deviations of 1.6 and 1.4 degrees, respectively. The lattice constants of stress-induced martensite were determined by in-situ XRD measurements, and the PTMC calculations were performed again using these lattice constants, resulting in deviations of 0.5 and 1.2 degrees from the observed habit planes, respectively. Incorporating the in-situ measured lattice constants into PTMC yields significantly better agreement with the experimental results.

P04_321

On interaction between deformation twins and LPSO phases in Mg alloys

Andrej Ostapovec
Institute of Physics of Materials CAS, Brno, Czech Republic

Long-periodic stacking ordered (LPSO) phases play important role in development of Mg alloys. LPSO phases are observed in Mg-TM (transition element)-RE(rare earth element) alloys and, in general, are considered as the element, which suppresses deformation twinning. The LPSO phases have structures similar to those of typical martensite phases in shape-memory alloys. However, formation of LPSO structures is connected to diffusive processes due to segregation of solute elements on stacking faults inside LPSO phase. On the other hand, it was demonstrated previously that stacking faults in hcp structure can grow or dissapear without diffusion in the cases when this growth is accompanied by interaction with twin boundaries. In the present work, interaction of growing twins with the stacking faults inside LPSO structure will be studied in order to describe mechanisms of LPSO structure destruction during this process.

P05_167

Lattice Distortion-Atomic Shuffle Coupling of the R phase in NiTi

Yuxuan Chen[1,2], Xiaobin Shi[3], Junsong Zhang[2], Shan Huang[1], Xinyu zhang[2], Riping Liu[2], Yinong Liu[4]
[1]Hebei Vocational University of Technology and Engineering, Xingtai, Hebei, China. [2]Yanshan University, Qinghuangdao, Hebei, China. [3]Anhui University of Technology, Maanshan, Anhui, China. [4]The University of Western Australia, Perth, WA, Australia

The R phase in NiTi is known to exhibit a lattice distortion relative to the B2 parent phase and an internal atomic shuffle. The lattice distortion, which can be described by a $[111]_{B2}$ stretch, changes the unit cell shape with a lattice strain output thus giving rise to the shape memory and pseudoelastic effects of the B2-R transformation. The atomic shuffle, which occurs on every third of the $(001)_R$ planes, does not change the unit cell shape, thus generating no lattice strain output. This implies that the lattice distortion may be directly affected by mechanical conditions either applied externally or occurring internally within the alloy matrix, such as nanograin size, whereas atomic shuffle may not. This study investigated the correlation between the two in a nanocrystalline $Ni_{48}Ti_{50}Fe_2$ alloy, where grain size confinement acts as a mechanical constraint to the lattice distortion, by means of *in situ* X-ray diffraction experiment and density functional theory (DFT) analysis. It was found that the atomic shuffle precedes lattice distortion, deviating the correlation from the minimum energy pathway predicted by DFT, and the deviation is more pronounced in matrices of smaller grain sizes (<15 nm). These findings provide insight to guide the development of novel martensitic alloys of extraordinary properties, such as strain glass alloys, where lattice distortions are largely suppressed while atomic shuffles remain active, enabling tailored functional properties.

P06_188

R-Phase transformation in Ti-Ni-Co alloys

Jaeil Kim, Heeun Choi
Dong-A University, Busan, Busan, Korea, Republic of

The R-phase transformation of Ti-Ni shape memory alloy exhibits small transformation hysteresis and thermo-mechanical stability compared to B2↔B19' transformation, Therefore, this is known to be candidate material for application of actuators. It is well known that the addition of ternary element, such as Fe, Co, Al, is effective method to introduce R phase transformation. In this study, R phase transformation in Ti-Ni-Co alloys are investigated systematically. The martensitic transformation and R phase transformation temperature decreased by 23.8K and 13.9K with 1at% increase of Co content, respectively. The R phase transformation temperature is hardly affected by annealing temperature in the equi-atomic Ti-Ni-Co alloy. This further means that dislocations introduced by cold working did not affect R-phase transformation temperature in contrast to the martensitic transformation temperature. In the Ni-rich Ti-Ni-Co alloy, R phase transformation temperature is affected by Ni content in the matrix sensitively, and is hardly affected by the distribution of precipitation(such as the size and density) by aging. Also R phase transformation temperature is little affected by the number of thermal cycle. This means that R-phase transformation temperature does not change even if dislocation is introduced by thermal cycle.

P07_286

Electrical Resistivity Changes during Successive Transformations in Ti-Ni Alloy under Stress Loading

Hidemasa Torihara[1,2], Yohei Soejima[1], Hiroki Cho[2], Sumio Kise[1], Minoru Nishida[1,3]
[1]Special Metals Division, Furukawa Techno Material Co., Ltd., Hiratsuka, Kanagawa, Japan. [2]Department of Mechanical Systems Engineering, Faculty of Environmental Engineering, The University of Kitakyushu, Kitakyushu, Fukuoka, Japan. [3]Department of Advanced Materials Science and Engineering, Faculty of Engineering Sciences, Kyushu University, Kasuga, Fukuoka, Japan

In Ti-Ni shape memory alloys annealed below the recrystallization temperature after cold working, successive transformations from the parent B2 phase to the trigonal R phase and subsequently to the monoclinic B19' phase during cooling have been confirmed via electrical resistivity measurements. However, since most studies have measured resistivity changes during transformation under stress-free conditions, the behavior of resistivity during successive transformations under tensile stress remains unclear.

This study investigates the effect of tensile stress on resistivity changes during the successive and the reverse transformations during cooling and heating, respectively. An electrical resistivity measurement system equipped with stress-loading and temperature-control mechanisms was used. The experiments were conducted on a Ti-50Ni at.% alloy wire, 0.075 mm in diameter, cold-drawn and heat-treated at 460 ℃.

Under stress-free conditions, the forward transformation process results in an increase in resistivity from B2 to R, followed by a decrease from R to B19'. During the reverse transformation process, resistivity increases from B19' to R and decreases from R to B2. These behaviors are consistent with previous studies. Under a tensile stress of 60 MPa, the resistivity changes during the forward transformation process are similar to those under stress-free conditions. However, during the reverse transformation, in addition to an increased transformation temperature, the rate of resistivity increase for B19' to R decreases, whereas the rate of resistivity decrease for R to B2 increases. At stresses exceeding even 100 MPa, resistivity changes during the forward transformation process still follow the B2 to R to B19' sequence. However, during the reverse transformation, no increase in resistivity corresponding to B19' to R is observed. Instead, resistivity decreases sharply due to the reverse transformation directly from B19' to the parent B2 phase. In other words, tensile stress suppresses the reverse transformation from B19' to R.

We will also discuss the mechanisms underlying changes in electrical resistivity in response to temperature variations under various stress conditions, as well as their application in thermal sensors.

P08_403

Effect of molten zone geometry on compositional homogeneity in NiMnGa crystals obtained by optical floating zone method

Valentina Moskvina, Jaroslav Čapek, Denys Musiienko, Oleg Heczko
FZU-Institute of Physics of the Czech Academy of Sciences, Prague, Czech Republic

The $Ni_{50}Mn_{25}Ga_{25}$ Heusler alloy exhibits a magnetic shape memory effect with reversible strains up to 10% in single crystals, enabled by the motion of martensitic twin boundaries [1]. The essential condition for the effect, the martensitic transformation and martensite structures are highly sensitive to small compositional deviations, particularly within Ni 48–52 at.% and Mn 23–27 at.% ranges, complicating functional property prediction. Therefore, precise compositional control during crystal growth is critical. The optical floating zone (OFZ) method is widely used to grow high-quality single crystals due to its crucible-free nature, reduced contamination, and capacity for directional solidification under controlled thermal gradients.

This study investigates the effect of growth parameters, particularly the molten zone (MZ) geometry on elemental distribution in OFZ-grown crystal from $Ni_{50}Mn_{25}Ga_{25}$ initial ingot. The figure shows the calculated molten zone height along the crystal length and experimental X-ray fluorescence (XRF) concentration profiles together with the calculated one. At the initial stage of ingot recrystallization, a sharp depletion of Mn and an increase in Ni and Ga concentrations occur. A stable MZ resulted in more gradual, diffusion-driven compositional changes slowly approaching the composition of the initial ingot. The drop of MZ height at the end of the growth process caused Mn accumulation and Ni and Ga depletion due to enhanced segregation. These results demonstrate that local temperature gradients and the molten zone geometry directly influence solute redistribution during solidification. The calculated compositional profiles match well with experimental ones and demonstrate the potential of modeling for optimizing single crystal growth conditions.

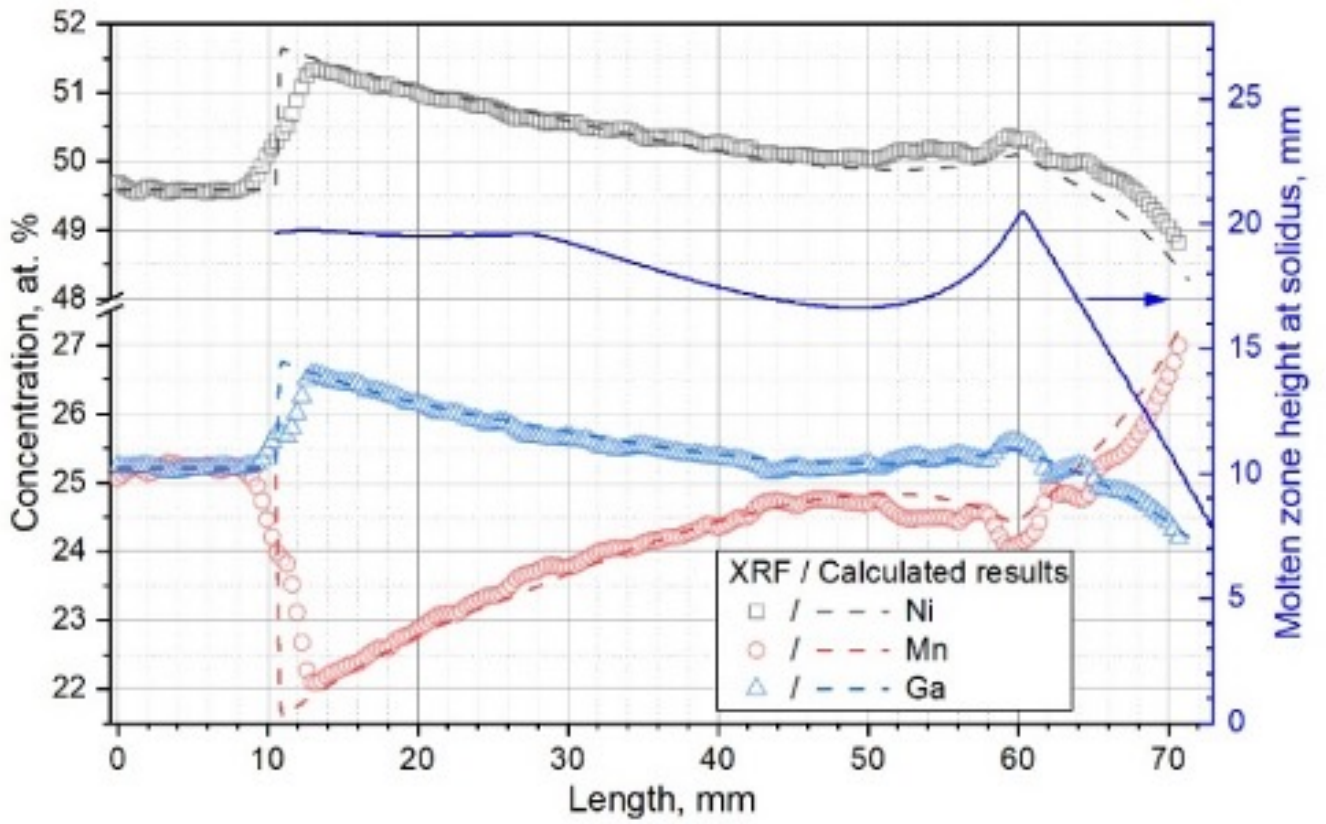

Fig. 1. Comparison of XRF-measured (symbols) and calculated (dashed lines) concentrations along the grown NiMnGa crystal combined with calculated MZ height profile (blue solid line).

Reference

[1] O. Heczko, Magnetic shape memory effect and highly mobile twin boundaries, Materials Science and Technology, 30(13a), 1559–1572 (2014).

Acknowledgments

This work was supported by OP JAK project No.CZ.02.01.01/00/22_008/0004591 and Czech Science Foundation Grant No. 24-11361S.

P09_185

Characterization of $Ti_{50}Ni_{50-X}Mo_X$ (X=2; 6) alloy produced by high-energy ball milling

Tomasz Goryczka, Grzegorz Dercz
Institute of Materials Engineering, University of Silesia in Katowice, Katowice, Poland

The $Ti_{50}Ni_{50-X}Mo_X$ (where X=2; 6) alloys belong to the family, which reveals shape memory effects. They differ in characteristics from a binary NiTi one in a temperature range and the course of the reversible martensitic transformation [1]. Both alloys were produced as powders using high-energy ball milling (HEBM). The milling time was applied as a variable parameter to assess the progress of alloying. The evolution of structure and phase composition was studied using X-ray diffraction, scanning, and transmission electron microscopy. After 20 hours of milling, the grains were fragmented, partially mixed, and joined into agglomerates (Fig 1a). The first alloying effects appeared after 40 hours. Solid solutions based on alloying elements began to form. Extending the milling time to 100 hours improved the distribution of the alloying elements (Fig. 1b) and resulted in the formation of an amorphous nanocrystalline mixture.

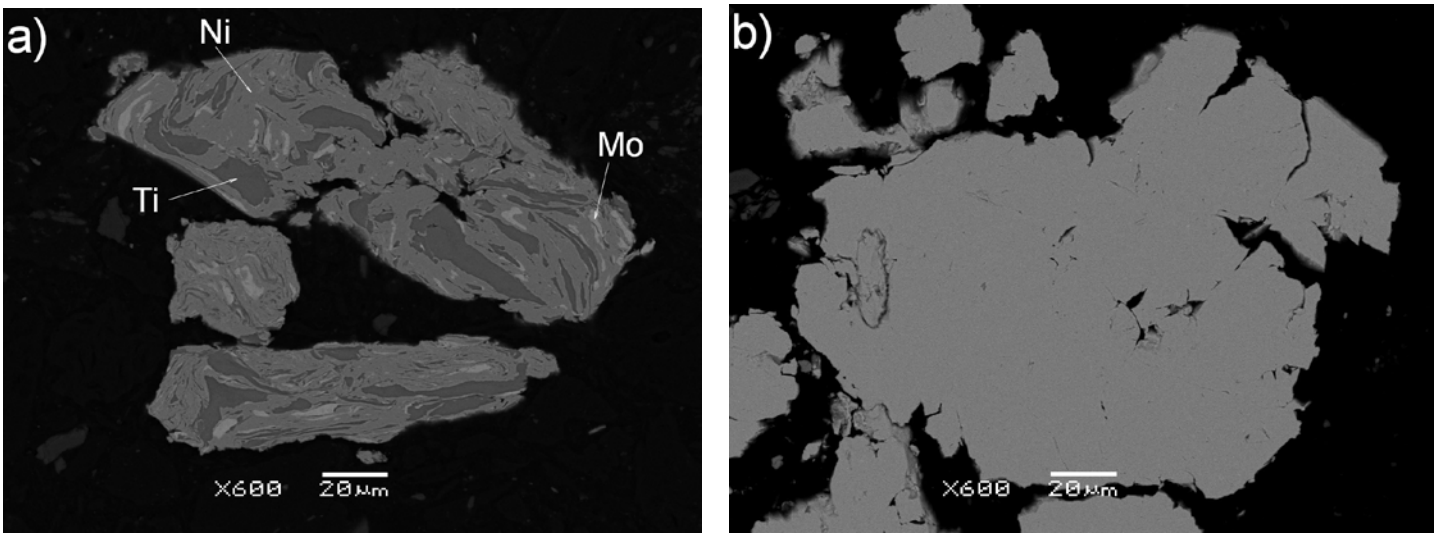

***Fig.1**.SEM_BSE images observed for $Ti_{50}Ni_{44}Mo_6$ alloy after milling for: 20 (a) and 100 hours (b).*

From the morphological point of view, the produced powders consisted of two fractions, fine and coarse, with an average grain size of 32 µm and 1800 µm, respectively. The crystallization process was studied based on measured thermograms using a differential scanning calorimeter (DSC). Crystallization appeared as a multi-stage in the range of temperatures 320 to 450ºC ($Ti_{50}Ni_{48}Mo_2$) and 350 to 506ºC ($Ti_{50}Ni_{44}Mo_6$). It required an enthalpy of about 147 J/g and 60 J/g. Both alloys, after crystallization, showed the presence of a reversible two-stage martensitic transformation with the participation of the R phase.

References

[1] J.V. Humbeeck, Shape Memory Materials: State of the art and requirements for future applications, J. Phys IV France 07, C5-3-12, 1997.

P10_264

Laser focal length influence in H13 Tool Steel Deposition Through L-DED

Rafael Ramos[1], Naiara Le Sénéchal[1], Paulo Dyer[2], José Eduardo Carvalho[3], Rodrigo Cardoso[3], Getulio De Vasconcelos[2], Andersan Paula[1]
[1]Instituto Militar de Engenharia (IME), Rio de Janeiro, RJ, Brazil. [2]Instituto de Estudos Avançados (IEAv), São José dos Campos, SP, Brazil. [3]Centro Brasileiro de Pesquisas Físicas (CBPF), Rio de Janeiro, RJ, Brazil

H13 tool steel is commonly applied in dies and molds due to good properties as hardness, toughness and thermal fatigue resistance. Its use in additive manufacturing (AM) is promising because those technologies would make possible tool fabrication with complex cooling systems and geometries. Laser-Direct Energy Deposition (L-DED) is prone to be used in tooling to build new parts and to repair and refurbish them, with process parameters defining microstructural and macroscopical characteristics of a built part. Thus, this study aimed to evaluate the laser focus height influence on the deposition of the twelve layers on substrate. H13 steel powder water atomized in a Brazilian company was deposited through a non-branded experimental equipment keeping all parameters constant, except for the laser focus height. Cross-section observation was performed, first macrographically and then microscopically by optical and scanning electron microscopies. Reduced focus height condition presented bigger specimen, indicating a better use of the laser energy. On the other hand, greater laser focus height led to a more compact specimen, like results for laser cladding. In both cases, densification good level was obtained.Also, different thermal cycles were experienced for each part position, the so-called intrinsic heat treatment (IHT), causing inhomogeneous microstructure. In conclusion, laser focus closer to the built part is useful to parts growing, whereas more distant one favored flattened layer. In all cases, for microstructural homogenization, post heat treatments are indicated.

P11_183

Influence of two-step aging treatment on precipitation behavior of as-built 18Ni-maraging steel fabricated by laser powder bed fusion

Sung Hwan Hong[1], Hae Jin Park[1], Gyeol Chan Kang[1], Jaiyoung Cho[2], Ki Buem Kim[1]
[1]Sejong University, Seoul, Korea, Republic of. [2]Hankook Tire & Technology Co., Ltd., DaeJeon, Korea, Republic of

Additive manufacturing (AM) is an advanced technology used for the manufacture of products that have intricate shapes and complex inner geometries. In commercial metallic material field, various metallic materials have been investigated to use AM processing. The microstructural features such as grain size and precipitates will differ profoundly from those obtained by casting, heat treatment and forming processing, which resulted from the rapid heating and cooling rates during AM. Therefore, the evolution in microstructure of metallic materials fabricated AM with post-treatment can give an opportunity to discover the enhanced mechanical properties of the metallic materials. In this study, the maraging steel powder with mean particle radius of 36 μm have been used in AM experiment. The specimens with bulk cuboidal shape were fabricated with the optimized laser power and scanning rate conditions. The as-built specimens were composed of α' martensite phase in applied AM condition. The density of as-built specimens reached ~ 8.03 g/cm^3, which is almost similar to the full density of maraging steel. The as-built specimens were aged at two different temperatures to form nanoscale precipitates in the α' martensite matrix. From the systematic microstructural analysis, it was found that the formation of nanoscale precipitates and its volume fraction depend on the aging temperature and time. After single aging treatment at 733 K exhibited Ni_3Ti type nano-precipitates. On the other hand, the specimens aged at two different temperatures contained two types of nano-precipitates. The microstructural evolution achieved by two-step aging treatment revealed an different precipitation behavior such as size and distribution of nanoscale precipitate in comparison with the specimen aged by single aging treatment. Moreover, the aging time for peak hardness was reduced by two-step aging treatment. From these results, it is suggested that the optimized microstructure and mechanical properties of 18Ni-maraging steel can be achieved by modulating the aging treatment condition.

P12_394

A Fast-Track Approach to Ti–20Nb–6Ta Alloy via PBF-LB for Biomedical Applications

João Felipe Queiroz Rodrigues, Mariana Sizenando Lyrio, Márcio Sangali, Gabriel Henrique Caetano, Rodolfo da Silva Teixeira, Alessandra Cremasco, Rubens Caram
University of Campinas, Campinas, São Paulo, Brazil

Ti–20Nb–6Ta alloy is a promising material for use in additively manufactured bone implants. The mechanical properties of Ti–20Nb–6Ta specimens produced by PBF-LB are controlled by the phases formed and the crystallographic orientation. Samples of the Ti-20Nb-6Ta (wt.%) alloy were produced by PBF-LB using a stripe strategy with a 400 W laser power, promoting melting pools of about 200-300 µm. The additive manufacturing process employed a stripe scanning strategy with a 400 W laser, generating melt pools of approximately 200–300 µm. This enables the use of a 150 µm layer thickness, resulting in a build rate 4–5 times faster than conventional additive manufacturing parameters. The samples were characterized using X-ray diffraction (XRD) and scanning electron microscopy (SEM). Texture analysis was performed at both macro and micro scales via XRD and electron backscatter diffraction (EBSD), respectively. Phase transformations were investigated using in-situ high-temperature XRD (HTXRD) and differential scanning calorimetry (DSC). Mechanical properties were assessed through Vickers microhardness and uniaxial tensile tests. The Ti–20Nb–6Ta powder exhibited a characteristic α″-martensitic phase, which decomposed into the stable α phase between 400 °C and 450 °C. During the additive manufacturing process, the α″-martensitic phase commonly observed in conventional 30 µm layer thickness samples was decomposed, leading to the formation of the equilibrium α phase. Texture analysis revealed a pronounced crystallographic alignment along the build direction. Hardness increased from 279 HV to 320 HV. The mechanical tests showed a Young's modulus of 69.9 ± 0.3 GPa, a yield strength of 830 ± 10 MPa, and an ultimate tensile strength of 926 ± 12 MPa. These results demonstrate that the selected processing parameters enable faster fabrication while enhancing mechanical strength and maintaining a low Young's modulus, making the alloy suitable for biomedical applications.

P13_399

Digital Image Correlation-Based Local Strain Evaluation in EBM-Additive Manufactured NiTi Part

Savas Dilibal[1], Asheesh Lanba[2], Tymur Sabirov[2], Gozde Peduk[1]
[1]Istanbul Gedik University, Istanbul, Turkey. [2]University of Southern Maine, Portland, ME, USA

Digital Image Correlation (DIC) is a non-contact, full-field optical technique that has gained prominence for its ability to measure strain and displacement in materials under mechanical loading. By tracking the deformation of a random speckle pattern applied to a specimen’s surface, DIC enables high-resolution, spatially resolved analysis of local deformation behavior throughout mechanical testing. This study explores the use of DIC to evaluate the mechanical performance of Nickel-Titanium (NiTi) shape memory alloy components fabricated via Electron Beam Melting (EBM), an additive manufacturing process capable of producing complex geometries and tailored microstructures. Tensile specimens were extracted from EBM-produced NiTi parts and tested under uniaxial loading to investigate local strain distribution. Preliminary results provide valuable insights into the deformation characteristics and mechanical integrity of the EBM-fabricated NiTi components. The findings highlight the capability of DIC to accurately capture strain localization and evolution, especially in heterogeneous and anisotropic microstructures typical of additively manufactured materials. These outcomes demonstrate the effectiveness of DIC as a powerful diagnostic tool for assessing localized mechanical behavior in advanced manufacturing contexts.

P14_327

Microstructural Aspects Ti6Al4V Alloy Processed by LBPF Investigated by EBSD Technique

Fábio Oliveira[1], Andersan Paula[2], Carlos Elias[2]
[1]National Institute of Technology, Rio de Janeiro, Rio de Janeiro, Brazil. [2]Military Engineering Institute, Rio de Janeiro, Rio de Janeiro, Brazil

In laser powder bed fusion (LPBF) of the Ti6Al4V alloy, the presence of reheated and remelted regions within the heat-affected zone (HAZ) induces complex thermal histories that significantly affect local phase stability and transformation pathways. This study investigates the formation of non-conventional martensitic structures in Ti6Al4V alloy processed by LBPF, beyond the commonly observed α′ phase, as a function of altered stoichiometry within the β-phase, driven by solute redistribution during successive thermal cycles during LPBF process. Modifications in the local composition of titanium, aluminum, and vanadium — stemming from differential diffusion and partitioning effects — were found to influence the stabilization and decomposition routes of metastable β, favoring the development of alternative martensitic products such as α″ or decomposed α′. Electron backscattering diffraction (EBSD) on the scanning electron microscopy (SEM) analyses revealed spatial heterogeneities in the crystallography of the phases detected in a significant fraction of the microstructure that distinguishes them from the body cubic centered phases-bcc (α and α') and compact hexagonal-hcp (retained β), indicating the role of localized solute enrichment or depletion. These findings highlight the intricate relationship between thermal gradients, solute mobility, and martensitic transformations under non-equilibrium solidification conditions typical of LPBF. The results advance the understanding of microstructural evolution in additively manufactured Ti-Al-V alloys and provide insight into controlling phase transformations for tailored mechanical performance in high-demand applications.

P15_338

Acoustic emission from displacive phase transitions: comparison of martensitic and ferroelectric model materials

Christoph Boehnke, Uwe Klemradt
RWTH Aachen University, Aachen, Germany

Acoustic emission is one of the most sensitive methods for detecting jerky, cooperative movements of atoms at an interface, especially at domain walls. The resulting acoustic signals, typically in the 100 kHz range, vary in amplitude, energy and duration over many orders of magnitude, opening up the possibility to study statistical properties of the associated dynamic structural changes. Such crackling noise is measured in various non-equilibrium processes, e.g. in ferroic transformations, compression of porous materials and switching processes [1]. Typically, power laws are found in the parameters of the acoustic wave trains, whose exponents are explained by avalanche criticality.

While acoustic emission in martensites is well established [2], its application to ferroelectrics has a much shorter history [3]. Here we report on studies of the austenite-martensite transition in the prototypical shape memory alloy Ni63Al37 (NiAl) compared to the model ferroelectric BaTiO3 (BTO) using the same experimental setup.

Whereas for BTO we find energy exponents expected from mean field theory, these exponents are significantly higher for NiAl. In addition, significant differences in the detailed time structure of the signals are observed. In particular, BTO satisfies the well-known Omori law for the rate of “aftershocks” in acoustic activity over more than five orders of magnitude in time, while there is no such behavior in NiAl.

[1] E.K.H. Salje and K.A. Dahmen, Annu. Rev. Condens. Matter Phys. 5, 233 (2014).

[2] P.C. Clapp, J. Phys. IV 5, C8-11 (1995); Proceedings of ICOMAT 95.

[3] G.F. Nataf and E.K.H. Salje, Ferroelectrics 569, 82 (2020).

P16_276

Characterization of permanent lattice defects and strain generated by forward or reverse martensitic transformation in NiTi wire

Orsolya Molnárová, Elizaveta Iaparova, Luděk Heller, Petr Šittner
Institute of Physics of the Czech Academy of Sciences, Prague, Czech Republic

During thermomechanical deformation of the NiTi wire incremental plastic strains are generated by martensitic transformation (MT) proceeding under external stress. In order to reveal the mechanism by which these plastic strains are generated, NiTi wires were cooled (heated) under various external stresses and permanent lattice defects generated by forward (reverse) MT within austenitic grains were analysed post-mortem in TEM. The ambition was to analyse all permanent lattice defects created by the forward (reverse) MT in analysed grains. Besides slip dislocations and austenite twin bands, the permanent lattice defects include lattice orientation gradient and lattice strain fields in grains.

It is found that no plastic strain and no permanent lattice defects were generated by forward MT upon cooling under stress below 500 MPa threshold (Figure 1a-c), whereas the reverse MT upon heating under stresses above 200 MPa generated plastic strains and permanent lattice defects (Figure 1d-f). Slip dislocations generated by forward and reverse MTs were found to be qualitatively different. The character of permanent lattice defects changed with the increasing applied stress. The higher the applied stresses under which the forward and reverse MT occurred, the larger misorientation of the austenite lattice across grain were observed. {114} austenite twins were observed in the microstructure of NiTi wires cooled or heated under highest stress 800 MPa. It is claimed that all observed permanent lattice defects were created in the martensite phase and only inherited by the austenite phase.

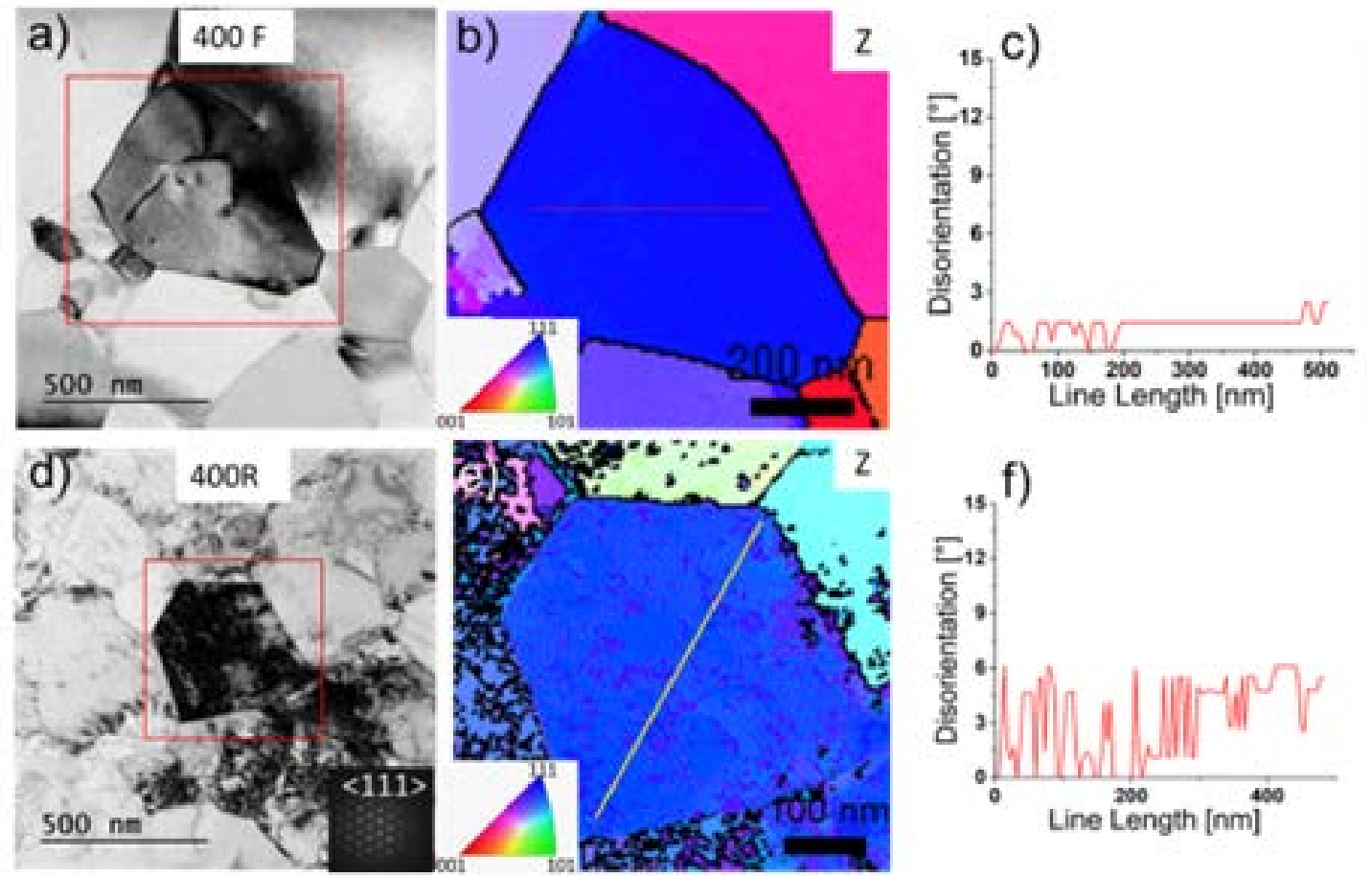

Figure 1. Comparison of austenitic microstructures observed by TEM in NiTi wires undergoing forward MT upon cooling (a,b,c) and reverse MT upon heating (d,e,f) under 400MPa stress: a) BF-TEM image of a grain oriented in <111> zone axis revealing only few isolated dislocations b) lattice orientation map of the grain, c) the disorientation of the austenite lattice evaluated along the line denoted in (b), d) BF-TEM image of a grain oriented in <111> zone axis revealing .

P17_351

In-situ Measurement of Elasticity During Thermally Induced Phase Changes Using Dove Prism-Enhanced Transient Grating Spectroscopy

Pavla Stoklasová, Jakub Kušnír, David Mareš, Tomáš Grabec, Hanuš Seiner
Czech Academy of Sciences, Institute of Thermomechanics, Prague, Czech Republic

In this contribution, we present an upgraded laser-ultrasonic setup for transient grating spectroscopy (TGS) that enables full 360° elastic characterization of materials undergoing thermally induced phase changes. TGS is a surface acoustic wave (SAW)-based method that allows for non-contact, in-situ monitoring of elastic changes with high directional sensitivity [Stoklasová et al., Ultrasonics 2015].

A major challenge in previous experiments has been to rotate samples placed inside a temperature-controlled chamber, which limited the angular coverage of the measurement. To overcome this, we have integrated a Dove prism into the optical path. Dove prisms rotate the image without deviating the beam, enabling rotation of both the probe and pump beams on the sample surface by simply adjusting the prism angle—without the need to move the sample itself. This advancement enables anisotropic elasticity data collection over the full 360° range, even with the sample fixed inside the temperature-controlled chamber.

To validate the method, benchmark measurements were performed on two materials exhibiting thermally induced changes in elasticity: a shape memory alloy (NiFeGaCo) and a metastable beta-phase alloy (Ti15Mo). In the case of NiFeGaCo, we observed pronounced softening of shear elasticity near the martensitic transformation. For Ti15Mo, decreasing temperature led to an increase in the number of athermal omega phase particles, resulting in stiffening and isotropization of the shear elastic response. These results confirm the capability of the upgraded TGS system to capture complex elastic behavior associated with temperature-induced phase changes.

This setup retains the advantages of the original TGS method, including k-selectivity and narrowband SAW generation by spatially modulated laser beams [Stoklasová et al., Exp Mech 2021], while expanding its capability to measure angularly resolved elasticity under thermal loading. Providing new opportunities for studying structural dynamics and phase changes in advanced functional materials.

This work was financially supported by the Ministry of Education, Youth and Sports of the Czech Republic in the frame of the project 'Ferroic multifunctionalities' (project No. CZ.02.01.01/00/22_008/0004591), co-funded by the European Union.

P18_334

Actuation characteristics of spring-biased NiTi shape memory alloy wires under pulsed current stimulation

Xiao Ma, Lianzhi Ding, Yanwen Bu, Shanshan Cao, Xinping Zhang
South China University of Technology, Guangzhou, China

NiTi shape memory alloys (SMAs) are widely used in making microactuators due to their high energy density and considerable output strain. One-way SMAs in combination with bias stress configurations possess significant advantages over two-way SMAs, as the former do not require a complex training process and are able to provide a stable driving strain when forming reciprocating actuators. The use of elastic spring as biasing element is easy to install and suitable for a wide range of applications compared to other methods such as constant force. Furthermore, the thermal-mechanical response characteristics of the coupled SMA and spring actuating apparatus can be tuned precisely by varying the stiffness of spring and the bias stress.

This work focuses on revealing the electro-thermal-mechanical characteristics, including actuation strain, actuation stress, actuation time and energy efficiency etc., of NiTi SMA wires combined with bias springs under different stimulating and biasing conditions. An evaluation platform is designed and built, which consists of a moving slider, laser displacement sensor, thermocouple and load cell as shown in Figure 1. A four-channel data acquisition system is programmed using the NI Labview software to record the real-time changes of the corresponding signals of electrical current, temperature, displacement and force. SMA wires of various diameters and bias springs with a range of stiffnesses can be conveniently installed on the platform, and the bias stress can be adjusted by rolling the handle of the moving slider. The SMA wire is heated by Joule heat generated by a pulsed current supplied by a DC power supply, with two electrode clips are attached to both ends of the SMA wire; and the heating and cooling times are programmed and controlled by timer relays.

The experimental results show that for a specific coupled SMA-spring configuration, the actuation strain and actuation force increase with increasing the bias stress; as the stiffness of spring increases, the actuation strain also increases. However, excessive bias stress and stiffness will lead to failure of the SMA-spring configuration where no actuation response is achieved. Energy efficiency is the ratio of work output to energy input, both of which can be calculated from experimental data acquired by the so-built evaluation platform. Further results and detailed analysis will be presented in the full-length paper.

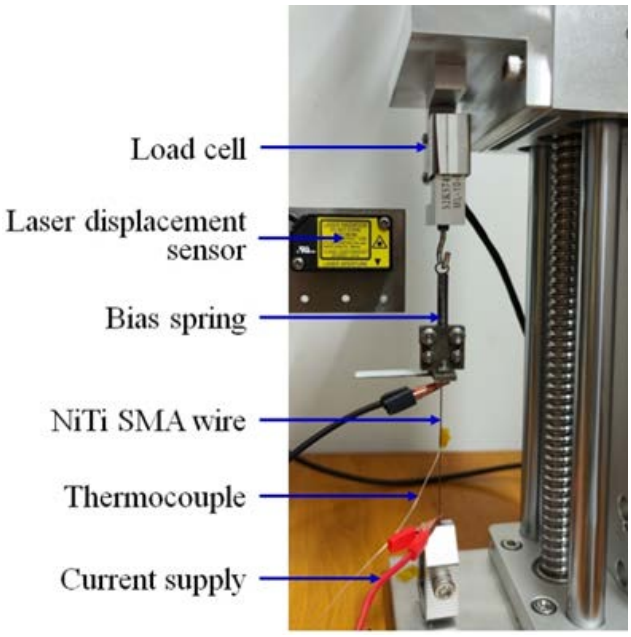

Fig. 1

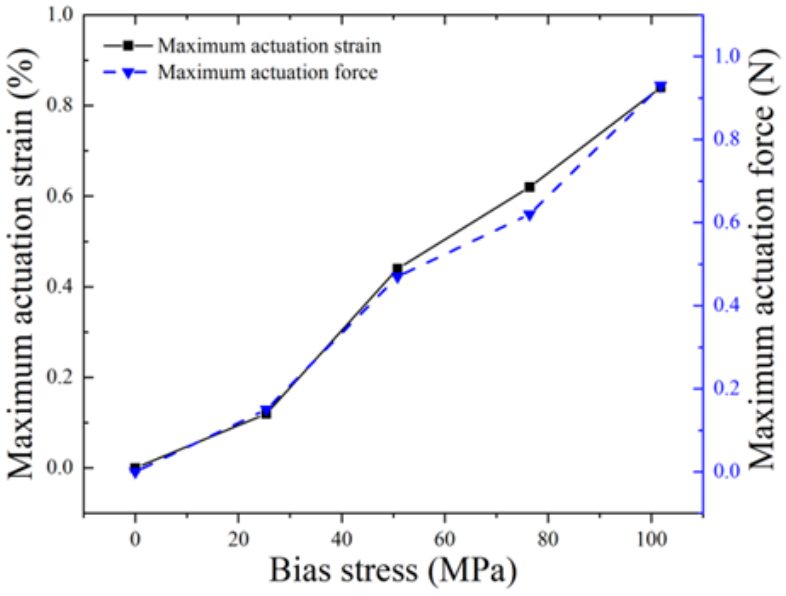

Fig. 2

P19_313

Thermomechanical Characterization of very thin $Ni_{50}Fe_{27}Ga_{23}$ Shape Memory Microwire

Limpat Nulandaya[1], Tomas Ryba[2], Rastislav Varga[1,2], Ludek Heller[1], Petr Sittner[1]
[1]Institute of Physics of the Czech Academy of Sciences, Prague, Prague, Czech Republic. [2]RVmagnetics, Kosice, Kosice, Slovakia

In this work, we present results of the thermomechanical characterization of 14 µm $Ni_{50}Fe_{27}Ga_{23}$ microwires [1-4] produced by Taylor Ulitovsky method [5,6]. The characterization was performed in the actuation regime using thermal cycles under constant stress and in the superelastic regime using stress-strain cycles at constant temperatures. The results of iso-stress tests strain-temperature curves with 12% reversible strains and stress independent thermal hysteresis of 65 °C up to maximum stress 200 MPa. The results of superelastic test show stable and reversible stress-strain responses up to 400 °C. Both experiments indicate same temperature dependence of the forward and reverse transformation stresses of 1.4 MPa/°C up to 200 °C. Beyond 200 °C, however, the superelastic plateau length increases from 11% (200 °C) up to 13% (400 °C) along with hysteresis widening from 50 MPa (200 °C) up to 150 MPa (400 °C). In addition, the temperature dependence of the forward and reverse transformation stresses deviate from the linearity. To sum up, 14 µm Ni50Fe27Ga23 microwires loaded in tension provide more than 10% recoverable transformation strain without functional fatigue in actuation cycling below 200 MPa and in superelastic cycling in wide temperature range 100-400°C.

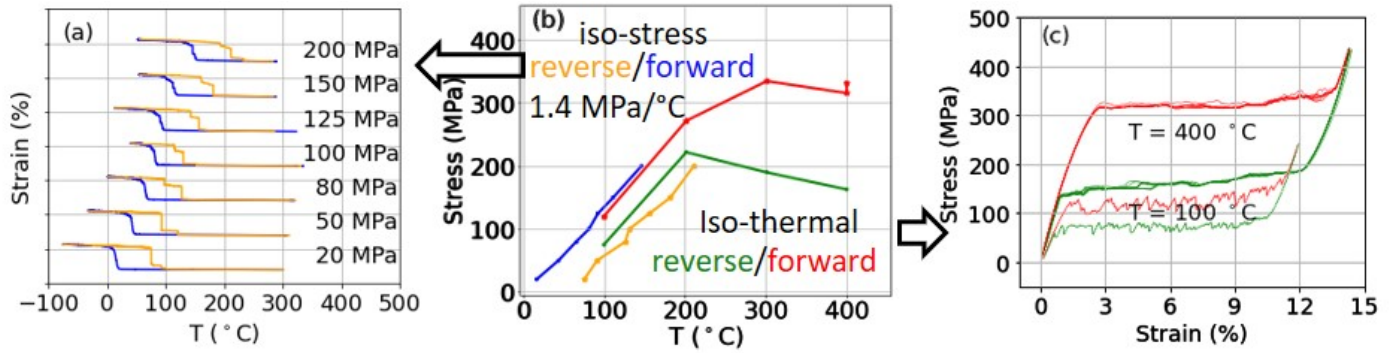

Figure: (a) Strain-temperature curves from iso-stress measurements by cooling/heating under various constant stresses from 20 MPa (3.1e-3 N) to 200 MPa (3.1e-2 N). (b) Stress-temperature diagram from the iso-stress and iso-thermal measurements. (c) Stress-strain curves from iso-thermal measurement showing super-elastic response at 400 °C (10 cycles of loading-unloading) and 100 °C (two cycles of loading-unloading).

[1] Applied Physics Letters, 2004, 84 (8), 1275-1277, doi.org/10.1063/1.1642277.

[2] Acta Materialia, 2015, 96, 420-427, doi.org/10.1016/j.actamat.2015.06.011.

[3] Materials Science and Engineering: B, 2021, 263, 114891, doi.org/10.1016/j.mseb.2020.114891.

[4] Journal of Magnetism and Magnetic Materials, 2022, 556, 169394, doi.org/10.1016/j.jmmm.2022.169394.

[5] Crystals, 2017, 7(6), 136, doi.org/10.3390/cryst7060136

[6] Physical Review Journals, 1924, 23, 655-660, doi.org/ 10.1103/PhysRev.23.655

P20_365

Influence of Sputtering Parameters on Functional and Mechanical Behavior of Ni-Rich NiTi Films

André Fontes[1], Patrícia Freitas Rodrigues[1], Andersan dos Santos Paula[2], Ana Sofia Ramos[1]
[1]Department of Mechanical Engineering, ARISE/ CEMMPRE-Centre for Mechanical Engineering Materials and Processes, University of Coimbra, Coimbra, Portugal. [2]Department of Materials Science, Military Institute of Engineering—IME, Rio de Janeiro, Rio de Janeiro, Brazil

Shape memory alloy films (SMAFs) represent a class of functional materials that exhibit remarkable properties. Their reduced dimensions enhance responsiveness, increase flexibility, and enable integration into micro-and nanoscale devices. NiTi SMAFs were prepared by DC magnetron sputtering from a compound NiTi target, aiming to investigate the influence of deposition parameters, such as power density, argon pressure, and deposition time, on their structural and functional properties. All films were deposited onto monocrystalline silicon substrates and subsequently heat-treated at 400 °C for 1 hour to promote crystallization.

Comprehensive characterization using SEM, EDS, AFM, synchrotron XRD, and nanoindentation was performed on both as-deposited and heat-treated films. The as-deposited films exhibited an amorphous structure with typical cauliflower-like surface morphology and columnar cross-sections, except under higher pressure, which yielded denser but less defined features. All films showed significant Ni enrichment (~60 at.%), resulting from the higher sputtering yield of Ni compared to Ti. Some as-deposited films present vein-like features characteristic of metallic glass films produced by sputtering.

Heat treatment led to the formation of the austenitic B2 phase along with Ni-rich precipitates, confirmed by synchrotron XRD. Grain growth and film densification were observed, especially in samples previously showing vein-like cross-sectional features. These structural transitions resulted in enhanced mechanical properties. Hardness increased to 8.1 GPa, Young's modulus exceeded 150 GPa, and the elastic recovery parameter (ERP) increased in all heat-treated films, indicating superelastic behavior. Interestingly, while the deposition pressure influenced the morphology and hardness of as-deposited films, other deposition parameters had limited impact on the films' properties.

These findings suggest that heat treatment enables superelastic functionality in Ni-rich NiTi thin films. The ability to change microstructure and mechanical performance through precise deposition and annealing strategies reinforces their potential for MEMS and other smart material applications.

P21_377

Martensitic transformation in Heusler alloy nanostructures

Michal Varga[1], Marek Vronka[1], Pavel Diko[2], Oleg Heczko[1]
[1]FZU—Institute of Physics of the Czech Academy of Sciences, Prague, Czech Republic. [2]Institute of Experimental Physics, Slovak Academy of Sciences, Kosice, Slovakia

The current challenge in the utilization of shape memory Heusler alloys for sensors and actuators remains in their downsizing [1,2]. Nanodimensional materials with shape memory capability can be prepared by multiple fabrication techniques [2, 3]. Electrodeposition presents a scalable method for fabrication of shape memory materials, which can be used for practical applications in the nanoscale.

Electrodeposition of Ni_2Fe-X (X = Ga, In, Tl) nanowires resulted in off-stoichiometric Heusler alloy compositions. The Ni-Fe-Ga and Ni-Fe-Tl nanowires show a phase transformation above room temperature, confirmed by structural and magnetic analysis.

First-order reversal curve analysis of an array of the fabricated nanowires reveals a change in their magnetization process before and after the phase transition, enabling contactless sensing mechanism of the nanowires' transformation [2, 4]. Thus, the observed phase transformation at the nanoscale demonstrates the application potential of the Heusler alloy nanowires in a wide range of applications related to the martensitic transformation capability.

References
[1] Frolova et al., "Smart Shape Memory Actuator Based on Monocrystalline Ni_2FeGa Glass-Coated Microwire," IEEE Trans Magn, vol. 54, pp. 1–5, Nov. 2018, doi: 10.1109/TMAG.2018.2848670.
[2] M. Varga et al., "FORC and TFORC analysis of electrodeposited magnetic shape memory nanowires array," J Alloys Compd, vol. 897, p. 163211, doi: 10.1016/j.jallcom.2021.163211.
[3] Zhang, H, et al., "Reversible phase transformations in a shape memory alloy In–Tl nanowires observed by in situ transmission electron microscopy" Materials Letters, vol. 70, p. 109-112, doi: 10.1016/j.matlet.2011.11.049
[4] M. R. Zamani Kouhpanji, A. Ghoreyshi, P. B. Visscher, and B. J. H. Stadler, "Facile decoding of quantitative signatures from magnetic nanowire arrays," Sci Rep, vol. 10, no. 1, p. 15482, doi: 10.1038/s41598-020-72094-4.

P22_353

Angular dependence in magnetically induced reorientation

David Hruška, Oleg Heczko
FZU-Institute of Physics of the Czech Academy of Sciences, Prague, Czech Republic

In the field of magnetic shape memory effect, *magnetically induced variant reorientation* is often considered in simplified configurations with the magnetic field applied along the [100] crystallographic direction of a single variant with the easy axis perpendicular to the field. In contrast, we investigate the angular dependence of twin boundary motion driven by an external magnetic field in Ni-Mn-Ga 10M martensite, taking into account arbitrary relevant orientations of twin boundaries and the associated martensitic variants without the restriction to a common plane with the applied field.

We consider a sample consisting of two martensitic variants separated by a mobile twin boundary (or multiple parallel boundaries), with each variant treated as several uniformly magnetized domains to capture demagnetization effects. The magnetization within each domain evolves according to a modified Stoner–Wohlfarth model that includes simplified interaction between domains and a rate-independent dissipation mechanism.

We present a relatively efficient numerical scheme for our model, which enables computation of switching fields and some related energetic quantities. This goes beyond previous approaches (e.g., [1]), which only considered reorientation at the maximum potential energy difference. Our model provides a more detailed picture of the reorientation process, including angular dependence of switching, domain interactions, and energy dissipation associated with the twin boundary motion.

Predictions of the model are compared with experimental measurements on a single crystal of Ni-Mn-Ga exhibiting a 10M martensitic structure.

Acknowledgements

This work was supported by OP JAK project No. CZ.02.01.01/00/22_008/0004591 and Czech Science Foundation grant No. 23-04806S.

References

[1] O. Heczko at al., Magnetic Shape Memory Phenomena in J.P. Liu et al. (eds.), Nanoscale Magnetic Materials and Applications, p. 399,

DOI 10.1007/978-0-387-85600-1 14, Springer Science+Business Media, LLC 200

P23_246

Elastic properties of Ni-Mn-Ga-1%Fe 10M martensite with incommensurate lattice modulation

Alexei Sozinov[1], Mariia Vinogradova[2], Andrey Saren[2], Ladislav Straka[3], Martin Zelený[4], Robert Chulist[5], Pavla Stoklasová[6], Hanuš Seiner[6], Kari Ullakko[2]
[1]Tikomat Oy, Savonlinna, Finland. [2]LUT University, Lappeenranta, Finland. [3]FZU, Prague, Czech Republic. [4]Faculty of Mechanical Engineering, Brno University of Technology, Brno, Czech Republic. [5]AGH University of Krakow, Krakow, Poland. [6]Institute of Thermomechanics of the Czech Academy of Sciences, Prague, Czech Republic

Ni-Mn-Ga-based Heusler-type alloys have garnered significant attention in recent years due to their capacity for achieving magnetic field-induced strains (MFIS) as high as 12%. The appealing MFIS properties, which are potential for numerous applications, are associated with exceptionally low twinning stresses. This low twinning stress is expected to correlate with low shear moduli along the relevant twinning planes and directions. Understanding lattice elastic properties is crucial for atomic and continuum-level modeling and understanding of high twin boundary mobility. The lack of a reliable elastic matrix limits the calculation of the mechanical properties of Heusler alloy modifications and their potential for commercialization.

The elastic matrix for 10M Ni-Mn-Ga-based martensite has been determined in the tetragonal approximation using methods that exclude the influence of twin boundaries. The *a/b* twin boundaries showed immobility due to the use of alloys with incommensurate lattice modulation. The effect of *a/c* twin boundaries was reduced by applying tensile stress along the *a*-axis or compression along the *c*-axis. The identified elastic matrix differs in a specific way from those previously found using transient grating spectroscopy (TGS) [1], confirming that the incommensurate structure strongly affects the elastic compliance along the (110) planes. The main difference was a threefold increase in Young's moduli along the [001] and [100] directions and in shear moduli G for the *a/b* and *a/c* twinning planes and directions in the absence of twin boundaries (TBs). When compared to the first principal calculation [2], we can see that the Young's modulus along the *a*-axis is more than twice as high in these calculations. This investigation highlights the importance of studying the mechanisms by which twin boundaries contribute to stress-induced deformation at low levels of excitation. We suggested and discussed two such mechanisms: highly mobile twin dislocations and modulated lattice instability to disappearance of monoclinity. The monoclinic instability is examined within the context of a recently proposed model for IC modulation [3], as well as models for hysteresis and strain glasses.

[1] K. Repček et al. Adv. Mater. (2024) 2406672.

[2] H. Seiner et al. Phys. Stat. Sol RRL–Rapid Res. Lett. 16(2022)2100632.

[3] P. Veřtát et al. (2025), https://doi.org/10.48550/ARXIV.2503.04379.

P24_410

Tuning magneto-structural transitions in Ni-Mn-Ga melt-spun ribbons through Co and Cu doping

Milena Kowalska[1], Mariana Rios[2], Patricia Lazpita[3], Volodymyr Chernenko[2,3,4], Daniel Salazar[2], Maciej J. Szczerba[1]
[1]Institute of Metallurgy and Materials Science, Polish Academy of Sciences, Kraków, Poland. [2]BCMaterials, Basque Center for Materials, Applications and Nanostructures, EHU Science Park, Leioa, Spain. [3]Department of Electricity and Electronics, Faculty of Science and Technology, University of the Basque Country, Bilbao, Spain. [4]Ikerbasque, Basque Foundation for Science, Bilbao, Spain

Ni-Mn-Ga-based ferromagnetic shape memory alloys have drawn considerable interest for actuator and sensor applications due to unique effects such as magnetic field-induced strain (MFIS) and magnetic field-induced bending (MFIB) [1-3]. MFIS arises from twin boundary motion in martensite variants, with strains up to ~11% in modulated phases of ternary Ni-Mn-Ga. Co and Cu doping can extend these effects to the non-modulated 2M martensite, where reduced twinning stress enables MFIS of ~12% [4]. MFIB, unlike MFIS, produces reversible bending without structural degradation and is enhanced in materials with a high length-to-width ratio, such as thin ribbons obtained by melt-spinning.

In this study, $Ni_{50-x}Mn_{25}Ga_{25-x}Co_xCu_x$ (x = 1–6 at.%) melt-spun ribbons were produced to stabilize the martensitic phase and tune transformation temperatures. X-ray diffraction at room temperature showed a transition from $L2_1$ austenite (x = 1–3) to non-modulated 2M martensite (x = 5–6), with both phases present at x = 4. Increasing Co and Cu from x = 1 to 6 raised martensitic transformation (MT) temperatures from 223 K to 499 K. The austenite Curie temperature rose from 373 K (x = 1) to 381 K (x = 3) before decreasing to 371 K (x = 4), while martensite Curie points were 296 K (x = 5) and 221 K (x = 6). A phase diagram mapping MT and magnetic transition temperatures as a function of composition revealed that only alloys with 4–5 at.% Co and Cu possess ferromagnetic martensite—an essential condition for MFIB. These compositions, combining suitable MT temperatures with favorable magnetic properties, are promising for flexible magneto-mechanical actuators. The constructed phase diagram offers guidance for tailoring Ni-Mn-Ga-based alloys for functional use near room temperature.

[1] M. Acet, Ll. Mañosa, A. Planes, Chapter Four, Handb. Magn. Mater., vol. 19, pp. 231-289 (2011).

[2] K. Ullakko, J. K. Huang, C. Kantner, R. C. O'Handley, V. V. Kokorin, Appl. Phys. Lett., vol. 69, p. 1966 (1996).

[3] N.J. Kucza, C. L. Patrick, D. C. Dunand, P. Müllner, Acta Mater., vol. 95, pp. 284-290 (2015).

[4] A. Sozinov, N. Lanska, A. Soroka, W. Zou, Appl. Phys. Lett., vol. 102, 021902 (2013).

P25_388

Substrate-induced martensitic transformation in thin epitaxial Ni-Mn-Ga films

Matěj Makeš[1,2], Jakub Zázvorka[2], Petr Veřtát[1], Michal Rameš[1], Martin Veis[2], Oleg Heczko[1]
[1]FZU-Institute of Physics of the Czech Academy of Sciences, Prague, Czech Republic. [2]Institute of Physics of Charles University, Prague, Czech Republic

Ni-Mn-Ga is a prototypical magnetic shape-memory alloy (MSMA). The origin of martensitic transformation in this material continues to be a subject of discussion. Magneto-optical measurements can provide an insight into this structural transformation as they are sensitive to small changes in the electronic structure of the material [1]. Here, we present a systematic study of optical and magneto-optical responses for a series of thin Ni-Mn-Ga films with different transformation behaviour depending on film thickness.

Studied Ni-Mn-Ga films were deposited by magnetron sputtering on 27 nm thick stress-mediating Cr layer and MgO substrate using single crystal target. The films grew epitaxially with their unit cells oriented as commonly observed, i.e., Ni-Mn-Ga(100)[011]/Cr(100)[011]/MgO(100)[001].

Structure characterization techniques including AFM, XRD and XRR revealed biaxial compressive stress induced by the substrate. Thinner films remain austenitic in the 5-400 K temperature range and the stress was found to increase with increasing thickness, while thicker films did undergo MT.

To probe changes of the electronic structure during the stress-induced transformation, we used variable-angle spectroscopic ellipsometry (VASE) and polar magneto-optical Kerr spectroscopy (PMOKES) across the 0.7-6.4 eV photon energy range (see figure). This allows the computation of complete linear permittivity tensor. The sensitivity of these methods to electronic structure changes was observed and strong correlations between lattice parameter, coercivity and magneto-optical properties were identified.

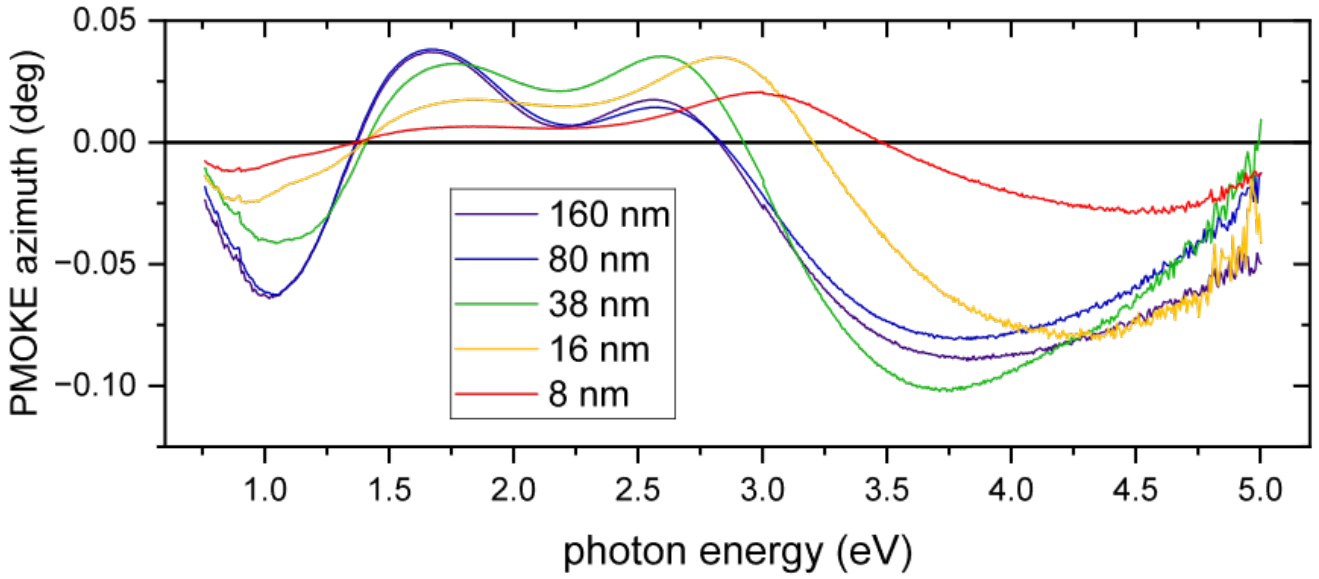

Reference

[1] M. Veis et al, J. App. Phys. 115, 17A936 (2014); doi: 10.1063/1.4867754

Acknowledgements

This work was supported by OP JAK project No. CZ.02.01.01/00/22_008/0004591, Czech Science Foundation grant No. 24-11361S and the Charles University grant SVV–2024–260720.

P26_361

Search for criterion for martensitic transformation in ferromagnetic Heusler alloys

Michal Rameš, Ladislav Straka, Vít Kopecký, Michal Varga, Petr Veřtát, Oleg Heczko
FZU-Institute of Physics of the Czech Academy of Sciences, Prague, Czech Republic

Ferromagnetic Heusler alloys, especially those based on Ni-Mn-Ga, may exhibit martensitic transformation as a prerequisite for magnetic shape memory (MSM) phenomena such as magnetically induced reorientation (MIR) and magnetic field induced strain (MFIS). Temperatures where martensite and MSM phenomena exist can be tuned via doping of stoichiometric compound by chemical elements. We systematically experimentally studied doping of stoichiometric Ni_2MnGa by 5 at.% of transitional elements from Cr to Cu and by Ga, where doping atoms occupied nominally only Ni, Mn, or Ga positions in the stoichiometric compound. The alloys were 19 arc-melted polycrystals, the martensitic transformation temperature T_M was measured using vibrating sample magnetometer (VSM) in the Physical Property Measurement System (PPMS). T_M of the doped Ni-Mn-Ga alloys depends strongly on doping element and on atomic position it occupies in the stoichiometric compound. We compared our data with those from other Heusler alloys and analyzed them as a function of valence electron concentration *e*/*a*. The data are plotted in the figure. For our alloys the dependence is non-trivial, without any clear tendency. For isoelectronic substitutions with varying atomic concentrations only of the elements with the same number of valence electrons, T_M is not a function of *e*/*a*. Also, the T_M dependences of *e*/*a* adopted from literature do not follow a single tendency. This calls for better criterion for T_M in Heusler alloys. Our proposed criterion seems to overcome these problems, helping thus to synthesize alloys with high T_M attractive for sustainable applications.

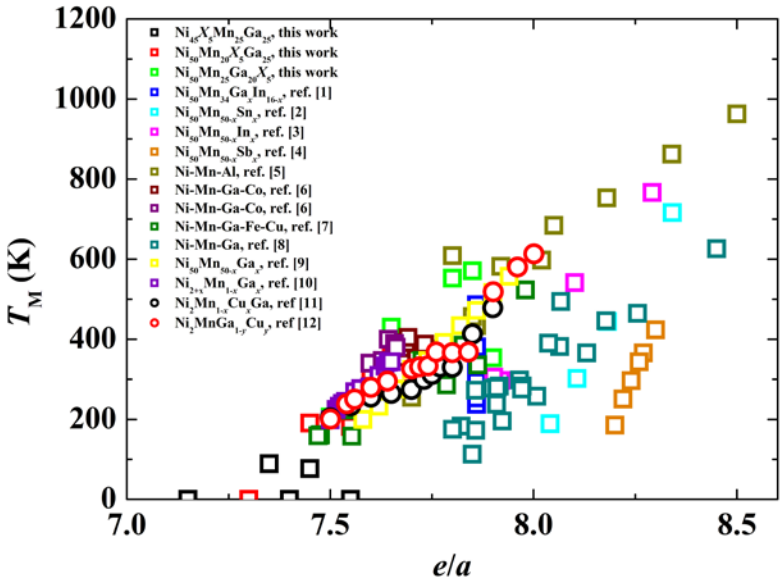

Acknowledgements

This work was supported by OP JAK project No. CZ.02.01.01/00/22_008/0004591 and Czech Science Foundation grant No. 22-22063S.

References

[1] Z.H. Liu, G.T. Li et al., *J. Alloys. Compd.* (2012)
[2] T. Krenke, M. Acet et al., *Phys. Rev. B* (2005)
[3] T. Krenke, M. Acet et al., *Phys. Rev. B* (2006)
[4] Y. Sutou, Y. Imano et al. *Appl. Phys. Lett.* (2004)
[5] R. Kainuma, H. Nakano et al., *Metal. Mater. Trans. A* (1996)
[6] K. Rolfs, R. C. Wimpory, W. Petry, R. Schneider, *J. Phys. Conf. Ser.* (2010)
[7] A. Armstrong, F. Nilsén et al., *Shap. Mem. Superelast.* (2020)
[8] V.A. Chernenko, E. Cesari et al., *Scr. Metall. Mater.* (1995)
[9] X. Xu, T. Kanomata et al., *Acta Mater.* (2014)
[10] V.V. Khovailo, K. Oikawa et al., *J. Appl. Phys.* (2003)
[11] M. Kataoka, K. Endo et al., *Phys. Rev. B* (2010)
[12] K. Endo, T. Kanomata et al., *Mater. Sci. Forum* (2011)

P27_385

Scanning twin boundary mobility in 10M martensite of Ni-Mn-Ga alloy from subatomic to macroscopic scale

Sergey Kustov[1], Andrey Saren[2], Alexei Sozinov[2], Boris Kustov[1,2], Kari Ullakko[2]
[1]University of Balearic Islands, Palma de Mallorca, Spain. [2]LUT University, Lappeenranta, Finland

We report studies of macroscopic motion and microscopic dynamics of a/c Type I and Type II single twin boundaries (TBs) in a $Ni_{50.0}Mn_{28.4}Ga_{21.6}$ alloy by combining direct measurements of the twinning stress (TS) with acoustic studies in non-linear regime of TB motion.

An ultrasonic resonant technique was used to derive the non-linear anelastic strain due to the TB motion and average friction stress acting on moving TB in “domain engineered” bar-shaped samples of 10M martensite containing three differently oriented variants. The central narrow variant had c-axis perpendicular to the sample length, whereas two variants with the c-axis parallel to the sample length occupied both ends of the bar. The variants were separated either by two Type I TBs or by one Type I and one Type II TB. The first configuration was used to study the mobility of Type I TB, the mobility of the Type II TB was tested in the second configuration. To account for the effect of a/b twins in the central variant, we performed the measurements for different distances between a/c TBs. For each TBs separation, the macroscopic TS was determined and compared with the characteristic stresses in acoustic experiment. For Type II TB, the values of anelastic strain ranged between ca. 10^{-11} and 10^{-6}, and of the friction stress between ca. 1 kPa and 0.03 MPa, the latter value being close to the macroscopic TS. Assuming the uniform displacement of the TB, the lower value of the anelastic strain would correspond to the TB displacements of much less than one interatomic distance, pointing to only local non-linear displacements of the small parts of the TB.

The motion of Type I TBs was always smooth on macroscopic and microscopic scales with a characteristic power law stress dependence of anelastic properties. The motion of Type II TBs in both acoustic and macroscopic experiments required an order of magnitude lower stresses. The acoustic experiments revealed three characteristic domains of qualitatively different Type II TB dynamics: (i) low stress regime of smooth motion and gradually increasing friction stress; (ii) intermediate regime of highly unstable and jerky dynamics and abrupt increase of the friction stress, reflecting initiation of the macroscopic displacement of the TB; (iii) high-amplitude relatively stable and essentially linear regime of TB motion. We conclude that the non-linear dynamics of the Type II TBs is controlled by their interaction with a/b twins which are anchored by Type I TB.

P28_344

Probing martensitic transformation in Ni-Mn-Ga via high-frequency ferromagnetic resonance

Sviatoslav Vovk, Denys Musiienko, Oleg Heczko, Luděk Kraus
FZU-Institute of Physics of the Czech Academy of Sciences, Prague, Na Slovance 1999/2, 182 00, Czech Republic

Magnetic shape memory (MSM) alloys based on Ni-Mn-Ga exhibit a strong coupling between magnetic and structural order parameters, leading to large magnetic-field-induced strains in the martensitic state. Understanding the temperature-dependent magnetic anisotropy in these systems is key to both theoretical modeling and future applications. Earlier ferromagnetic resonance (FMR) studies on bulk Ni-Mn-Ga single crystals at X-band frequencies revealed temperature-and angle-dependent behavior [1]; however, the extracted anisotropy constants substantially differed from those determined from the magnetization measurements, probably due to multivariant sample studied.

In this work, we employ broadband FMR (4–40 GHz) to investigate a $Ni_{50}Mn_{28.1}Ga_{21.9}$ single crystal in single variant state over a wide temperature range (20–140 °C). A sharp discontinuity in the resonance field is observed near the martensitic transformation temperature (~46 °C) as it shown at Figure 1, reflecting a significant change in magnetocrystalline anisotropy. Below the transformation, in the single-variant martensitic state, the resonance field corresponds to the Kittel model, with a gyromagnetic ratio g = 2.0 and strong uniaxial anisotropy with easy axis along the c-axis parallel to the field direction in agreement with our previous results [2]. Above transition the resonance field is shifted to higher fields due to weak anisotropy in the austenitic phase.

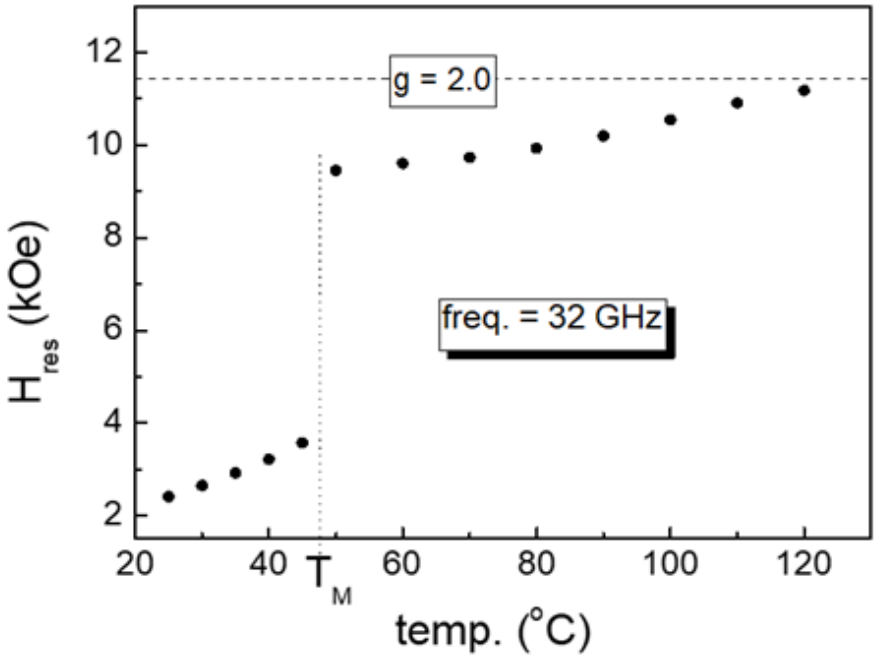

Additionally, multivariant martensite states were analyzed, with preliminary data suggesting the importance of inter-twin magnetic coupling. Planned measurements at multiple frequencies aim to further resolve the evolution of the effective anisotropy field and magnetic damping across the transformation.

Acknowledgements

This work was supported by OP JAK project No. CZ.02.01.01/00/22_008/0004591 and Czech Science Foundation grant No. 22-22063S.

References

[1]V. G. Gavriljuk *et al.*, “A study of the magnetic resonance in a single-crystal $Ni_{50.47}Mn_{28.17}Ga_{21.36}$ alloy,” *J. Phys. Condens. Matter*, vol. 18, no. 32, pp. 7613–7627, Jul. 2006, doi: 10.1088/0953-8984/18/32/010.

[2] L. Kraus, O. Heczko, “Magnetic order in Mn excess Ni-Mn-Ga Heusler alloy single crystal probed by ferromagnetic resonance, ” *J. Magnetism and Magnetic Materials* 532 (2021) 167983, https://doi.org/10.1016/j.jmmm.2021.167983

P29_259

Elastocaloric effect in polycrystalline NiMnGa produced through hot-rolling powder consolidation

Francesca Villa[1,2], Elena Villa[1], Francesca Passaretti[1], Enrico Bassani[1], Corrado Tomasi[3], Riccardo Casati[2]
[1]CNR ICMATE, Lecco, Italy. [2]Politecnico di Milano, Milano, Italy. [3]CNR ICMATE, Genova, Italy

NiMnGa ferromagnetic shape memory alloy has been extensively studied for its peculiar functional and magnetic properties and magnetocaloric effect. However, the intrinsic brittleness of this alloy represents a significant limitation for practical applications. Therefore, microstructural tuning of polycrystalline NiMnGa alloys has been investigated to improve their mechanical properties and to reduce their typical brittleness. For this reason, increasing interest has been devoted to the development of various fabrication routes, such as powder metallurgy processes. In the present study, a polycrystalline $Ni_{50}Mn_{30}Ga_{20}$ (atomic %) alloy is produced by means of an unconventional powder metallurgy route which involves a *powder-in-tube* approach. This method involves the canning of powders inside a metallic sheath and the subsequent processing by hot rolling. In this way, powders are effectively compacted and fully-dense NiMnGa samples are obtained. This process was implemented according to the results obtained by means of the open die pressing (ODP) sintering of NiMnGa which was investigated in a previous work. A heat treatment at 925 ◦C for 6 h was applied and allowed achieving a maximum adiabatic ΔT of +6.3 °C and-4.5 °C with a strain of 4 % and a strain rate of 400 %/min in compression. The aim of this work is the development of an innovative and cost-effective powder metallurgy route to mitigate polycrystalline NiMnGa brittleness issue. The mechanical performance of NiMnGa was enhanced, enabling its potential use in elastocaloric applications and magneto-elastic coupling.

P30_384

Microstructure and Elastocaloric Effect of a Ti-Ni-Zr-Sn Shape Memory Alloy

Zhiyong Gao, Lingjiao Kong, Xianglong Meng
School of Materials Science & Engineering, Harbin Institute of Technology, Harbin, China

Elastocaloric refrigeration, as a novel solid-state cooling technology, is considered to be the most promising alternative to the traditional vapour-compression-based technology in a 2014 report of US Department of Energy. The shape memory alloys (SMAs) exhibit excellent elastocaloric effect because of the latent heat of the uniaxial stress-induced reversible martensitic transformation during loading-unloading process. Recently, some superelastic β-Ti SMAs have been designed, providing a new material family to explore elastocaloric properties. In the present study, it is found that a Ti-Ni-Zr-Sn alloy after proper thermomechanical treatment show good elastocaloric effect in a wide temperature range. The nano-scale domains, originated from the strain glass, should be responsible for it. The elastocaloric effect deteriorates during loading-unloading cycles because the formation of stress-induced w phase and the increase of the residual martensite. The evolution of microstructure during the loading-unloading cycling was investigated. Some feasible methods to improve the elastocaloric effect were suggested.

P31_392

Modulation of NI_2MnGa described by generalized susceptibility based on Wannier functions.

Dominik Váňa, Jaroslav Hamrle
Faculty of Nuclear Sciences and Physical Engineering, Czech Technical University, Prague, Czech Republic

The generalized susceptibility describes the tendency (energy stability) of the cubic phase to become modulated. A typical example is the modulation of Ni_2MnGa [1] which can undergo structural transformation from austenite to a modulated structure. The generalized susceptibility is calculated using occupation probability (Fermi-Dirac distribution), however, this approach omits the dependence which the coupling coefficient of the electron-lattice interaction has on electronic states. The goal of this work is to express generalized susceptibility with calculated coupling coefficients. As the first step, we express generalized susceptibility using Wannier functions, modifying the original approach of Motizuki [2], based on a linear combination of atomic orbitals.

- [1] O. Söderberg et al, *Ni-Mn-Ga multifunctional compounds*, Mater. Sci. Eng. A **481**, 80 (2008)
- [2] K. Motizuki, N. Suzuki, Microscopic Theory of Structural Phase Transitions in Layered Transitional-Metal Compounds, D. Reidel Publishing Company (1986)

P32_209

Tensile deformation of cold rolled Fe-Ni-C metastable austenitic steel investigated by in-situ synchrotron XRD

Naoki Harada, Si Gao, Nobuhiro Tsuji
Graduate School of Engineering, Kyoto University, Yoshida Honmachi, Sakyo-ku, Kyoto, Japan

Metastable austenitic steels exhibit excellent strength and ductility due to deformation induced martensitic transformation (DIMT). However, fully recrystallized austenitic steels usually show low yield strength due to the soft FCC crystal structure. Plastic deformation is an effective way to enhance the yield strength of austenite phase by strain hardening, but its impact on DIMT and deformation behavior during subsequent tensile deformation remains unclear. The present study aims to investigate effects of cold rolling on tensile properties and DIMT behavior of a metastable austenitic steel.

An Fe-24Ni-0.5C (mass%) metastable austenitic steel with a fully recrystallized coarse-grained austenite microstructure was used as the starting material in the present study. The starting material was cold rolled by 50% reductions in thickness to obtain the cold rolled specimen. Tensile tests at room temperature were performed to access their mechanical properties, and microstructural observations were conducted using SEM-EBSD. Digital Image Correlation (DIC) method was also used to evaluate local strains of the specimens showing inhomogeneous deformation during tensile deformation. In-situ synchrotron X-ray diffraction measurements during tensile tests were performed at SPring-8 BL13XU to quantitatively measure DIMT behavior during deformation.

The room temperature tensile tests showed that the starting material had a yield strength of 200 MPa and a total elongation of 71%. For the 50% cold-rolled material, the yield stress rose significantly to 1100 MPa and the total elongation decreased to 54%, still exhibiting a combination of high strength and large ductility. Notably, the cold-rolled material exhibited Lüders-type inhomogeneous deformation after yielding, with a Lüders strain of 12%. The in-situ XRD measurements revealed that both the starting material and the cold-rolled material did not have martensite before the tensile deformation. DIMT was observed in both materials during the deformation. After the tensile deformation, the volume fraction of martensite increased to 25% for the starting material and 35% for the cold-rolled specimen. Additionally, the in-situ XRD measurement highlighted significant differences in the phase internal stresses between austenite and martensite phases in the cold-rolled specimen, which accounted for its high strain hardening rate. The results of the combined DIC and in-situ XRD analysis will be discussed in the presentation.

P33_302

Mechanical Testing at Elevated and Cryogenic Temperatures with Concurrent Acoustic Emission and Electrical Resistivity Monitoring

Jan Čapek, Michal Knapek
Charles University, Prague, Czech Republic

Understanding the deformation mechanisms of materials under extreme temperature conditions is crucial for their reliable application. This study presents an advanced mechanical testing methodology that integrates acoustic emission (AE) and electrical resistivity measurements during tensile loading at both elevated and cryogenic temperatures. The combination of AE and resistivity monitoring provides real-time insights into microstructural changes, and phase transformations. The results highlight the correlation between mechanical behavior, and defect evolution, offering a comprehensive approach to material characterization under non-ambient conditions.

P34_271

Surface Microstructures Formed by Shot-Peening of Fe-33mass%Ni Alloy

Marie Kondo, Hisashi Sato, Takuma Kishimoto, Yoshimi Watanabe
Nagoya Institute of Technology, Nagoya, Aichi, Japan

Shot-peening (SP) is surface treatment processing which countless hard-particles hit on the surface of materials. When the Fe-33%Ni alloy with only austenite phase (γ) is shot-peened, the strain-induced martensitic transformation occurs [1]. On the other hand, in the case of the Fe-33%Ni alloy containing large amount of martensite phase (α'), the reverse transformation from α' to γ occurs by the SP. Moreover, as the SP is prolonged, the volume fraction of γ is the same between these two kinds of the SPed Fe-33%Ni alloy. In this way, although the phase transformation caused by the SP of the Fe-33%Ni alloy is different depending on the initial microstructure, the final microstructure is independent of the initial microstructure [1]. However, its detailed microstructures, such as grain size, orientation relationship (OR) between α' and γ, have not been clear. In this study, the surface microstructures of the SPed Fe-33%Ni alloy are investigated.

The Fe-33%Ni alloy specimens were austenitized at 1100 °C for 30 min and then water-quenched. Some of the specimens were subzero-treated in liquid nitrogen for 30 min to obtain α'. Finally, two kinds of the specimens were obtained. One is the specimen containing only γ (A-specimen) while the other one is the specimen containing 82 vol% of α' (M-specimen). Using these specimens, the SP was performed at 0.6 MPa in pressure for 3 min and 20 min. Then, the SPed surfaces were polished and its microstructures were observed by electron backscattered diffraction (EBSD) with spherical indexing method.

Figures 1 (a) and (b) show microstructure of the A-specimen and the M-specimen SPed for 20 min, respectively. In both specimens, the α' and γ grains are refined and these grains have granular shape. In addition, the α' has {111} fiber texture, where <111> is parallel to peening direction, while the γ has {110} fiber texture, where <110> is parallel to the peening direction. Since the SP often forms the fiber textures, these textures are formed by the SP. Furthermore, the α' and the γ in the both specimens have OR close to Greninger-Troiano OR. It is concluded that the surface microstructure is formed by the severe plastic deformation and the phase transformation due to the SP.

[References]
1. H. Sato, T. Nishiura, T. Moritani, Y. Watanabe, Surf. Coat. Technol., 462 (2023) 129470.

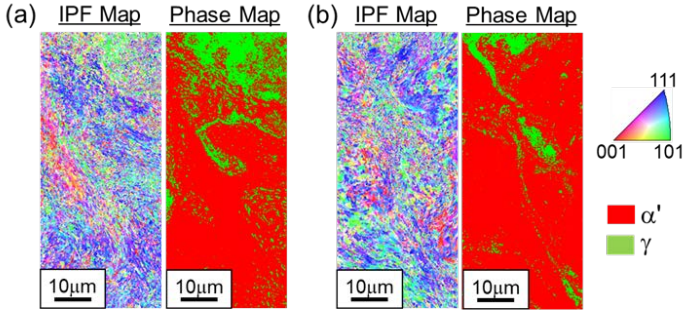

Fig. 1 Inverse pole figure (IPF) and phase maps on the surface of (a) A-specimen and (b) M-specimen SPed at 0.6 MPa for 20 min.

P35_292

Acoustic emission measurements during plastic deformation of FeMn(Cr) TWIP steel.

Lajos Daróczi[1], Asmaa A. Azim[1,2], Erzsébet Nagy[3], László Z. Tóth[1], Valéria Mertinger[4], Dezső L. Beke[1]
[1]University of Debrecen, Debrecen, Hungary. [2]Ain Shams University, Cairo, Egypt. [3]MTA-ME Material Science Research Group, Miskolc, Hungary. [4]University of Miskolc, Miskolc, Hungary

Stress induced martensitic transformation and twinning in the martensitic phase play determining role in the plastic deformation of manganese TWIP steels, resulting high toughness and deformability. It was shown [1] that starting from as quenched state (with about 85% *e* martensite and 15% austenite) the stress induced transformation at different temperature led to different phase compositions below 150ºC and above. Below 150ºC the *a* martensite was also always present in the end-product, while only the ratio of volume fractions of the austenite and *e* martensite changed above 150ºC. The above processes can cause significant acoustic emission activity during stress induced transformations. Acoustic emission was measured during tensile test of Fe 17.7wt%Mn 2.26wt%Cr steel in the 25 ^{0}C-300 ^{0}C temperature range. Yield stress and the cumulative acoustic energy values drop to a low level above 150 ^{0}C. Below 150 ^{0}C the noise activity is concentrated to the first part of the stress-strain curve (where the versus curve starts to deviate from the linear behaviour), while above 150 ^{0}C low level almost uniform noise activity can be observed in the whole deformation range. The statistical analysis of the acoustic noise was also performed. The probability distribution densities of the noise parameters are power functions characteristic to driven critical processes.

[1] A Talgotra et al. 2018 IOP Conf. Ser.: Mater. Sci. Eng. 426, 012046

P36_186

Novel sub-grain structures in B2 of a cold-rolled TiNi shape memory alloy with unique property

Qianglong Liang[1], Dong Wang[1], Xiangdong Ding[1], Yunzhi Wang[2], Michael Mills[2]
[1]Xi'an Jiaotong University, Xi'an, Shaanxi, China. [2]The Ohio State University, Columbus, Ohio, USA

Plastic deformation significantly alters the microstructure and properties of TiNi shape memory alloys. This work investigates the formation of a unique herringbone-like sub-grain structure with extended twin boundaries in the B2 phase of a cold-rolled $TiNi_{50.8}$ (at. %) and its impact on the superelasticity of the alloy. Detailed electron back-scatter diffraction (EBSD) analysis reveals abundant sub-grain areas in different orientations distinct from the matrix grain after multiple passes in cold-rolling deformation. Notably, unique band and herringbone structures emerge within the sub-grain areas, with all the boundaries identified as coincident site lattice (CSL) boundaries. Further analysis reveals spontaneous CSL boundary generation following periodic $<011>_{B2}$ and $<001>_{B2}$ tilt axes perpendicular to the normal direction of the deformed surface in $[100]_{B2}$ oriented grains, forming a characteristic quadruple junction within the herringbone structure, distinct from the single $[011]_{B2}$ tilt axis identified in the band structure. Transmission electron microscopy (TEM) identifies B2 twin relations corresponding to the special CSL Σ boundaries, while dark-field and high-angle annular dark-field (HAADF) images show B19′ martensitic nanodomains decorating the twin boundaries. This extended twin boundary structure enhances drastically cyclically stable superelasticity characterized by much more limited functional fatigue, 27% lower modulus and 76% larger recoverable strain as compared to the solution-treated sample after 100 training cycles. Our study provides new insights into the microstructure evolution and enhancement of the superelastic properties of TiNi SMAs by cold-rolling, offering a novel approach to optimize the functionality of SMAs by introducing special sub-grain structures with martensitic-nanodomains-nested B2 twins through simple cold-rolling process.

P37_218

Effect of excess Ti solutes on the martensitic transformation behavior and microstructure of Ti-rich $Ti_{50+x}Ni$ (x = 0, 0.5, 1, 1.5, 2) shape memory alloys via rapid solidification

Nian-Hu Lu, His-Chao Lin, Chih-Hsuan Chen
National Taiwan University, Taipei, Taiwan

Martensitic transformation behavior and microstructural characteristics of Ti-rich TiNi shape memory ribbons fabricated by the melt-spinning method were investigated. The experimental results showed that the fraction of Ti_2Ni phase in the bulk samples increased from 2.3 % to 14.6 % as the Ti content increased. Compared with the bulk samples, no Ti_2Ni phase was observed in the ribbon samples due to the rapid solidification process, forming supersaturated TiNi SMA with excess Ti solutes. One-step B2↔B19' martensitic transformation was exhibited in all bulk samples, while a two-step martensitic transformation from B2↔R↔B19' was observed in the rapid solidified ribbons. When the Ti content increased from 50 to 52 at. %, the B2 to B19' transformation peak temperature of the bulk samples increased by 28.0 ºC. In contrast, the B2 to R and R to B19' transformation peak temperatures of the ribbons increased significantly by 61.5 ºC and 74.2 ºC, respectively, with increasing Ti content increased from 50 to 51 at. %. Due to the limited solubility of Ti element in the bulk samples, the Ti in the matrix slightly increased with increasing Ti content (matrix composition increased from 50.0 at. % to 50.8 at. %), leading to a minor increase in their transformation temperature. In contrast, the excess Ti element was dissolved in the matrix of ribbons during the rapid solidification process, resulting in a significant increase in their transformation temperature. However, when the Ti content of the ribbon exceeded 51 at. %, the B2 to R transformation peak temperature remained unchanged, while R to B19' one decreased by 68.2 ºC. Ti-rich G. P. zones were observed in ribbons with Ti content exceeding 51 at. % and their average length decreased from 7.0 nm (51 at. % Ti) to 3.3 nm (52 at. % Ti), while their density increased accordingly. Since the R-phase transformation involves smaller deformation, it is less sensitive to the stress field of G. P. zones, resulting in no significant change in its transformation temperature. On the other hand, the formation of the B19' phase was significantly suppressed by the high density of G. P. zones, leading to a decrease in its transformation temperature. In summary, excess Ti solutes can be introduced in the TiNi SMA via rapid solidification technique, and their martensitic transformation behavior and microstructure can be adjusted, thereby expanding their applications across various temperature ranges and enabling functional modifications.

P38_335

Superelasticity over a wide temperature range in a NiTiCu shape memory alloy via laser powder bed fusion

Haizhou Lu[1,2], Zhijie Zhou[1], Hongwei Ma[2], Shuo Yin[3], Chao Yang[2]
[1]Guangdong Polytechnic Normal University, Guangzhou, China. [2]South China University of Technology, Guangzhou, China. [3]Trinity College Dublin, Dublin, Ireland

Additively manufactured NiTi-based shape memory alloys (SMAs) can achieve good superelasticity at specific temperatures; however, the realization of superelasticity over a wide temperature range in additively manufactured NiTi-based SMAs has rarely been reported. To the best of our knowledge, this is the first study to present the in situ synthesis of $(Ni_{50.4}Ti_{49.6})_{95}Cu_5$ ternary SMA via laser powder bed fusion (LPBF) additive manufacturing process using a mixture of pre-alloyed $Ni_{50.4}Ti_{49.6}$ and elemental Cu powders to expand the temperature range for applications of superelastic NiTi-based SMAs via additive manufacturing. The alloy displayed relatively good compressive superelastic recovery strain (0.94–2.40%) within the temperature range from −75–50 °C. The distorted Ti(Ni, Cu) B2 austenite matrix and high-density stacking faults formed because the supersaturated Cu atoms significantly strengthened the matrix and impeded dislocation formation during stress-induced martensitic transformation. In addition, supersaturated Cu atoms introduced numerous lattice distortion regions into Ti_2(Ni, Cu) precipitates and impeded dislocation movement, effectively strengthening the matrix. The synergistic effect of these factors contributes to the superelasticity of LPBF $(Ni_{50.4}Ti_{49.6})_{95}Cu_5$ over a relatively wide temperature range. These findings pave the way for achieving superelasticity over a wide temperature range in LPBF-NiTi-based SMAs.

P39_172

Antwerp outreach activity for children

Dominique Schryvers, Nathalie Claes, Saied Pourbabak, Jan Popelier, Wim Huyge
University of Antwerp, Antwerp, Belgium

Each year the Flemish community organises a Day of the Sciences during which researchers from universities and other academic and research institutes can show their recent findings to the general public. The focus is on children, although some activities are more directed towards (young) adults. Shape memory and superelastic material is ideal for demonstrations, but to organise an active workshop for children is not trivial. After several lab tests we designed a metal frame with screws and bolts onto which children (10-14 year) can fold and clamp a 0.5 mm diameter Ni-Ti wire with Ms around 70°C. The activity was organised in two sessions of 10 kids, each receiving such a metal frame and a piece of wire of appr. 0.5 m. (total cost appr. € 120) Before shaping the wire onto the frame, the children were asked to first draw the wanted shape on a piece of paper showing the settings of the screws on the frame. When they were happy with the drawing, they could fold the wire around the screws and fix the end points. All 10 frames with wires were then-per set of 5-heated in a furnace for 5 to 10 min at 400°C. Frames and wires were then quenched in water after which the kids could retrieve their wire from the frames and test the shape memory in flat dishes with hot water. To keep the memory and demonstrate this spectacular material to family and friends, kids can take their piece of Ni-Ti wire home.

Next to the tables on which the kids can design and fix their wires, two posters were displayed on which parents and other visitors could read about the history and physics of SMA.

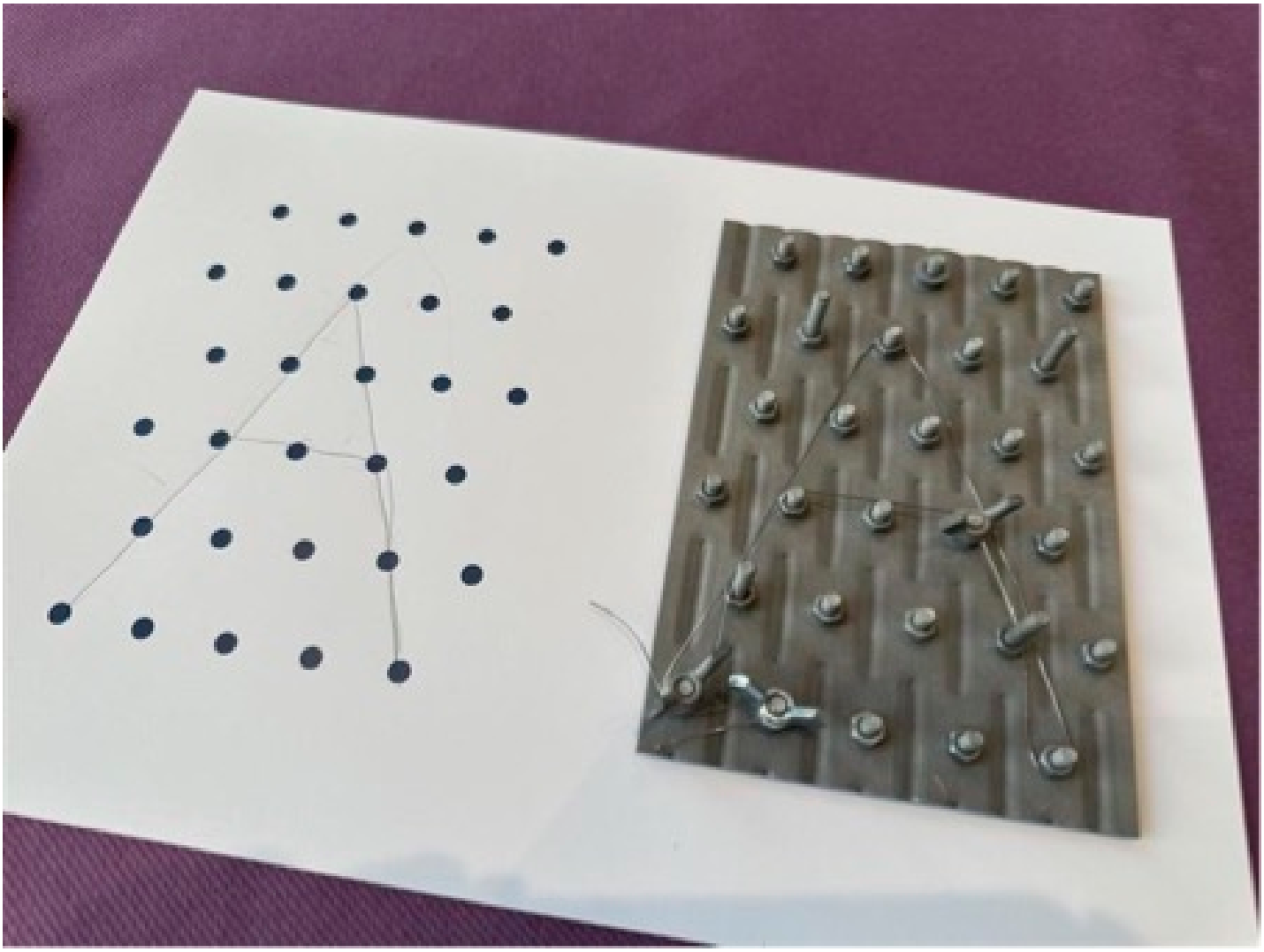

Fig.: Example of the letter A drawn on paper and as wire on the frame.

P40_308

Strain glass boundary in TiNiCu alloys showing enhancement of superelasticity over a wide temperature range

Yang Yang, Andong Xiao, Xingxing Song
Xi'an Jiaotong University, Xi'an, Shanxi, China

In ferroelectric materials, the piezoelectric properties are significantly enhanced at the morphotropic phase boundary (MPB), which is a composition-induced boundary between different ferroelectric phases. Based on the physical parallelism between ferroelectrics and ferroelastics, we design a strain glass boundary in plastic deformed TiNiCu shape memory alloy, which is a composition-induced boundary between two strain glasses with different local symmetries (B19' and R). At the strain glass boundary, the tensile strain increases by 50% and the yield strength increases by 30% over a wide temperature range. Therefore, the designed strain glass boundary enabled the alloy to exhibit narrow hysteresis and high strength (~1.05 GPa) superelasticity (~6.4%) over a wide temperature range from 123 K to 333 K. The work provides new insights into the development of high-performance superelastic alloys.

P41_309

Martensitic transformation behaviors and damping properties of Cu-Al-Fe-Co high-temperature shape memory alloys

Shihang Zhang, Guangqi Liu, Weiting Guo
National Yilan Universitu, Yilan, Taiwan

The present study investigated the microstructure, martensitic transformation behavior, and internal friction of the Cu-14Al-4Fe-*x*Co (*x* = 0-2 wt.%) high-temperature shape memory alloys (SMAs). Cu-14Al-4Fe-*x*Co SMAs all exhibited a single β → γ_1' martensitic transformation in cooling and a single γ_1'→ β martensitic transformation in heating. The martensitic transformation peak temperatures of the Cu-14Al-4Fe-*x*Co SMAs gradually increased with the amount of Co addition. However, the Δ*H* values of the Cu-14Al-4Fe-*x*Co SMAs gradually decreased simultaneously. The grain size of the Cu-14Al-4Fe-*x*Co SMAs reduced significantly with the increase of Co content. Some precipitates began to appear when the Co content was above 1.5%. The size and the amounts of precipitates further increased when the Co content in the Cu-14Al-4Fe-*x*Co SMAs increased to 2 wt.%. Increasing the Co content of the Cu-14Al-4Fe-*x*Co SMAs caused the internal friction peak temperature to approximately 200 °C. Nevertheless, the damping capacity of the internal friction peak decreased significantly at the same time.

P42_295

Damping characteristics of Cu-13.5Al-4Ni-xTi shape memory alloys

Kai-Min Huang, Shih-Hang Chang, Kuan-Ying Chu
ILAN University, ILAN, ILAN, Taiwan

This study investigated the damping properties of Cu-13.5Al-4Ni-xTi (x=0, 1, 2, 3 wt.%) shape memory alloys (SMAs). X-ray diffraction and differential scanning thermal analysis results showed that Cu-13.5Al-4Ni-XTi SMAs all exhibited a $\beta_1(DO_3) \rightleftarrows \beta'_1(18R)$ martensitic transformation. The martensitic transformation temperature of Cu-13.5Al-4Ni-xTi SMAs gradually increased with the increase of Ti content. Scanning electron microscopy observation showed that the amounts of X-phase precipitates in the Cu-13.5Al-4Ni-XTi SMAs increased with Ti addition. Dynamic mechanical analyzer results revealed that adding Ti atoms into Cu-13.5Al-4Ni SMA decreased the damping capacity of the $\beta_1(DO_3) \rightarrow \beta'_1(18R)$ internal friction peak as the X-Phase precipitates hinder the movements of parent/martensitic interface and the twin bounding of the transformed $\beta'_1(18R)$ martensite.

P43_284

Effects of Au addition on the internal friction of Cu-Al-Mn shape memory alloys

Wei-Jhen Hsu, Shih-Hang Chang, Wan-Yu Liao
National Ilan University, Ilan, Taiwan

This study investigated the effect of Au addition on the damping properties of the internal friction peak (IF) and intrinsic internal friction peak ($IF_{PT}+IF_I$) of the Cu-Al-Mn shape memory alloys (SMAs). Experimental results revealed that Cu-12Al-5Mn-xAu (x = 0, 1, 2, and 3 wt.%) SMAs all possessed a $\beta(L2_1) \rightleftarrows \beta'_1(18R)$ martensitic transformation. The martensitic transformation temperatures of the Cu-12Al-5Mn-xAu SMAs gradually decreased with the increase of the amounts of Au addition. The grain size of the Cu-12Al-5Mn-xAu SMAs reduced after adding Au elements into the alloys. The tan δ values of the $(IF_{PT})_{\beta(L21)\rightarrow\beta'1(18R)}$ and $(IF_{PT} + IF_I)_{\beta(L21)\rightarrow\beta'1(18R)}$ peaks both increased after Au addition because the increase of the martensite interface density facilitated the energy dissipation by twins sliding during vibration. However, adding Au element with more than 2 wt.% into Cu-12Al-5Mn SMAs caused the formation of precipitates and grain refinement, impeding the sliding of the interfaces and deteriorating the damping properties of the alloys.

P44_360

Influence of Particle Size and Microstructure on the First-Order Magnetostructural Phase Transition in Ni-Mn-Sn Heusler Alloy

Johannes Puy, Enrico Bruder, Oliver Gutfleisch, Franziska Scheibel
Technical University of Darmstadt, Darmstadt, Germany

Ni-Mn-X (X= Sn, In, Sb) Heusler alloys are promising candidates for solid-state caloric cooling applications, as they show a significant inverse magnetocaloric and conventional elastocaloric effect [1,2]. Optimizing the caloric performance of Ni-Mn-X requires a comprehensive understanding of the influence of the microstructure on the underlying first-order magnetostructural phase transition (FOMST).

In this study, we examine the influence of particle size and microstructure on the temperature-induced FOMST in Ni-Mn-Sn. Spherical gas-atomized powders and sintered powder with varying relative density, prepared by spark-plasma-sintering (SPS), are used. Gas-atomized powders minimize the conflicting effects of particle morphology and defects, commonly introduced by milling techniques [3, 4]. Magnetometry on powder reveals that decreasing the particle size from 150 µm to < 20 µm results in a sharper FOMST with reduced transition width (M_S-M_F) and increased thermal hysteresis ΔT_{hyst}. Magnetic and in-situ SEM characterization on individual particles show a sharp, jump-like FOMST (M_S-M_F < 1 K) for particles < 20 µm, whereas larger particles exhibit a continuous transition (M_S-M_F > 10 K). Electron backscatter diffraction shows an average grain size of 20 µm for all particles, indicating that the size dependence of the FOMST correlates with the single-and polycrystalline nature of the particles.

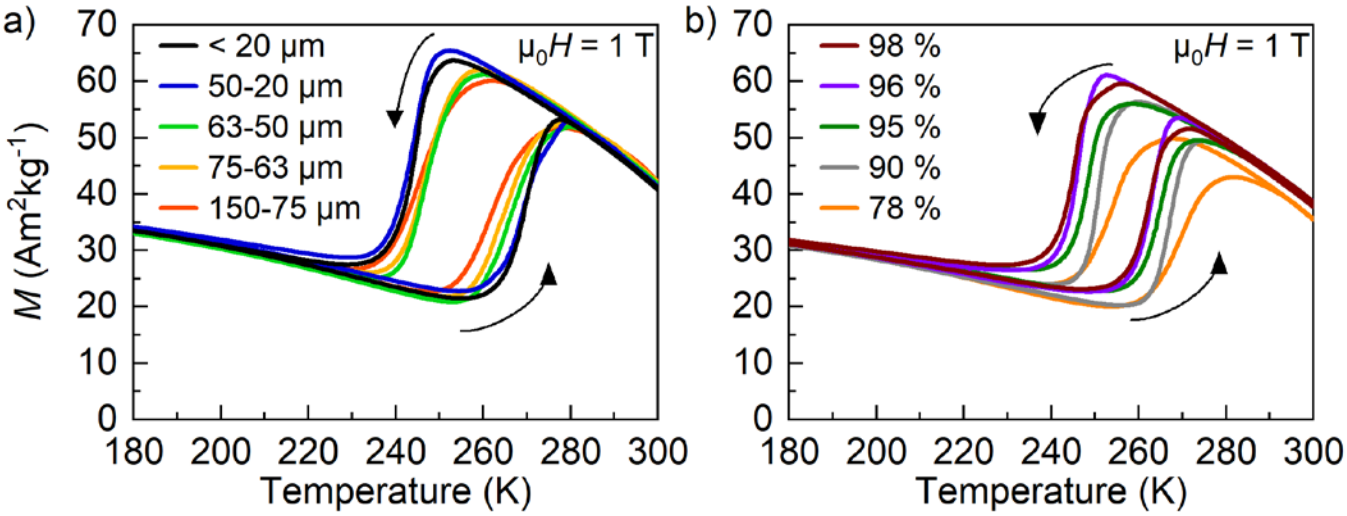

Figure 1. *M(T)*-curves of a) gas-atomized Ni-Mn-Sn with particle size between 150-75 µm and < 20 µm revealing size effect of FOMST and b) SPS Ni-Mn-Sn with relative density between 98 % and 78 % revealing effect of porosity on FOMST.

In SPS Ni-Mn-Sn, the relative density is adjusted between 77 % and 98 % to study the effect of porosity on the FOMST. A higher relative density narrows (M_S-M_F) from 18 K to 9 K and lowers the transition temperature from 263 K to 254 K. In-situ optical microscopy shows that martensite nucleation occurs preferentially at free particle surfaces in 77 %-dense samples, while nucleation is predominantly observed at sintering necks in 98 %-dense samples.

This work was supported by the Deutsche Forschungsgemeinschaft within the CRC/TRR 270 (Project ID No. 405553726).

References

[1] L.Pfeuffer, … O.Gutfleisch, *Acta Mater.*, **2021,** *217***,** 117157.
[2] A.Gràcia-Condal, … L. Mañosa, *Appl. Phys. Rev.,* **2020,** *7*, 041406.
[3] G.Cavazzini, … M.Solzi, *J.Alloys Compd.*, **2022**, *906*, 164377.
[4] T.Gottschall, … O.Gutfleisch, *Adv. Funct. Mater.*, **2017**, *27*, 1606735.

P45_337

Low melting point composites based on metamagnetic Ni-Co-Mn-In-Cu alloy for magnetic refrigeration

Vicente Sánchez-Alarcos[1], Paulo La Roca[2], Elisa Gabriela Herrera[1], Vicente Recarte[1], Antonio Urbina[1], José Ignacio Pérez-Landazábal[1], Rubén Santamarta[3], Jaume Pons[3], Concepció Seguí[3]
[1]Departamento de Ciencias (INAMAT2) Universidad Pública de Navarra, Pamplona, Navarra, Spain. [2]Centro Atómico Bariloche (CNEA), CONICET, Bariloche, Argentina. [3]Departamento de Física, Universitat de les Illes Balears, Palma de Mallorca, Spain

Refrigeration is becoming increasingly essential in various aspects of daily life. Conventional vapor-compression technology not only relies on volatile substances that severely harm the ozone layer but also is approaching its efficiency limits. An interesting alternative approach involves magnetic refrigeration based on metamagnetic shape memory alloys, which exhibit a giant magnetocaloric effect linked to a magnetically induced structural martensitic transformation. However, these materials are highly brittle, leading to poor mechanical integrity in cyclic processes. In this context, a new composite material made of a low-melting-point metal matrix embedding metamagnetic shape memory alloy particles is proposed as an alternative solution to address the inherent brittleness of bulk alloys while showing good heat transfer during operation

Magnetocaloric composites were produced by isostatically pressing a mixture of Ni-Co-Mn-In(Cu) microparticles and Sn-Pb powders. The martensitic transformation and the magnetic properties of the active microparticles, obtained from ball milling of the bulk alloys, were optimized prior to their incorporation into the metal matrix. A significant pressure-induced martensite stabilization is observed in all freshly produced composites, regardless of the initial state of the milled microparticles. Furthermore, upon heating to 473 K, above the Sn-Pb melting temperature, the eutectic structure of the matrix becomes unified all along the composite, while, interestingly, the macroscopic form is still preserved. The aged composites show not only a very high magnetocaloric effect but also an excellent mechanical consistency.

P46_356

Optimizing NiTi Interatomic Potentials Through Atomic Cluster Expansion

Petr Šesták[1,2], Petr Jaroš[1], Miroslav Černý[2], Petr Sedlák[1]
[1]Institute of Thermomechanics of the CAS, Prague, Czech Republic. [2]Brno University of Technology, Brno, Czech Republic

Atomistic simulations provide a way to observe atomic behavior at the nanoscale level. There are two main approaches: the first is based on quantum mechanics (ab initio simulations), and the second relies on Newton's mechanics (molecular dynamics). However, despite advancements in computer science, including quantum computing, both approaches remain limited. Ab initio simulations are constrained by the size of the simulation cell and the necessity to perform quasi-static simulations at T = 0 K due to their complexity and high computational demands, while molecular dynamics primarily suffer from the accuracy of interatomic potentials. Many of these limitations can be mitigated through machine learning, which enables the construction of interatomic potentials from training sets obtained in ab initio simulations.

In this work, we present an interatomic potential for NiTi based on the Atomic Cluster Expansion, developed using the Pacemaker software package. We validate this potential by comparing it against the results of simulations using other interatomic potentials, quantum-mechanical calculations, as well as our own experimental data. Our quantum-mechanical calculations utilize density functional theory (DFT) within the generalized gradient approximation (GGA) to determine the ground-state structural, electronic, thermodynamic, and elastic properties of NiTi in low-temperature (martensitic) phase. The target properties include elastic constants, phonon spectra calculations, and vacancy formation energy. Specifically, the stress-strain method was employed to compute the full tensor of the second-order elastic constants and assess the mechanical stability of the studied phases, ensuring that the results are consistent with those obtained using other established potentials.

P47_243

Phase-field study on austenite-martensite interface formation in Shape Memory Alloys

Bingqian Wang, Chengguan Zhang, Ziad Moumni, Yongjun He
LMI, UME, ENSTA Paris, Paris, France

The microstructure of the interface at the habit plane between austenite and twinned-martensite in the Shape Memory Alloys can affect the material behavior such as the energy dissipation and the fatigue behavior [1-5]. In this paper, the microstructure of the austenite-twinned martensite interface obtained by the thermal-induced phase transition under different temperature gradient is studied using finite-strain phase-field model. As shown in Fig.1, the microstructure is assumed periodic and two-dimensional plane strain, and the boundary condition only considers the temperature gradient. It's shown that interface temperature ($\Theta_{interface}$) deviates from the equilibrium temperature Θ_0 at which the austenite and martensite have the same chemical energy. In addition, the edges of the zigzag-shaped interface are not fully compatible structures between the martensite variants and the austenite in 2D case. These results can be used to better understand the stress concentration around the interface, which can affect the fatigue behavior of SMA during phase transformation.

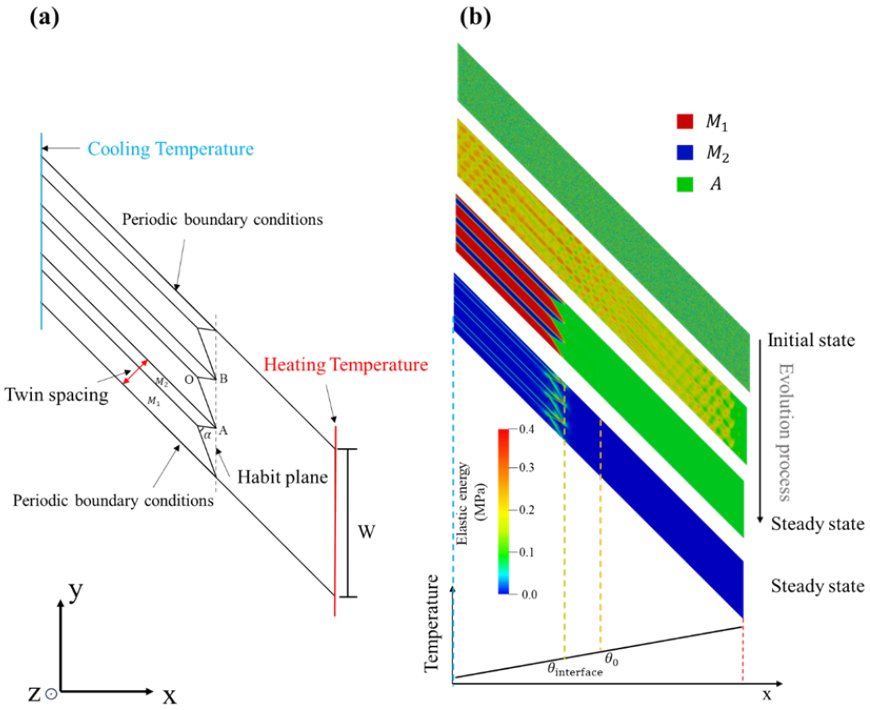

Figure 1. (a) Schematic diagram of simulated interface layer (b) The automatic microstructure evolution to the equilibrium interface pattern (distributions of the phases and the associated elastic energy) under a given temperature gradient.

Reference

[1] Tůma K, Stupkiewicz S. Int. J. Solids Struct. 2016;97-98:89-100.
[2] Zhang Z, James RD, Müller S. Acta Mater. 2009;57(15):4332-52.
[3] Bronstein E, Faran E, Shilo D. Acta Mater. 2019;164:520-9.
[4] Zhang C, Chen X, Gao X, Brisset F, Hubert O, He Y. Acta Mater. 2024;281.
[5] Zhang Y, Moumni Z, You Y, Zhang W, Zhu J, Anlas G. Int. J. Plast. 2019;115:307-29.

P48_326

Automated Classification of Martensitic Microstructures in Ti6Al4V via Transfer Learning: A Metallographic and Literature-Based Approach

Edilvando Eufrazio, Fábio Oliveira, Leonardo Linhares
National Institute of Technology, Rio de Janeiro, Rio de Janeiro, Brazil

This study investigates the martensitic microstructure of the titanium aluminum vanadium alloy (Ti6Al4V), produced through additive manufacturing, by integrating metallographic experiments with a comprehensive literature review. High-resolution images capturing the distinct features of the martensitic phase were obtained under carefully controlled experimental conditions, while the literature provided essential insights into the phase transformation mechanisms and morphological characteristics intrinsic to additively manufactured Ti6Al4V.

Leveraging the synergy between experimental observations and literature-derived knowledge, we propose an innovative computational framework based on transfer learning using a pre-trained convolutional neural network (CNN), specifically VGG16. VGG16 is a widely recognized deep learning model renowned for its simplicity and robust performance in image analysis tasks. It features a uniform architecture consisting of 16 layers, including 13 convolutional layers with small (3×3) filters and 3 fully connected layers, originally culminating in a softmax output layer. The network's modular design allows it to effectively extract hierarchical features from metallographic images, capturing both fine-grained textures and broader structural patterns critical to understanding the martensitic transformation.

In our approach, VGG16 is employed primarily for its powerful feature extraction capabilities, tailored by fine-tuning its later layers to accommodate the specific nuances of metallographic images of additively manufactured Ti6Al4V. This strategy simplifies the implementation by reducing the need for an extensive training dataset and accelerates the computational training process while ensuring high-fidelity recognition of microstructural details such as grain boundaries and phase distributions.

The proposed methodology offers substantial opportunities for further expansion. Future investigations will refine the deep learning model, integrate larger datasets, and explore a broader spectrum of microstructural variations. This ongoing research is expected to continuously bridge the gap between traditional metallographic characterization and advanced computational techniques, driving significant advancements in materials analysis and enhancing quality control for additively manufactured alloys.

P49_216

Phase-field simulation of martensitic transformation during continuous cooling in polycrystalline low-carbon steel

Takumi Okamoto, Yuhki Tsukada, Toshiyuki Koyama
Nagoya University, Nagoya, Aichi, Japan

Lath martensite in low-carbon steel is an essential microstructure for high-strength structural components. The crystal structure change from austenite (γ-fcc) to martensite (α'-bct) during martensitic transformation (MT) is accompanied by large lattice deformation, generating an elastic field inside the material. Part of the internal elastic strain energy is relaxed by the formation of multivariant structures consisting of multiple crystallographic orientation variants (OVs) of the α' phase and the slip of the α' and γ phases during MT. In this study, the microstructure evolution during MT accompanying slip of the α' and γ phases in low-carbon steel was investigated using the phase-field (PF) method.

A simulation of MT at a cooling rate of 1 K / s was performed for an Fe–0.1 mass% C alloy. The total free energy of microstructure was formulated as the sum of chemical free energy, gradient energy, and elastic strain energy. The Gibbs energy difference between the γ and α-bcc phases was used for the driving force for MT. The temperature dependence of the lattice parameters and elastic constants was considered in the elastic strain energy calculation. The α'/γ interface mobility was determined so that the experimental data on the change in volume fraction of the α' phase during the initial stages of MT [1] could be reproduced by simulation. The simulation started with a γ-phase polycrystalline structure.

Simulation result shows that as the temperature decreases, a multivariant structure composed of three OVs (Bain variants) is formed. Analysis of the elastic field during MT reveals that the formation of multivariant structures is favorable from the perspective of elastic strain energy relaxation. The dislocation density in the α' phase increased rapidly at the beginning of MT and then became almost constant. Meanwhile, the dislocation density in the γ phase gradually increased by two orders of magnitude during MT. These behaviors are consistent with results obtained from in-situ neutron diffraction and X-ray diffraction experiments [2,3]. Compared with previous simulation results at 300 K [4], the change in dislocation density simulated in this study is close to the experimental result

[1] C. Mao *et al*., Mater. Des. **197** (2021) 109252.
[2] J. Macchi *et al*., Mat. Sci. Eng. A **800** (2021) 140249.
[3] W. Gong *et al*., Acta Mater. **250** (2023) 118860.
[4] Y. Tsukada *et al*., Proceedings of the 7th International Symposium on Steel Science (ISSS 2024), pp. 49–54 (2024).

P50_340

Regular Twinning in Epitaxial Rh_2MnSb Thin Films

Artem Shamardin, Stanislav Cichoň, Esther de Prado, Oleg Heczko
FZU-Institute of Physics of the Czech Academy of Sciences, Na Slovance 1999/2, 18200, Prague, Czech Republic

Epitaxial thin films of Rh_2MnSb grown on MgO substrates by DC magnetron sputtering exhibit a pronounced tiled morphology, indicating regular twinning. Microstructural studies revealed that films deposited at 600 °C have a clearly pronounced mosaic surface with minimal surface roughness that does not exceed 4 nm (Fig.1 a). Increasing the deposition temperature leads to an increase in surface heterogeneity and suppression of the visibility of twinning. TEM analysis showed the presence of X-type twin configurations [1] with alternating light and dark bands inclined at an angle of 47°-50° to the substrate (Fig 1 b). XRD measurements confirmed the epitaxial growth of the films and the presence of $L2_1$ structural ordering. Analysis of the pole figures revealed a unique central pole for the symmetric (004) reflection, indicating the perpendicularity of the c-axis of the unit cell to the substrate, and four weaker spots for the symmetric (400) reflection, confirming the presence of four twin domains, which are symmetrically distributed azimuthally. The results obtained are consistent with an X-type model of twinning in which variants of twins with the c-axis perpendicular to the surface predominate with only a small fraction of variants with the a-axis (Fig 1 c).

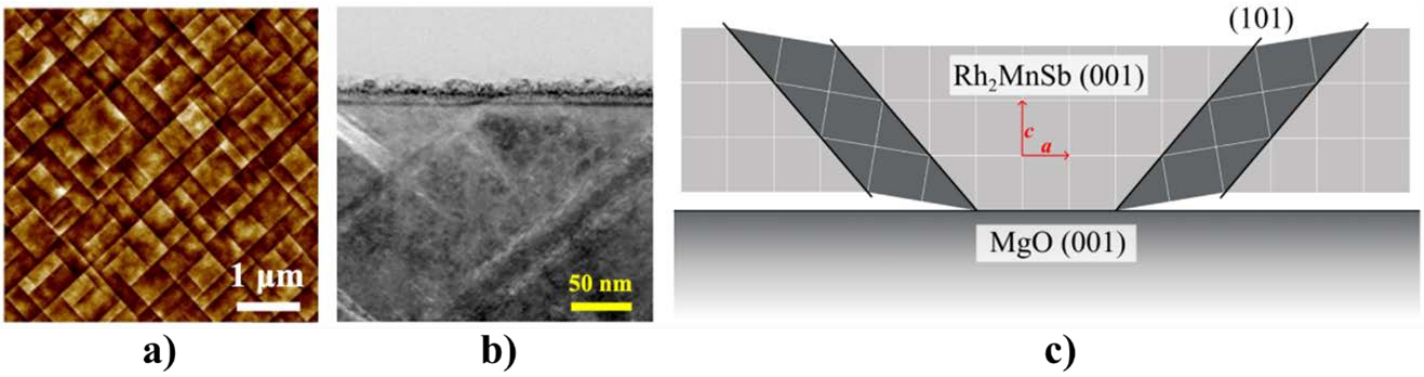

Fig.1. Microstructure of the Rh_2MnSb thin film prepared at 600 °C: a) AFM; b) TEM cross-section; c) schematic twinning geometry of tetragonal martensite in film

Reference

[1] R. Niemann et al., Nucleation and growth of hierarchical martensite in epitaxial shape memory films, Acta Materialia 132 (2017) 327-334 http://dx.doi.org/10.1016/j.actamat.2017.04.032

Acknowledgements

This work was supported by OP JAK project No.CZ.02.01.01/00/22_008/0004591 and Czech Science Foundation Grant No.24-11361S.

P51_223

Effect of Carbon Content on Microstructures of Low-Carbon Lath Martensite

Shigekazu Morito, Taisuke Hayashi, Anh Hoang Pham
Shimane University, Matsue, Shimane, Japan

Lath martensite has been incorporated into high-strength low-alloy steels. The increasing use of lath martensite for this purpose necessitates an understanding of its mechanical behaviour within the low-carbon range. The size of the lath martensite structure in low-carbon steel varies significantly with the amount of carbon. To elucidate this structural change, an analysis of lath martensite in low-carbon steel containing carbon ranging from 0.0023 to 0.1 mass% was conducted.
The specimens were composed of Fe–1.5 mass% Mn with 0.0023, 0.01, and 0.1 mass% carbon. The heat treatment involved austenitising at 1200°C, followed by water or ice brine quenching. Examination by optical microscopy confirmed that all the specimens had a fully martensitic structure. Further analyses of the microstructures were performed using optical microscopy, SEM and SEM-EBSD.
Optical microscopy revealed that the block thickness decreased with increasing carbon content. Additionally, the morphologies of the blocks and packets, which are composed of a set of blocks, changed to an entangled structure for the higher carbon specimens. Quantitative analyses using EBSD maps revealed that, in the specimen containing 0.01 mass% carbon, there are “coarse” blocks and relatively fine and fragmented blocks within the coarse blocks. The fine blocks, most of which are included in the adjacent coarse blocks, are approximately 1 μm in width. The coarse blocks and fine-inclusion-type blocks are mostly related by a near-twin orientation relationship, which is a frequently observed orientation relationship in the martensite. The coarse and fine block pairs are adjacent to each other along high-angle boundaries that are nearly parallel to the habit plane of the martensite. These fine blocks, which are separated from the “host” blocks by high-angle boundaries, are not observed in the 0.0023% C steel, and it is speculated that the carbon addition causes the nucleation and growth of these fine-inclusion-type blocks. The fine-inclusion-type blocks could be “nuclei” of medium-sized blocks and are key to the refining of blocks; the fine block structure would be caused by the growth of a part of these fine blocks in steels with higher carbon content.

P52_180

Phase-field modeling of martensitic transformation in ferrous shape memory alloy exhibiting superelasticity

Miyu Takagi, Yuhki Tsukada, Toshiyuki Koyama
Nagoya University, Nagoya, Aichi, Japan

Fe–Mn–Al–Ni shape memory alloy exhibiting superelasticity has attracted considerable attention due to its low material cost and small temperature dependence of the critical stress for martensitic transformation (MT) between the bcc (α) matrix and fcc (γ′) martensite phases. The nanoscale NiAl (B2) phase precipitated in the α phase is presumed to play an important role in exhibiting superelasticity, but its specific role is unknown. In this study, the effect of the B2 phase on the microstructure evolution during α→γ′ MT was investigated by the phase-field method.

First, the microstructure of the nanoscale B2 phase precipitated in the α phase was prepared by simulating the spinodal decomposition at 300 K in Fe–34Mn–15Al–7.5Ni (at. %) single crystal alloy. Next, the obtained (α + B2) structure was used for simulating α→γ′ MT under external compressive stress along the $[100]_{\alpha}$ direction at 300 K. In the phase-field model used for the simulations, the chemical free energy was formulated based on the Gibbs energies of the constituent phases calculated using a thermodynamic database of equilibrium phase diagram. Furthermore, the elastic strain energy was formulated considering the eigenstrain arising from both the precipitation of the B2 phase and the α→γ′ MT.

The simulation result showed that two of the three Bain variants emerged along with the progression of MT. When the magnitude of the external stress reached 700 MPa and the external stress was removed, γ′→α reverse transformation occurred. The macroscopic stress-strain curve along the external stress axis was also obtained in the simulation, which exhibited superelasticity, with the critical stress for MT being approximately 400 MPa. The γ′→α reverse transformation was observed to be initiated from the retained α phase adjacent to the B2 phase. It was confirmed that the B2 phase is energetically stable even when the external compressive stress of 700 MPa is applied, and can act as the initiation site for the γ′→α reverse transformation.

P53_405

In-situ characterization of supercritical martensitic phase transformations in NiFeGaCo single crystals using high-energy diffraction microscopy

Timothy Thompson[1], Abdulhamit Sarac[1], Sangwon Lee[1], Amlan Das[2], Fei Xiao[3], Ashley Bucsek[1]
[1]University of Michigan, Ann Arbor, MI, USA. [2]Cornell High Energy Synchrotron Source, Ithaca, NY, USA. [3]Shanghai Jiao Tong University, Shangai, China

Superelastic behavior, enabled by reversible martensitic phase transformations, has been observed in many multiferroic materials like shape memory alloys. Typically, martensitic phase transformations involve the formation and migration of interfacial stress fields at phase interfaces, causing hysteresis and degradation of superelastic behavior. However, recent research indicates that above a critical temperature (in a supercritical thermodynamic state), the transformation occurs with exceptional cyclic stability and no hysteresis. This study uses high-energy diffraction microscopy (HEDM) to characterize martensitic phase transformations below ("subcritical") and above ("supercritical") the critical temperature during compression of NiFeGaCo ferromagnetic shape memory alloys. In-situ HEDM experiments are supported by in-situ differential interference contrast (DIC) optical microscopy. Results reveal the evolution of martensite within single crystals and changes in phase interfaces. These findings will enhance the fundamental understanding of supercritical martensitic phase transformations.

P54_251

Hydrogen-Induced Modifications in Nickel-Titanium Alloys: Correlating Electronic Transport and Phase Transformations

Torben Tappe[1,2], Finn Hingmann[1], Jan Frenzel[3], Gabi Schierning[1,2], Klara Lünser[1,2]
[1]Applied Quantum Materials, Institute for Energy and Materials Processes, University of Duisburg-Essen, Duisburg, Germany.
[2]Research Center Future Energy Materials and Systems, Research Alliance Ruhr, Bochum, Germany. [3]Chair for Materials Science and Engineering, Institute for Materials, Ruhr University Bochum, Bochum, Germany

Hydrogen embrittlement poses a significant challenge in the development of hydrogen-based technologies, as hydrogen can degrade the mechanical properties of metals and alloys. Nickel-titanium (NiTi) alloys, renowned for their shape memory and superelastic behavior, are not exempt from this issue. Understanding the way hydrogen interacts with the electronic transport properties of NiTi is particularly relevant for elucidating the mechanisms underlying hydrogen embrittlement, especially in contexts where NiTi components may be exposed to high-pressure hydrogen atmospheres. In this study, we examine how hydrogen affects both the electronic transport properties and phase transitions of NiTi (51.00 at.% Ni, 49.00 at.% Ti), aiming to gain insight into the structural and electronic modifications that occur under hydrogen uptake.

NiTi samples were placed in an autoclave at elevated pressures and temperatures in a hydrogen-containing atmosphere. Subsequently, Seebeck measurements and differential scanning calorimetry (DSC) were conducted to investigate how hydrogen exposure influences the martensitic and austenitic phase transitions, as well as the material’s overall electronic transport properties.

The experimental data indicate variations in the Seebeck coefficient, suggesting a potential interaction between hydrogen and the free electrons in NiTi. In parallel, the DSC results reveal shifts in the transformation temperatures, implying that hydrogen may affect the stability of different crystallographic phases, either by occupying specific lattice sites or by modifying the local electronic environment.

These observations demonstrate that hydrogen influences both the electronic transport properties and phase transitions of NiTi, highlighting the importance of electronic factors in the study of hydrogen embrittlement in intermetallic alloys.

P55_240

Microstructural Studies of Fe-Pd Martensitic Crystals using Elastic and Inelastic Neutron Scattering

Trevor Finlayson[1], Garry McIntyre[2], Kyle Portwin[3], Kirrily Rule[2], Jun Cui[4]
[1]University of Melbourne, Melbourne, Victoria, Australia. [2]ANSTO, Sydney, NSW, Australia. [3]University of Wollongong, Wollongong, NSW, Australia. [4]Iowa State University, Ames, Iowa, USA

Fe-x at. % Pd alloys for $30 \leq x \leq 32$, transform martensitically, exhibiting quite complex structural behaviour on being cooled to low temperatures, as illustrated in the published phase diagram[1]. From x-ray diffraction studies for an Fe-30.2 at. % Pd crystal, Seto *et al.*[2] suggested an "intermediate state" between the austenite (fcc) and martensite (fct) phases characterised by a "two-tetragonal-mixed" phase. From neutron scattering studies, the same authors[3] observed quasi-elastic scattering which increased as the crystal temperature approached the fcc to "intermediate phase" transition, which they interpreted as "embryonic fluctuations" of the low-temperature structure. Earlier work[4] employing inelastic neutron scattering, suggested the fcc to fct transformation was driven by a softening of low-q, TA_1 phonons. In addition, these alloys are ferromagnetic with Curie temperatures in the vicinity of 600K[4]. Consequently, they exhibit a significant magnetostrictive coefficient[5] and the magnetic shape memory effect, which could lead to technological applications.

In the current research, two crystals have been studied, employing both elastic and inelastic neutron scattering using instruments at the Australian Research Reactor, OPAL. For each crystal satellite reflections have been observed in the vicinity of certain Bragg peaks. In this presentation the temperature and field dependence for these microstructural features will be presented and the results discussed in relation to the existing published data for Fe-Pd shape memory materials.

1. M. Sugiyama, R. Oshima and F.E. Fujita, *Trans. Japn. Inst.Met.* **25**, 585-592 (1984).
2. H. Seto, Y. Noda and Y. Yamada, *J. Phys. Soc. Japn.* **59**, 965-977 (1990).
3. H.Seto, Y. Noda and Y. Tamada, *J. Phys. Soc. Japn.* **59**, 978-986 (1990).
4. M. Sato, B.H. Grier, S.M. Shapiro and H. Miyajima, *J. Phys. F: Met. Phy.*, **12**, 2117-2129 (1982).
5. T. Kakeshita, T. Fukuda and T. Takeuchi, *Mater. Sci. and Eng. A*, **438-440**, 12-17 (2006).

P56_278

Analysis of Fatigue Behavior of Martensitic Steel Using Digital Holographic Microscope

Yusuke Matsui, Albert Guevara, Junya Inoue
The University of Tokyo, Tokyo, Japan

This study investigates the fatigue behavior of low-carbon martensitic steel, focusing on the quantitative analysis of Persistent Slip Band (PSB) growth and its relationship with martensitic substructures. We employ a multi-modal approach that combines in-situ Digital Holographic Microscopy (DHM) with ex-situ Scanning Electron Microscopy (SEM), utilizing Electron Backscatter Diffraction (EBSD) and Electron Channeling Contrast Imaging (ECCI).

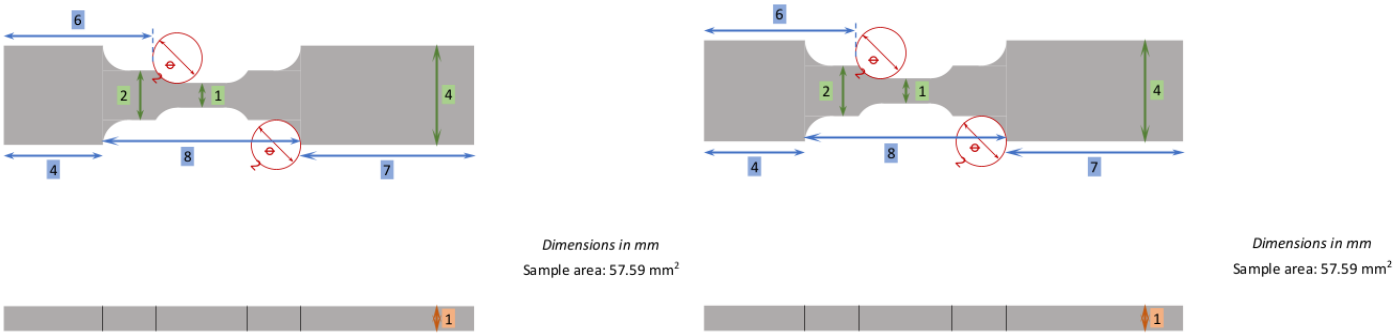

Fig 1. Fatigue specimen

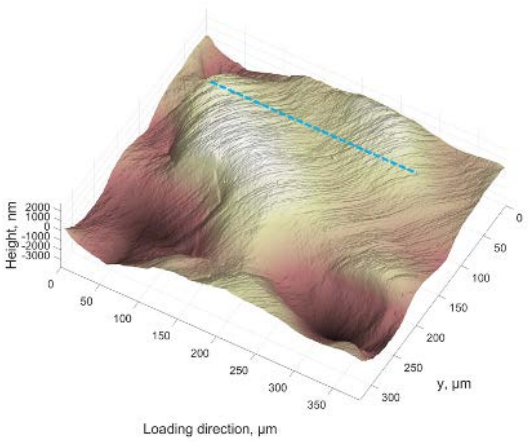

Fig.2 Reconstructedsurface morphology of fatigue specimen

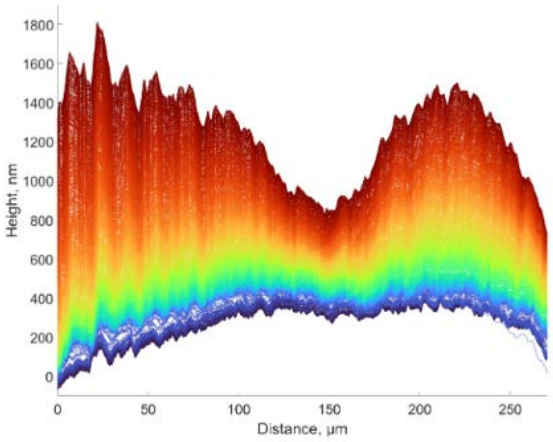

Fig.3 Height profilechange along a blue dotted line in Fig. 2

Chromium-molybdenum steel SCM415 was austenitizedat 1100℃ for 10 minutes and quenched in water to achieve a fully martensitic microstructure. Fatigue specimens (Fig. 1) were fabricated using electrical discharge machining (EDM), and the observation surface was mechanically polished. Low-cycle pulsating tensile fatigue tests were conducted, accompanied by in-situ observations of the specimen surface using DHM. Preliminary in-situ DHM observations during the fatigue test show the evolution of PDB height profiles (Fig. 2).Height profile changes along the cross-section (blue dotted line in Fig. 2) within PSB regions were reconstructed from continuous image sequences and demonstrate the growth of individual slip lines in the depth direction asdeformation increases (Fig. 3).

Fatigue tests will be conducted using the fabricated specimens, and the initiation of PSBs will be dynamically and quantitatively observed using DHM. The obtained observations will be analyzed with crystallographic analysis using SEM-EBSD and dislocation structure analysis using SEM-ECCI to elucidate the mechanism.

P57_316

Hybrid Modeling Framework for Shape Memory Alloys

Dimitris C Lagoudas, Haoyi Tian
Texas A&M University, College Station, Texas, USA

Data-driven constitutive modeling approaches have gained popularity due to their ability to capture complex material behaviors without presuming the functional form of the response. However, there exist some commonly cited drawbacks, including the requirement of large amounts of training data, poor extrapolation performance, and unguaranteed reliability. Hybrid models have emerged as a means of addressing these issues by combining the versatility of data-driven methods with the robustness of traditional models grounded in mechanics and thermodynamics. In this work, a hybrid approach is explored for the modeling of Shape Memory Alloys (SMAs) through the integration of Artificial Neural Networks (ANNs) into a rate independent thermomechanical phenomenological model for SMAs. First, the transformation hardening function is replaced with an ANN trained on experimental data to establish a hybrid model which can capture the first-order stress and temperature induced phase transformation behavior of SMAs with improved accuracy. Extensions towards advanced effects of SMAs, such as tension-compression asymmetry and irrecoverable strains, are also explored through data-driven representations of the transformation function and evolution equations. The thermodynamic consistency of the proposed hybrid model is evaluated as a check for model robustness. The hybrid model is trained on experimental data and its performance in comparison to traditional SMA modeling approaches is discussed, along with application of the hybrid constitutive model towards finite element analysis. The hybrid approach in this work is useful in accurately capturing various complex behaviors and non-proportional loading paths of SMAs. Furthermore, because of the high degree of variability in SMA behavior despite manufacturing controls, the ability to train constitutive models directly on experimental data may be advantageous.

P58_409

A Multiphase-Field Model for Grain Boundary-Induced Martensitic Transformations in Polycrystals at Finite Strains with Scale Dependence.

Newton ., Anup Basak
Indian Institute of Technology Tirupati, Tirupati, Andhra Pradesh, India

Martensitic phase transformation (PT) in polycrystalline materials, induced by grain boundaries(GBs) and their triple junctions (TJs), is studied using a thermodynamically and physically consistent nanoscale multiphase-field (MPF) approach of the Ginzburg-Landau type at large strain considering the interfacial stresses. The present model employs N order parameters (OPs) to describe the N grains in the sample and M + 1 OPs to describe the austenite (A) ↔ martensite (M) transformation and M martensitic variants. Unlike the previous MPF models, our model considers distinct energy and intrinsic size of the dry GBs and TJs energies, providing a more realistic representation. GB energies are assumed to be isotropic and vary due to PTs. A double-obstacle potential for the grains and a double-well potential for the MTs are assumed, ensuring no ‘spurious phases’ within the GBs and phase boundaries appear. The strong effect of intrinsic length scales, including dry GB widths and grain size, on the temperature of barrierless phase transformations, kinetics, and complex microstructural evolution is studied during the forward (A → M) and reverse (M → A) transformations. The simulation results show that an intermediate stationary state between A and M, called premartensite (PM), nucleate barrierlessly within the GB network at a temperature well above the critical temperature for A → M PT. As the temperature of the sample decreases, more volume fraction of the twinned microstructures evolves within the grains. The forward and reverse transformation paths differ, indicating the transformations involve hysteresis. The elastic and structural stresses within the samples are also studied.

P59_332

Structure and Microstructure-based Elastic Property study on a Co41Ni32Al27 Ferromagnetic Shape Memory Alloy Melt-spun ribbon

Rajini Kanth Bhogoju[1,2], Sarowar Hossain Md[3,2], Tusar Saha Saha[3], Mukhopadhyay Pratip Kumar[2]
[1]LSMS, TKR Centre for Research and Innovation, T. K. R. College of Engineering and Technology, Hyderabad 500097, India, Hyderabad, Telangana, India. [2]LCMP, S.N. Bose National Centre for Basic Sciences, Salt Lake, Kolkata-98, Kolkata, West Bengal, India. [3]Department of Physics, American International University-Bangladesh, Dhaka 1229, Bangladesh, Dhaka, Dhaka, Bangladesh

Co-Ni-Al FSMA is a fascinating system due to the coexistence and interplay of FSMA *β* (B2) phase grains and non-FSMA *γ* (A1)-phase, precipitated at the grain boundaries [1-3]. In the present study, a comprehensive investigation was performed on the structure, microstructure, and elastic properties of a $Co_{41}Ni_{32}Al_{27}$ melt-spun ribbon. Structural analysis through X-ray diffraction (XRD) and Rietveld refinement revealed the presence of *β* (B2, BCC) and *γ* (A1, FCC) phases, with the β phase being dominant (92.2%) and exhibiting a low atomic packing fraction, indicative of structural non-ideality. Microstructural features observed via FESEM and 3D surface profiling showed polycrystalline grain morphology with an average grain size of ~1.65 µm. Crystallite size and internal strain were further evaluated using the Scherrer and modified Williamson–Hall methods(UDM, USDM, UDEDM), revealing nanocrystalline grain dimensions (~83–142 nm), intrinsic strain, and a deformation energy density of ~43.6 kJ/m³. Dynamic Mechanical Analysis (DMA) measured the elastic response under stress, indicating dual elastic regions with Young's modulus values ranging from ~35 MPa to ~1956 MPa. These findings suggest that the unique structural and microstructural characteristics of the Co-Ni-Al ribbon significantly influence its mechanical behavior, highlighting its potential for microscale actuation and magneto-mechanical applications.

Keywords: Co-No-Al FSMA, Microstructure, Lattice Strain, Deformed Energy Density, and Stress-Induced Strain

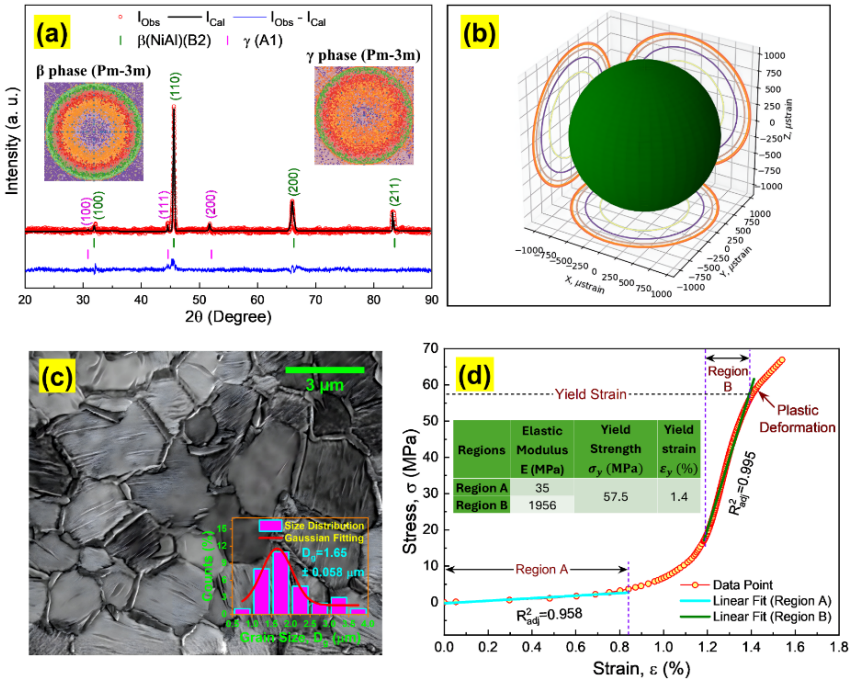

Regions	Elastic Modulus E (MPa)	Yield Strength σ_y (MPa)	Yield strain ε_y (%)
Region A	35	57.5	1.4
Region B	1956		

Fig. 1. (a) Rietveld refinement of XRD data, **(b)** micro-strain of $Co_{41}Ni_{32}Al_{27}$ ribbon, **(c)** microstructure with the inset showing Gaussian fitting of grain size distributions, **(d)** Stress-induced strain (%) obtained for $Co_{41}Ni_{32}Al_{27}$ ribbon.

Acknowledgements

BRK acknowledges DST SERB for sanction of DST Project Ref No. SR/FTP/PS-108/2009. He also acknowledges Mrs. Ramya Madam at ARCI Chennai, for the DMA data and the Principal, and Management of TKR College of Engg &Tech for constant encouragement and support, and the then Director, S. N. Bose Center for the Visiting Associateship. SH is thankful to the TWAS-Bose fellowship.

References

[1] M. S. Hossain, B. R. Kanth, P.K. Mukhopadhyay, Shape Mem. Superelasticity 3 (2017) 199.
[2] M. S. Hossain, T. Ghosh, B.R. Kanth, P.K. Mukhopadhyay, Cryst. Res. Technol. 54 (2019) 1800153.
[3] B. Rajini Kanth, N. V. Ramarao, A.K. Panda, R. Gopalan, A. Mitra, P. K. Mukhopadhyay, J. Alloys Compd. 491 (2010) 22-25.

P60_383

Structural-functional integrated TiBw/Ti–V–Al lightweight shape memoryalloy composites

Xianglong Meng, Kuishan Sun
School of Materials Science & Engineering, Harbin Institute of Technology, Harbin, China

To meet the requirements of light weight, high strength and large recoverable strain of shape memory alloys for intelligent interference sealing connections in aerospace and weapon fields, a lightweight TiB/Ti-V-Al shape memory composite with high strength and large recovery strain was obtained by introducing the TiB phase into the Ti-V-Al alloy. In present study, a TiBw/Ti–V–Al lightweight shape memory alloy composites were prepared with large recoverable strain (>5 %), high specific strength (>200 MPa cm3/g) and good elongation (>20 %). The satisfied structural and functional performances are attributed to the unique gradient microstructure, including TiB whiskers, short-range martensitic nanodomains and long-range martensitic microdomains. TiBw with the optimized orientation exhibits high load-bearing capacity. The transition area between TiBw and matrix is composed of short-range martensitic nanodomains. Nanodomains are affected by the diffused interstitial B atoms and local internal stress field regulated by TiBw. The elastic interaction energy between nanodomains and TiBw are calculated according to the Eshelby method. Upon deformation, nanodomains grow to long-range martensitic laths. The long-range martensitic laths keep stable after unloading. The microstructure evolution ties well with the Landau free energy model. It achieves effective loading transfer from matrix to reinforcement phase, resulting in less irreversible defects and better shape memory effect. In addition, grain refinement strengthening, loading transfer strengthening and solution strengthening are utilized to achieve the improvement of the strength and plasticity. The finding offers a promising inspiration for the development of new type shape memory alloy composites with integrated structural and functional properties.

P61_336

High tensile stress actuation with NiTiHf high-temperature shape memory alloys additively manufactured via laser powder bed fusion

Hongwei Ma[1,2], Petr Šittner[2], Orsolya Molnárová[2], Haizhou Lu[3], Eduardo Alarcón[2], Luděk Heller[2], Chao Yang[1]
[1]South China University of Technology, Guangzhou, Guangdong, China. [2]Institute of Physics of the Czech Academy of Sciences, Prague, Prague, Czech Republic. [3]Guangdong Polytechnic Normal University, Guangzhou, Guangdong, China

NiTiHf high-temperature shape memory alloys (HTSMAs) fabricated via laser powder bed fusion (LPBF) are commonly suffering from poor tensile strength and unstable actuation preventing their successful use in engineering applications. We managed to fabricate defect-free NiTiHf alloy via LPBF with superior tensile strength (821 MPa) and high tensile stress stable actuation properties, which significantly surpasses the actuation properties of the cast NiTiHf alloy of the same nominal chemical composition. The LPBF NiTiHf alloy exhibits lower recoverable strain than the cast alloy but stable actuation with 2.34% strain under 300 MPa. The improved actuation properties of the LPBF NiTiHf alloy are ascribed to the strengthening effect of nano-precipitates introduced during the LPBF which prevents detwinning of martensite variant microstructure created upon cooling under external stress restricting thus dislocation slip in martensite responsible for the cyclic instability.

P62_237

Phase transformation and texture evolution in a metastable medium entropy alloy

Ibrahim Ondicho[1], Germanas Peleckis Peleckis[1], Hyoung Seop Kim[2], Azdiar Gazder[1]
[1]University of Wollongong, Wollongong, New South Wales, Australia. [2]Pohang University of Science and Technology, Pohang, Korea, Republic of

Medium-and high-entropy alloys (MEAs/HEAs) have garnered significant attention due to their superior yield strength (YS), ultimate tensile strength (UTS), and ductility. However, most face-centred cubic (fcc) MEAs and HEAs exhibit insufficient strength for structural applications. A promising approach to improving the strength-ductility balance in fcc MEAs/HEAs is by promoting deformation-induced martensitic transformation, which can be achieved by reducing the stacking fault energy (SFE) to ≤15 mJ/m² through precise chemical composition adjustments.

In this study, the deformation mechanisms and texture evolution of a metastable Fe45Co35Cr10V10 MEA were investigated. After casting and homogenisation at 1100°C for 6 h, the alloy exhibited a single-phase fcc (γ) microstructure. During cold rolling (CR), deformation-induced martensitic transformations occurred via γ → ε → α' and γ → α' pathways, governed by Shoji-Nishiyama (S-N), Burgers, and Kurdjumov-Sachs (K-S) orientation relationships (ORs) with variant selection. Additionally, a finer initial grain size in the γ phase was found to favour the γ → α' transformation pathway. Furthermore, with increasing cold rolling thickness reduction, the γ to α'-martensite OR transitioned from Kurdjumov-Sachs (K-S) to Nishiyama-Wassermann (N-W) at 40% thickness reduction, highlighting a critical transformation threshold.

Beyond 40% CR thickness reduction, the γ phase develops a brass-type texture due to the preferential transformation of Cu_g and S_g orientations to ε and α' martensite, accompanied by shear banding. The ε-martensite texture features ~ (01-15) $[3\text{-}742]_e$ and ~$(11\text{-}26)[\text{-}1\text{-}121]_e$ orientations along the {hkil}-fibre, arising from Cu_g and S_g orientations via the S-N OR and variant selection. Similarly, the α'-martensite texture aligns along the alpha and gamma fibres after 80% CR typical of bcc materials, with the former originating from G_g, Br_g , Cu_g and S_g orientations, and the latter mainly from Br_g and S_g via the K-S OR and variant selection.

P63_253

Functional properties comparison for high entropy and conventional shape memory alloys: few application perspectives

Vira Filatova[1], Georgiy Firstov[1], Yuriy Koval[1], Valeriy Odnosum[1], Grigoriy Gerstein[2], Hans Jurgen Maier[2]
[1]G. V. Kurdyumov Institute for Metal Physics of the National Academy of Science of Ukraine, Kyiv, Ukraine. [2]Institut fur Werkstoffkunde (Materials Science) Leibniz Universitat Hannover, Garbsen, Germany

Shape memory alloys (SMA) in general were in focus of numerous engineering applications due to the possibility to restore significant deformation amounts under certain stress–temperature conditions due to the martensitic diffusionless phase transformation involved. It was possible to exploit not only so-called 'shape-memory' effect, but also superelasticity and high damping capacity. Over the years, thousands of patents on SMA were filed, appreciating not only the possibility to exploit the energy transformation to ensure the response (feedback) at the change in independent thermodynamic parameters (temperature, stress, pressure, electric or magnetic field, etc.), but the significant work output as well. The envisaged shape memory components covered applications in the automotive, aerospace, machine building and civil construction industries.

At present, amongst SMA the high entropy ones exhibit certain structural peculiarity, namely, a lattice distortion that lead to the suppression of shear. The definite positive effect of this is the significant resistance to the irreversible plastic deformation, while the martensitic reversible strain is still possible [1].

The present report is going to show that high entropy shape memory alloys (HESMA) of multiple principal element intermetallic kind are able to exhibit work output 7 times higher comparing to conventional SMA. It will be also shown that the perfect stable shape memory is accompanied by significant damping (loss factor tand over 0.2) in these HESMA. Some of these issues will be illustrated in the frame of our recent application attempts including bleeding control devices, smart materials for communal services etc. The reasons for important differences and similarities in functional behavior will be discussed.

[1] G. S. Firstov, Yu. M. Koval, V. S. Filatova, V. V. Odnosum, G. Gerstein, and H. J. Maier, *Progress in Physics of Metals*, 24, No. 4: 819–837 (2023); https://doi.org/10.15407/ufm.24.04.819

P64_355

Microstructural aspects of bcc-hcp-fcc displacive transformations in annealed HEA melt spun ribbons

Wojciech Maziarz[1], Anna Wojcik[2], Arkadiusz Szewczyk[2], Nikodem Poreba[2], Norbert Schell[3], Robert Chulist[2]
[1]Institute of Metallurgy and Materials Science, Polish Academy of Sciences, Krakow, Poland. [2]AGH University of Science and Technology, Faculty of Metals Engineering and Industrial Computer Science, Krakow, Poland. [3]Institute of Materials Physics, Helmholtz-Zentrum Hereon, Geesthacht, Germany

The $Co_{47}Fe_{23.5}Al_{17.7}Cr_{11.8}$ (at%) HEA melt-spun ribbons have been investigated using high-energy synchrotron diffraction, EBSD and transmission electron microscopy (TEM). The melt-spinning process was employed to refine the microstructure and produce metastable, disorder phases by rapid quenching. This process can be compared to severe plastic deformation process as both result in highly disordered states. It is known that in HEA, a martensitic fcc-to-hcp transformation can be induced by a stress of 14 GPa [1]. Additionally, twinning-induced plasticity (TWIP) strengthening mechanisms are active during martensitic twinning transformation in a metastable refractory element-based bcc-HEA [2]. In this work, we present a sequence of displacive transformations from bcc to fcc through an intermediate hcp phase during the annealing of melt-spun ribbons. Particular attention was devoted to the microstructural effects related to atomic rearrangement, including the formation of stacking faults and twin configurations during this transformation. Local chemical composition measurements of particular phases after various stages of annealing showed that diffusion processes were not involved in this transformations.

[1] Cameron L. Tracy, Sulgiye Park, Dylan R. Rittman, Steven J. Zinkle, Hongbin Bei, Maik Lang, Rodney C. Ewing & Wendy L. Mao, High pressure synthesis of a hexagonal close-packed phase of the high-entropy alloy, CrMnFeCoNi, Nature Communications, (8:15634), DOI: 10.1038/ncomms15634.

[2] Y. Huang, J. Gao, V. Vorontsov, D. Guan, R. Goodall, D. Dye, S. Wang, Q. Zhu, W. M. Rainforth, I. Todd, Martensitic twinning transformation mechanism in a metastable IVB element-based body centered cubic high-entropy alloy with high strength and high work hardening rate, Journal of Materials Science & Technology, 124, (2022), 217–231
Acknowledgment:
Financial support of the National Science Centre, Poland (project no. 2022/47/B/ST8/03298) is greatly acknowledged.

P65_273

In-situ Observation of the Formation of Lath Martensite Microstructurein Fe-Ni-Cr-C Alloy

Wataru Aoki[1], Nozomi Takahashi[1], Ryutaro Matsumura[1], Yuri Shinohara[2], Hiroyuki Kawata[3], Tomonari Inamura[1]
[1]Institution of Science Tokyo, Yokohama, Kanagawa, Japan. [2]The University of Electro-Communications, Chofu, Tokyo, Japan. [3]Nippon Steel Corporation, Futtsu, Chiba, Japan

We have clarified the effect of the geometric compatibility condition (rank-1 connection condition) on the variant pairing for martensitic structures in steel in thin plate, lenticular, and butterfly martensite [1][2][3]. We revealed that the variant pairing that occur preferentially have small geometric incompatibility, whereas the V1/16 (Variant number definition follows Morito [4].) pair occurs at a high frequency despite exhibiting significantly larger incompatibility compared to other preferentially occurring variant pairs. As for the lath martensite, it has already been reported that V1/16 pairs appear frequently in the early stages of transformation [5]; however, their formation process and the relationship with geometric incompatibility remain unclear. In this study, we clarify the effect of geometric compatibility condition on the variant pairing of lath martensite in Fe-Ni-Cr-C alloys with Ms below room temperature using in-situ observations with optical microscopy and EBSD.

Fe-22.8Ni-2.1Cr-0.18C(wt%) alloy was vacuum melted, hot forged, and then homogenized at 1000 ℃ for 1 hour, followed by water cooling. The sample surface was electropolished to smoothen it, and the martensitic transformation process was observed under an optical microscope with a cooling stage (1.0 ℃/min, from room temperature to -40 ℃). Subsequently, variant pairs were identified by EBSD measurements and evaluated based on Rank-1 connection conditions.

It was revealed through in-situ observation that V1/16 pairs formed in the early stage of transformation, followed by the formation of V1/2 and V1/4 pairs at high frequency and growth into packets, and that the frequency of V1/16 pair with large incompatibility was remarkably high in the early stage of transformation and decreased from 7.5% to 2.1%, less than half, as the transformation progressed. This indicates that V1/16 pairs are formed in the early stage of transformation in spite of their large incompatibility. Possible factors promoting the formation of the V1/16 pair are discussed.

[1] Y. Shinohara et al., Sci. Rep., 2021, 11, 14597.
[2] Y. Shinohara et al., Acta Mater., 2023, 259, 119275.
[3] N. Takahashi et al., ISIJ Int., 2024, 64, 202.
[4] S. Morito et al., Acta Mater., 2003, 51, 1789.
[5] T. Kohne et al., Metall. Trans. A., 2022, 53, 3034.

P66_236

Tensile properties and deformation-induced martensitic transformation in Fe-Ni-C steel

Ryoya Oishi, Si Gao, Myeong-Heom Park, Nobuhiro Tsuji
Kyoto University, Kyoto, Japan

TRIP (Transformation-Induced Plasticity) steels exhibit both high strength and good ductility due to deformation-induced martensitic transformation (DIMT). DIMT is strongly affected by the amount of interstitial carbon content of the alloys. On one hand, increasing the carbon content would stabilize austenite and suppress the transformation rate of DIMT during deformation. On the other hand, the higher carbon content increases the hardness of the transformed martensite, which would positively contribute to the strain hardening caused by DIMT. Our previous work [1] demonstrated an Fe-24Ni-0.3C (wt%) TRIP steel exhibiting a high tensile strength of 1000 MPa and a large uniform elongation of 70% due to the DIMT. However, the effect of further increase of carbon content on the mechanical properties and the DIMT in the Fe-Ni-C steel remains unclear.

In the present study, an Fe-24Ni-0.8C (wt%) was used to investigate the effects of high carbon content on DIMT and mechanical properties of Fe-Ni-C TRIP steels. The as-received material was cold rolled by 90% thickness reduction and annealed at 950℃ for 10 minutes. Tensile test was performed at room temperature and microstructures were observed by SEM-BSE and SEM-EBSD.

EBSD observation revealed that the annealed material consisted of 100% austenite phase with fully recrystallized grains with a mean grain size of 12.1 μm. Tensile test showed a yield strength of 240 MPa, an ultimate tensile strength (UTS) of 828MPa and a high tensile elongation of 106%. Compared to the Fe-24Ni-0.3C alloy, the Fe-24Ni-0.8C alloy exhibited a lower UTS but a significantly higher tensile elongation. SEM-BSE observation showed that dislocation slip was predominant at early stage of tensile deformation. Deformation-induced martensite was first observed at the tensile elongation of 50%, and its fraction gradually increased from 1.3% to 13.2% during the tensile elongation increased up to 106%. The slow martensite transformation rate and the high hardness of the martensite are believed to play important roles in the excellent combination of tensile strength and elongation of the present Fe-24Ni-0.8C alloy, which will be discussed in detail in the presentation.

[1] Mao W., Gao S., Gong W., Bai Y., Harjo S., Park M. H., Shibata A., Tsuji N. *Acta Mater.* **256**, 119139 (2023).

ORBITUARIES

Obituary: Ken’ichi Shimizu (1928-2024)

Ken’ichi Shimizu, Professor Emeritus of Osaka University and Honorary member of Japan Institute for Metals, passed away at the age of 96 on November 12, 2024. We felt deep sorrow at his passing, since he was a sincere and friendly person, who was a regular attendee of ICOMAT conferences and established good rapport with members of the ICOMAT society.

Prof. Shimizu was born in Hokkaido in 1928. He graduated from the Department of Physics, Faculty of Science, Tohoku University in March 1951, and joined the Institute of Scientific and Industrial Research, Osaka University in April of the same year as a research assistant. He was promoted to assistant professor and associate professor before being promoted to professor in 1966.

He retired from Osaka University in 1992 and was awarded the title of Professor Emeritus in April of the same year. He then continued to work as professor at Kanazawa Institute of Technology until 2008 (and as visiting professor since 2006).

Prof. Shimizu has made several world-leading achievements in the fundamentals and applications of martensitic transformations in metallic materials. Specifically, he has elucidated the crystallographic mechanism of formation and growth for martensitic transformation in ferrous and nonferrous alloys, the mechanisms of shape memory effect and superelasticity, closely related to the transformation, and the effects of stress, magnetic field, and hydrostatic pressure on the transformation.

He also devoted himself to the development of materials analysis techniques using electron microscopes, and was the first to develop and apply a five-lens ultra-high-voltage electron microscope capable of selected-area electron diffraction in the nano-area, and an analytical electron microscope with a field-emission electron gun capable of simultaneously performing high-resolution observations and compositional analysis.

For these research achievements, he received the Seto Award from the Japanese Society of Electron Microscopy in 1962, the title of Fellow from ASM International in 1985, the Honda Memorial Award in 1996, and the Japan Institute of Metals Award in 2002; his research achievements have been highly evaluated worldwide.

In international exchange, he played a leading role as the chairman of the organizing committee for the first and fifth International Conference on Martensitic Transformations and as a member or advisor of the International Committee of the same conference. In addition, as the first president of the Shape Memory Alloy Association (ASMA, Japan) from 1993 to 2006, he contributed greatly to the development of industrial applications of this alloy.

By Tomoyuki Kakeshita;
President of Fukui University of Technology, Professor Emeritus of Osaka University

Orbituary to Professor Kazuhiro Otsuka (1937-2023)

Professor Kazuhiro Otsuka passed away on 19th August, 2023, after a long and productive career researching aspects of shape memory alloys and superelastcity. His M.S. at the University of Illinois in 1966 under the supervision of Professor Marvin Wayman, not only was the commencement of a long-lasting friendship but also put him in contact with Professor Ken'ichi Shimizu from Osaka University where he found his first appointment on his return to Japan. There followed a D.Eng from the University of Tokyo in 1972, a promotion to Associate Professor at Osaka in 1972 and a Professorship at the University of Tsukuba in 1979. On becoming Professor Emeritus from the University of Tsukuba in 2000, he was able to continue his productive research career at the National Institute for Materials Science and the National Institute for Advanced Interdisciplinary Research, both in Tsukuba, until his retirement in March 2017.

Some of Professor Otsuka's most significant research outputs will be summarised during this tribute, as well as his regular contributions to the international scientific community via the ICOMAT and Solid→Solid Phase Transformations series. His most memorable legacies to the field of shape memory and superelasticity are his book, "Shape Memory Materials" (Cambridge University Press, 1988) in collaboration with Professor Wayman, and his publication on Ti-Ni-based alloys, "Physical Metallurgy of Ti-Ni-based Shape Memory Alloys" K. Otsuka and X. Ren, in *Progress in Materials Science,* **50**: 511-678 (2005).

This Tribute Presentation has been prepared in collaboration with Professor Yasukzu Murakami (Kyushu University, Japan), Professor Antoni Planes (University of Barcelona, Spain), Professor Xiaobing Ren (National Institute for Materials Science, Japan) and Dr Avadh Saxena (Los Alamos National Laboratory, U.S.A.)

Professor Trevor Finlayson
University of Melbourne
Victoria, Australia.

Orbituary to Professor Pat Kelly (1935-2025)

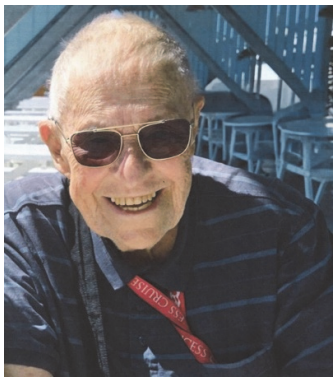

Patrick Manning Kelly (or Pat to his friends and colleagues) was born in Panama City, Republic of Panama on 25th March, 1935. His father came from Jamaica and his mother from Barbados. When Pat was four the family moved to Colon on the Atlantic side of Panama where Pat attended an American elementary school. His secondary schooling, thanks to his staunchly British parents, was at a boarding school in Barbados. He was awarded a Barbados government scholarship which enabled him to attend Cambridge University, U.K. from where he graduated B.Sc. (Hons) and Ph.D., with a specialisation in electron microscopy. Following a short period as a Lecturer in the Department of Metallurgy at Leeds University, U.K., he was recruited by the Australian Atomic Energy Commission (now the Australian Nuclear Science and Technology Organisation (ANSTO)) to join their Materials Institute for which he eventually became the Institute Head. Pat moved back into academia as an Associate Professor in the Department of Metallurgy at the University of Queensland in the early 1990s. He sadly passed away as the consequence of an aggressive cancer, on 11th August this year.

Pat's life-long research focussed on crystallography, particularly using electron microscopy and electron diffraction. He carried out research on steels, aluminium and titanium alloys, as well as the ceramic, magnesia partially stabilised zirconia. For a number of years he was a member of the ICOMAT International Committee and was the Chair of the Organising Committee for ICOMAT1989 which had been awarded to Australia and which was held in Sydney from 3rd to 7th July, 1989.

Professor Trevor Finlayson
University of Melbourne
Victoria, Australia.